VOLUME 37 OCTOBER 1959 NUMBER 10

Canadian Journal of Chemistry

Published by THE NATIONAL RESEARCH COUNCIL

OTTAWA CANADA

Canadian Journal of Chemistry

Under the authority of the Chairman of the Committee of the Privy Council on Scientific and Industrial Research, the National Research Council issues THE CANADIAN JOURNAL OF CHEMISTRY and five other journals devoted to the publication, in English or French, of the results of original scientific research. Matters of general policy concerning these journals are the responsibility of a joint Editorial Board consisting of: members representing the National Research Council of Canada; the Editors of the Journals; and members representing the Royal Society of Canada and four other scientific societies.

The Chemical Institute of Canada has chosen the Canadian Journal of Chemistry as its medium of publication for scientific papers.

Manuscripts for publication should be submitted to Dr. Léo Marion, Editor-in-Chief, Canadian Journal of Chemistry, National Research Council, Ottawa 2, Canada.
(For instructions on preparation of copy, see **Notes to Contributors** (inside back cover).)

Proof, correspondence concerning proof, and orders for reprints should be sent to the Manager, Editorial Office (Research Journals), Division of Administration and Awards, National Research Council, Ottawa 2, Canada.

Subscriptions, renewals, requests for single or back numbers, and all remittances should be sent to Division of Administration and Awards, National Research Council, Ottawa 2, Canada. Remittances should be made payable to the Receiver General of Canada, credit National Research Council.

The journals published, frequency of publication, and prices are:

Canadian Journal of Biochemistry and Physiology	Monthly	$9.00 a year
Canadian Journal of Botany	Bimonthly	$6.00 a year
Canadian Journal of Chemistry	Monthly	$12.00 a year
Canadian Journal of Microbiology	Bimonthly	$6.00 a year
Canadian Journal of Physics	Monthly	$9.00 a year
Canadian Journal of Zoology	Bimonthly	$5.00 a year

The price of regular single numbers of all journals is $2.00.

Canadian Journal of Chemistry

Issued by THE NATIONAL RESEARCH COUNCIL OF CANADA

VOLUME 37 OCTOBER 1959 NUMBER 10

SELF-DIFFUSION IN POLYCRYSTALLINE NICKEL[1]

J. R. MACEWAN,[2] J. U. MACEWAN, AND L. YAFFE

ABSTRACT

The self-diffusion of nickel has been studied in polycrystalline samples by a sectioning technique. There is evidence of grain boundary diffusion below temperatures of 1150° C. The results obtained between 1150° and 1400° C are representative of volume diffusion and are represented by the expression

$$D = 3.36\, e^{-69,800/RT}.$$

A comparison is made with the results of other self-diffusion studies using Zener's hypothesis.

INTRODUCTION

The most precise measurements made on the rate of volume self-diffusion in metals have been carried out with single crystal specimens. Measurements made with polycrystalline specimens have been in good agreement with those made with single crystal specimens only when the diffusion study was confined to temperatures close to the melting point of the metal. None of the reported investigations (1, 2, 3) made of the self-diffusion of nickel in polycrystalline samples have satisfied this criterion. Therefore, it was thought worth while to report some work on the rate of nickel self-diffusion in the temperature range 1050° to 1400° C.

EXPERIMENTAL

Diffusion coefficients were obtained by the standard sectioning method (4) and by a modification of Gruzin's integral residue method (5). In some cases both techniques were employed to analyze the same specimen, which permitted a direct comparison of the results obtained with each.

The nickel tracer employed contained two long-lived isotopes, Ni^{63} decaying with the emission of a 67-kev β-particle and Ni^{59} decaying by K-electron capture with the emission of a Co K_α X-ray (6). A Co^{58}, gamma-emitting impurity present in the tracer solution was completely removed by an ion exchange procedure (7). In the 2π internal source proportional counter employed, the ratio of detected disintegrations of Ni^{63} to Ni^{59} was in excess of 5×10^3 for almost all sources counted. Thus, with one exception which will be discussed later, it was assumed that the tracer consisted of a single active species, Ni^{63}.

The diffusion specimens consisted of polycrystalline nickel cylinders about 0.60 in. in diameter with the active tracer electroplated on one face. The total analyzed impurity

[1]*Manuscript received May 22, 1959.*
Contribution from the Department of Metallurgical Engineering and the Radiochemistry Laboratory, Department of Chemistry, McGill University, Montreal, Que., with financial assistance from the Defence Research Board.

[2]*Present address: Fuel Development Branch, Atomic Energy of Canada Limited, Chalk River, Ontario.*

content in the cylinders was less than 0.08%, with the principal impurities being Fe, 0.04; Co, 0.015; and Cu, 0.01%. Each cylinder was annealed at 1400° C for 24 hours to produce a coarse stable grain size prior to the electrodeposition of the tracer from an ammonia – ammonium sulphate solution. Grain diameters in individual specimens varied from 3 to 10 mm. Thickness of the tracer layer was about one micron. Uniformity of the active plating was checked by measuring the counting rate at nine positions on the active surface through an aluminum diaphragm with a 3/32-in. hole. These counting rates were converted to thicknesses with a self-absorption curve for Ni^{63} (8), and specimens with thickness variations greater than ±3% were rejected.

For the diffusion anneal, duplicate specimens were positioned in recrystallized alumina crucibles with the active faces touching to minimize loss of the tracer by evaporation. This assembly was placed in a preheated tube furnace with a constant temperature zone 5 in. in length where the samples were surrounded by a pure hydrogen atmosphere to prevent oxidation. By charging and discharging the samples to and from a hot furnace, errors in the length of the diffusion anneal were less than 0.2%, even for the shortest times. Temperatures were controlled to within ±0.5° C by backing off most of the potential from the Pt/(Pt – 13% Rh) control thermocouple with a standard potential source and feeding the amplified difference to a Speedomax proportional temperature controller. The temperature of the specimens was measured during each run with a certified Pt/(Pt–Rh) thermocouple, corrections being made for thermocouple sheath losses. The diffusion anneal temperatures should be accurate to ±2.0° C.

After the diffusion anneal, one of the duplicate specimens was sectioned in the standard manner. The specimen was mounted in a lathe-collet so that the face ran true to ±0.002 mm, and at least 1.2 mm was removed from the diameter to eliminate edge effects. Then successive facing cuts from 0.025 to 0.040 mm, in thickness were made to provide samples for activity measurements. The turnings were weighed to determine the slice thickness for comparison with direct micrometer measurements made on the specimen. As the nickel cuttings did not represent a suitable source for counting of the low energy Ni^{63} β-particles, the cuttings were dissolved in concentrated hydrochloric acid and the nickel electroplated on to copper planchets to form a 0.70-in. diameter deposit. The method employed has been described elsewhere (8). In all cases, sufficient nickel was deposited to form an infinitely thick source (4.5 mg/cm² or greater), so that the observed counting rate was directly proportional to the specific activity of the source. The reproducibility in preparing sources in this manner was better than ±1%. Whenever possible, sufficient counts were recorded to give counting statistics of ±1%.

The second specimen was treated in an identical fashion except for the following change in procedure. Before taking each facing cut, the activity of the active face was measured by mounting the specimen in the 2π internal source counter using a special baseplate. A diaphragm with a central hole smaller than the specimen diameter prevented β-particles emitted from the specimen sides being detected. The activity measured in this manner represents the specific activity of the Ni^{63} in a layer less than one micron below the surface. Previous work (8) on the self-absorption of Ni^{63} showed that over half the detected activity in an infinitely thick sample of uniform specific activity is emitted from a depth within 0.5 μ of the sample surface. Thus in a diffusion couple where the activity is decreasing in a Gaussian manner with increasing depth below the surface, the counting rate measured on the surface can be assumed to be proportional to the specific activity of the metal forming the surface layer.

RESULTS AND DISCUSSION

For volume diffusion, the concentration $C(x, t)$ of the tracer isotope in a layer at distance X below the surface after an annealing time t is given by the equation,

$$C(x, t) = C_0/\sqrt{\pi Dt}\, e^{-X^2/4Dt},$$

where C_0 is the total quantity of tracer deposited on the specimen face and D is the diffusion coefficient. The diffusion coefficient is calculated from the slope of the straight line plot of log $\bar{C}$ versus $\bar{X}^2$. Typical plots obtained at temperatures of 1197° and 1152° C are shown in Fig. 1. The plot at 1197° C is typical of those obtained at all temperatures equal to or above 1200° C. It can be seen that log $\bar{C}$ varies as $\bar{X}^2$ for all values of $\bar{X}$ indicating that the diffusion occurring at these temperatures is typical of volume diffusion. However, in the concentration penetration curve obtained at 1152° C, log $\bar{C}$ varies as $\bar{X}^2$ for shallow penetrations, while at deeper penetrations log $\bar{C}$ varies as $\bar{X}$. This mixed type of penetration curve is obtained when neither grain boundary nor volume diffusion predominate in a diffusion couple. Wajda (9) has shown that with this type of specimen the volume diffusion coefficients obtained from the initial linear portion of the log $\bar{C}$ versus $\bar{X}^2$ are generally higher than those obtained from single crystal specimens at the same temperature.

Excellent agreement, within 1%, was obtained between duplicate diffusion couples treated by the standard sectioning method. However, when the same specimen was treated by both surface-activity-sectioning and sectioning techniques, the D values for the former method were always slightly lower. For the five samples treated by both methods, this difference varied from 1.5 to 9.0%, with an average deviation of 5.6%. This is reflected in Fig. 1 where the penetration curve determined by the surface-sectioning method has a steeper slope than that obtained in the conventional manner for the same specimen. About one per cent of this diffusion is a result of neglecting the enhanced counting rate at the surface for low values of $\bar{X}$ due to detection of the more penetrating Ni^{59} radiation from much deeper portions of the diffusion specimen. This effect would tend to make the diffusion coefficients obtained with the surface-activity-sectioning method too low. The diffusion coefficients obtained by the normal method are about 1.0% too high as a result of using slices of finite thickness. No convincing explanation can be offered for the residual discrepancy of 3.6%.

The activation energy, Q, and frequency factor, D_0, for volume diffusion are related by the Arrhenius equation:

$$D = D_0\, e^{-Q/RT}.$$

To obtain values for Q and D_0, the measured values of D were plotted against $1/T$ as in Fig. 2. The open circles represent the average values found by the normal sectioning method for the duplicate specimens annealed at one time, while the solid points represent the surface-activity-sectioning value for one of these specimens. A correction was made to the diffusion constants for lattice expansion, but no allowance was made for an isotopic mass effect. Johnson's (10) original work, which suggested that Graham's law applied to metallic diffusion as well as to gaseous diffusion, has not been substantiated by more recent work (11).

It can be seen that the values found for the temperature range 1150° to 1400° C lie on a straight line. The coefficients measured below 1150° C lie above the extrapolated line of best fit for the high temperature results indicating that sufficient grain boundary

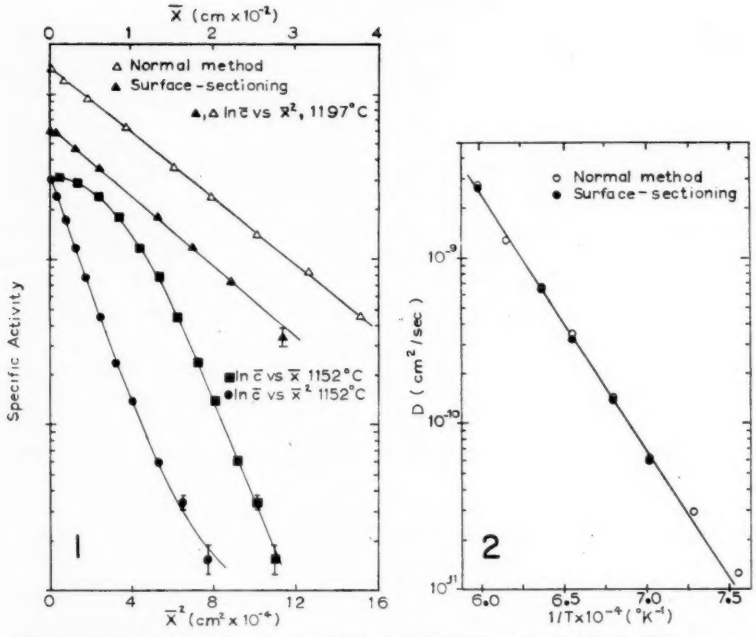

FIG. 1. Concentration penetration curves obtained at 1152° C and at 1197° C. The curves at 1152° C assume the form generally associated with grain boundary diffusion.
FIG. 2. Activation energy plot.

diffusion has occurred in those specimens to invalidate the results. To obtain a comparison between the results obtained by both methods employed, both sets of data were fitted individually by least mean squares. For the standard sectioning method

$$D = 3.66\, e^{-(70{,}000 \pm 1700)/RT}$$

and for the surface-activity-sectioning method

$$D = 3.04\, e^{-(69{,}000 \pm 600)/RT}.$$

The results obtained by the two methods of analysis are in good agreement although the surface-activity-sectioning data have a slightly smaller standard deviation. Thus this work gives an average value of 3.36 cm^2/sec for the frequency factor, D_0, and 69.8 kcal/mole for the activation energy, Q.

For comparison, the values found in other investigations are tabulated below:

TABLE I

Self-diffusion data for nickel

Reference	Q (kcal/mole)	D_0 (cm^2/sec)	Temp. range (° C)	Method
(1)	61–65	—	250–1250	Surface activity
(2)	66.8	1.27	1150–1250 870–1230	Sectioning surface activity
(3)	63.8	0.33	1100–1175	Sectioning
This work	69.8	3.36	1150–1400	Sectioning

Burgess and Smoluchowski's work, apparently incomplete, can be regarded only as a preliminary study. Their results were obtained by a surface activity technique, not specified in detail, below a temperature of 1250° C. No value was reported for the frequency factor.

The activation energy obtained by Reynolds *et al.* in a study of nickel self-diffusion throughout the Au–Ni system cannot be given too much weight because of the narrow temperature range investigated. However, their measured diffusion coefficients differ by only 4% from those obtained in this work.

Hoffman, Pikus, and Ward's reported diffusion coefficients in the temperature range 1150–1250° C are also in good agreement with the results obtained in this work. The differences in activation energy are reflected in a small but consistent difference in D values at temperatures outside the range where the two investigations overlap. Hoffman *et al.* employed a decrease in surface activity technique for their measurements below 1150° C. However, inspection of their data shows that all their diffusion coefficients obtained above a temperature of 1147° C, both by surface activity and sectioning techniques are consistent with an activation energy higher than that reported. Therefore, if their low temperature measurements yielded results which were high, their reported activation energy would be low.

There are two factors which could cause high values for the D values obtained by the decrease in surface activity method employed in the investigation by Hoffman *et al.*: grain boundary diffusion or an incorrect choice of k, the absorption coefficient of the β-radiation from Ni^{63}. Direct measurements of k by the present authors (8) and by Schweitzer *et al.* (12) for self-absorption of Ni^{63} in a 2π geometry have shown that at least two absorption coefficients are needed to explain the observed results assuming exponential absorption of radiation. One of these coefficients is much larger than, and the other comparable to, that obtained in an external absorption measurement. The narrow angle counter geometry employed by Hoffman will tend to minimize this effect but certainly not eliminate it. The combined effect of these two absorption coefficients is to make self-absorption more rapid in the source than anticipated and will lead to high values for D in samples where little diffusion has taken place, i.e. at low temperatures.

Zener (13) in a theoretical analysis of the activation process for diffusion in face-centered cubic metals proposed the following correlation between the entropy of activation for diffusion, ΔS, the temperature coefficient of Young's modulus, μ^1/μ_0, and the activation energy

$$(\Delta S/R) = \ln (D_0/a^2\nu) = \lambda(\mu^1/\mu_0)(Q/R)$$

where a is the lattice parameter, R the gas constant, and ν the Debye frequency. The particular choice of the constant, $\lambda = 0.55$, was such as to make the correlation exact for the accurately determined values of D_0 and Q for the self-diffusion of silver (14).

A plot of $\Delta S/R$ versus $(\mu^1/\mu_0)(Q/R)$ is given in Fig. 3 for the commonly accepted self-diffusion data for Ag, Au, Cu, Ni, Pb, and Pt. The straight line shown has a slope of 0.55, corresponding to Zener's suggested value for the constant λ. The dotted lines connecting various points for the same metal are not intended to have any particular significance, but rather to simplify inspection of the graph.

Inspection of the graph shows that there is a rough correlation between values of $\Delta S/R$ and $(\mu^1/\mu_0)(Q/R)$. A point of some interest is that the value from Makin, Rowe, and LeClaire's (15) recent careful study of gold self-diffusion falls just above the curve.

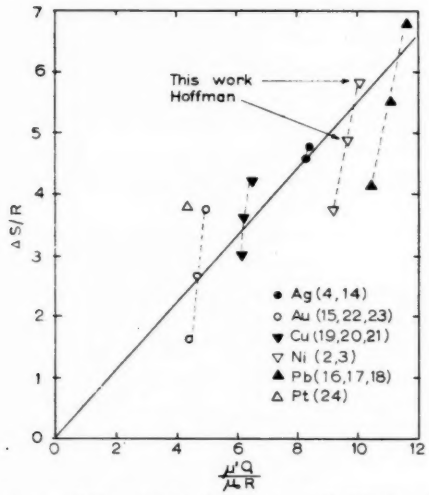

FIG. 3. Correlation between $\Delta S/R$ and $(\mu^1/\mu_0)(Q/R)$ for self-diffusion in various face-centered cubic lattice metals.

Thus, if we accept Zener's correlation with $\lambda = 0.55$ as exact, it is apparent that the activation energy for self-diffusion in nickel falls somewhere between that found in this work and that found by Hoffman *et al.* While there is no real justification for this observation, it is interesting to note that with $\lambda = 0.57$, the correlation line would pass through or close to points representing self-diffusion studies in Au, Ag, Cu, Pb, and the value found for nickel in this research.

ACKNOWLEDGMENT

The authors wish to express their gratitude to the Defence Research Board for grants received.

REFERENCES

1. BURGESS, H. and SMOLUCHOWSKI, R. J. Appl. Phys. **26**, 491 (1955).
2. HOFFMAN, R. E., PIKUS, F. W., and WARD, R. A. Trans. A.I.M.E. **206**, 483 (1956).
3. REYNOLDS, J. E., AVERBACH, B. L., and COHEN, M. Acta Met. **5**, 29 (1957).
4. JOHNSON, W. A. Trans. A.I.M.E. **143**, 107 (1941).
5. GRUZIN, P. L. Doklady Akad. Nauk S.S.S.R. **86**, 289 (1952).
6. BROSI, A. R., BORKOWSKI, C. J., CONN, E. E., and GREISS, J. C., JR. Phys. Rev. **81**, 391 (1951).
7. MOORE, G. E. and KRAUS, K. A. J. Am. Chem. Soc. **73**, 9 (1951); **74**, 843 (1952).
8. MACEWAN, J. R., MACEWAN, J. U., and YAFFE, L. Can. J. Chem. **37**, 649 (1959).
9. WAJDA, E. S. Acta Met. **2**, 184 (1954).
10. JOHNSON, W. A. Trans. A.I.M.E. **166**, 114 (1946).
11. LAZARUS, D. and OKKERSE, B. Phys. Rev. **105**, 1677 (1957).
12. SCHWEITZER, G. K., STEIN, B. R., and NEHLS, J. W. J. Phys. Chem. **56**, 692 (1952).
13. ZENER, C. J. Appl. Phys. **22**, 372 (1951).
14. SLIFKIN, L., LAZARUS, D., and TOMIZUKA, T. J. Appl. Phys. **23**, 1032 (1952).
15. MAKIN, S. M., ROWE, A. H., and LECLAIRE, A. D. Proc. Phys. Soc. B, **70**, 545 (1957).
16. SEITH, W. and KEIL, A. Z. Metallk. **25**, 104 (1933).
17. NACHTREIB, N. H. and HANDLER, G. S. J. Chem. Phys. **23**, 1569 (1955).
18. OKKERSE, B. Acta Met. **2**, 551 (1954).
19. MAIER, M. S. and NELSON, H. R. Trans. A.I.M.E. **147**, 39 (1942).
20. RAYNOR, C. L., THOMASSEN, L., and ROUSE, L. J. Trans. Am. Soc. Metals, **30**, 313 (1942).
21. KUBASCHEWSKI, O. Trans. Faraday Soc. **46**, 713 (1950).
22. OKKERSE, B. Phys. Rev. **103**, 1246 (1956).
23. GATOS, H. C. and KURTZ, A. D. Trans. A.I.M.E. **200**, 616 (1954).
24. KIDSON, G. V. and ROSS, R. Intern. Conf. on Radioisotopes in Scientific Research, Unesco/NS/RIC/216 (1957).

DIFFUSION OF Ni^{63} IN IRON, COBALT, NICKEL, AND TWO IRON–NICKEL ALLOYS[1]

J. R. MacEwan,[2] J. U. MacEwan, and L. Yaffe

ABSTRACT

The self-diffusion of nickel and the diffusion of Ni^{63} into iron, cobalt, and two iron–nickel alloys was studied using the technique of decrease in surface activity, The nickel self-diffusion results are compared to previously reported values. Nickel is found to diffuse more slowly than iron in the iron-rich portion of the iron–nickel system. The rate of nickel diffusion increases with increasing nickel content. A comparison is made between the present results for diffusion of Ni^{63} into iron, cobalt, and nickel with reported values for diffusion of Co^{60} and Fe^{59} in the same metals. In each solvent, the magnitudes of the activation energies, Q, are such that $Q_{Ni} > Q_{Co} > Q_{Fe}$.

INTRODUCTION

The transition elements iron, cobalt, and nickel are interesting both theoretically and experimentally because they exhibit marked similarities in properties. All assume a face-centered cubic lattice structure at high temperatures and possess nearly similar atomic radii. Therefore, it was thought worth while to investigate the rate of diffusion of Ni^{63} in pure iron, cobalt, and nickel. The studies were in a temperature range where only face-centered cubic lattice phases exist, and all diffusion data refer to the three metals in this condition. These results should permit some conclusions to be drawn concerning diffusion in these metals as other investigators have already reported data for diffusion of cobalt and iron tracers in iron, cobalt, and nickel.

The rate of self-diffusion of nickel in the iron-rich portion of the iron–nickel system was investigated to complement work reported by other investigators on the rate of self-diffusion of iron in the same region. The results should permit a comparison to be made between rates of diffusion of iron and nickel atoms in this technologically interesting portion of the iron–nickel system.

EXPERIMENTAL

The self-absorption characteristics of Ni^{63} β-radiation are such that, in a thick sheet containing the tracer isotope, over half the activity detected over a face comes from radiation emitted within 0.5 μ of that surface (1). Since the specific activity of the tracer decreases in a Gaussian manner below the diffusion interface, it has been shown (2) that in a specimen where diffusion has taken place the counting rate determined over the surface is directly proportional to the specific activity of the tracer on the surface. This characteristic of Ni^{63} β-radiation suggested the use of the following technique for measuring diffusion coefficients.

The solution to Fick's law corresponding to the diffusion of an infinitely thin layer of tracer into a semi-infinite medium, the diffusion coefficient D assumed constant, is

$$[1] \qquad C(x,t) = (C_0/\sqrt{\pi Dt})\, e^{-x^2/4\,Dt}$$

where C_0 is the quantity of tracer deposited on the surface, $C(x,t)$ is the concentration in a layer at distance x below the surface, and t is the diffusion time. For the limiting

[1]*Manuscript received June 9, 1959.*
Contribution from the Department of Metallurgical Engineering and the Radiochemistry Laboratory, Department of Chemistry, McGill University, Montreal, Que., with financial assistance from the Defence Research Board.

[2]*Present address: Fuel Development Branch, Atomic Energy of Canada Limited, Chalk River, Ontario.*

case where $x = 0$ the above equation becomes

$$C(0,t) = C_0/\sqrt{\pi Dt}. \quad [2]$$

If C_0 is evaluated, the diffusion coefficient can then be determined by measuring the change of surface activity with time. This method overcomes the necessity of knowing accurately the self-absorption coefficients for Ni^{63} β-radiation.

The purified tracer isotope employed contained two long-lived isotopes, Ni^{63} decaying by the emission of a 67-kev β-particle and Ni^{59} decaying by K-electron capture with the emission of a Co K_α X-ray (3). Even in a specimen diffused for a long time, the contribution of the more penetrating Ni^{59} radiation to the counting rate measured at the active surface was less than 0.5%. Therefore, it was assumed that the tracer contains only one active species, Ni^{63}. All samples were measured in a 2π internal source counter (1).

The rate of diffusion of Ni^{63} was studied in five metals, 99.92% purity nickel, 99.91% purity iron, 99.5% purity cobalt, and two iron–nickel alloys prepared from electrolytic iron and nickel containing 5.79 and 14.88% Ni. All these metals were melted and cast *in vacuo*. The three pure metals were obtained from National Research Corporation, Cambridge, Mass., and we are indebted to Mr. H. V. Kinsey, Mines Branch, Department of Mines and Technical Surveys, Ottawa, Ontario, for preparing the two alloys. Disks, 0.650 in. in diameter and 0.15 in. thick, were machined from these metals for diffusion specimens. After each specimen was annealed at 1400° C for 24 hours, it was carefully faced on a lathe followed by grinding on a series of polishing papers, finishing on 4/0 grade. Aliquots containing equal amounts of Ni^{63} tracer then were electrodeposited on the face of each specimen from an ammonia – ammonium sulphate electroplating solution. The active deposit was about one micron in thickness. Satisfactory deposits were obtained only when the specimens were given an anodic pretreatment in a 25% sulphuric acid solution to remove the oxide layer. Specimens where the tracer was non-uniformly plated or where the total quantity deposited differed by more than ±1.5% from the intended amount were discarded.

Ten specimens, a pair for each metal investigated, were placed in a recrystallized alumina crucible and diffusion-annealed simultaneously. Loss of tracer by evaporation was minimized by placing the faces of duplicate specimens in contact. Welding of the specimens was prevented by washing the active faces with a dilute suspension of fine alumina powder in alcohol. The furnace was maintained at the annealing temperature and specimens were introduced and removed at this temperature. Corrections were made when necessary to keep the error in the effective diffusion time within 0.4% by a method suggested by Ham, Parke, and Herzig (4). The furnace had a constant temperature zone 5 in. in length and was controlled to ±0.5° C. The specimen temperatures were measured to ±1.5° C with a certified Pt/(Pt – 10% Rh) thermocouple. An atmosphere of purified hydrogen was employed to prevent oxidation of the specimens.

At least four successive annealing treatments at the desired annealing temperature were employed to obtain each diffusion coefficient. These times were chosen to give equal intervals on a $1/\sqrt{t}$ axis. The surface activities were measured using a diaphragm with an opening 0.55 in. in diameter over the active surface to minimize edge effects arising from surface diffusion.

In addition to the slope of the plot of $C(0,t)$ versus $1/\sqrt{t}$, it is necessary to know C_0, in order to calculate the diffusion coefficient. The following procedure was selected as giving the most accurate value for C_0. Two nickel specimens, annealed at 1209° C, were sectioned on a lathe. Before each section was removed, the counting rate of the

exposed face was measured to determine $C(x,t)$ for various values of x. The area under the curve of $C(x,t)$ versus x was integrated to determine a value for C_0. Agreement between the duplicate specimens was within 1%. The diffusion coefficient calculated from equation [2] for the mean value of C_0 was in excellent agreement with that calculated from the sectioning data in the normal manner using equation [1]. This agreement indicates that good results should be obtainable with this surface activity technique. As an identical quantity of tracer was deposited on each specimen, it was sufficient to measure C_0 in this manner for one pair of specimens.

RESULTS AND DISCUSSION

The experimental curves for all specimens at a diffusion temperature of 1209° C are shown in Fig. 1, and are typical of those obtained at all temperatures. For surface activities below 4500 c.p.m., the curves are linear conforming to equation [2] and extrapolate to pass through the origin. However, for the diffusion of nickel into iron, cobalt, and the two iron–nickel alloys the plots are curved in the initial region, the curvature corresponding to a decrease in the diffusion coefficients with time. This curvature represents either a concentration dependence of the diffusion coefficient or a failure to satisfy the boundary conditions of equation [2] by using a tracer layer of finite thickness. This latter supposition was not substantiated, as a check experiment showed that a plot of $C(0,t)$ versus $1/\sqrt{t}$ is linear for nickel self-diffusion even for diffusion times short enough to promote much less diffusion than that obtained in those specimens where curvature was observed. Therefore, while the tracer layer was thin enough to satisfy the boundary

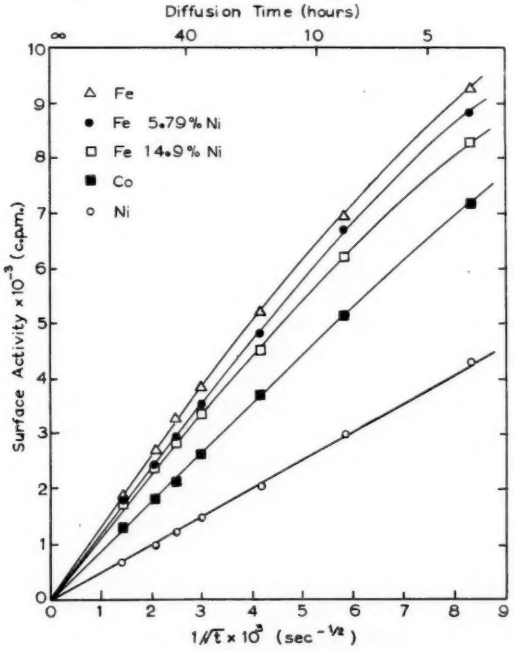

FIG. 1. Variation of surface activity with diffusion time for Ni^{63} diffusing into various metals and alloys at 1209° C.

conditions of equation [2], it appears to have been thick enough to cause a concentration effect.

A similar time dependence of the diffusion coefficient was observed by Martin, Johnson, and Asaro (5), who studied the rate of diffusion of Au^{198} into copper at low solute concentrations. At 1000° C the diffusion coefficient varied with annealing time, decreasing steadily for the first 30 hours and then assuming a constant value for longer times. No noticeable improvement was obtained when the thickness of the Au^{198} layer was decreased by a factor of 50. Therefore, this time dependence of the diffusion coefficient for short annealing times may not be entirely associated with a dependence of the diffusion coefficient on concentration, but it may be partially associated with an enhanced rate of diffusion caused by lattice strains introduced by the large concentration gradient existing at the start of an experiment.

The diffusion coefficients were calculated in each case from the linear portions of the plots. In this region, the concentration of tracer atoms has decreased sufficiently that each diffusing tracer atom is completely surrounded by host atoms so that there is a negligible concentration effect. Diffusion coefficients were obtained for each system at the following temperatures: 1152°, 1209°, 1271°, 1327°, and 1400° C.

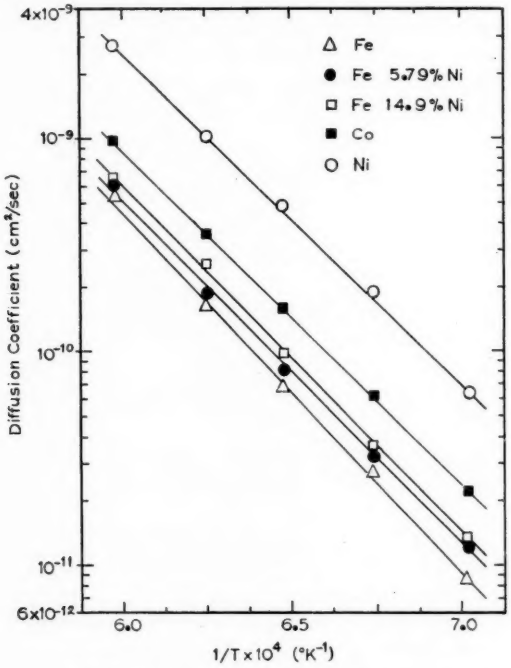

FIG. 2. Activation energy plots for Ni^{63} diffusion.

The activation energy, Q, and frequency factor, D_0, for volume diffusion are related by the Arrhenius equation:

$$D = D_0 e^{-Q/RT}.$$

To obtain values for Q and D_0, the experimental D values were plotted against $1/T$ as

in Fig. 2. A correction was made to each coefficient to compensate for lattice expansion. The data for each system were fitted by the method of least squares, on the assumption that the temperatures were correct, and gave the values for the activation energy and frequency factor shown in Table I.

TABLE I

Values of Q and D_0 for Ni^{63} diffusion

Solvent	D_0 (cm^2/sec)	Q (kcal/mole)
Ni	5.12	71.0±1.8
Co	1.25	72.1±1.4
Fe	6.92	77.6±2.0
Fe 5.8% Ni	2.11	73.5±2.0
Fe 14.88% Ni	5.00	75.6±1.2

A comparison of the present results for self-diffusion of nickel with those of a previous investigation (2) shows that the two studies are in close agreement as is shown in Table II where the values are tabulated. Both investigations gave higher values for the activation energy than that reported by Hoffman, Pikus, and Ward (6).

TABLE II

Summary of D_0 and Q values for nickel self-diffusion

Reference	D_0 (cm^2/sec)	Q (kcal/mole)	Method
(6)	1.27	66.8	Sectioning and surface activity
(2)	3.36	69.8	Sectioning
This work	5.12	71.0	Surface activity

The slightly higher activation energy found in this investigation compared with that previously reported by the same authors may be a result of slight errors introduced by evaporation of tracer from the active face, as a surface activity method is more sensitive to these losses than a sectioning method. However, any losses must have been negligible as no traces of activity were found on the supporting crucible even after the anneals at 1400° C. The good agreement between this and the previous investigation where a sectioning method was employed can be taken as evidence for the accuracy of the surface activity method employed in this investigation. No comparison of these results for nickel self-diffusion to those for other face-centered metals will be attempted here, as this topic was fully discussed when the previous results were reported (2).

Theoretical attempts to correlate the diffusion rate of various solutes in the same solvent at low solute concentration have been based on two different concepts. Lazarus (7) has deduced expressions for D_0 and Q for solute diffusion in a monovalent solvent taking into account the screened coulombic potential surrounding the impurity atom. These expressions suggest that elements to the left of the solvent atom in the periodic table should diffuse more slowly with higher values of D_0 and Q, while those to the right should diffuse more rapidly with lower values of D_0 and Q. This theory has had partial success in correlating the results for various solute atoms in silver and copper. Swalin (8) has attempted to correlate the results for the diffusion of various solutes in nickel solely on a size effect. He argues that the increased strain induced when solute

atoms larger than the solvent atoms pass through the saddle point should result in slower rates of diffusion and higher values for D_0 and Q, and the converse for smaller impurities.

The three transition elements iron, cobalt, and nickel are interesting from the theoretical viewpoint because of the similarity in their properties. All assume a face-centered cubic structure at high temperatures and have atomic radii which are nearly equal. Therefore, any differences in diffusion rates should be associated with the valency these atoms assume when dissolved in one another. Thus a comparison of the activation energies for self-diffusion and tracer-impurity diffusion is of interest. The appropriate values of Q and D_0, are tabulated in Table III for diffusion in the solvents iron, cobalt, nickel, and copper.

TABLE III

D_0 and Q values for self-diffusion and tracer-impurity diffusion in some transition elements

Solute	Solvent	D_0 (cm^2/sec)	Q (kcal/mole)	Reference
Fe		1.0	69.0	(9)
Co	Fe	1.2×10^5	104.0	(10)
Ni		6.92	77.6	This work
Fe		0.21	62.7	(11)
Co	Co	0.83	67.7	(11)
Ni		1.25	72.1	This work
Fe		8.4×10^{-3}	51.0	(12)
Co	Ni	1.46	68.3	(13)
Ni		5.12	71.0	This work
Fe		1.4	51.8	(14)
Co	Cu	1.93	54.1	(14)
Ni		2.70	56.5	(14)
Cu		0.32	46.8	(14)

Before discussing the significance of the data in Table III it should be pointed out that the data for the diffusion of iron into nickel and for cobalt into iron seem questionable. The value of D_0 found for diffusion of Fe^{59} into nickel is 8.4×10^{-3} cm^2/sec. This is suspect on the basis of Zener's (16) theory because it corresponds to a negative entropy of activation. The activation energy for the diffusion of Co^{60} into iron seems very high. It will be interesting to see if these values are confirmed in future investigations.

As observed by Mackliet (14) in the case of diffusion in the solvent copper, the tracer impurities iron, cobalt, and nickel all have larger activation energies than was obtained for copper self-diffusion. This is in general agreement with the Lazarus screening theory which predicts that elements which have a negative value of excess valency, Z, should have higher activation energies than for solvent self-diffusion. However, he found that $Q_{Ni} > Q_{Co} > Q_{Fe}$, which is contrary to the predictions expected if we assign to these elements their excess valence on a basis of their position in the periodic table. It is of interest to note that this trend also holds when the solvents are respectively iron, cobalt, and nickel with the single exception for diffusion of cobalt into iron. An explanation of this trend in activation energies for these transition elements will have to await clarification of the concept of valence in these metals.

Darken (17) has deduced expressions relating the interdiffusion coefficients, D_e, in a binary alloy at a given composition to the self-diffusion coefficients D_a^* and D_b^* of the

individual species in the same alloy. In the case of the iron–nickel system, which is thermodynamically ideal in the gamma region (18), these expressions reduce to

$$[3] \qquad D_c = N_{Fe}D_{Ni}^* + N_{Ni}D_{Fe}^*$$

where N_{Fe} and N_{Ni} are the atomic fractions of iron and nickel in the alloy. The variation of the interdiffusion coefficient, D_c, with composition in the iron–nickel system was investigated by Wells and Mehl (19) at 1300° C. Their data for D_c are plotted along with our data obtained for D_{Ni}^* in Fig. 3. A complete study of the variation of D_{Fe}^* with composition in the iron–nickel system was made by Neiman and Shinyaev (20) in the temperature range 1055 to 1148° C. Unfortunately their data are suspect at the nickel-rich end, because their D_0 values for diffusion in this range are low enough to correspond to negative entropies of activation. Therefore, in Fig. 3, we have only shown Gruzin's data for D_{Fe}^* in pure iron (9), and for D_{Fe}^* in two iron–nickel alloys containing 20% and 25% nickel (21).

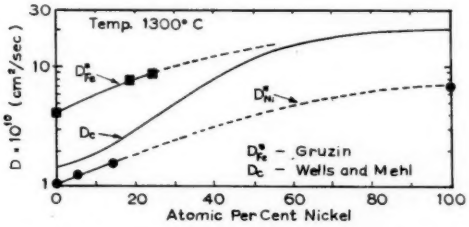

FIG. 3. Variation of the diffusion coefficients with composition in the iron–nickel system.

Considering that the data represent the results of four separate investigations, the correlation is remarkably good. While there is no evidence to justify the extrapolations shown, it is apparent that nickel atoms diffuse at about one-quarter the rate of iron atoms in the iron-rich portion of this system and probably throughout the entire system. This is in agreement with the observations of Seith and Kottman (22), who observed porosity in the iron-rich portion of an iron–nickel couple during a Kirkendall-effect experiment (23). While the data are not in sufficient agreement to test the validity of Darken's equations it is interesting to note that $D_c \rightarrow D_{Ni}^*$ as $N_{Fe} \rightarrow 1$ in agreement with equation [3].

Examination of the data in Table II indicates that there may be a trend towards lower activation energies for nickel self-diffusion in this system with increasing nickel content. There is a definite trend towards faster rates of nickel self-diffusion with increasing nickel content, which also suggests that the activation energy should decrease.

ACKNOWLEDGMENT

The authors wish to express their gratitude to the Defence Research Board for grants received.

REFERENCES

1. MACEWAN, J. R., MACEWAN, J. U., and YAFFE, L. Can. J. Chem. **37**, 649 (1959).
2. MACEWAN, J. R., MACEWAN, J. U., and YAFFE, L. Can. J. Chem. **37**, 1623 (1959).
3. BROSI, A. R., BORKOWSKI, C. L., CONN, E. E., and GREISS, J. C., JR. Phys. Rev. **81**, 391 (1951).
4. HAM, J. L., PARKE, R. M., and HERZIG, A. J. Trans. Am. Soc. Metals, **31**, 877 (1943).
5. MARTIN, A. B., JOHNSON, R. P., and ASARO, F. J. Appl. Phys. **25**, 369 (1954).
6. HOFFMAN, R. E., PIKUS, F. W., and WARD, R. A. Trans. A.I.M.E. **206**, 483 (1956).

7. LAZARUS, D. Impurities and imperfections. Impurities and imperfections in metallic diffusion. American Society for Metals, Cleveland, Ohio. 1955. Chap. 5.
8. SWALIN, R. A. Acta. Met. **5**, 443 (1957).
9. GRUZIN, P. L., KORNEV, N. Y., and KURDYUMOV, G. V. Reports Acad. Sci. Ukr.S.S.R. **80**, 49 (1951).
10. GRUZIN, P. L. Doklady Akad. Nauk S.S.S.R. **94**, 681 (1954).
11. MEAD, H. W. and BIRCHENALL, C. E. Trans. A.I.M.E. **203**, 994 (1955).
12. NEIMAN, M. B., CHINYAEV, A. YA., and DZANTIEV, B. G. Doklady Akad. Nauk S.S.S.R. **91**, 265 (1953).
13. RUDER, R. C. and BIRCHENALL, C. E. Trans. A.I.M.E. **191**, 142 (1951).
14. MACKLIET, C. A. Phys. Rev. **109**, 1964 (1958).
15. RAYNOR, C. L., THOMASSON, L., and ROUSE, L. S. Trans. Am. Soc. Metals, **30**, 313 (1942).
16. ZENER, C. J. Appl. Phys. **22**, 372 (1951).
17. DARKEN, L. S. Trans. A.I.M.E. **175**, 184 (1948).
18. KUBASCHEWSKI, O. and GOLDBECK, O. Trans. Faraday Soc. **45**, 948 (1949).
19. WELLS, C. and MEHL, R. F. Trans. A.I.M.E. **145**, 329 (1941).
20. NEIMAN, N. B. and SHINYAEV, A. YA. Doklady Akad. Nauk S.S.S.R. **102**, 969 (1955).
21. GRUZIN, P. L. and KUZNETSOV, E. V. Doklady Akad. Nauk S.S.S.R. **93**, 809 (1953).
22. SEITH, W. and KOTTMAN, A. Angew. Chem. **64**, 379 (1952).
23. SMIGELSKAS, A. D. and KIRKDENDALL, E. O. Trans. A.I.M.E. **171**, 130 (1947).

THE REACTION BETWEEN DIPHENYLAMINE AND NITRATES IN ULTRAVIOLET LIGHT[1,2]

B. B. Coldwell and S. R. McLean[3]

ABSTRACT

Under the activating influence of short-wave ultraviolet light, diphenylamine and nitrate ions in solution or on filter paper react to yield a yellow-colored product. Between pH 4 and 10 this consists mainly of 2-nitrodiphenylamine and 4-nitrodiphenylamine. Over this range of pH, the absorption maxima at 405 mμ did not shift; however, the intensity of absorption appeared to reach a minimum at or near neutrality and then increase rapidly as the solution was made more alkaline. The reaction rate was not affected by lowering the concentration of diphenylamine from 0.38% to 0.038%. A similar change in nitrate concentration decreased the rate 5.4 times. No evidence of nitroso compounds was found. Possible mechanisms are suggested.

INTRODUCTION

In a previous paper (1), it was noted that diphenylamine and nitrate ions reacted to form a yellow-colored product when irradiated with short-wave ultraviolet light. The reaction appeared specific and was made the basis of a spot test for inorganic nitrates. Subsequently, Hayward (2) found the reaction applicable to nitrate esters and used it for detecting these on paper chromatograms. We have confirmed Hayward's observation and, also, have found the reaction useful in identifying various kinds of explosives (3). The present work is concerned mainly with the identification of the products of the photochemical reaction.

EXPERIMENTAL AND RESULTS

(*A*) *Identification of Products Formed on Paper*

Sixty sheets of Whatman No. 1 filter paper (18×22 in.) were immersed for a few seconds in aqueous 1% sodium nitrate solution, air-dried, then immersed again in an ethanolic solution of diphenylamine (1% in 95% ethanol), air-dried, and exposed to short-wave ultraviolet radiation for 10 minutes on each side. The source and filters used have been described (1). The yellow-colored material was extracted from the paper with 95% ethanol in a modified Soxhlet assembly. The alcoholic extract was evaporated to dryness under vacuum on a constant temperature bath at 80° C. A total of 14.4 g, mostly unreacted diphenylamine, was recovered.

The material was dissolved in warm, redistilled petroleum ether (boiling range 30–50° C), and chromatographed on alumina columns (1×30 cm) which were prewashed with ethyl ether followed by petroleum ether. The columns were developed with petroleum ether. Two yellow bands separated, one (1P) weakly and the other (2P) very strongly absorbed by the alumina. Fraction 1P together with most of the unreacted diphenylamine was eluted from the columns with petroleum ether; the eluates were combined and evaporated to dryness under vacuum on a constant temperature bath at 35° C. Approximately 12.4 g were recovered. Repeated passes through the column eventually gave a fraction (44.8 mg) whose absorption maxima (see Table I) in the visual

[1]*Manuscript received June 5, 1959.*
Contribution from the Crime Detection Laboratories, Royal Canadian Mounted Police, Ottawa, Canada.
[2]*Published with the permission of the Commissioner, R.C.M.P., Ottawa.*
[3]*Present address: Canadian Titanium Pigments Ltd., Montreal, Quebec.*

TABLE I

Spectrophotometric properties of diphenylamine, nitro derivatives, and fractions isolated from the photochemical reaction between diphenylamine and nitrate

Substance	Position of maxima, mμ		Position of minima, mμ	
	Literature (4)	Observed*	Literature (4)	Observed*
Diphenylamine	285	283–285	249	248–249
2-Nitrodiphenylamine	422–423 257–259	415–425 257–259	323–327 238–239	319–324 237–239
Fraction 1P		415–420 256–260		324–328 236–239
Fraction 1S		418–422		
4-Nitrodiphenylamine	390 257	386–388 254–256	305–306	304–306
Fraction 2P		386–390 254–257		308–312 240–242
Fraction 3S		388–394 254–256		290–300 234–237
Fraction 2S		442–450 291–293 256–257 243–245 233–234		374–380 272–274 249–250 240–242
Fraction 4S (acidic solution)		575–580 237–239		465–475 226–228
Fraction 4S (basic solution)		575–580 239–241		450–470 228–229

*Spectra determined with a Spectracord using 1-cm silica and Corex cells and absolute ethanol as solvent.

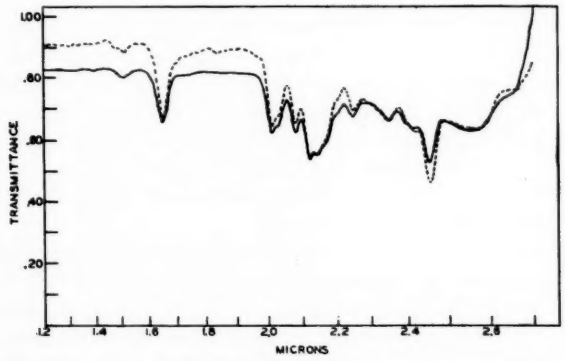

FIG. 1. Near infrared spectra of 2-nitrodiphenylamine (———) and fraction 1P (– – –) in carbon tetrachloride. Obtained with Spectracord using 1-cm silica cells.

and ultraviolet regions were in good agreement with those reported for 2-nitrodiphenylamine (4). The near- and far-infrared spectra of this fraction also were identical with those of 2-nitrodiphenylamine (see Figs. 1 and 2). From the absorptivity of 2-nitrodiphenylamine and the absorbance at 420–425 mμ, it was calculated that fraction 1P contained approximately 80% of 2-nitrodiphenylamine. The spectra, melting point[4] (35–50° C),

[4]*All melting points are uncorrected.*

and adsorbent characteristics of a 4 to 1 mixture of 2-nitrodiphenylamine and diphenylamine were identical with those of fraction 1P. It was concluded, therefore, that the yellow component of fraction 1P was 2-nitrodiphenylamine.

Fraction 2P was eluted from the adsorbent with acetone and evaporated to dryness under vacuum at 35° C. Approximately 0.24 g was recovered. This was rechromatographed on alumina using benzene – petroleum ether (1:1) as the developing solvent.

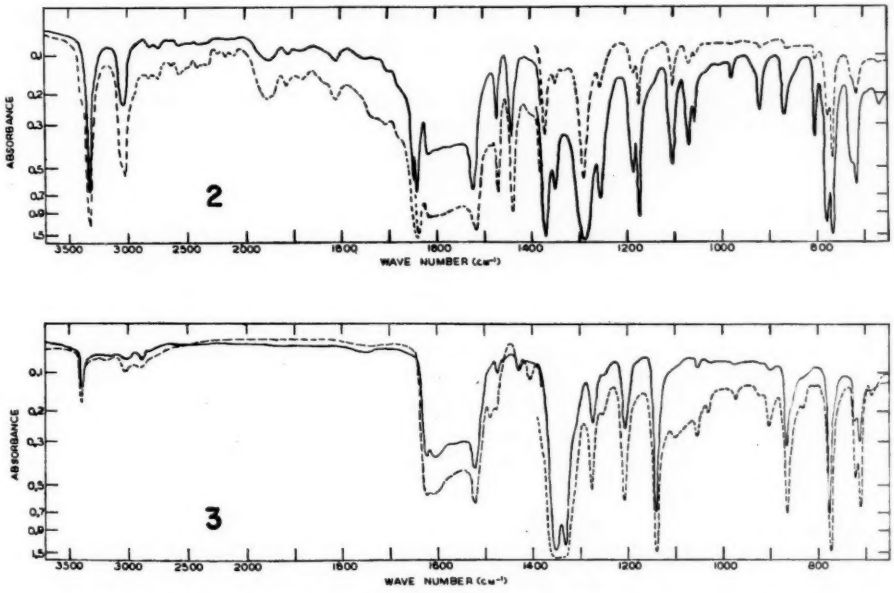

FIG. 2. Infrared spectra of 2-nitrodiphenylamine (———) and fraction 1P (– – –). Instrument: Perkin–Elmer Model 21, double beam, with sodium chloride optics. Solvent: carbon tetrachloride from 3600 to 1385 cm^{-1}, carbon disulphide from 1385 to 650 cm^{-1}.

FIG. 3. Infrared spectra of 4-nitrodiphenylamine (———) and fraction 2P (– – –). Conditions: as given in Fig. 2.

The colored eluate when concentrated gave 187.5 mg of yellow crystals. After recrystallizing twice from carbon tetrachloride the material melted at 133.5–134° C. A mixed melting point determination with a known[5] sample of 4-nitrodiphenylamine (m.p. 136–137° C) gave no depression. Absorption maxima in the ultraviolet and visible spectral regions were in agreement with those reported for 4-nitrodiphenylamine (see Table I). The infrared spectra of 2P and 4-nitrodiphenylamine were also identical (see Fig. 3). It was concluded that fraction 2P was 4-nitrodiphenylamine.

(B) Identification of Products Formed in Solution

A saturated solution of calcium nitrate tetrahydrate in 95% ethanol was made 1% with respect to diphenylamine. Ten 100-ml aliquots of this solution in a 1-l. beaker were exposed to short-wave ultraviolet radiation for 1 hour. The solutions were combined, taken to dryness, and chromatographed on alumina using petroleum ether to develop the chromatogram, as described above. Four bands gradually developed. The first band

[5]*Obtained from Dr. K. N. Trueblood, Department of Chemistry, University of California, Los Angeles, whose assistance is gratefully acknowledged.*

(1S), yellow in color, was eluted with petroleum ether. To elute the remaining bands off the column, ethyl ether was added to the petroleum ether, the proportions being increased gradually from 4:1 to 1:1. The second (2S) and third (3S) bands were orange and yellow, respectively. The fourth band (4S) was colored blue and remained at the top of the column. It was removed from the adsorbent with 95% ethanol.

Fraction 1S was concentrated and rechromatographed several times until finally crystals were obtained having an absorption maximum in the visible region characteristic of 2-nitrodiphenylamine (see Table I). Because of the difficulty in separating diphenylamine from 2-nitrodiphenylamine, additional purification of this fraction was not attempted.

Fraction 2S was concentrated and rechromatographed with 1:1 petroleum ether – ethyl ether. The absorption maxima exhibited in the ultraviolet and visible regions are given in Table I. There was insufficient material available to characterize this fraction further.

Fraction 3S was concentrated to a small volume and the orange-yellow crystals which separated were recrystallized twice from carbon tetrachloride (m.p. 132–132.5° C) and identified as 4-nitrodiphenylamine by a mixed melting point determination. The absorption maxima in the ultraviolet and visual regions (see Table I) and the infrared spectra of this material corresponded to those of 4-nitrodiphenylamine.

The wavelengths of maximum and minimum absorption of fraction 4S were almost identical in acidic and alkaline solutions (see Table I). The blue-colored material was insoluble in water. It appeared to be different from the blue quinoidal compound formed on the oxidation of diphenylamine with strong oxidizing agents (5). The latter on dilution with alcohol changed from a deep blue to a brownish yellow with the formation of a greenish brown precipitate. Similar changes were not observed with fraction 4S.

(C) Effect of pH on Reaction in Solution

Mixtures of diphenylamine and sodium nitrate, each 0.38% in aqueous ethanol (13 parts ethanol to 8 parts distilled water by volume), were adjusted to a known pH with hydrochloric acid or potassium hydroxide and exposed to short-wave ultraviolet radiation for 30 minutes without stirring. The pH, color, and visual spectra were then recorded. Some of the data are summarized in Table II and in Fig. 4.

TABLE II

Effect of pH on the ultraviolet-light-induced reaction between diphenylamine and nitrate. (Diphenylamine, 0.38%; sodium nitrate, 0.38%; solvent, ethanol 13 parts and water 8 parts; exposure, 30 minutes)

pH				
Initial	After exposure	Position of maxima,* mμ	Absorbance	Color of solution
3.0	3.0	398–401	0.240	Dark blue
		525–550	0.500	
4.0	5.5	402–408	0.595	Red-brown
		525–550	0.220	
5.0	7.2	405	0.490	Dark yellow
6.0	7.3	405	0.480	Yellow
8.0	8.0	405	0.565	Yellow
10.0	9.0	405	0.780	Yellow

*Determined with Spectracord using 1-cm Corex cells.

At pH 3, the main end product of the reaction appears to be the blue-colored substance found in fraction 4S. This is quite evident from curve 1, Fig. 4. As the pH rises,

the blue substance disappears and the absorption at 405 mμ becomes more pronounced. There is evidence that the absorption at 405 mμ reaches a maximum at pH 4, decreases to a minimum at or near neutrality, and then rises sharply as the solution is made more alkaline. This trend is evident from the data in Table II and was observed in another series of experiments where the concentration of diphenylamine and nitrate was 0.038% for each. The production of 2-nitrodiphenylamine and 4-nitrodiphenylamine would appear to be responsible for the absorption at 405 mμ. A 1 to 1 mixture of these two compounds in 13 to 8 ethanol–water exhibited an absorption maximum at 403–404 mμ, which shifted to 406 mμ when the mixture contained twice as much 2-nitrodiphenylamine as 4-nitrodiphenylamine.

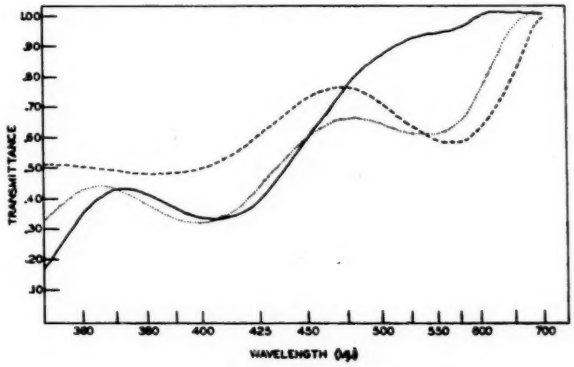

FIG. 4. Effect of pH on the visible spectra of diphenylamine–nitrate solutions irradiated with ultraviolet light. Solvent: 13 parts ethanol to 8 parts distilled water by volume. Concentration: diphenylamine and sodium nitrate each 0.38% (w/v). Exposure time: 30 minutes. Instrument: Spectracord with 1-cm Corex cells. Curve 1: – – –, pH 2.5. Curve 2: . . . , pH 3.0. Curve 3: ———, pH 5.0.

The magnitude of the absorbance at 405 mμ was not affected by lowering the diphenylamine concentration from 0.38% to 0.038% but was decreased 5.4 times by the same change in the nitrate concentration. At these concentrations a linear relationship was observed between absorbance and time of exposure, over a period of 2.5 hours.

(D) Nitrite and Diphenylamine

A solution of sodium nitrite (0.038%) and diphenylamine (0.038%) in aqueous ethanol (13 parts ethanol to 8 parts water by volume) was colorless between pH 11.0 and 6.2 and exhibited no absorption between 360 and 700 mμ. When irradiated for 1 hour the mixture turned a light yellow color and showed weak absorption in the region of 435 to 460 mμ (also given by irradiated diphenylamine solution) and strong absorption below 360 mμ (not shown by irradiated diphenylamine solution).

Increasing the acidity, without exposure to ultraviolet light, caused the solution to turn yellow. At pH 5.1 relatively sharp absorption maxima were observed at 388, 372, and 358 mμ. As the pH was lowered still further, the absorption below 360 mμ became stronger and overshadowed the absorptions at higher wavelengths which appeared as a shoulder between 370 and 390 mμ. Neutralization of the acidic solution did not change its visible spectrum. The spectrum at pH 2 was similar to that at pH 10 and resembled that of N-nitrosodiphenylamine. Similar results were obtained with more concentrated solutions.

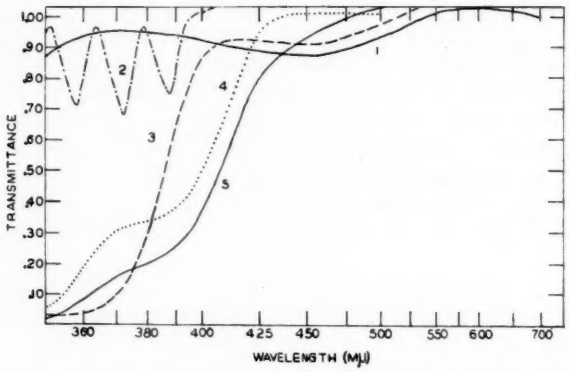

FIG. 5. The effect of ultraviolet radiation and pH on the visible spectra of diphenylamine, diphenylamine–nitrite solutions, and N-nitrosodiphenylamine. Solvent: ethanol 13 parts and distilled water 8 parts by volume. Instrument: Spectracord with 1-cm Corex cells. Curve 1: 0.038% diphenylamine exposed 1 hour to short-wave ultraviolet light. Curve 2: a solution of diphenylamine and sodium nitrite, each 0.038%, pH 5.1. Curve 3: same as curve 2, pH 7.5, irradiated 1 hour. Curve 4: same as curve 2, pH 2 and pH 10. Curve 5: N-nitrosodiphenylamine (0.1%).

The spectra of acidic (pH 5.5) diphenylamine–nitrite solutions could not be duplicated by exposing the corresponding original mixtures (pH 7.5) to short-wave ultraviolet light for varying periods of time. The spectrum of irradiated N-nitrosodiphenylamine (0.1% in 13 to 8 ethanol–water solution) was unchanged from the original. These results are illustrated in Fig. 5.

DISCUSSION

It is evident that between pH 4 and 10 the yellow end products formed during short-wave ultraviolet radiation of diphenylamine–nitrate mixtures, either in solution or on paper, consist largely of 2-nitrodiphenylamine and 4-nitrodiphenylamine. While the actual mechanism whereby these derivatives are formed remains uncertain, two pathways appear possible, (*a*) direct N-nitrosation of diphenylamine followed by rearrangement to the C-nitroso compound and subsequent oxidation (6), and (*b*) direct nitration of the phenyl rings (7).

Nitrate ion is reduced to nitrite ion by ultraviolet light, particularly at wavelengths below 2650 Å and around 3000 Å (8, 9). The reduction proceeds more rapidly in alkaline than in neutral or acidic solutions (10). It is claimed also that solid nitrate salts form nitrite near the surface when irradiated at 2500 Å (11, 12). Under our experimental conditions, the concentration of nitrite, determined with a modified Griess reagent (13), in aqueous alcoholic sodium nitrate solutions increased linearly with time of exposure to short-wave ultraviolet radiation. A 10-fold increase in nitrate concentration increased the rate of nitrite production by a factor of 3.

Further, the concentration of nitrite increased with rising pH, the amount present at pH 10 being more than twice that present at pH 3. These results agree with those of Villars (7) and Warburg (8). Thus, with increasing alkalinity there is an increase in the amount of yellow product and nitrite. Both of these increase linearly with time of exposure and both are affected in a similar manner by a change in concentration of nitrate. Warburg (8) pictures the reduction of nitrate by light as a unimolecular reaction in which the nitrate ion becomes activated by absorption of a quantum of light energy (90 to 100 kcal) and subsequently dissociates into nitrite and oxygen:

$$NO_3^- + h\nu \rightarrow (NO_3^-)^1 \rightarrow NO_2^- + O.$$

These facts suggest that the nitro derivatives might have resulted from very rapid oxidation of the C-nitroso derivatives of diphenylamine. In the presence of oxygen, oxidation of the labile nitroso compounds would be expected to take place rapidly, particularly in alkaline solution. This may explain why no evidence of nitroso derivatives was found on chromatographing the yellow reaction products or on spectral examination of irradiated diphenylamine–nitrate solutions. Certainly, the differences in the reactions taking place in irradiated diphenylamine–nitrate solutions, irradiated diphenylamine–nitrite solutions, and acidified solutions of the latter, as evidenced from a study of their spectra, suggest atomic oxygen plays a key role.[6]

On the other hand, the absence of nitroso compounds in the reaction products enhances the possibility of derivative formation through direct nitration of the ring. The activated nitrate radical might react with diphenylamine in this manner.

ACKNOWLEDGMENT

The authors are indebted to Mr. R. Ironside, Division of Applied Chemistry, National Research Council, Ottawa, for recording the infrared spectra.

REFERENCES

1. COLDWELL, B. B. and McLEAN, S. R. Can. J. Chem. **36**, 652 (1958).
2. HAYWARD, L. D. Private communication.
3. COLDWELL, B. B. Analyst. In press.
4. SCHROEDER, W. A., WILCOX, P. E., TRUEBLOOD, K. N., and DEKKER, A. O. Anal. Chem. **23**, 1740 (1951).
5. KEHRMANN, F. and MICEWITZ, ST. Ber. **45**, 2641 (1912).
6. DAVIS, T. L. and ASHDOWN, A. A. Ind. Eng. Chem. **17**, 674 (1925).
7. SCHROEDER, W. A., MALMBERG, E. W., FONG, L. L., TRUEBLOOD, K. N., LANDERL, J. D., and HOERGER, E. Ind. Eng. Chem. **41**, 2818 (1949).
8. GILLAM, A. E. and MORTON, R. A. J. Soc. Chem. Ind. (London), **46**, 415 (1927).
9. VILLARS, D. S. J. Am. Chem. Soc. **49**, 326 (1927).
10. WARBURG, E. Z. Elektrochem. **25**, 334 (1919).
11. NARAYANSWAMY, L. K. Trans. Faraday Soc. **31**, 1411 (1935).
12. KRISHNAN, K. S. and GUHA, A. C. Proc. Indian Acad. Sci. A, **1**, 242 (1934).
13. SNELL, F. D. and SNELL, C. T. Colorimetric methods of analysis. Vol. 2. 3rd ed. D. Van Nostrand Co., Inc., New York. 1949. p. 804.

[6]*The Referee has suggested that under these conditions it appears likely atomic oxygen would react first with the solvent, by electron capture or otherwise, to form intermediate products which could function as the oxidizing agent. This is certainly a possibility.*

A STUDY ON THE STRUCTURE OF THE CYCLOPENTADIENYL ANION WITH C^{14} AS TRACER[1]

R. TKACHUK[2] AND C. C. LEE

ABSTRACT

Starting with formaldehyde-C^{14}, 1,2-dibromocyclopentane-4-C^{14} (XI) was synthesized in eight steps. Conversion of XI to cyclopentadiene was accomplished in three different ways, namely: the dehydrobromination of XI with quinoline at 195–198° C, the preparation of 1,2-bis-(trimethylammonium)-cyclopentane-4-C^{14} hydroxide from XI followed by thermal decomposition, and the conversion of XI to 3,5-dibromocyclopentene followed by reaction of the latter with magnesium in dry ether. Degradations of the samples of cyclopentadiene obtained by these three synthetic routes showed a completely randomized distribution of the C^{14} activity, with 20% of the total activity on each of the five carbon positions. These results led to the conclusion that these preparations of cyclopentadiene very likely involved ionization to the cyclopentadienyl anion. The randomized distribution of C^{14} in the resulting products thus furnishes a strong indication that all five carbon positions in the cyclopentadienyl anion are equivalent.

INTRODUCTION

The acidity of cyclopentadiene was first recognized in 1900 by Thiele (1), and its potassium salt was prepared in 1901 (2). This salt is stable, though very reactive. The reason for the stability of salts containing the cyclopentadienyl anion has been given as early as 1928, by Goss and Ingold (3), and is that this ion has six (π) electrons, distributed over the entire five-membered ring, thus constituting a stable aromatic system similar to benzene. The resonance energy of this ion has been calculated to be about 42 kcal per mole (4).

Salts of cyclopentadiene with organic cations are also known. Pyridinium cyclopentadienylide has been described by Lloyd and Sneezum (5) and by Kosower and Ramsey (6). Triphenylphosphonium cyclopentadienylide has also been reported (7).

From theoretical considerations and physical chemical measurements, a number of workers (4, 8–12) have predicted that the negative charge on the cyclopentadienyl anion will not be localized on a particular carbon atom but will be distributed over the

(I)

ion as a whole, as depicted by I. In the present study, attempts were made to obtain, by the tracer technique, some direct experimental evidence in support of these theoretical predictions.

If it were possible to synthesize cyclopentadiene-5-C^{14} (II), conversion of this compound to its potassium salt followed by regeneration should yield a cyclopentadiene in which the C^{14} distribution could provide definitive evidence for the structure of the cyclopentadienyl anion. Should the anion have the symmetrical electronic structure I, on

[1]*Manuscript received June 8, 1959.*
Contribution from the Department of Chemistry, University of Saskatchewan, Saskatoon, Sask.
[2]*Canadian Industries Limited Fellow, 1956–1958.*

regeneration of cyclopentadiene from the anion, the proton would have an equal probability of attaching itself to any one of the five equivalent carbons, resulting in the formation of a mixture of equal amounts of cyclopentadiene with the C^{14} label on the 1-, 2-, 3-, 4-, or 5-position.

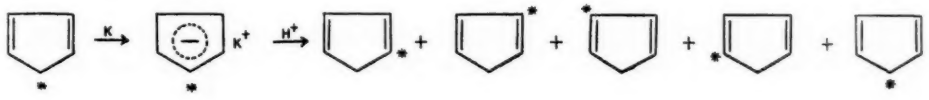

(II) (I)

Effectively, on degradation, one-fifth of the original C^{14} activity in II would be located on each carbon position of the sample of regenerated cyclopentadiene.

RESULTS AND DISCUSSION

As a suitable precursor for the attempted syntheses of cyclopentadiene-5-C^{14} (II), *trans*-1,2-dibromocyclopentane-4-C^{14} (XI) was chosen because it can give rise to cyclopentadiene by a number of different routes. The synthesis of XI was accomplished according to the following sequence of transformations.

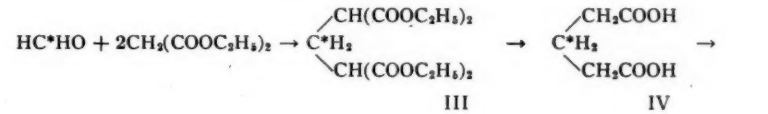

III IV

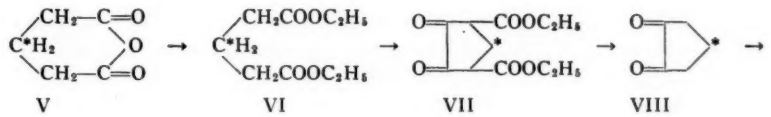

V VI VII VIII

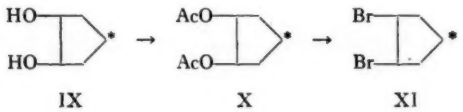

IX X XI

Tetraethyl propane-1,1,3,3-tetracarboxylate-2-C^{14} (III) was prepared by the condensation of formaldehyde-C^{14} and diethyl malonate. It was hydrolyzed to give glutaric acid-3-C^{14} (IV), which was, in turn, converted to glutaric anhydride-3-C^{14} (V) by treatment with acetic anhydride. Esterification of V gave diethyl glutarate-3-C^{14} (VI), which, on a Dieckmann condensation with diethyl oxalate, yielded 3,5-dicarboethoxy-1,2-cyclopentanedione-4-C^{14} (VII). Hydrolysis of VII afforded 1,2-cyclopentanedione-4-C^{14} (VIII). Reduction of VIII with sodium borohydride in water gave *trans*-1,2-cyclopentanediol-4-C^{14} (IX), which in turn was acetylated with acetic anhydride in pyridine to give *trans*-1,2-diacetoxycyclopentane-4-C^{14} (X). Treatment of X with hydrogen bromide in anhydrous acetic acid yielded *trans*-1,2-dibromocyclopentane-4-C^{14} (XI). The over-all yield of XI from formaldehyde-C^{14} was 11.4%.

To ascertain that *trans*-1,2-dibromocyclopentane-4-C^{14} (XI) was labeled as designated, it was degraded by the following scheme.

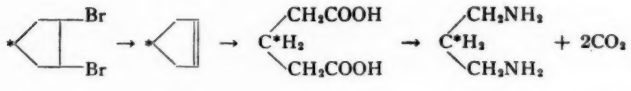

XI XII XIII XIV XV

The debromination of XI with zinc dust in ethanol yielded cyclopentene-4-C^{14} (XII). Ozonolysis of XII gave glutaric acid (XIII), which was degraded by the Schmidt reaction to give trimethylene-1,3-diamine (XIV) and carbon dioxide (XV). Radioactivity assays were carried out on the glutaric acid (XIII), on the diamine (XIV) as its dihydrogen bromide, and on the carbon dioxide (XV) precipitated as barium carbonate. The results, given in Table I, indicated that XIV contained all and XV contained none of the activity originally present in XI, showing that the label was not in positions 1 and 2. Thus, the designation that XI was labeled only in position 4 was likely correct.

TABLE I

C^{14} activities in products from degradation of 1,2-dibromocyclopentane-4-C^{14}

Compound analyzed	C^{14} activity[a] (mμc/mmole)
Glutaric acid (XIII)	415
Trimethylene-1,3-diamine dihydrogen bromide from XIV	421
Barium carbonate from XV	0.18

[a]C^{14} activity in millimicrocuries per millimole of sample was assayed as CO_2 gas with a vibrating reed electrometer supplied by Nuclear-Chicago Corporation.

The synthesis of cyclopentadiene from XI was accomplished by three different routes. The first synthesis was effected by the heating of XI with quinoline at 195–198° C to give cyclopentadiene-*x*-C^{14} (XVI*a*). The procedure was similar to one reported in 1904 for the preparation of 1,3-cyclohexadiene from 1,2-dibromocyclohexane (13). The second synthesis involved the thermal decomposition of 1,2-bis-(trimethylammonium)-cyclopentane-4-C^{14} hydroxide (XVIII) according to the following sequence of conversions.

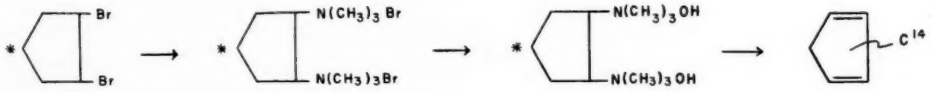

(XI) (XVII) (XVIII) (XVIb)

Treatment of XI with trimethylamine in acetone gave 1,2-bis-(trimethylammonium)-cyclopentane-4-C^{14} bromide (XVII). In turn, XVII was converted to XVIII with silver oxide in water. The decomposition of XVIII at 150° C afforded another sample of cyclopentadiene-*x*-C^{14} (XVI*b*). The third synthesis was carried out according to procedures reported fairly recently in the literature. It involved first the conversion of XI to cyclopentene-4-C^{14} (XII). Treatment of XII with N-bromosuccinimide and benzoyl peroxide in carbon tetrachloride gave 3,5-dibromocyclopentene (XIX)(14). Reaction of XIX with magnesium in dry ether (15) yielded a third sample of cyclopentadiene-*x*-C^{14} (XVI*c*).

The samples of cyclopentadiene-*x*-C^{14} obtained from the various syntheses were degraded by the following series of reactions.

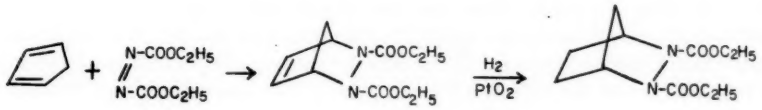

(XX) (XXI)

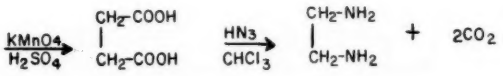

(XXII) (XXIII) (XXIV)

A Diels–Alder type of reaction between cyclopentadiene-*x*-C^{14} and diethyl azodicarboxylate gave the adduct, the diethyl ester of 2,3-dihydrazabicyclo (2.2.1)-5-heptene-2,3-dicarboxylic acid-*x*-C^{14} (XX). Hydrogenation of XX gave the diethyl ester of 2,3-dihydrazabicyclo (2.2.1) heptane-2,3-dicarboxylic acid-*x*-C^{14} (XXI). To yield succinic acid (XXII), XXI was oxidized with potassium permanganate. A Schmidt reaction with XXII resulted in the formation of ethylene-1,2-diamine (XXIII) and carbon dioxide (XXIV); XXIII was isolated as the dihydrogen bromide and XXIV as barium carbonate. C^{14} assays were carried out on XXI, XXII, the dihydrogen bromide from XXIII, and the barium carbonate from XXIV; XXI contained the total activity originally present in the cyclopentadiene-*x*-C^{14}. The difference in activities between XXI succinic acid (XXII) represented the activity in the 5-position (the methylene position) of cyclopentadiene. The activity in the 1- and 4-positions of cyclopentadiene was represented by the C^{14} in the carbon dioxide (XXIV) as well as by the difference between the activities of succinic acid (XXII) and ethylene-1,2-diamine (XXIII). Finally, the activity in the 2- and 3-positions of cyclopentadiene was given by the C^{14} in XXIII. The results of the C^{14} measurements are summarized in Table II.

TABLE II

C^{14} activities in products of degradation of cyclopentadiene-*x*-C^{14}

Source of cyclopentadiene	Compound analyzed	C^{14} activity (mμc/mmole)	% activity (XXI = 100)	% activity calc. for randomized distribution
Synthesis No. 1[a]	Hydrogenated Diels–Alder adduct (XXI)	26.73	100	100
	Succinic acid (XXII)	21.76	81.3	80
	Ethylene-1,2-diamine dihydrogen bromide from XXIII	10.78	40.3	40
	Barium carbonate from XXIV	10.92	40.9	40
Synthesis No. 2[b]	Hydrogenated Diels–Alder adduct (XXI)	43.56	100	100
	Succinic acid (XXII)	35.00	80.2	80
	Ethylene-1,2-diamine dihydrogen bromide from XXIII	17.44	40.1	40
	Barium carbonate from XXIV	17.64	40.5	40
Synthesis No. 3[c]	Hydrogenated Diels–Alder adduct (XXI)	2.09; 5.10[d]	100; 100[d]	100
	Succinic acid (XXV)	1.65; 3.97[d]	79; 78[d]	80
	Barium carbonate from XXIV	0.96	46	40

[a] Dehydrobromination of 1,2-dibromocyclopentane-4-C^{14} with quinoline.
[b] Thermal decomposition of 1,2-bis-(trimethylammonium)-cyclopentane-4-C^{14} hydroxide.
[c] Reaction of 3,5-dibromocyclopentene with magnesium in dry ether.
[d] Duplicate run.

The data in Table II clearly show that the samples of cyclopentadiene-*x*-C^{14} (XVI*a*, XVI*b*, XVI*c*) obtained from *trans*-1,2-dibromocyclopentadiene-4-C^{14} (XI) by the three synthetic routes were not the hoped for cyclopentadiene-5-C^{14}. Instead, they were samples of cyclopentadiene with the C^{14} activity completely randomized over all the five carbon positions. Such a distribution of C^{14} activity may be explained on the assumption that the cyclopentadienyl anion with symmetrical structure I is involved in these preparations. In the dehydrobromination of XI with quinoline (synthesis No. 1), the cyclopentadiene formed may immediately undergo reversible ionization-regeneration with quinoline acting as proton acceptor.

Considering the thermal decomposition of 1,2-bis-(trimethylammonium)-cyclopentane-4-C^{14} hydroxide (XVIII) (synthesis No. 2), first of all, the designation of the C^{14} location in XVIII is most probably correct since the conversion of XI to XVIII involved an S_N2 type of direct displacement and a double decomposition reaction both of which are not likely to cause isotope position rearrangements. Moreover, XVIII was prepared in a manner analogous to the synthesis of *n*-propyl-3-C^{14}-trimethylammonium hydroxide, which has been found to undergo successful thermal decomposition to propene-1-C^{14} (16). The randomized C^{14} distribution in the cyclopentadiene from synthesis No. 2 may, therefore, be again explained on the basis that the cyclopentadiene formed immediately undergoes reversible ionization-regeneration.

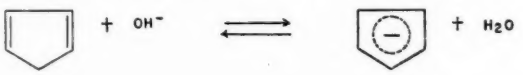

The interpretation of the results from synthesis No. 3 is more difficult. In the conversion of cyclopentene-4-C^{14} (XII) to 3,5-dibromocyclopentene (XIX) by treatment with N-bromosuccinimide and benzoyl peroxide, the possibility of allylic shifts cannot be excluded. Thus, the location of the C^{14} labels in XIX cannot be definitely designated. Furthermore, the mechanism for the transformation of XIX to cyclopentadiene in the presence of magnesium and dry ether is not well understood. Therefore, it is uncertain at what stage of the synthesis randomization of the C^{14} activity occurs. If one were to assume that there is no isotope position rearrangement in the conversions of XII to XIX and XIX to cyclopentadiene, then the randomized C^{14} distribution in the cyclopentadiene obtained from synthesis No. 3 might be explained in the same manner as in syntheses 1 and 2, namely, the cyclopentadiene formed immediately undergoes a reversible ionization-regeneration. Under the conditions employed in this synthesis, a Grignard reagent type of species may be present and serve as a base in promoting the ionization of the cyclopentadiene to its anion.

From the above considerations, it is clear that although the original intention of securing evidence on the structure of the cyclopentadienyl anion via cyclopentadiene-5-C^{14} was not successfully realized, the C^{14} distribution found in the samples of cyclopentadiene synthesized in these experiments does have a bearing on the problem under study. The completely randomized distribution of the C^{14} labels in the synthetic cyclopentadiene, at least in the samples from syntheses No. 1 and 2, likely resulted from an

involvement of the cyclopentadienyl anion during the synthetic processes. Thus, this randomization of the C^{14} activity in the cyclopentadiene furnishes a strong, though indirect, indication that all five carbon positions in the cyclopentadienyl anion are equivalent, as depicted in structure I.

EXPERIMENTAL

The condensation of formaldehyde-C^{14} with diethyl malonate to give tetraethyl propane-1,1,3,3-tetracarboxylate-2-C^{14} (III), the hydrolysis of III to glutaric acid-3-C^{14} (IV), and the conversion of IV to glutaric anhydride-3-C^{14} (V) were carried out according to procedures given in Cason and Rapaport (17). Starting with 16 g (0.53 mole) of formaldehyde-C^{14} (0.5 mc) as 35% formalin and 160 g (1.0 mole) of diethyl malonate, the yield of III, b.p. 163–166° C at 1.4 mm (lit. (17), b.p. 168–171° C at 4 mm), was 138.5 g (83%). Hydrolysis of the 138.5 g of III in 138 ml of concentrated hydrochloric acid gave a crude glutaric acid (IV), which was heated at 100° C for 1 hour with 85 ml of acetic anhydride to give glutaric anhydride-3-C^{14} (V). After vacuum distillation and crystallization from benzene and dry ether, the yield of product, m.p. 55–56° C (lit. (17), m.p. 55–56° C), was 24.8 g (52% based on the tetraethyl ester III).

Diethyl Glutarate-3-C^{14} (VI)

The conversion of glutaric anhydride-3-C^{14} to the diethyl ester was effected by treatment with absolute ethanol in the presence of toluene and concentrated sulphuric acid. The method used was similar to that given by Micovic for the preparation of diethyl adipate (18). From 24.8 g of V, 40 g (99% of theoretical) of diethyl glutarate-3-C^{14}, b.p. 84–85° C at 1.4 mm (lit. (19*a*), b.p. 103–104° C at 7 mm), was obtained.

3,5-Dicarboethoxy-1,2-cyclopentanedione-4-C^{14} (VII)

The Dieckmann condensation between diethyl glutarate-3-C^{14} (40.0 g, 0.21 mole) and diethyl oxalate (31.5 g, 0.22 mole) was carried out according to a procedure given by Hauser and Hudson (20). The product (VII), crystallized twice from ethanol and water, melted at 116–117° C (lit. (20), m.p. 115° C). The yield was 41.4 g (81%).

1,2-Cyclopentanedione-4-C^{14} (VIII)

Under an atmosphere of carbon dioxide, a mixture of 41.3 g (0.17 mole) of 3,5-dicarboethoxy-1,2-cyclopentanedione-4-C^{14} and 160 g of 20% sulphuric acid was refluxed gently in a wax bath for 2.5 hours. The reaction mixture was cooled, saturated with ammonium sulphate, and then continuously extracted with ether for 10 hours. A carbon dioxide atmosphere was also maintained throughout the extraction period. After removal of the ether from the extract, the residue was distilled under reduced pressure to give 12.7 g (76%) of product, b.p. 67–69° C at 1.4 mm; m.p. 54–55° C (lit. (21), m.p. 56° C).

Air rapidly decomposes this diketone, especially at room temperature. However, when kept under nitrogen or carbon dioxide at approximately −5° C, it is stable for at least two years.

trans-1,2-Cyclopentanediol-4-C^{14} (IX)

To 4.0 g (0.041 mole) of 1,2-cyclopentanedione-4-C^{14} in 50 ml water, 2.31 g (0.61 mole) of sodium borohydride was slowly added with cooling and shaking. The reaction which took place was quite vigorous, and the mixture turned yellowish during the reduction. After standing at room temperature for 3 hours, the solution was heated to boiling to destroy any excess sodium borohydride. The resulting solution, after cooling, was extracted continuously with ether for 72 hours. On removal of the ether from the extract and vacuum distillation of the residue, 2.3 g (65%) of product was obtained with a b.p.

of 80–82° C at 1.2 mm (lit. (22), b.p. 93° C at 2 mm). The di-*p*-nitrobenzoate derivative melted alone and on admixture with the same derivative from authentic *trans*-1,2-cyclopentanediol at 141–142° C (lit. (22), di-*p*-nitrobenzoate derivative, m.p. 143° C). It is reasonable that only the *trans*-isomer was isolated since the *cis*-isomer is known to form a stable complex with boric acid (23).

trans-1,2-Diacetoxycyclopentane-4-C^{14} (X)

The *trans*-1,2-cyclopentanediol-4-C^{14} was acetylated by treating 2.3 g (0.023 mole) of the diol with a mixture of 20 ml of acetic anhydride and 40 ml of pyridine at 100° C for 4 hours. After cooling, the reaction mixture was neutralized with 10% hydrochloric acid and then extracted three times with 35-ml portions of ether. The extract was dried over potassium carbonate, the ether removed, and the residue vacuum-distilled to give 2.7 g (65%) of product, b.p. 61–65° C at 1.4 mm (lit. (24), b.p. 85.5–86.5° C at 3.5 mm). Analysis: Calc. for $C_9H_{14}O_4$: C, 58.05%; H, 7.58%; acetyl, 46.3%. Found: C, 57.88%; H, 7.54%; acetyl, 46.4%.

In another preparation of the diacetate (X), 0.81 g of the diol (IX), 4.0 g of acetic anhydride, and 12 ml of pyridine were refluxed for 1.5 hours, the reaction mixture being protected from atmospheric moisture by means of a drying tube containing Drierite. The excess acetic anhydride and pyridine were removed under reduced pressure with a water aspirator pump and the residue vacuum-distilled, yielding 1.4 g (95%) of product boiling at 60° C at 1.2 mm.

trans-1,2-Dibromocyclopentane-4-C^{14} (XI)

This preparation was carried out in a manner similar to that used in the synthesis of 2,3-dibromobutane from 2,3-diacetoxybutane (25).

Into a 12-mm (O.D.) Pyrex glass tube with wall thickness of 1 mm was placed 1.38 g of *trans*-1,2-diacetoxycyclopentane-4-C^{14} and 7.0 ml of saturated hydrogen bromide in acetic acid, the latter prepared by saturating pure acetic acid with dry hydrogen bromide gas at 35° C. The glass tube was sealed and then heated for 2 hours in boiling water. During this period, the reaction mixture darkened appreciably. After the mixture had cooled, the tube was opened and the solution poured onto crushed ice, neutralized with sodium bicarbonate solution, and extracted three times with 40-ml portions of low boiling petroleum ether. The extract was dried with anhydrous sodium carbonate, the solvent removed, and the residue vacuum-distilled, yielding 1.33 g (78%) of product, b.p. 44–46° C at 1.4 mm (lit. (26), b.p. 76.5–77.5° C at 18.5 mm). Analysis: Calc. for $C_5H_8Br_2$: Br, 70.2%. Found: Br, 70.8%.

Degradation of trans-1,2-Dibromocyclopentane-4-C^{14} (XI)

Cyclopentene-4-C^{14} (XII)

Cyclopentene-4-C^{14} (XII) was prepared from XI by a method similar to that used in the preparation of 2-pentene from 2,3-dibromopentane (27). To 2.0 g of granular, 20-mesh zinc metal in 3 ml of ethanol at 50° C, 1.3 g (0.0057 mole) of *trans*-1,2-dibromocyclopentane-4-C^{14} was added dropwise over a period of 10 minutes. A vigorous reaction took place, the cyclopentene being distilled over as it was formed into a receiver cooled in a dry ice – acetone bath. To insure complete recovery of the cyclopentene, the reaction mixture was heated just to the boiling point of ethanol. The weight of the product was 0.35 g (84%).

Ozonolysis of Cyclopentene-4-C^{14}

Ozonolysis of cyclopentene-4-C^{14} (XII) was effected in the same manner as reported

for the ozonolysis of cyclohexene (28). Starting with a solution of XII from 1.3 g of XI in 20 ml of absolute methanol, ozonization followed by decomposition of the ozonide in formic acid and hydrogen peroxide gave 0.62 g (87% based on the dibromide XI) of glutaric acid-3-C^{14} (XIII), m.p. 97° C (lit. (19*a*), m.p. 97–98° C).

The Schmidt Reaction on Glutaric Acid-3-C^{14}

This was carried out according to procedures already described in the literature (29, 30). From 198 mg (1.5 mmoles) of XIII, the yield of barium carbonate from the carbon dioxide absorbed in carbonate-free sodium hydroxide solution was 300 mg (52%), while the yield of trimethylene-1,3-diamine-2-C^{14} dihydrogen bromide was 49.5 mg (14%). Analysis: Calc. for $C_3H_{12}N_2Br_2$: C, 15.27%; H, 5.13%; N, 11.87%; Br, 67.7%. Found: C, 15.32%; H, 5.05%; N, 12.02%; Br, 68.0%.

Cyclopentadiene-x-C^{14} (XVI*a*) *from Dehydrobromination of trans-1,2-Dibromocyclopentane-4-*C^{14} (XI) *with Quinoline* (*Synthesis No. 1*)

In a 25-ml pear-shaped flask with a side arm as gas inlet was placed 2.82 g (0.0124 mole) of XI and 7.98 g (0.0168 mole) of freshly distilled quinoline. The flask was also fitted with a reflux condenser whose jacket temperature was kept at 45–47° C. The whole system was swept with dry nitrogen leading to a receiver cooled in a dry ice – acetone bath. The reaction mixture was heated in a wax bath to 195–198° C, whereupon a reaction set in as evidenced by much charring and bubbling. After the main evolution of volatile material had ceased, the mixture was kept at 198° C for an additional 10 minutes to insure complete reaction. The product in the receiving vessel was distilled into a calibrated centrifuge tube by heating the original receiver to 50–53° C. This distillation separated the cyclopentadiene from higher boiling materials such as quinoline that may have been present. The volume of product was 0.5 ml, corresponding to an approximate yield of 50% if all this product were pure cyclopentadiene.

A solution of the above product in ether was treated with maleic anhydride giving rise to the cyclopentadiene – maleic anhydride adduct which melted at 162–163° C (lit. (15), m.p. 163–164° C).

Another derivative of the above cyclopentadiene was the liquid adduct formed with diethyl azodicarboxylate which, on reaction with bromine, yielded the diethyl ester of 2,3-dihydraza-5,6-dibromobicyclo (2.2.1) heptane-2,3-dicarboxylic acid, m.p. 66–67° C (lit. (31), m.p. 67° C).

There was some indication that some cyclopentene may also have been formed in this reaction. After treatment of the redistilled product with excess diethyl azodicarboxylate, a small amount of liquid boiling at 39–41° C (lit. (19*b*), b.p. for cyclopentene, 44–46° C) was recovered. This liquid was unsaturated and showed an infrared spectrum similar to that of authentic cyclopentene.

Cyclopentadiene-x-C^{14} (XVI*b*) *from Thermal Decomposition of 1,2-Bis-(trimethylammonium)-cyclopentane-4-*C^{14} *Hydroxide* (*Synthesis No. 2*)

1,2-Bis-(trimethylammonium)-cyclopentane-4-C^{14} *Bromide* (XVII)

A mixture of 0.639 g (0.0028 mole) of *trans*-1,2-dibromocyclopentane-4-C^{14} (XI) and 2.0 ml of acetone[3] containing 2.65 g (0.045 mole) of trimethylamine was placed in a Pyrex glass tube, 12 mm O.D., with 1 mm wall thickness. The tube was sealed and heated at 80° C for 66 hours. During this period a mass of white crystals was deposited in the

[3]*A search for a suitable solvent for this reaction showed that acetone gave the best results as compared with nitromethane, nitrobenzene, acetonitrile, benzyl alcohol, and acetophenone* (*cf. discussion of the effects of solvent on the Menschutken reaction given by Streitwieser* (*32*)).

reaction mixture. After the mixture had cooled, the sealed tube was opened and the solvent and excess trimethylamine evaporated off. The product was recrystallized from a mixture of ethanol and ethyl acetate. The yield of the quaternary ammonium salt (XVII) was 1.11 g (76%). Analysis: Calc. for $C_{11}H_{26}N_2Br_2$: C, 38.15%; H, 7.57%; N, 8.10%; Br, 46.2%. Found: C, 38.24%; H, 7.39%; N, 8.07%; Br, 46.2%.

1,2-Bis-(trimethylammonium)-cyclopentane-4-C^{14} *Hydroxide* (XVIII)

To a solution of 1.11 g of 1,2-bis-(trimethylammonium)-cyclopentane-4-C^{14} bromide (XVII) in 20 ml of water, moist, freshly prepared silver oxide was slowly added until the color of silver oxide persisted after the solution had been standing for 1 hour at room temperature. The silver bromide which precipitated was filtered off and washed with 15 ml of water. The filtrate and washings were combined, and the water removed at 45–50° C with the aid of a water aspirator pump. The quaternary ammonium hydroxide, which remained behind as a yellowish oil, was used directly for the next reaction.

Cyclopentadiene-x-C^{14} (XVI*b*)

The above quaternary ammonium hydroxide (XVIII) was transferred to a 15-ml pear-shaped flask equipped with a nitrogen bubbler and a reflux condenser with its jacket temperature maintained at 50° C. The reflux condenser was connected to a receiver immersed in a dry ice – acetone bath. With a slow stream of dry nitrogen flushing through the system, the reaction flask was heated in a wax bath to 150° C whereupon a smooth reaction took place. The reaction temperature was kept at 150° C for 10 minutes and then raised to 160° C for an additional 15 minutes. The product trapped in the receiver was dissolved in 15 ml of low boiling petroleum ether containing 0.4 g of ordinary cyclopentadiene as carrier. This solution of diluted cyclopentadiene-*x*-C^{14} was washed four times with 15-ml portions of cold water, dried with Drierite, and then it was used directly for degradation to determine the C^{14} distribution. In preliminary preparations, the yield of cyclopentadiene, identified by the formation of the maleic anhydride adduct, m.p. 162–163° C, was found to be of the order of 20%.

Cyclopentadiene-x-C^{14} (XVI*c*) *from Reaction of 3,5-Dibromocyclopentene with Magnesium in Dry Ether* (*Synthesis No. 3*)

Cyclopentene-4-C^{14} (XII)

Cyclopentene-4-C^{14} (XII) was prepared from *trans*-1,2-dibromocyclopentane-4-C^{14} (XI) as described under the method of degradation of XI.

3,5-Dibromocyclopentene-x-C^{14} (XIX)

One gram (0.015 mole) of cyclopentene-4-C^{14} was brominated by refluxing for 4 hours with a mixture of 5.4 g (0.030 mole) of N-bromosuccinimide and 50 mg of benzoyl peroxide in 70 ml of carbon tetrachloride. The product, recovered as described by Cope and co-workers (14), weighed 2.12 g (64%), b.p. 50–60° C at 1.2 mm (lit. (14), b.p. 52–73° C at 3 mm).

Cyclopentadiene-x-C^{14} (XVI*c*) (*15*)

In a 15-ml pear-shaped flask fitted with reflux condenser, dropping funnel, and inlet to provide a nitrogen atmosphere was placed 0.432 g (0.018 mole) of magnesium turnings and 5.0 ml of absolute ether. The magnesium was activated by the addition of a few drops of ethyl bromide. Then with frequent shaking, 2.00 g (0.0088 mole) of 3,5-dibromocyclopentene-*x*-C^{14} (XIX) in 5.0 ml of absolute ether was added dropwise over a period of 15 minutes. The reaction was very vigorous. After the addition of XIX was completed, the mixture was allowed to stand at room temperature for 30 minutes with frequent shaking. The product, along with ether, was distilled, the distillate being

collected in a dry-ice-cooled receiver. This distillate was used directly for the degradation of the cyclopentadiene-*x*-C^{14}. In preliminary preparations, the cyclopentadiene was identified by the formation of the adduct with maleic anhydride, m.p. 162–163° C.

Degradation of Cyclopentadiene-x-C^{14}

Diethyl Ester of 2,3-Dihydrazabicyclo (2.2.1)-5-heptene-2,3-dicarboxylic Acid (XX)

An ether solution containing 0.50 g (0.0076 mole) of cyclopentadiene-*x*-C^{14} and 1.32 g (0.0076 mole) of diethyl azodicarboxylate, the latter prepared from reaction of hydrazine with ethyl chloroformate followed by oxidation with chlorine (33), was heated in a sealed tube at 45° C for 12 hours. After removal of the solvent, the residue was distilled under vacuum, yielding 1.73 g (95%) of a very viscous product, b.p. 110–113° C at 0.12 mm (lit. (31), b.p. 121° C at 0.5 mm). On addition of bromine, the dibromo derivative obtained melted at 66–67° C (lit. (31), m.p. 67° C).

Diethyl Ester of 2,3-Dihydrazabicyclo (2.2.1) heptane-2,3-dicarboxylic Acid (XXI)

In the glass liner of the hydrogenator bomb were placed 2.00 g (0.0083 mole) of the above Diels–Alder adduct (XX) in 20 ml of absolute ethanol and 0.05 g of platinum oxide. Hydrogenation was effected by shaking the system for 4 hours under a hydrogen pressure of about 450 p.s.i. The required drop in pressure for the small quantity of reactant used was negligible so it was not recorded. The product was isolated by filtering off the catalyst, removing the ethanol by means of a water aspirator pump, and vacuum-distilling the residue. The fraction collected weighed 1.77 g (88%), b.p. 112–114° C at 0.2 mm (lit. (31), b.p. 121° C at 5 mm).

Succinic Acid (XXII) *from* XXI

A mixture of 1.00 g (0.0041 mole) of hydrogenated ester XXI, 6.5 g (0.041 mole) of potassium permanganate, and 100 ml of water was heated on a steam bath with occasional shaking for 25 minutes. After the mixture had cooled, the excess permanganate and manganese dioxide were reduced by slow addition of sodium bisulphite. The resulting colorless solution was continuously extracted with ether for 48 hours. The extract was dried with Drierite, the ether removed by distillation, and the residue maintained at 60–70° C under water pump vacuum until a yellowish, crystalline residue remained. This residue, after being washed with chloroform, weighed 0.253 g (52%). It was purified by three successive recrystallizations, suitable solvent for the recrystallization being diethyl ketone, anhydrous tetrahydrofuran, or water acidified with hydrochloric acid. The m.p. of the purified product was 184–185° C (lit. (19*c*), m.p. 184.5–185° C).

Schmidt Reaction with Succinic Acid

Succinic acid (50 mg, 0.42 mmole) was converted to succinic anhydride by treatment with 30 λ (0.34 mmole) of phosphorus oxychloride, and then the anhydride was subjected to reaction in 0.43 ml of 100% sulphuric acid containing 85 mg (1.3 mmoles) of sodium azide. The detailed procedure has been reported by Phares and Long (34). The carbon dioxide liberated was trapped in carbonate-free sodium hydroxide solution and then precipitated as barium carbonate. The yield of barium carbonate was in the order of 80%. The reaction mixture was made basic with sodium hydroxide solution and distilled to give an aqueous solution of ethylene-1,2-diamine as described by Phares and Long (34). Isolation of the ethylene-1,2-diamine as a solid derivative was effected by acidifying the distillate with hydrobromic acid, evaporating almost to dryness, adding ethanol, and collecting the crystalline product formed. The yield of ethylene-1,2-diamine dihydrogen bromide was 52 mg (55%). Analysis: Calc. for $C_2H_{10}N_2Br_2$: N, 12.63%; Br, 72.0%. Found: N, 12.59%; Br, 72.4%.

ACKNOWLEDGMENTS

The award of the C-I-L Fellowship to one of us (R.T.) and the financial support given by the National Research Council of Canada are gratefully acknowledged.

REFERENCES

1. THIELE, J. Ber. **33**, 666 (1900).
2. THIELE, J. Ber. **34**, 68 (1901).
3. GOSS, F. R. and INGOLD, C. K. J. Chem. Soc. 1268 (1928).
4. ROBERTS, J. D., STREITWIESER, A., JR., and REGAN, C. M. J. Am. Chem. Soc. **74**, 4579 (1952).
5. LLOYD, D. and SNEEZUM, N. S. Chem. & Ind. (London), 1221 (1955); Tetrahedron, **3**, 334 (1958).
6. KOSOWER, E. M. and RAMSEY, B. G. J. Am. Chem. Soc. **81**, 856 (1959).
7. RAMIREZ, F. and LEVY, S. J. Org. Chem. **21**, 488 (1956); J. Am. Chem. Soc. **79**, 67 (1957).
8. HÜCKEL, E. Z. Physik, **70**, 204 (1931); Grundzüge der Theorie ungesättigter und aromatische Verbindungen. Verlag Chemie, G.M.B.H., Berlin. 1938. pp. 71–85.
9. WHELAND, G. W. J. Chem. Phys. **2**, 474 (1934).
10. DOERING, W. VON E. and KNOX, J. H. J. Am. Chem. Soc. **76**, 3203 (1954).
11. WILKINSON, G. W., COTTON, F. A., and BIRMINGHAM, J. M. J. Inorg. & Nuclear Chem. **2**, 95 (1956).
12. FRITZ, H. P. Ber. **92**, 780 (1959).
13. CROSSLEY, A. W. J. Chem. Soc. 1403 (1904).
14. COPE, A. C., ESTER, L. L., JR., EMERY, J. R., and HAVEN, A. C., JR. J. Am. Chem. Soc. **73**, 1199 (1951).
15. REID, E. B. and YOST, J. F. J. Am. Chem. Soc. **72**, 1807 (1950).
16. FRIES, B. A. and CALVIN, M. J. Am. Chem. Soc. **70**, 2235 (1948).
17. CASON, J. and RAPAPORT, H. Laboratory text in organic chemistry. Prentice-Hall Inc., New York. 1950. pp. 289–291.
18. MICOVIC, M. V. Organic synthesis. Collective Vol. II. John Wiley & Sons, Inc., New York. 1943. p. 264.
19. HEILBRON, I. and BUNBURY, H. M. Dictionary of organic compounds. Eyre and Spottiswoode, Ltd., London. 1953. (*a*) Vol. II, p. 606; (*b*) Vol. I, p. 647; (*c*) Vol. IV, p. 383.
20. HAUSER, C. R. and HUDSON, B. E., JR. Organic reactions. Vol. 1. John Wiley & Sons, Inc., New York. 1942. p. 284.
21. HESSE, G. and BÜCKING, E. Ann. **563**, 31 (1949).
22. OWEN, L. N. and SMITH, P. N. J. Chem. Soc. 4026 (1952).
23. HERMANS, P. H. Z. anorg. u. allgem. Chem. **142**, 83 (1925).
24. VERKADE, P. E., COOPS, J., JR., VERKADE-SANDBERGEN, A., and MAAN, C. J. Ann. **477**, 279 (1930).
25. WINSTEIN, S. and LUCAS, H. J. J. Am. Chem. Soc. **61**, 1581 (1939).
26. ZELINSKY, N. D. and LEWINA, R. J. Ber. **66**, 477 (1933).
27. LUCAS, H. J., SCHLATTOR, M. J., and JONES, R. C. J. Am. Chem. Soc. **63**, 22 (1941).
28. BAILY, P. S. J. Org. Chem. **22**, 1548 (1957).
29. LOFTFIELD, R. B. J. Am. Chem. Soc. **73**, 4707 (1951).
30. ROBERTS, J. D., SEMENOV, D. A., SIMMONS, H. E., JR., and CARLSMITH, L. A. J. Am. Chem. Soc. **78**, 601 (1956).
31. DIELS, O., BLOM, J. M., and KOLL, W. Ann. **443**, 242 (1925).
32. STREITWIESER, A., JR. Chem. Revs. **56**, 571 (1956).
33. RABJOHN, N. Org. Syntheses, **28**, 58 (1948).
34. PHARES, E. F. and LONG, M. V. J. Am. Chem. Soc. **77**, 2556 (1955).

A PRELIMINARY STUDY OF THE VAPOR PERMEABILITY OF CELLOPHANE[1]

W. L. ARCHER[2] AND S. G. MASON

ABSTRACT

The water vapor permeability of cellophane was measured over adsorption–desorption cycles and was found to parallel the sorption isotherm. When a constant vapor pressure was applied on the low pressure side of the membrane, the mass flow rate was independent of the vapor pressure used and showed hysteresis on desorption. The permeabilities of methanol, ethanol, and benzene were found to increase with increasing vapor pressure.

INTRODUCTION

In this note we describe some rather careful measurements of the diffusion of water and other substances through cellophane when a controlled difference in vapor pressure was maintained across the membrane. The measurements were made originally to determine their usefulness in studying swelling phenomena in cellulose. Because the measurements were time-consuming and the permeation phenomena complicated, the technique was abandoned in favor of liquid permeability methods (1, 2).

Since the transmission of gases and vapors through polymeric films is receiving considerable attention (3, 4), our results may prove to be of some interest. Doty, Aiken, and Mark (5) have shown that the water vapor permeability of cellophane varies non-linearly with the vapor pressure gradient. They proposed a mechanism of vapor transfer comprising an activated diffusion by the sorption and desorption of water molecules at active spots on the internal surface of the cellulose.

Several investigators have pointed out the similarity in shape between the water sorption isotherm and permeability of cellophane (6, 7). This observation has been confirmed and extended in the present study.

EXPERIMENTAL PART

Apparatus

Measurements were made in an evacuated system consisting essentially of a vapor source, a cellophane barrier, and a cold trap to condense the permeating vapor. The sorption of the vapor by a separate piece of cellophane was measured simultaneously on the high pressure side of the membrane.

The same cellophane membrane was used in all the permeability measurements and was held in a stainless steel cell (Fig. 1). The cell consisted of two half-cells bolted together at central flanges by eight symmetrically placed steel bolts. The membrane was clamped between the inner lapped ring surfaces of the flanges. A groove B cut in the flanges provided a mercury well to seal the edges of the membrane. The free area of membrane was 19.68 cm^2.

The cell was connected to the vacuum system by two tapered ends machined to fit female standard ground glass joints. Effective bonding of the steel and glass was obtained with high vacuum cement. The cell was immersed in a constant temperature water bath. A vacuum of 10^{-4} mm Hg was readily obtained.

[1]*Manuscript received June 10, 1959.*
Contribution from the Physical Chemistry Division, Pulp and Paper Research Institute of Canada, and the Department of Chemistry, McGill University, Montreal, Quebec.
[2]*Holder of Studentships (1947–48 and 1948–49) from the National Research Council.*

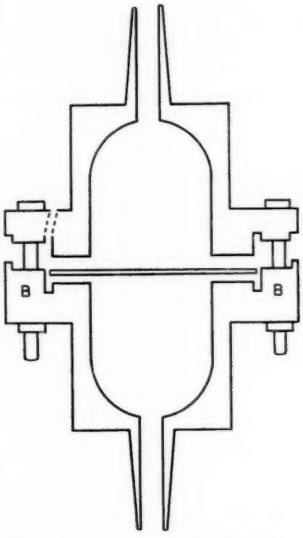

FIG. 1. Vapor permeability cell.

Vapor was supplied from bulbs at C (Fig. 2), thermostatted separately from the permeability cell to provide the required relative vapor pressures next to the membrane. Saturated solutions of potassium acetate and potassium thiocyanate, and distilled water, provided a complete range of relative humidities. A mixture of methanol and glycerol provided low methanol vapor pressures. Due to the low loss rate of vapor by permeation, mechanical agitation of the reservoir was not required. Dissolved air was removed by several cycles of freezing and thawing under vacuum. The temperature of the vapor tube bath was controlled to $\pm 0.02°$ C.

The vapor pressure gradient across the membrane was measured by mercury manometers at D and E (Fig. 2).

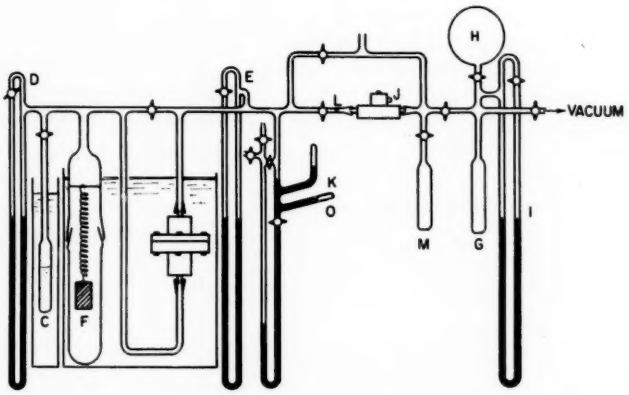

FIG. 2. Vapor permeability apparatus.

Sorption measurements were carried out with a cellophane sample suspended by a quartz spiral spring (sensitivity = 1.08 mg/mm) in a sorption cell at F. Vapor sorption was determined by measuring the extension of the quartz spring with a cathetometer, and was expressed as a percentage of the dry weight.

The vapor passing through the membrane was condensed in a cold trap G using liquid nitrogen, and measured by subsequent expansion into a known volume of the system. A calibrated volume H was used both to determine the volume of this portion of the system and to provide extra space for the expansion of large amounts of condensate. The resulting pressures were measured with a mercury manometer I.

Constant vapor pressures were maintained as required on the "dry" or low pressure side of the membrane by a solenoid-operated needle valve J. Valve action was controlled by a mercury contact switch K operating through a relay. For increased sensitivity, a fine orifice L was inserted in advance of the needle valve. Dry side vapor pressures were maintained constant to ±0.1 mm Hg.

Materials

Both the permeability membrane and the sorption sample were cut from a single sheet of Canadian Industries Limited PT 600 (non-waterproofed) cellophane. The glycerol plasticizer was removed by extraction in water at 60° C for 2 hours.

Procedure

For several days prior to each sorption–desorption cycle, the system was continuously evacuated to remove sorbed vapors and gases from the glass tubing and the cellophane. During the time required to reach a constant transmission rate, the vapors passing through the membrane were collected in a cold trap M (Fig. 2). For a permeability measurement, this cold trap was closed off and the transmitted vapor collected in cold trap G.

All permeability and sorption measurements were carried out at 30±.01° C.

The permeabilities were expressed in terms of the mass flow rate q in g sec^{-1}, and a vapor permeability P_v defined by

$$[1] \qquad q = P_v A(\Delta p)$$

where A is the area of membrane (= 19.68 cm^2), and (Δp) is the vapor pressure difference across the membrane in dynes/cm^2. In view of the uncertainty of the thickness of the partially swollen membrane and of other complications, no attempts were made to calculate absolute permeability coefficients.

RESULTS AND DISCUSSION

Permeability to Water Vapor

1. Steady State

To ensure that a constant vapor transmission rate was attained, a series of flow rate measurements was made at each relative humidity until a constant flow rate was reached. A typical curve illustrating the change in flow rate accompanying an increase in relative humidity on the "wet" side is shown in Fig. 3. The time to reach a constant flow rate was found to decrease with increasing relative humidity, and to be shorter during sorption than during desorption. These trends were evident from the times to half-value, i.e. the time for the initial 50% change in flow rate to occur. The corresponding times to half-value for sorption were approximately one-half those of P_v at low R.H.; above 40% R.H. the times were substantially the same.

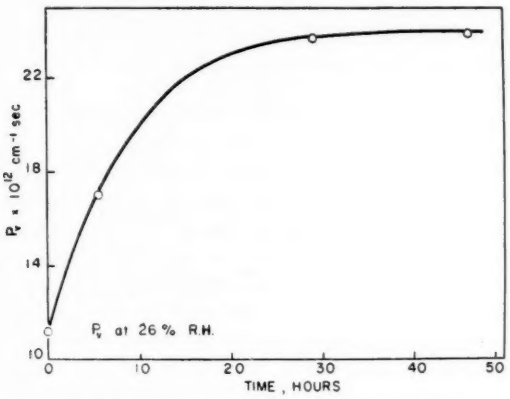

FIG. 3. Approach of permeability to equilibrium value on increasing relative humidity from 26 to 40%. Dry side at 0% R.H. The time to half-value in this experiment was 6.0 hours.

2. Permeability at Zero Back Pressure

Permeabilities for a complete sorption–desorption cycle are given in Table I. These measurements were made with zero vapor pressure on the low pressure side of the membrane.

TABLE I

Water vapor permeability (zero back pressure)

Relative humidity (wet side), %	Δp, mm Hg	$q \times 10^8$, g sec^{-1}	$P_v \times 10^{12}$, cm^{-1} sec	Moisture content, %
Adsorption				
11	3.5	6.12	0.67	4.5
26	8.2	24.2	1.12	6.5
40	12.8	79	2.38	8.3
55	17.5	234	5.03	10.8
80	25.5	1000	14.8	17.9
Desorption				
94	30.0	2000	25.1	30.6
80	25.5	1016	15.0	19.1
60	19.1	294	5.80	12.8
40	12.8	116	3.43	10.0
26	8.2	56.4	2.61	8.1
11	3.5	13.6	1.47	5.8

The permeabilities in Table I are approximately four times those reported by Doty *et al.* (5) for a comparable grade of cellophane. This is not a serious discrepancy in view of the wide variations in permeability reported by these authors for commercial films of different manufacture.

The permeability and sorption data are plotted in Fig. 4 and as others have found (6, 7) roughly parallel one another. During desorption, the curve of Fig. 4 is seen to exhibit a permeability hysteresis at relative humidities below 60%. This behavior was confirmed several times. Both the adsorption and desorption portions of the P_v curve in Fig. 4 extrapolate smoothly to the origin indicating that dry cellophane is impervious to water.

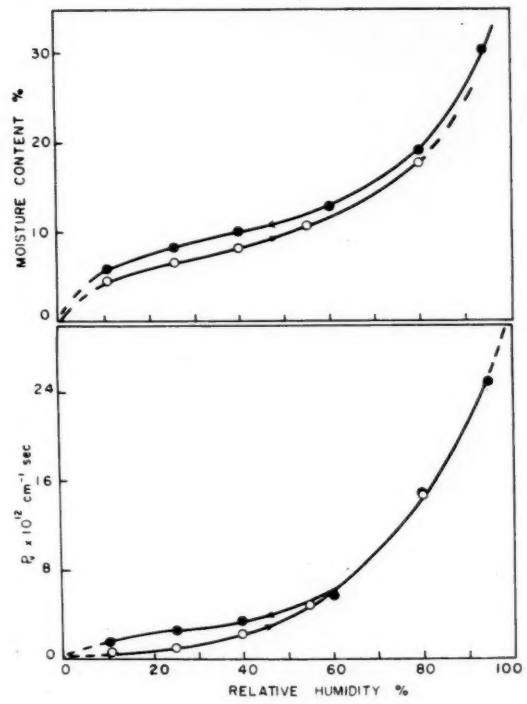

FIG. 4. Water vapor sorption (upper part) and permeability at zero back pressure (lower part) for adsorption (open circles) and desorption (solid circles).

3. Reduced Moisture Gradients

The effect of reducing the moisture gradient across the membrane was studied by introducing constant water vapor pressures on the low pressure side of the membrane. The results obtained with pressures corresponding to 20% R.H. are given in Table II

TABLE II

Water vapor permeability
(20% relative humidity on low pressure side)

Relative humidity (wet side), %	Δp, mm Hg	$q \times 10^8$, g sec^{-1}	$P_v \times 10^{12}$, cm^{-1} sec
Adsorption			
26	1.8	12.9	2.7
55	11.2	360	12.1
65	14.1	730	21.2
75	17.0	1320	29.2
Desorption			
70	15.5	1080	26.2
65	14.1	920	24.8
55	11.2	500	16.8
33	4.2	105	9.5

for a complete cycle. These data together with values at 0, 10, and 15% R.H. are shown in Fig. 5. In order to show the trends more clearly, values of q have been plotted.

Figure 5 shows that the reduction in moisture gradient across the membrane has caused an increase in the vapor transmission rate at all relative humidities. The q curves during adsorption for the three back pressures used coincide, indicating that the increase in q is independent of the pressure used.

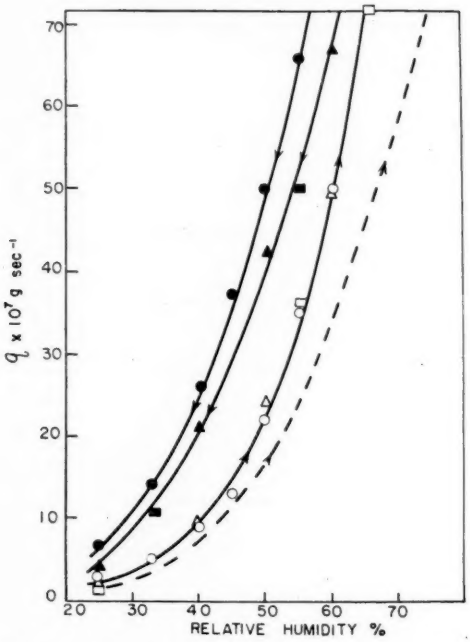

FIG. 5. Water vapor flow rates during adsorption (open points) and desorption (solid points) at 10% (circles), 15% (triangles), and 20% (squares) relative humidity on the low pressure side. The broken line is for adsorption at zero R.H. on the low pressure side.

A second effect of a reduced moisture gradient is seen in the extension of the permeability hysteresis to relative humidities above 60%. There also appears to be a trend toward a reduction in the magnitude of the hysteresis as the low pressure side relative humidity is increased.

TABLE III

Organic vapor permeabilities (zero back pressure)

Permeant	Δp, mm Hg	$q \times 10^8$, g sec^{-1}	$P_v \times 10^{14}$, cm^{-1} sec	% sorption
Methanol	45.5	1.47	1.21	1.4
	81.9	10.5	4.85	1.8
	133	94	26.7	6.9
Ethanol	40.0	0.93	1.08	—
	60.1	2.50	1.57	—
	79.0	7.09	3.39	—
Benzene	67.6	2.32	1.3	0.03
	97.7	7.26	2.8	0.08

Permeability to Organic Vapors

Various organic vapors are adsorbed less than water and it was thought that P_v might be independent of Δp when the sorption became negligible. The permeabilities of methanol, ethanol, and benzene at zero back pressure are given in Table III. These data show that the permeability to organic vapors is considerably less than to water vapor. The flow rate of methanol vapor, for example, at 45.5 mm Hg pressure is less than 1/600 that of water vapor at 25.5 mm Hg pressure (Table I).

Sorption measurements on methanol and benzene are included in Table III and show that P_v increases with the sorptions.

It is seen from Table III that P_v did not remain constant but in all cases increased with increase in Δp.

REFERENCES

1. CARROLL, M. and MASON, S. G. Can. J. Technol. **30**, 294 (1952).
2. KUZMAK, J., ARCHER, W. L., and MASON, S. G. To be published.
3. WAACK, R., ALEX, N. H., FRISCH, H. L., STANNET, V., and SZWERC, M. Ind. Eng. Chem. **47**, 2524 (1955).
4. BARRER, R. M. Diffusion in and through solids. Cambridge Univ. Press, London. 1941.
5. DOTY, P. M., AIKEN, W. H., and MARK, H. Ind. Eng. Chem. Anal. Ed. **16**, 686 (1944).
6. CHARCH, W. H. and SCROGGIE, A. G. Paper Trade J. **101**, 201 (1935).
7. TAYLOR, R. L., HERRMANN, D. B., and KEMP, A. R. Ind. Eng. Chem. **28**, 1255 (1936).

PARTIAL SPECIFIC VOLUME MEASUREMENTS BY DIFFERENTIAL SEDIMENTATION[1]

W. G. MARTIN, C. A. WINKLER,[2] AND W. H. COOK

ABSTRACT

The partial specific volumes of several macromolecules were determined from their sedimentation rates in aqueous and heavy water solutions with results comparable to those obtained by conventional methods. Corrections for the changes in weight due to isotopic exchange were obtained from measurements on small quantities of material with a quartz spiral balance. Measurements of the partial specific volumes of bovine plasma albumin, polyvinyl alcohol, glycine, and triglycylglycine in both aqueous and heavy water media, made with a magnetic float apparatus, indicate that isotopic exchange has no significant effect on the macromolecular volume. The sedimentation method is therefore a micro method that does not require a knowledge of the concentration of macromolecules and which is applicable to mixtures that are resolvable during sedimentation.

INTRODUCTION

In a recent paper (1) it was shown that measurement of the differential rate of sedimentation of macromolecules dissolved in water or deuterium oxide solvents could yield a sufficiently accurate estimate of their partial specific volume ($\bar{v}$) to be useful in estimating molecular size by sedimentation methods. Although the inherent accuracy is less than that of the conventional methods (pycnometry and magnetic float), the procedure has several advantages: it can be used when only small amounts of material (ca. 10 mg) are available; other methods require purified material whereas the sedimentation method should be applicable to mixtures, provided the boundaries can be resolved; finally, this method is applicable to materials (lipoproteins) where density and other properties are altered by contact with immiscible organic liquids used to establish density gradient columns. These advantages are so great in the preparative stages of any new biological macromolecule, or with any scarce material, that further study and development of the method were well justified.

As mentioned in the earlier paper (1), other investigators (2) have used salts and nonelectrolytes to alter the density of the media of sedimentation. Since these substances interacted with the sedimenting solutes and brought about spurious results, Sharp *et al.* (3) sedimented viruses in heavy water media. Recently polystyrene latex spheres were sedimented in aqueous and heavy water mixtures (4, 5), but here hydration and isotopic exchange of labile hydrogen were not involved. Katz and Schachman (6) have obtained an adequate value of $\bar{v}$ from sedimentation of deoxyribonucleic acid at constant concentration in media in which the density was altered by the addition of heavy water. However, with most biological macromolecules it is necessary to consider the extent of exchange of labile hydrogen atoms in heavy water media. True, as in our earlier paper, isotopic exchange may be estimated for well-known materials, but not so for new unknown macromolecules. Therefore a procedure for determining the degree of substitution on micro quantities of material by direct weighing was developed and critically compared with the substitution indicated by density methods. In addition to measurements on

[1]*Manuscript received June 15, 1959.*
Contribution from the Division of Applied Biology, National Research Council, Ottawa, Canada, and the Physical Chemistry Laboratory, McGill University, Montreal, Quebec. This paper constitutes part of a thesis submitted to the Graduate School, McGill University, by W.G.M., in partial fulfillment of the requirements for the degree of Doctor of Philosophy.
Issued as N.R.C. No. 5320.
[2]*Department of Chemistry, McGill University, Montreal, Quebec.*

proteins, some relatively extensive measurements were made on glycine and triglycylglycine where substitution is proportionately higher. Finally, the aqueous – heavy water sedimentation procedure was tested on mixtures of proteins of known and unknown $\bar{v}$ to confirm the applicability and accuracy of the procedure as applied to such systems.

MATERIALS

Crystalline bovine plasma albumin lot No. A1201 (Pentex Inc.), crystalline bovine β-lactoglobulin lot No. 0053B (Armour and Co.), and triglycylglycine lot No. 7484 (Nutritional Biochemicals Corp.) were used without further purification and will be referred to as BPA, βLG, and TGG, respectively. Polyvinyl alcohol (Shawinigan Chemicals Ltd.), termed PVA, was dissolved in distilled water, centrifuged, filtered, and then lyophilized. The PVA had a remnant of 12 acetate groups per 100 mers owing to incomplete alcoholysis. Glycine (Eastman) was dissolved in warm water and filtered from a slurry of charcoal and celite, then precipitated with methanol, washed with methanol–ether, and dried at 45° C *in vacuo*.

Livetin (7), the water-soluble protein of hen egg yolk, was separated into its α–β-components and γ-components by the procedures of Martin *et al.* (8, 9). Lipovitellin of yolk was prepared by the method of Joubert and Cook (10). It was possible to store the α–β-livetin in a lyophilized condition but the lipovitellin and γ-livetin had to be stored at 5° C in solution.

A stock of distilled water was prepared by adding potassium permanganate to alkaline tap water and distilling with a minimum of reflux. The distillate, redistilled with a minimum of reflux, was assumed to have a density of 0.997074 g/ml at 25.000° C.

Deuterium oxide (99% D_2O) and a quartz spiral were purchased from Merck & Co., Inc., and Microchemical Supply Co., respectively.

METHODS

The sedimentation procedures were as described previously (1) with some modifications. Solutes in appropriate solvents were dialyzed at 5° C against solvent. Suitable dilutions were then made using diffusate as diluent. Viscosity and density measurements on diffusates were made with Ostwald–Fenske type viscometers and with a Mohr–Westphal balance, respectively, at 20° C, since sedimentation experiments were controlled at this temperature. Solute concentrations were determined from measurements with a differential refractometer (11) from previously determined values of the specific index increments. Transfer of solutions was effected by use of dry syringes to minimize exchange of heavy water with atmospheric moisture.

In order to interpret the changes in $\bar{v}$ of macromolecules brought about by isotopic exchange, the direct weight increase upon exposure to heavy water was measured on a McBain–Bakr quartz spiral balance (Fig. 1). The balance apparatus consisted of vacuum pump A, oil diffusion pump B, gas inlet control system C and D, trap E, ionization gauge F, pyrex glass balance case containing quartz spiral and sample basket, and movable permanent magnets L. Capillary tube G permitted insertion of syringe needles. Heater M containing thermometer N was removable. Auxiliary apparatus could be connected at H.

Aluminum foil baskets were dipped into silicone grease dispersed in benzene, and then dried at 110° C. Baskets with capacity of 1 or 2 ml weighed about 40 to 60 mg. The spiral was calibrated *in vacuo* by measuring the extension caused by the addition of calibrated platinum weights. Extensions were measured with a Wild cathetometer

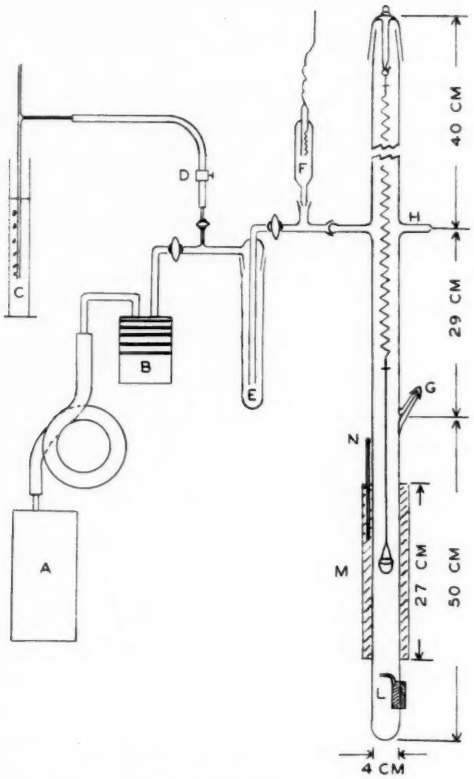

FIG. 1. Quartz spiral balance apparatus.

at 25° C to 0.01 mm with a precision of reading of ±0.02 mm. The sensitivity of the spiral was 1.00±0.02 mg/mm extension with loads ranging from 24 to 198 mg.

Measurements were made of spiral extension *in vacuo* with the empty basket suspended and the trap E immersed in liquid nitrogen. Then nitrogen gas was slowly admitted to the system through the trap until atmospheric pressure was reached. About 150 mg of sample was added to the basket and the system evacuated until constant weight was reached. Nitrogen gas was admitted to the system through the trap and about 1 ml of water was directed into the basket through capillary G while the basket was supported by the magnets. After an equilibrium period of 15 to 20 hours the basket was lowered in the balance case and the sample was frozen *in situ*. Lyophilization was brought about and evacuation continued until constant weight again occurred. Similarly, two to three applications of deuterium oxide were applied to the sample and sometimes followed by two more applications of water. Equilibrium weights were also obtained at selected temperatures (< 105° C) by adjustment of the movable furnace M about the basket. Once a sequence of exchanges had commenced, the trap E was kept immersed in liquid nitrogen. When deuterium oxide was added to samples, a small flow of nitrogen gas passed through the system by way of the trap.

To provide a standard of comparison with $\bar{v}$ obtained by the sedimentation method, $\bar{v}$ was also determined from measurements of density made with a magnetic float apparatus (12, 13). Usually weighed quantities of diffusate were placed in the float chamber and then weighed amounts of concentrated stock solutions were added, with density measurements being made upon each addition. However, owing to the impossibility of dialysis of glycine or TGG solutions, solvents were obtained by cryosublimation from their frozen solutions, and solvents and residual concentrated solutions used in the manner of the diffusates and solutions mentioned above.

Solute concentrations for the float measurements were based on dry weight. Deuterated samples were brought to constant weight, then two additions of water were made with intervening drying to get the dry weight of the protonated sample. At the temperature of 105° C *in vacuo*, employed for the other materials, glycine samples failed to reach constant weight, and therefore the effect of temperature on glycine was examined with the spiral balance. Based on these measurements, glycine was brought to constant weight at 70° C *in vacuo*.

RESULTS

Difficulty in achieving constant dry weight of glycine samples at 105° C *in vacuo* is understandable in view of the results shown in Fig. 2 for the spiral extension when the basket containing glycine was heated to various temperatures. Rapid loss of weight, accompanied by sublimation of the sample, occurred *in vacuo* at temperatures above 74° C. The other materials presented no serious drying difficulties. Even with the lipid-containing lipovitellin, only a slight loss in weight occurred between 25 and 91° C *in vacuo*.

The extent of exchange of deuterium for hydrogen atoms in the materials is shown in Table I, 97.4% deuterium oxide being the exchange medium. In a few instances experiments with the spiral balance had to be repeated owing to dusting or loss of small pieces of the material during drying. Concentrated solutions gave less trouble in this respect.

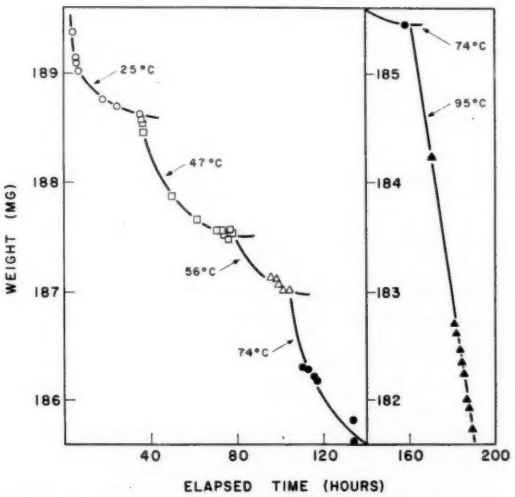

FIG. 2. Weight (extension) of glycine as a function of temperature and heating time *in vacuo*.

TABLE I

Labile hydrogen exchange*

Sample	Weight increase observed, %	Theoretical weight increase, %
BPA	1.52	1.52
βLG	—	1.5
PVA	1.79	1.75
Glycine	3.84	3.89
TGG	—	2.4
Lipovitellin + X protein	1.33	—
α- + β-Livetin	1.32	—
γ-Livetin	1.36	—

*Based upon 97.4% of D_2O and equilibrium at 25° C.

The isotopic exchange of deuterium with the labile hydrogen atoms of BPA was investigated at intermediate concentrations of heavy water and the results shown in Fig. 3 illustrate the essential linearity of the relation between volume per cent of heavy water and the percentage weight increase of the material.

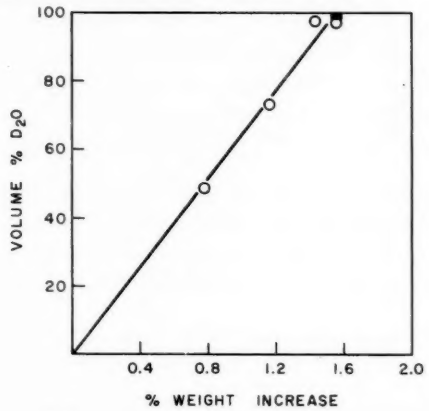

FIG. 3. Relation between D_2O concentration and weight increment of bovine plasma albumin. ○ Experimental. ■ Calculated.

From the exchange measurements or, lacking these, published data, the value of k (1) was calculated from

$$k = 1+[(\Delta w)(d_1-d_0)/\Delta d] \quad [1]$$

where Δw is the weight increase per gram of sample, (d_1-d_0) is the increment in density of the solvent due to deuterium oxide, and Δd is the increment in density of 100% deuterium oxide over the density of water.

$$f\eta s = Mk(1-\bar{v}k^{-1}d) \quad [2]$$

was given in the previous paper (1), where f, η, s, M, d are the frictional coefficient, solvent viscosity, sedimentation coefficient, molecular weight of the macromolecule, and solvent density, respectively. As shown in Fig. 4 the relation between $\eta s/k$ and d/k for BPA and PVA (concentration 0.4 g/100 ml) in media of varying concentrations of heavy water

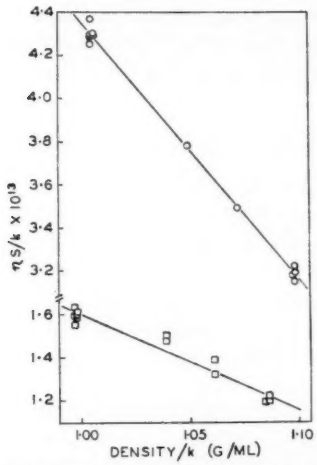

FIG. 4. Relation between $\eta s/k$ (solvent) and d/k (solvent) for bovine plasma albumin and polyvinyl alcohol. ○ BPA. □ PVA.

is essentially linear, as expected from inspection of equation [2]. Moreover, from the intercepts at the values of $\eta s/k$ equal to zero, where $\bar{v}$ equals the reciprocals of the intercepts d/k, $\bar{v}$ was 0.735±0.003, and 0.735±0.013, for BPA and PVA, respectively.

Since the above results and those of others (2, 3, 6) demonstrate the linearity of equation [2] when heavy water is used to alter the density of the solvent, the equation

$$[3] \qquad \bar{v} = (\eta_2/\eta_1 - ks_1/s_2)(d_1\eta_2/\eta_1 - d_2s_1/s_2)^{-1},$$

derived in the earlier paper (1), was used to calculate $\bar{v}$ from sedimentation experiments on macromolecules including single solutes and mixtures. Sedimentation coefficients were extrapolated to zero solute concentration by use of relative values of diluted initial stock solutions and are recorded in Table II, as are also the related solvent viscosities

TABLE II

Summary of sedimentation results and related measurements

Materials	Temp., °C	s^0 uncorr., Svedbergs		η, centipoise		d, g/ml		k
		1	2	1	2	1	2	
Individual macromolecules								
BPA, 0.2 *N* NaCl	25	4.78±0.04	2.97±0.03	0.912	1.117	1.005	1.113	1.015
PVA, 0.2 *N* NaCl	25	2.14±0.03	1.22±0.03	0.912	1.117	1.005	1.113	1.018
α-β-Livetin, 0.2 *N* NaCl	20	3.77±0.05	2.36±0.01	1.030	1.269	1.008	1.112	1.013
γ-Livetin, buffer*	20	7.28±0.06	4.67±0.07	1.033	1.274	1.012	1.116	1.014
In mixtures								
BPA (with βLG), 0.2 *N* NaCl	20	4.36±0.05	2.76±0.06	1.026	1.259	1.006	1.112	1.015
βLG (with BPA), 0.2 *N* NaCl	20	2.74±0.08	1.66±0.05	1.026	1.259	1.006	1.112	1.015
Lipovitellin (with X), buffer†	20	9.71±0.01	5.31±0.01	1.101	1.357	1.019	1.122	1.013
Protein X (with lipovitellin), buffer†	20	6.36±0.16	3.34±0.29	1.101	1.357	1.019	1.122	1.013

*Glycine, pH or pD 9.5, μ 0.2.

†Glycine, pH or pD 9.0, μ 0.3 + 0.05 *M* $MgSO_4$.

s, η, and d values refer to the solvents and temperatures indicated.

1 refers to aqueous solvent.

2 refers to heavy water solvent.

and densities. The values of k were based upon measured values (Table I) except for βLG, where k was estimated from the amino acid composition (14). Values of $\bar{v}$ obtained by the sedimentation method are shown in Table III. The errors were calculated according to equation

$$[4] \qquad \Delta\bar{v} = \eta_1\eta_2(kd_1-d_2)(s_1+s_2)(d_1s_2\eta_2-d_2s_1\eta_1)^{-2}[(\Delta^2s_1 + \Delta^2s_2)/2]^{\frac{1}{2}}$$

where Δ is to be read "the standard error of" (1).

From measurements of density with the magnetic float apparatus of solutions BPA, PVA, glycine, and TGG in water and heavy water, $\bar{v}$ values were computed for the protonated and deuterated macromolecules, as shown in Tables III and IV. Based upon the measured $\bar{v}$, the fractional changes in $\bar{v}$ upon exchange of labile hydrogen atoms with deuterium atoms were calculated and compared with the values to be expected from the degree of substitution given in Table I.

TABLE III

Partial specific volumes of macromolecules (ml/g)

Material	Calculated	Published or observed by conventional methods	Sedimentation method	
			Alone	In mixtures
BPA	0.734* (15)	0.734$_9$† (13) 0.7342±0.0002†	0.734±0.001†	0.72±0.02* (with βLG)
PVA	0.75*	0.766±0.001†	0.78±0.01†	
βLG	0.746* (15)	0.751* (17)	—	0.75±0.03* (with BPA)
Lipovitellin	—	0.781† (10)	—	0.779±0.003* (with X)
Protein X	—	—	—	0.79±0.03* (with lipovitellin)
γ-Livetin	—	0.726±0.001† (9)	0.70±0.02*	—
α-β-Livetin	—	—	0.72±0.02*	—

NOTE: Temperatures applicable, *20° C, †25° C.
PVA contains 12 acetate groups per 100 mers.
Values without references are from this work.

In Table III the calculated values of $\bar{v}$ for BPA and βLG were reported by McMeekin and Marshall (15), while that of PVA was obtained by use of the atomic volume increments derived by Traube (16). Of the published values of $\bar{v}$, that of BPA (13), lipovitellin (10), and γ-livetin (9) were obtained by use of a magnetic float, while that of βLG (17) was obtained presumably by use of pycnometers.

DISCUSSION

The weight increases (Table I) that occur upon exchange of labile hydrogen atoms with deuterium atoms are accompanied by changes in $\bar{v}$ as shown by the data in Table IV. The experimentally determined decreases in $\bar{v}$ of PVA, TGG, and glycine were in reasonable agreement with the values calculated on the assumption that the volume occupied by deuterium atoms in a material is similar to that of the displaced hydrogen atoms. The decrease in $\bar{v}$ of BPA was less than the theoretical value, although complete exchange would be expected on the basis of the spiral balance measurements. However, Robertson (18) has reported that an expansion is likely to occur in the direction of the hydrogen bonds upon deuteration, an effect of greater importance in BPA than in PVA, TGG, or glycine. The extent of such an effect on proteins would be unpredictable owing to the several types of hydrogen bonding. Errors in $\bar{v}$ due to measurements with the

TABLE IV

Partial specific volumes from float apparatus measurements

	Substance			
	BPA	PVA	TGG	Glycine
$\bar{v}_p \times 10^3$, 25° C, ml/g	734.2±0.2	765.9±0.6	590.7±1.2	575.4±1.5
$\bar{v}_D \times 10^3$, 25° C, ml/g	728.2±1.3	754.4±3.5	576.6±1.9	544.9±0.8
$(-\Delta\bar{v}/\bar{v}_p) \times 10^3$ (found)	8.2±1.3	15.0±3.5	24±3	53±3
$(-\Delta\bar{v}/\bar{v}_p) \times 10^3$ (theory)	15.5	17.9	24	40

NOTE: Subscripts p and D refer to protonated and deuterated TGG and glycine values at $c \to 0$.

float apparatus have already been discussed (12, 13) and, even with the added difficulties of dealing with heavy water, are not enough to account for the small $\Delta\bar{v}$ for BPA.

Specific volumes of organic substances with known composition and functional groups can be calculated from atomic volume increments derived by Traube (16) and recently employed by others to evaluate $\bar{v}$ of proteins (19, 15). Calculated and experimental values of $\bar{v}$ for BPA and other proteins agree well if the decrease in volume due to charged groups (electrostriction) is ignored. Electrostriction should occur in proteins as it does in amino acids and peptides. Cohn and Edsall (19) report electrostriction values of 13.5, 16.1, and 16.1 for glycine, glycylglycine, and diglycylglycine, while in this work values of 12.6 and 19.1 ml/mole were obtained for glycine and triglycylglycine, respectively. Thus the effect of electrostriction in proteins must be nullified by a compensating factor. There may be a steric effect due to the folding and packing of the peptide chains whereby a small volume (excluded volume) is rendered inaccessible to solvent (20, 13), although the exchange reactions in heavy water showed a ready accessibility in BPA.

The available and observed $\bar{v}$ values for the macromolecules used in this study are summarized in Table III. Obviously, calculated values can be reported only for materials of known composition and functional groups. Clearly, the sedimentation method with BPA permits evaluation of $\bar{v}$ in complete agreement with calculated and magnetic float values, despite the small $\Delta\bar{v}$ value discussed above. Applied to a mixture of BPA and βLG, the value of $\bar{v}$ for BPA was about 1.5% lower and that for βLG in agreement with the calculated and reported values. The agreement of $\bar{v}$ of lipovitellin by the sedimentation and float methods indicates the applicability of the sedimentation method to lipoproteins. The minor sedimenting component, termed protein X, which always accompanies lipovitellin at pH 9.0, had a $\bar{v}$ value of 0.79±0.03 by the sedimentation method, which serves to distinguish it from γ-livetin, which had a $\bar{v}$ of 0.70±0.02 by sedimentation and 0.726±0.001 by the float method, although these two substances have similar sedimentation and electrophoretic characteristics in aqueous media. It is likely that protein X is a lipoprotein. Although the α–β-livetins could not be resolved sufficiently for accurate measurement of their individual $\bar{v}$ values, the value obtained for the mixture is reasonable for protein material.

It is worth mentioning, perhaps, that values of $\bar{v}$ are obtainable by sedimentation measurements without recourse to knowledge of solute concentration. In fact, the evaluations of $\bar{v}$ from the experiments on mixed macromolecules were made on the basis of relative concentrations only. Also, since the concentrations of the macromolecules in the mixtures were low and extrapolations were made to zero concentration, the Johnston–Ogston effect (21) would be small. In any case, the effect would be similar in aqueous and heavy water solutions.

Thus it would be possible to obtain $\bar{v}$ of macromolecules even in impure preparations in which resolvable boundaries are evident upon sedimentation in aqueous and heavy water media. A 1-ml sample containing about 10 mg of solute may be dialyzed versus solvent, dilutions made, and sedimentation coefficients determined. Density and viscosity may easily be measured upon the diffusate. The extent of isotopic exchange may be estimated or measured by direct weight increase on a quartz spiral balance of suitable sensitivity. By differentiation of equation [3] it may be estimated that neglect of this factor will introduce an error of about four to six per cent in $\bar{v}$. However, by taking an estimated figure of about 1.015 for k of protein, the error involved would be within the error of the sedimentation method of evaluating the partial specific volumes.

ACKNOWLEDGMENTS

The authors wish to thank Mr. J. Giroux and Mr. D. R. Muirhead for valuable technical assistance.

REFERENCES

1. MARTIN, W. G., COOK, W. H., and WINKLER, C. A. Can. J. Chem. **34**, 809 (1956).
2. LAUFFER, M. A. and BENDET, I. J. The hydration of viruses. *In* Advances in virus research. Vol. II. Academic Press, Inc., New York. 1954. p. 241.
3. SHARP, D. G., BEARD, D., and BEARD, J. W. J. Biol. Chem. **182**, 279 (1950).
4. SHARP, D. G. and BEARD, J. W. J. Biol. Chem. **185**, 247 (1950).
5. CHENG, P. Y. and SCHACHMAN, H. K. J. Polymer Sci. **16**, 19 (1955).
6. KATZ, S. and SCHACHMAN, H. K. Biochim. et Biophys. Acta, **18**, 28 (1955).
7. PLIMMER, R. H. A. J. Chem. Soc. **93**, 1500 (1908).
8. MARTIN, W. G., VANDEGAER, J. E., and COOK, W. H. Can. J. Biochem. and Physiol. **35**, 242 (1957).
9. MARTIN, W. G. and COOK, W. H. Can. J. Biochem. and Physiol. **36**, 153 (1958).
10. JOUBERT, F J. and COOK, W. H. Can. J. Biochem. and Physiol. **36**, 389 (1958).
11. BRICE, B. A. and HALWER, M. J. Opt. Soc. Am. **41**, 1033 (1951).
12. MACINNES, D. A., DAYHOFF, M. O., and RAY, B. R. Rev. Sci. Instr. **22**, 642 (1951).
13. CHARLWOOD, P. A. J. Am. Chem. Soc. **79**, 776 (1957).
14. SPRINGALL, H. D. The structural chemistry of proteins. Butterworth Scientific Publications, London. 1954.
15. MCMEEKIN, T. L. and MARSHALL, K. Science, **116**, 142 (1952).
16. TRAUBE, J. Ann. **290**, 43 (1896).
17. PEDERSEN, K. O. Biochem. J. **30**, 961 (1936).
18. ROBERTSON, J. M. Organic crystals and molecules. Cornell Univ. Press, Ithaca, N.Y. 1953.
19. COHN, E. and EDSALL, J. T. Proteins amino acids and peptides, Reinhold Publishing Corp., New York. 1943.
20. EDSALL, J. T. The proteins. Vol. IB, *Edited by* H. Neurath and K. Bailey. Academic Press, Inc., New York. 1953.
21. JOHNSTON, J. P. and OGSTON, A. G. Trans. Faraday Soc. **42**, 789 (1946).

THE MECHANISM OF THE PHOTOOXIDATION OF ACETALDEHYDE AT ROOM TEMPERATURE[1]

JACK G. CALVERT AND PHILIP L. HANST[2]

ABSTRACT

The initial rates of product formation in the photooxidation of acetaldehyde at room temperature have been determined through the use of infrared spectrometry. The rates of formation of the products peroxyacetic acid, carbon monoxide, carbon dioxide, methanol, formic acid, and acetic acid were determined in experiments with various pressures of acetaldehyde, oxygen, and added gases. The amounts of methylhydroperoxide and acetylperoxide formed in all of the experiments were below the detection limit of the analytical methods. The results require that some modification and corrections be made to the mechanism suggested by McDowell and Sharples.

INTRODUCTION

Recently McDowell and Sharples (1) published a series of kinetic studies of the photooxidation of acetaldehyde and propionaldehyde. The reactions were followed by the titration of the peroxyacid formed. Reported here is a study of the photooxidation of acetaldehyde in which a more detailed product analysis has been made through infrared absorption spectroscopy. The results show that the simple mechanism which McDowell and Sharples have inferred from their rate studies is very incomplete, and in some respects, it is incorrect. Some suggested modifications and corrections to their mechanism are presented.

EXPERIMENTAL

Apparatus and Materials

Our experiments were basically similar to those of McDowell and Sharples (1). We used comparable amounts of acetaldehyde in oxygen, and we photolyzed at room temperature with light in the range 3000–3300 Å. In order to accelerate the rates and facilitate the identification of the products of the chain-initiating and chain-terminating reactions, we used intensities about 1000 times those employed by McDowell and Sharples.

The acetaldehyde (Eastman-Kodak, white-label, fractionated at reduced pressure), oxygen (Linde tank gas), and other added gases were mixed in a 10-cm Pyrex-body infrared absorption cell which was mounted in the sample beam of a Perkin–Elmer Model 21 double beam infrared spectrometer. The side of the cell was exposed to the radiation from a Pyrex-jacketed, water-cooled, high pressure mercury arc (AH-6) which was fastened about 10 inches from the cell. The absorption characteristics of the water jacket and the cell body limited the effective radiation to the range 3000–3300 Å. The maximum intensity of the light absorbed by the aldehyde was near 3100 Å.

The other reactant gases and standards for analysis were obtained as follows: tetramethylethylene was the research grade Phillips product; peroxyacetic acid and acetylperoxide were obtained from Becco and purified by distillation at reduced pressure; ozone was prepared as needed by a simple ozonizer apparatus; the oxides of carbon were reagent gases of the Air Reduction Co.; methanol was the Mallinckrodt Analytical

[1]*Manuscript received May 25, 1959.*
Contribution from the McPherson Chemical Laboratory, The Ohio State University, Columbus 10, Ohio.
[2]*Present address: Physics Section, AVCO Research and Advanced Development, Wilmington, Massachusetts, U.S.A.*

Reagent; acetic acid was the DuPont Reagent product; nitrogen was the Linde dry tank gas.

Procedures and Results

The total pressure of the reaction mixture was adjusted to about 740 mm by the addition of nitrogen gas. Infrared absorption spectra of the products of the runs and standard gases were measured under similar conditions of pressure, resolution, and absorption.

The scale expansion feature of the Perkin–Elmer Model 21 infrared spectrometer made possible the determination of initial rates of formation of the products. Since it appears that similar application of this valuable technique has not been made in previous published kinetic studies, we wish to describe the method briefly. The scale expansion enables one to magnify small absorptions by selection of a 5-, 10-, or 20-fold signal amplification. With this amplification "initial" rates are easily measurable on amounts of material which normally would escape detection by infrared analysis. In the study here reported an accurate rate could be determined after only a few tenths of one per cent conversion of the reactants. The concentrations of the products were determined at the characteristic absorption regions: peroxyacetic acid, 8.1 and 3.05 μ; acetic acid, 7.7 μ; carbon dioxide, 4.31 μ; carbon monoxide, 4.63 μ; methanol, 9.68 μ; formic acid, 9.05 μ; methylhydroperoxide, 12.2 μ; acetylperoxide, 8.6 and 11.75 μ; methane, 7.7 μ; ethane, 12.4 μ; acetaldehyde, 3.7, 5.69 μ. There were no unexplained regions of absorption. Illustrative of the rate data obtained by this method is that given in Fig. 1

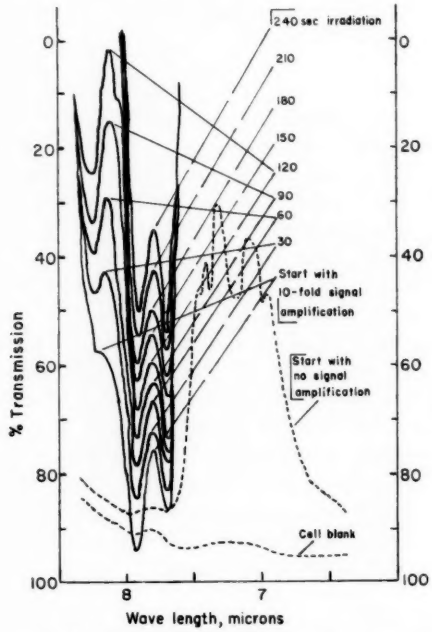

FIG. 1. A typical portion of the infrared absorption spectrum of an irradiated acetaldehyde–oxygen mixture, recorded during run 2 of Table I: the upper dotted curve shows the initial absorption of the mixture without amplification; the multiple peaks at 7.8 (due to CH_3CO_2H) and 8.1 μ (due to CH_3CO_3H) were recorded with a 10-fold signal amplification after successive 30-second exposures.

TABLE I

Initial rates of product formation in the photooxidation of acetaldehyde (3000–3300 Å, temperature 20°)

Run No.	Pressure of reactant or added gases, mm			Initial rates of product formed, mm/min					R_{CH_3OH}	$R_{CO_2} + R_{CH_3OH}$
	O_2	CH_3CHO	Added gas	CO_2	CH_3OH	CO	CH_3CO_2H	CH_3CO_3H	R_{CO_2}	$2R_{CH_3CO_3H}$
1	690	42.5	None	0.11	0.13	0.29	—	—	1.2	—
2	650	42.5	N_2, 50	0.12	0.13	0.30	0.020	0.55	1.1	0.23
3	247	42.5	N_2, 471	0.12	0.14	0.32	0.009	0.59	1.2	0.22
4[a]	43	42.5	N_2, 640	0.27	0.32	0.29	0.014	1.15	1.2	0.26
5	25	42.5	N_2, 670	0.29	0.34	0.29	0.015	1.13	1.2	0.28
6	8	42.5	N_2, 680	0.61	0.53	0.29	0.021	1.88	0.9	0.30
7	2	42.5	N_2, 700	—	—	—	0.021	2.29	—	—
8[b]	0	42.5	N_2, 700	0.00	0.00	0.09_4	0.000	0.00	—	—
9	745	5.0	None	0.0059	0.0052	0.026	0.0057	< 0.01	0.9	> 0.56
10	8	5.0	N_2, 730	0.022	0.017	0.025	0.0053	0.026	0.8	0.75
11	650	42.5	CH_3CO_3H, 4	0.14	0.14	—	0.14	loss	1.0	—
12	12	42.5	CH_3CO_3H, 4 N_2, 680	0.31	0.27	0.24	0.063	0.38	0.9	—
13	700	42.5	O_3<1	0.87[c]	0.90[c]	0.29	—	—	1.0	—
14[d]	676	42.5	$Me_2C{=}CMe_2$, 20	0.017	0.046	0.18	0.0057	< 0.05	2.7	—
15[d]	11	42.5	$Me_2C{=}CMe_2$, 12	0.0081	0.053	0.12	0.0041	< 0.05	6.5	—

[a]After 10 minutes' exposure there was no detectable amount of CH_3O_3H (on 20-fold amplification) at its absorption band at 12.2 μ or $(CH_3CO_2)_2$ at its 8.6- and 11.8-μ bands; $R_{CH_3O_2H} < 0.003$ mm/minute; $R_{(CH_3CO_2)_2} < 0.0005$ mm/minute.

[b]Other measurable product rates in this O_2-free run were: $R_{C_2H_6} = 0.01_4$; $R_{CH_4} = 0.083$.

[c]These rates have been corrected for a large thermal reaction, so the accuracy of them is not large.

[d]Possible traces of CH_3COCH_3 formed as detected at the characteristic band near 8.2 μ.

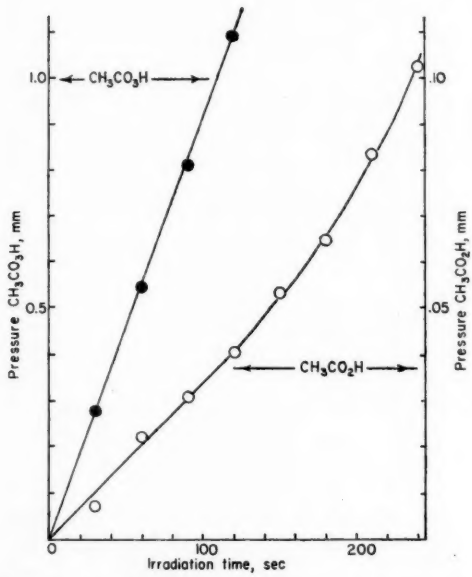

FIG. 2. Pressures of the peracetic acid and acetic acid products as a function of irradiation time (calculated from the data of Fig. 1, and recorded during run 2 of Table I).

(obtained for run 2 of Table I). Shown are the 7.8- (acetic acid) and 8.1-μ (peroxyacetic acid) regions scanned with 10-fold signal amplification after successive exposures each of 30 seconds' duration. These data yielded the product pressure – time plot of Fig. 2. All of the initial product rate data summarized in Table I were obtained from similar absorption measurements.

One of the products of the reaction, formic acid, is not shown in Table I since it was impossible to determine it accurately with small conversions; the major absorption bands

TABLE II

Mass balance of the products of the photooxidation of acetaldehyde at room temperature (experiments with 30 minutes' exposure)

	Run	
	1	2[a]
Pressure O_2, mm	670	670
Pressure CH_3CHO, mm	34	32
Products pressure in mm		
Peroxyacetic acid	2.8	1.4
Acetic acid	0.4	0.2
Methanol	2.6	0.5
Formic acid (as monomer)	2.2	0.5
Carbon dioxide	1.8	0.5
Carbon monoxide	2.0	0.7
Acetylperoxide	None detected	None detected
Methylhydroperoxide	None detected	None detected
Acetaldehyde, unreacted	27.3	29.4
Total acetaldehyde accounted for	34.8	32.4

[a]Intensity of run 2 is about one-third that of run 1; the arc-to-cell distance was increased.

overlapped those of the reactant, acetaldehyde. A test for the mass balance of the products was made in similar experiments in which a more extensive conversion was allowed (exposure time 30 minutes). These results are shown in Table II. It is seen that an adequate accounting can be made for all of the acetaldehyde which has reacted.

There was no measurable dark reaction between oxygen and acetaldehyde under any of the conditions used. When ozone was added to the oxygen–aldehyde mixture a rapid dark reaction occurred for which correction was made to estimate the "photochemical" rates (run 13, Table I).

DISCUSSION

Limitations of the McDowell and Sharples Mechanism

Our data show that the McDowell and Sharples mechanism (1) of acetaldehyde photooxidation should be revised in several important respects. First, the conventional chain-initiating steps which they suggest involving peroxy radicals seem unimportant for this system:

$$CH_3CHO + h\nu \rightarrow CH_3 + CHO \qquad [I]$$

$$R + O_2 \rightarrow RO_2 \ (R = CH_3 \text{ or } CHO) \qquad [1]$$

$$RO_2 + CH_3CHO \rightarrow RO_2H + CH_3CO. \qquad [2]$$

Methylhydroperoxide, one of the expected products of reaction [2], was below the detection limit of the infrared equipment using the most sensitive 20-fold signal amplification. We estimate that the rate of formation of this product, if formed at all, must be less than 0.003 mm/minute. If this result is coupled with the facts that the chain lengths are relatively short in our experiments,* and methylhydroperoxide is comparatively stable under the conditions used (2), then reaction [2] of the McDowell and Sharples mechanism must be unimportant in the photooxidation of acetaldehyde.

Secondly, the expected product of the termination step of the McDowell and Sharples mechanism, acetylperoxide, was not formed in detectable quantities in our experiments; its rate of formation in run 4 of Table I must have been less than 0.0005 mm/minute, if it was formed at all. Obviously, one should question the McDowell and Sharples assignment of the kinetic rate constant of the termination reaction derived from rotating sector experiments to the reaction [3]:

$$2CH_3CO_3 \rightarrow (CH_3CO)_2O_2 + O_2. \qquad [3]$$

Thirdly, cognizance should be taken of the variety of products other than peroxyacetic acid which are formed in the photooxidation of acetaldehyde, as they are not insignificant, and a proper consideration of them should help in the correct mechanism choice.

Revised Mechanism of Acetaldehyde Photooxidation

In view of our findings in the study of the azomethane photooxidation (2) and data here presented, we favor a mechanism of acetaldehyde photooxidation involving ozone as an intermediate product. Ozone has not been detected by direct spectroscopic observations in the irradiated acetaldehyde–oxygen system. However, it is a reasonable extrapolation

*$\Phi_{CO} \cong 0.2$ *in the oxygen-free acetaldehyde photolysis at 25° and 3130 Å (3). Using the rate data of Table I, run 8 (in the absence of oxygen) and run 7, one estimates the maximum chain length for peroxyacetic acid formation in these experiments to be about 20; this assumes that the primary efficiency of free radical formation in acetaldehyde photolyses at 3130 Å is 0.2 (4, 5). The estimate of chain length represents a maximum since the primary efficiency may be considerably higher (0.8) in experiments at low oxygen pressures. See the discussion in the section on the primary efficiency.*

to this system from the systems in which it has been observed. If we accept the hypothesis of ozone participation in the mechanism, we expect the steady state concentration of ozone to be very low (10^{-3} to 10^{-5} mm) because of its rapid reaction [4] with free radicals.

$$O_3 + R \rightarrow RO + O_2 \qquad [4]$$

Reaction [4] would not have the three-body restriction which has been observed for the reaction of methyl radicals with O_2 (6, 7, 8), and it would be considerably faster. We consider the mechanism here proposed to be a reasonable postulate which is consistent with the facts at hand and is worthy of further testing.

Chain-initiating Steps

It is probable that the formation of CH_3O_2 (and CHO_3) radicals in the photooxidation of acetaldehyde occurs as the first step in the reaction of CH_3 (and CHO) with O_2. The fact that the expected products, CH_3O_2H and HCO_3H, are not found in the photooxidation of acetaldehyde, but rather CH_3OH and HCO_2H are observed, suggests the rapid removal of these radicals by some other path than H-abstraction. We feel that the removal of CH_3O_2 (and HCO_3) may occur either by the mechanism of Bell and coworkers (9),

$$2CH_3O_2 \rightarrow 2CH_3O + O_2, \qquad [5]$$

or by the alternative reactions which we have favored in the azomethane photooxidation (2);

$$CH_3O_2 + O_2 \rightarrow CH_3O + O_3 \qquad [6]$$

$$HCO_3 + O_2 \rightarrow HCO_2 + O_3. \qquad [7]$$

In either case chain initiation in the photooxidation of acetaldehyde is presumed to involve the CH_3O and HCO_2 radicals; this interpretation is consistent with the observed products. If reaction [5] were the source of CH_3O we would expect some H-abstraction from aldehyde and a detectable yield of CH_3O_2H (the rate of [5] is proportional to $[CH_3O_2]^2$); to expect this reaction to occur to the exclusion of [2], whose rate is proportional to $[CH_3O_2][CH_3CHO]$, seems unrealistic. Thus we favor the alternative mechanism of CH_3O and HCO_2 formation in reactions [6] and [7].

Chain-termination Reactions

Some obvious alternatives to the unobserved acetylperoxide formation for chain termination are reactions [8], [9], and [10]:

$$2CH_3O \rightarrow CH_3OH + CH_2O \qquad [8]$$

$$CH_3O + CH_3CO_3 \rightarrow CH_2O + CH_3CO_3H \qquad [9]$$

$$CH_3O + CH_3CO_2 \rightarrow CH_2O + CH_3CO_2H. \qquad [10]$$

Under our conditions CH_2O would be rapidly converted to CHO_2H, with small amounts of CO, CO_2, and possibly other products (2).

The Efficiency of Radical Formation in Acetaldehyde Photooxidation

Note in Fig. 3 the increase in the rate of formation of the peroxyacetic acid, methanol, and carbon dioxide products as the oxygen pressure is lowered. We interpret this to indicate an increased quantum efficiency of radical formation at the lower oxygen pressures. That is, a certain fraction of the excited acetaldehyde molecules are deactivated by oxygen, and the fraction so deactivated before the possible decomposition into radicals decreases with decrease in oxygen pressure. With this interpretation we estimate from

the relative rates of CH_3CO_3H formation at the high and the low oxygen pressures that about 76% of the electronically excited ($\lambda \cong 3100$ Å) molecules of acetaldehyde which normally decompose in the absence of oxygen can be deactivated at the high concentrations of oxygen. This value checks well with the observed deactivation of 3130 Å light-activated acetaldehyde by added iodine. In this case it has been estimated that 75% of the electronically excited aldehyde molecules which decompose in the absence of iodine are deactivated when iodine is added (10).

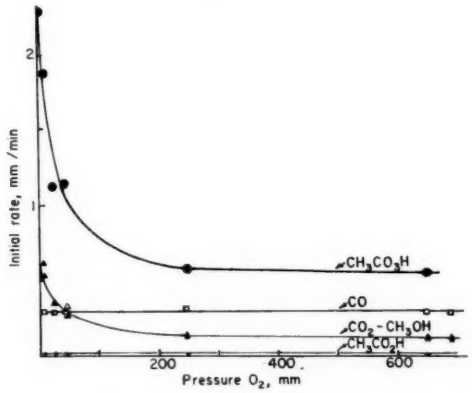

FIG. 3. Initial rates of formation of products of the photooxidation of acetaldehyde as a function of oxygen pressure: $P_{CH_3CHO} = 42.5$ mm; $P_{N_2} + P_{O_2} + P_{CH_3CHO} \cong 740$ mm; wave lengths of absorbed light, 3000–3300 Å; temperature, 20°.

Mechanism of Formation of CO_2 *and* CH_3OH

From the data of Table I the ratio R_{CH_3OH}/R_{CO_2} is seen to be near unity. In Fig. 3 it is seen that the rate of increase of CO_2 and CH_3OH at low oxygen pressures parallels that for CH_3CO_3H. In view of these results we first postulated that the CO_2 and CH_3OH arose from the thermal or photochemical decomposition of a portion of the primary product peroxyacetic acid. However, the initial rates of formation of CO_2 and CH_3OH are not measurably increased when peroxyacetic acid is added at the start of the run (see runs 11 and 12 of Table I), so that these products clearly are not derived from peroxyacetic acid. The only difference in the runs with added peroxyacid is the acceleration of the rate of CH_3CO_2H formation. This effect will be described later.

If we accept the conversion of CH_3 to CH_3O in the acetaldehyde–oxygen system, then there are several alternatives which may be considered in the explanation of the CO_2 and CH_3OH rate data.

$$CH_3CO_3 + M \rightarrow CH_3O + CO_2 + M \quad [11]$$

$$CH_3CO_3 + O_2 \rightarrow CH_3CO_2 + O_3 \quad [12]$$

$$CH_3CO + O_3 \rightarrow CH_3CO_2 + O_2 \quad [13]$$

$$CH_3CO_2 \rightarrow CH_3 + CO_2. \quad [14]$$

The relative constancy of the ratio, $(R_{CO_2} + R_{CH_3OH})/2R_{CH_3CO_3H}$, of Table I, is consistent with the occurrence of reaction [11], provided that the CH_3CO_3 radical decomposition is in the second order region and that [11] is usually followed by CH_3OH formation

by H-abstraction. It is likely that peroxyacetic acid is formed in the chain-propagating reaction [15], which is commonly proposed.

$$CH_3CO_3 + CH_3CHO \rightarrow CH_3CO_3H + CH_3CO. \qquad [15]$$

If we assume that [11] and [15] are homogeneous reactions and that these reactions are the major sources of the CO_2, CH_3OH, and CH_3CO_3H, then we can explain the small variation of the ratio, $(R_{CO_2} + R_{CH_3OH})/2R_{CH_3CO_3H}$, in terms of the differences in the efficiencies of CH_3CHO, O_2, and N_2 as M in reaction [11]. However, the increase in this ratio at low aldehyde pressures suggests that CH_3CHO is a poorer M than N_2 and O_2, a result which is unexpected.

We favor the alternative reactions for CO_2 and CH_3OH formation, [12], [13], and [14]; these suggest the formation and participation of ozone. In terms of this mechanism choice, the observed simultaneous increase in CH_3OH, CO_2, and CH_3CO_3H can be rationalized as follows: as the oxygen pressure is lowered, the rate of radical formation from the photodecomposition of acetaldehyde is increased; assuming reactions [6] and [7], we expect the ozone concentration to increase, and thus [13] and [14] would become more important. As the ratio of $[O_2]/[CH_3CHO]$ is increased, one expects that the fraction of the CH_3CO_3 radicals which form peroxyacetic acid in [15] would decrease compared to that reacting by [12]. This is the trend observed in the last column of Table I.

Some support for the participation of ozone in the photooxidation of acetaldehyde was obtained in runs 13, 14, and 15 of Table I. In run 13 a small quantity of ozone was added at the start of the run. Ozone initiates the thermal oxidation of acetaldehyde, and dark reaction was observed. However, after correction for the large dark rates, the "photochemical" rates of CO_2 and CH_3OH formation were much in excess of their normal values; compare runs 2 and 13 of Table I. The conclusions from this experiment are not unambiguous, but the results provide indirect support of the reactions [13] and [14]. In experiments 14 and 15 quantities of tetramethylethylene were added to the acetaldehyde–oxygen mixture. The indication of a trace of infrared light absorption near 8.2 μ suggests the formation of CH_3COCH_3 in these experiments. We have interpreted this as evidence for the presence of ozone in these experiments; ozone reacts rapidly with tetramethylethylene to form acetone (2). The amount of acetone formed in these experiments was much less than that found in the azomethane–oxygen–tetramethylethylene experiments reported previously (2), but the thermal reactivity of ozone with acetaldehyde might account for the difference.

Until the spectroscopic tests for ozone in the irradiated acetaldehyde–oxygen mixtures are made, one can consider ozone participation only as an interesting possibility, but we feel that there is strong indirect evidence that favors its consideration.

The Formation of Carbon Monoxide and Acetic Acid

The mechanism of formation of carbon monoxide and acetic acid is by no means clear from this work. It has been demonstrated that peroxyacetic acid is converted to acetic acid in the irradiated aldehyde–oxygen mixtures (see runs 11 and 12 of Table I). The acceleration of rate of formation of acetic acid with time is apparent in Fig. 2, even after only 2 minutes of irradiation. However, initial rates of formation of acetic acid do not parallel those of the peroxyacetic acid, so that the origin of the acetic acid formed initially by the conversion of peroxyacetic acid is ruled out. Perhaps the acetic acid is formed from CH_3CO_2 radicals which do not react entirely by [14] but to a minor extent abstract hydrogen from acetaldehyde or disproportionate with CH_3O reaction [11]. The alternative of acetic acid formation directly from electronically excited acetaldehyde molecules can not be excluded.

There are several possible sources of CO, for example, CH_2O photodecomposition, or reactions of the radicals, HCO, HCO_3, and CH_3CO. It appears to be formed in non-chain processes at a rate proportional to the absorbed light intensity.

In conclusion it should be stated that the photooxidation of acetaldehyde is a complex process, quite different from the simple oxidation mechanism which seems to be accepted currently. Much additional experimentation will be necessary to establish many of the interesting details of this reaction.

ACKNOWLEDGMENT

The authors gratefully acknowledge the financial support of this work by the United States Public Health Service, National Institutes of Health, Bethesda, Maryland.

REFERENCES

1. McDowell, C. A. and Sharples, L. K. Can. J. Chem. **36**, 251 (1958).
2. Hanst, P. L. and Calvert, J. G. J. Phys. Chem. **63**, 71 (1959).
3. Leighton, P. A. and Blacet, F. E. J. Am. Chem. Soc. **55**, 1766 (1933).
4. Blacet, F. E. and Heldman, J. D. J. Am. Chem. Soc. **64**, 889 (1942).
5. Blacet, F. E. and Loeffler, D. E. J. Am. Chem. Soc. **64**, 893 (1942).
6. Hoare, D. E. and Walsh, A. D. Trans. Faraday Soc. **53**, 1102 (1957).
7. Christie, M. I. Proc. Roy. Soc. (London), A, **224**, 411 (1958).
8. Sleppy, W. C. and Calvert, J. G. J. Am. Chem. Soc. **81**, 769 (1959).
9. Bell, E. R., Raley, J. H., Seubold, F. H., and Vaughan, W. E. Discussions Faraday Soc. **10**, 242 (1951).
10. Calvert, J. G., Pitts, J. N., Jr., and Thompson, D. D. J. Am. Chem. Soc. **78**, 4239 (1956).

THE STUDY OF ELECTRICALLY DISCHARGED O_2 BY MEANS OF AN ISOTHERMAL CALORIMETRIC DETECTOR[1]

L. Elias, E. A. Ogryzlo,[2] and H. I. Schiff

ABSTRACT

Molecular oxygen was subjected to an electrodeless discharge in the pressure range 0.1–3 mm Hg. The oxygen atom concentration was measured as a function of time in a flow system by means of a movable atom detector which consisted of a platinum wire coated with a suitable catalyst for atom recombination. The atom concentration was calculated from the heat liberated when the detector was operated under isothermal conditions. The surface recombination was found to be first order in the atom concentration. A value of 7.7×10^{-5} was obtained for the recombination coefficient (γ) on Pyrex. No temperature dependence for γ was observed. The gas phase recombination of oxygen atoms was found to be consistent with the mechanism

$$O + O_2 + M \rightarrow O_3 + M$$
$$O + O_3 \rightarrow 2O_2$$

The rate constant for the third-order reaction was found to have a value of 1.0×10^{14} cc^2 mole^{-2} sec^{-1}, and a small negative temperature dependence.

Evidence was also obtained for the presence of considerable amounts of excited molecular oxygen in electrically activated O_2.

INTRODUCTION

Considerable interest has been shown recently in the reactions of atomic oxygen, particularly those which occur in the upper atmosphere. To study the rates of recombination or reaction of oxygen atoms, it is necessary to know how their concentration changes with time. Such rapid reactions are often best studied in flow systems with movable atom detectors. Of the various methods available for measuring atom concentrations, isothermal calorimetry appears to be the most readily adaptable for use as a movable probe. This method was used successfully by Tollefson and Le Roy (1) to study the kinetics of hydrogen atom reactions. They measured the heat liberated by the recombination of H-atoms on a platinum or tungsten wire mounted on an adjustable column of mercury. The same technique has been used in the present study with minor modifications.

The present work was undertaken to study the kinetics of the recombination of oxygen atoms obtained by subjecting molecular oxygen to an electrical discharge. In the course of the investigation, evidence was obtained which strongly suggests the presence of considerable amounts of excited molecular oxygen.

EXPERIMENTAL

Principle of the Method

Normal oxygen is passed over a spiral of platinum wire coated with a material of high catalytic activity for recombining atoms. A known electric current "i_0" is passed through the wire, and its resistance R is measured. The gas is then activated by electrical discharge. The atoms which reach the wire are recombined on its surface. To compensate for the heat liberated by the atom recombination, the current through the wire is reduced to some new value "i", such that its resistance, and consequently its temperature, is restored

[1]*Manuscript received June 18, 1959.*
Contribution from the Department of Chemistry, McGill University, Montreal, Quebec. This work has been supported in part by the Air Force Cambridge Research Center under Contract No. AF19(604)-1488, and in part by the Defence Research Board of Canada.
[2]*Holder, National Research Council Fellowship 1956–58.*

to the initial value. The difference in electrical energy required to keep the wire isothermal can readily be calculated from the relation:

[1] $$\Delta W = R(i_0^2 - i^2).$$

Since the temperature of the wire is the same in the presence and in the absence of atoms, loss of heat by radiation or conduction through the leads should be unaltered. Thus, if the wire removes all the atoms from the gas stream, the flow rate of atoms F_0 can be deduced from the equation

[2] $$F_0 = \Delta W/\Delta H$$

where ΔH is the heat of atom recombination, 58.5 kcal/mole of O-atoms. The validity of this relation will be considered below.

Materials

Reproducible results could be obtained only when the nitrogen content in the oxygen was low. The presence of this impurity could be detected readily from the afterglow produced by the reaction of O-atoms with the NO formed in the discharge. U.S.P. grade tank oxygen supplied by Linde Air Products, rated at less than 0.1% nitrogen, was used. Oxygen was also produced by thermal decomposition of $KMnO_4$ and from liquified tank oxygen from which the first 80% of the distillate had been discarded. The oxygen from all three sources gave identical results for the recombination rates.

Nitric oxide, obtained from the Matheson Company, was purified by repeated trap-to-trap distillations; NO_2 was made by reaction of NO with O_2. All other gases were commercial products of reagent grade purity.

Apparatus

A conventional flow system was used for all experiments. A linear velocity of 20 to 40 cm/sec and a pressure of 0.5 to 5 mm Hg was found to be suitable for atom recombination studies. The flow rates of all gases were adjusted by means of fine-control needle valves and measured by calibrated U-tube flowmeters. All mercury surfaces were covered with "octoil".

The oxygen was activated by a "Raytheon" microwave generator operating at 2450 Mc/sec with a maximum power output of 125 w. The discharge could be excited in a 13 mm O.D. quartz tube over a pressure range from 0.1 to 20 mm Hg. The use of a Pyrex rather than a quartz tube resulted in some foreign material being liberated from the glass which produced erratic results.

The discharge tube was connected at A by a 20-cm length of Pyrex tubing to the reaction tube shown in Fig. 1; the inner diameter was 17.5 mm and its length was 35 cm. It was surrounded by a jacket B through which thermostatted liquid could be circulated and which was, in turn, surrounded by a vacuum jacket C. Inert gases, NO and NO_2 were introduced at G into the gas stream through a multiple jet located a few centimeters below the top of the jackets. The pressure was measured by McLeod gauges connected at M_1 and M_2. The reaction tube was cleaned frequently with dilute solutions of HF.

The detector D_1 was mounted on a rack which could be moved by rotation of a pinion attached to a standard taper joint equipped with an "O"-ring. The platinum ring R was attached to the top of the rack to ensure that the detector maintained a central position in the reaction tube.

The movable detector D_1, and the stationary detector D_2, were made of 60-cm lengths of No. 30 gauge platinum wire coiled into spirals. Since platinum was found to be in-

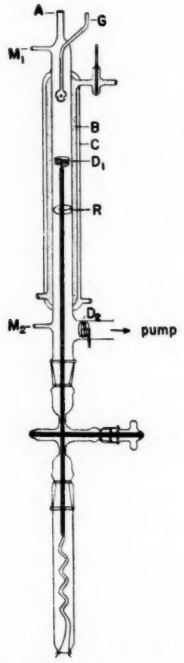

FIG. 1. Reaction tube: A, O_2 and O entry; G, multiple jet for reactant entry; M_1 and M_2, McLeod gauges; B, thermostatting jacket; C, vacuum jacket; D_1, movable detector; D_2, fixed detector.

efficient in recombining O-atoms, a layer of silver was deposited on the wire by electrolysis. A more adherent coating was obtained by heating the electroplated wire until the surface became shiny. When subjected to an atmosphere containing O-atoms, the metal is rapidly converted to the oxide, which forms an excellent catalyst for O-atom recombination.[3]

The oxides of cobalt, nickel, manganese, and copper were also found to be good catalysts. For the length of platinum wire used, zinc and cadmium coatings were only about half as efficient in destroying the atoms.

The detector formed one arm of a Wheatstone bridge. The current through the detector was determined from the potential drop across a standard resistor forming the adjacent arm of the bridge. To keep the bridge in balance when the oxygen was activated, the current through the detector was altered by means of a variable resistor in series with the bridge.

RESULTS AND DISCUSSION

(*1*) *Test of Detector*

Equation [2] is valid only if the detector removes all the atoms from the gas stream. To test this, measurements were made simultaneously with detectors D_1 and D_2. When the movable detector D_1 was above the pumping lead, D_2 showed no heat effect. When D_1 was lowered below the pumping lead, D_2 showed the same change in wattage previously shown by D_1 when it was just above the pumping lead.

A further test for the catalytic activity of the detector is obtained when a small amount

[3]*A stable detector could not be made from silver metal, since the thickness of the oxide layer would change with time.*

of NO is added to the gas stream. The green glow resulting from the reaction

$$O + NO \rightarrow NO_2 + h\nu$$

provides a very sensitive test for the presence of O-atoms.[4]

The glow was found to be completely extinguished by the detector. The sharp discontinuity of the glow at the detector also indicated that the rate of removal of atoms from the gas stream was controlled by the linear flow rate of the gas, and not by diffusion resulting from the atom concentration gradient established at the detector.

If the heat measured corresponds to the heat of recombination of all the atoms, it should be independent of the detector temperature. For the silver detector used, this was found to be true up to a detector temperature of 100° C. At higher temperatures the measured atom concentration decreased, and the NO–O glow was seen to extend beyond the detector. The temperature at which this occurs depends on the size of the detector. This indicated that, as the temperature increases, the silver oxide surface becomes less efficient, so that a larger surface area is required to effect complete recombination.

This observation is interesting for another reason. The method can be criticized on the grounds that the temperature distribution along the detector will be different when it is heated electrically only, and when the upper rings of the spiral are also heated by atom recombination, even though the electrical resistance may be the same in both cases. However, the atom concentration measured when the atoms are recombined on the first few rings (at the lower temperatures) was the same as when a number of rings were required (at higher temperatures). This effect must therefore be negligible.

(2) *Effect of Thermal Conductivity*

If the detector is to operate under truly isothermal conditions, it is necessary for the rate of heat loss to be identical in the presence and in the absence of atoms. This condition will be satisfied for radiation and conduction along the leads. However, the heat lost by conductivity in the gas could be altered if the gas temperature or composition changes upon activation of the gas.

The temperature of the discharged gas was measured by substituting a 1-mm glass-covered thermistor for the detector. Argon and helium, passed through the discharge at the same pressure, showed no increase in temperature at distances greater than 10 cm beyond the discharge. A maximum temperature rise of 2° C was observed in the center of an activated O_2 stream at the same distance. To determine the effect of such a temperature change on the detector readings, normal oxygen, initially at 25° C, was passed through the reaction tube which was thermostatted at 5° C. The difference in electrical energy required to keep the temperature of the wire constant at the top and in the middle of the reaction tube was found to be less than 0.004 *w*. This can be compared with a maximum value of 0.03 w calculated from the heat capacity of the oxygen. The heat given to the detector by atom recombination is in the order of 1.0 w. Thus, the effect of a 2° rise in gas temperature will be well within experimental error.

The change in thermal conductivity due to change in composition of the oxygen when it is subjected to electrical discharge will also have a negligible effect on the detector readings. The steady-state ozone concentration is very low, while excited molecular oxygen will not be expected to have a thermal conductivity appreciably different from normal oxygen. The slight change in thermal conductivity due to the presence of O-atoms above the detector would be expected to produce a change in detector reading which is less than the experimental error.

[4] *The glow also provides a good test for the design of the inlet jet, since the mixing pattern can be readily observed. Furthermore, it can be used to determine the upper limit of reactant flow rate in an* O-*atom reaction which can be used before encountering back diffusion of reactant.*

(3) *Comparison with other Techniques for Determining Atom Concentrations*

Experiments with discharges through mixtures of oxygen and argon or helium at a fixed total pressure showed that the ratio of atomic to molecular oxygen increased as the partial pressure of oxygen in the mixture decreased. An attempt was therefore made to prepare a known atom concentration by complete dissociation. However, the maximum atom concentration measured by the detector never exceeded 85% of that corresponding to complete dissociation. It is possible that complete dissociation could not be achieved in this way.

A comparison was made between the atom concentrations measured by the detector and by a Wrede gauge (2). The gauge was constructed from a fritted disk having a maximum pore diameter of 5 μ; the pressure difference across the disk was measured with a sensitive pressure transducer (Statham Instrument Co.). A small silver coil was placed near the disk, on the transducer side, to ensure complete atom recombination. Comparisons were made over the pressure range 0.7 to 3.3 mm. In this region the atom concentration measured by the detector was proportional to that measured by the Wrede gauge but higher by about 10%.

An attempt was made to measure the atom concentration by chemical titration. This method had previously been found to be very successful in testing the accuracy of a platinum detector in measuring deuterium atom concentrations (3). Since the reaction between D-atoms and ethylene is very rapid, introduction of an excess of C_2H_4 consumed all the D-atoms within a few millimeters of the inlet jet. The amount of deuterium atoms in the products was determined mass spectrometrically and used to calculate the atom concentration. The concentrations determined in this manner were found to agree with those determined by the detector within 0.5%.

Kaufman (4) has recently used an NO_2 titration for estimating O-atom concentrations. The reaction

$$NO_2 + O \rightarrow NO + O_2 \qquad [1]$$

is much faster than the light-emitting reaction

$$NO + O \rightarrow NO_2 + h\nu. \qquad [2]$$

Consequently, if the flow rate of NO_2 is gradually increased, a glow will be observed until the NO_2 concentration equals the O-atom concentration. At this point all the O-atoms will be consumed by reaction [1] and the glow will recede to the jet. This method was found by us to yield the same atom concentration within experimental error as the method of Spealman and Rodebush (5). These workers titrated the O-atoms with a large excess of NO_2, trapped the products at liquid air temperature, and measured the amount of NO formed. The O-atom concentration measured by NO_2 titration was found to be proportional to that measured by the silver oxide detector but lower by approximately 25%.

(4) *Evidence for the Existence of Excited Molecules*

The discrepancy between the atom concentrations determined by the detector and by the NO_2 titration may be due to the presence of some other species which does not react with NO_2 but which liberates heat on the detector. A cobalt oxide detector was found to show an even greater discrepancy with the titration value, which suggests that it is an even more efficient surface for deactivating the second species. To test this suggestion, a number of additional experiments were performed.

When the movable detector D_1 (Fig. 1) was coated with cobalt oxide while the fixed

detector D_2 was coated with silver oxide, no heat was liberated on D_2. However, when D_1 was silver oxide while D_2 was cobalt oxide, an appreciable amount of heat was measured by D_2.

When a sufficient amount of C_2H_4 was introduced through the inlet jet to consume all the atoms, the cobalt oxide detector still measured an appreciable quantity of heat. When an excess of NO_2 was used to destroy all the atoms, a silver oxide detector at D_1 measured only a very small amount of heat, while a cobalt detector below this at D_2 measured an amount of heat which was even greater than it measured before the NO_2 was introduced. This could be due to the additional excited O_2^* formed in the reaction

$$NO_2 + O \rightarrow NO + O_2^*.$$

When a mercury mirror was deposited just beyond the discharge tube, no atoms passed this point, as evidenced from the lack of glow when NO was introduced through the inlet jet. Nevertheless, heat was liberated on the cobalt detector, which corresponded to over 25% of the heat measured by the detector in the absence of the mercury mirror. The magnitude of this heat effect decreased only very slowly down the reaction tube, thus indicating a long lifetime for the excited species.[5]

Addition of NO, NO_2, CO_2, and C_2H_4 after the mercury mirror had no effect on the heat measured by the cobalt detector. The new species therefore does not appear to be ozone, which is known to react rapidly with NO and C_2H_4.

Norrish and co-workers (6) have presented evidence that vibrationally excited O_2 molecules are deactivated in approximately one collision in 5000 by CO_2, and in one collision in 500 by NO_2. However, addition of these gases in large amounts did not decrease the heat measured by the detector. The species therefore does not appear to be vibrationally excited molecules.

The most likely excited species appears to be electronically excited O_2. If these molecules are in the $^1\Delta g$ state as suggested by Foner and Hudson (7), and by Herron and Schiff (8), the observed heat effect would correspond to about 10% of the gas being present in this form, in agreement with estimates made by these authors.

As a result of these studies, it was learnt that a freshly prepared silver oxide coated detector of the dimensions given would recombine all the atoms but deactivate only a negligible amount of the excited molecules. After five or six experiments the detector measured an increasing proportion of excited molecules and was then replated. Freshly prepared detectors were used to measure the recombination of oxygen atoms.

(*5*) *Recombination of* O-*Atoms*

The oxygen atom concentration was measured along a 20-cm length of the reaction tube over a pressure range from 0.5 to 5 mm Hg. Figure 2 shows typical second-order, and Fig. 3 typical first-order, plots for the atom concentration – time dependence. It is apparent that the atom recombination follows first-order kinetics. The following mechanism is consistent with these observations:

$$O + \text{wall} \rightarrow \tfrac{1}{2}O_2 + \text{wall} \quad [3]$$

$$O + O_2 + M \rightarrow O_3 + M \quad [4]$$

$$O + O_3 \rightarrow 2O_2 \quad [5]$$

where M is any third body.

[5]*The same effect could be obtained if the atoms were destroyed by addition of* NO_2 *rather than by the mercury deposit.*

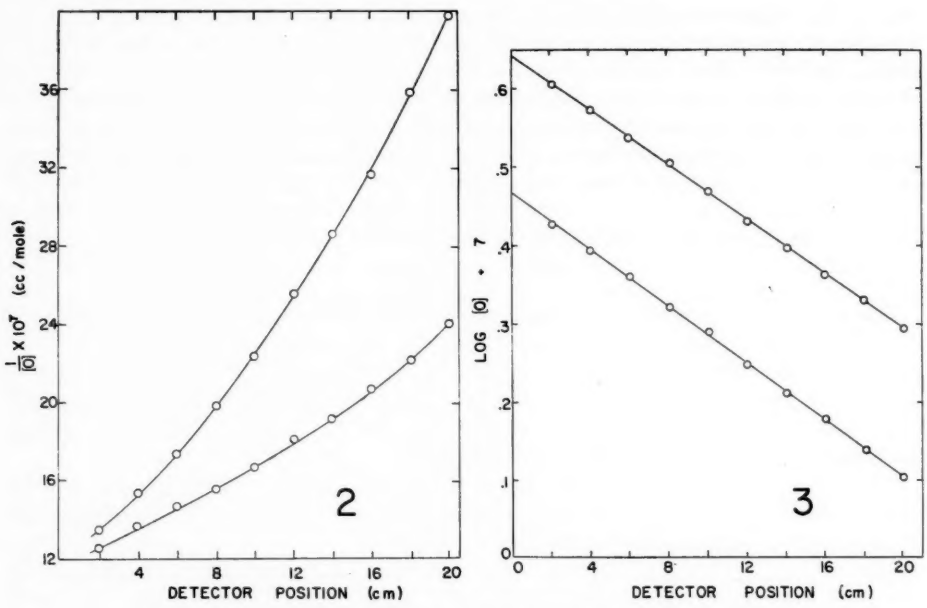

FIG. 2. Typical second-order plots of oxygen atom disappearance.
FIG. 3. Typical first-order plots of oxygen atom disappearance.

A steady-state condition can be assumed for the ozone concentration. Benson and Axworthy (9) give values of 1.3×10^9 cc mole^{-1} sec^{-1} for k_5, and 7.9×10^{13} cc^2 mole^{-2} sec^{-1} for k_4 at 293° K. If O-atoms form 10% of the gas leaving the discharge, calculations show that 70% of the steady-state ozone concentration is attained before the gas enters the reaction vessel at 0.5 mm Hg pressure, and virtually 100% at higher pressures. With this assumption the rate equation for the atom disappearance can be integrated to give:

$$\frac{1}{t}\ln\frac{[O_0]}{[O]} = k_3 + 2k_4[O_2][M]$$

where $[O_0]$ is the atom concentration at the top of the reaction tube, where t is taken as zero.

Figure 4 shows a plot of the left-hand side of this equation against $[O_2][M]$ for M = O_2. The intercept of this curve, k_3, can be used to calculate the surface recombination coefficient γ from the relation:

$$\gamma = 2k_3r/c$$

where r is the radius of the reaction tube and c is the average velocity of the atoms.

The average value of γ obtained from several sets of measurements was 0.77×10^{-4}. This can be compared with the value of 1.2×10^{-4} obtained by Linnett and Marsden (10) and 0.2×10^{-4} by Kaufman (11). Kistiakowsky and Volpi (12) deduced a minimum value of 2×10^{-4} from indirect measurements of N-atom reactions. Herron and Schiff (8) reported a value of 1.1×10^{-4} based on the assumption that all recombinations occur on the wall, and their figure therefore represents an upper limit.

The slopes of the curves in Fig. 4 yielded an average value for k_4 of 1.0×10^{14} cc^2 mole^{-2} sec^{-1}. This figure is in good agreement with the value of 2×10^{14} cc^2 mole^{-2} sec^{-1} reported by Kaufman (4) and the value of 0.79×10^{14} cc^2 mole^{-2} sec^{-1} obtained by Benson and Axworthy (9) from the thermal decomposition of ozone.

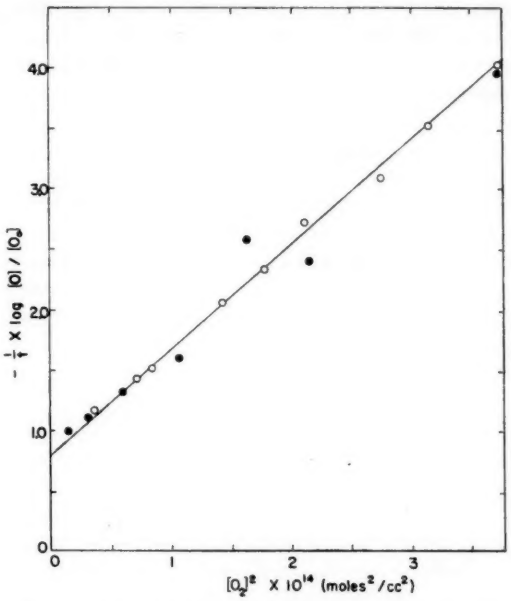

FIG. 4. The dependence of the oxygen atom disappearance on the pressure.

No differences in the rate of recombination were observed when helium or argon molecules were used as third bodies. Addition of CO_2 increased the rate of recombination but in a somewhat erratic way. If CO_2 acts simply as a third body, i.e.

$$O + O_2 + CO_2 \rightarrow O_3 + CO_2, \qquad [6]$$

the integrated rate equation could be written in the form

$$\frac{1}{t}\ln\frac{[O_0]}{[O]} - 2k_4[O_2]^2 = k_3 + 2k_6[O_2][CO_2].$$

A plot of the left-hand side of this equation against $[O_2][CO_2]$ should yield a straight line with slope $2k_6$. However, the data deviated from linear behavior to a larger extent than the estimated experimental error. No unequivocal explanation can be offered for this deviation at the present time. The best straight line through the data gave a value of $k_6 = 2.6\times10^{14}$ cc^2 mole^{-2} sec^{-1}. Thus the relative efficiency of M in reaction [4] was found to be 1.0, 1.0, 1.0, and 2.6 for O_2, He, A, and CO_2 respectively. Kaufman (4) found relative values of 1.0, 1.0, 1.0, and 10 for O_2, A, N_2, and CO_2. Benson and Axworthy (9) found relative values of 1.0, 0.78, 0.93, and 2.4 for O_2, He, N_2, and CO_2.

In order to estimate the effect of temperature on the rate of atom recombination, measurements were made with the reaction tube thermostatted at $-60°$ C. The results are plotted as closed circles in Fig. 4. They suggest that the temperature coefficients for both the gas phase and wall recombinations are zero.

However, at this temperature it is doubtful whether the assumption of a steady-state ozone concentration is justified. Benson and Axworthy (9) have reported an activation energy of 6 kcal mole^{-1} for reaction [5], which yields a rate constant for this reaction at $-60°$ C of 2×10^{7} cc mole^{-1} sec^{-1}. Assuming that the room temperature steady-state O_3 concentration is achieved before the gas enters the reaction zone, then, at this temperature and at the pressures used in these experiments, the rate of removal of O-atoms by reaction [5] is 400 times slower than by reaction [4], and can therefore be neglected. The integrated rate equation for atom recombination then becomes:

$$\frac{1}{t}\ln\frac{[O_0]}{[O]} = k_3+k_4[O_2][M].$$

On this basis the results obtained indicate no temperature coefficient for k_3 but a small negative Arrhenius activation energy of about 0.7 ± 0.2 kcal mole^{-1} for k_4, which can be compared with a value of 0.6 kcal mole^{-1} reported by Benson and Axworthy (9).

Oxygen atoms recombine much more slowly in the gas phase than do other atoms such as iodine (13, 14, 15), bromine (13, 16), nitrogen (17, 18), or hydrogen (19). Moreover, these atoms recombine by the reaction

$$X + X + M \rightarrow X_2 + M \qquad [7]$$

which is second order in the atom concentration, while the recombination of oxygen atoms was found to be first order in the atom concentration.

The rate of oxygen atom recombination by reactions [4] and [5] relative to recombination by reaction [7] when $M = O_2$ would be

$$\frac{2k_4}{k_7}\frac{[O_2]}{[O]}.$$

Since k_4 was found to be 1.0×10^{14} cc^2 mole^{-2} sec^{-1} and $[O_2]/[O] \simeq 20$ for most of the experiments, the relative rates are $4\times10^{15}/k_7$. If 10% of the recombination had occurred by reaction [7], curvature would have been found in the first-order plots. This leads to the conclusion that $k_7 \leqslant 4\times10^{14}$ cc^2 mole^{-1} sec^{-1}.

Third-order recombination reactions such as [7] can be expressed in terms of elementary reactions by at least three mechanisms:

$$[A]\quad X + X \rightleftharpoons X_2^* \qquad [a]$$
$$X_2^* + M \rightarrow X_2 + M \qquad [b]$$
$$[B]\quad X + M \rightleftharpoons XM^* \qquad [c]$$
$$XM^* + X \rightarrow X_2 + M \qquad [d]$$
$$[C]\quad X + M \rightleftharpoons XM^* \qquad [c]$$
$$XM^* + M' \rightleftharpoons XM + M' \qquad [e]$$
$$XM + X \rightarrow X_2 + M \qquad [f]$$

If reactions [*a*], [*c*], and [*e*] represent equilibria, the rates of atom recombination will be: by mechanism [*A*]

$$-d[X]/dt = K_a k_b[X]^2[M],$$

by mechanism [*B*]

$$-d[X]/dt = K_c k_d[X]^2[M],$$

by mechanism [*C*]

$$-d[X]/dt = K_c K_e k_f[X]^2[M].$$

Mechanism [*A*] predicts the correct order of magnitude for the third-order rate constant for many atom recombinations on the basis of simple collision theory. However, it encounters difficulties in explaining the variation of the rate constant with the nature of the third body, and the negative temperature coefficients observed for these reactions. Keck (20) has recently suggested means of circumventing these difficulties.

Mechanism [*B*] was originally proposed by Rabinowich (21) and is capable of explaining the effects of different third bodies, and the negative temperature coefficients.

Mechanism [*C*] has been strongly supported by Bunker and Davidson (15) to explain their observations of the recombination of iodine atoms. It possesses several inherent advantages over mechanism [*B*]. The negative temperature coefficient is immediately accounted for by the difference in bond strength of XM and the activation energy of reaction [*f*]. The relative efficiencies of third bodies can be explained in terms of the XM bond strength.

The results of the present study can be considered in the light of mechanism [*C*]. In the presence of large amounts of oxygen, $M = O_2$ and $MX = O_3$. Since the bond strength in O_3 is 24 kcal/mole, $k_e \gg k_{-e}$, and a steady-state rather than an equilibrium ozone concentration is established. The mechanism then reduces to that proposed earlier for the disappearance of O-atoms. Under these conditions the over-all third-order reaction becomes first order in [O], in agreement with experiment—a fact which cannot be explained by mechanism [*A*] or [*B*] alone.

Bunker and Davidson (15) have attributed the large differences in the third-body efficiencies for iodine recombination to the differences in the XM bond strengths. In the case of O-atom recombination, added inert gas can only influence reaction [*e*] and only small differences in third-body efficiencies should be observed. Although this is found to be true, Benson and Axworthy (9) report the same order of efficiencies for third bodies in the O-atom system as do Bunker and Davidson (15) in the I-atom system. Further studies of relative third-body efficiencies seem indicated.

REFERENCES

1. Tollefson, E. E. and Le Roy, D. J. J. Chem. Phys. **16**, 1057 (1948).
2. Wrede, E. Instrumentkunde, **48**, 201 (1928).
3. Toby, S. Ph.D. Thesis, McGill University, Montreal. 1955.
4. Kaufman, F. Proc. Roy. Soc. (London), A, **247**, 123 (1958).
5. Spealman, M. L. and Rodebush, W. H. J. Am. Chem. Soc. **57**, 1474 (1935).
6. Libscomb, F. J., Norrish, R. G. W., and Thrush, B. A. Proc. Roy. Soc. A, **233**, 455 (1956).
7. Foner, S. N. and Hudson, R. L. J. Chem. Phys. **25**, 601 (1956).
8. Herron, J. T. and Schiff, H. I. Can. J. Chem. **36**, 1159 (1958).
9. Benson, S. W. and Axworthy, A. E. J. Chem. Phys. **26**, 1718 (1957).
10. Linnett, J. W. and Marsden, D. G. H. Proc. Roy. Soc. (London), A, **234**, 489 (1956).
11. Kaufman, F. J. Chem. Phys. **28**, 352 (1958).
12. Kistiakowski, G. B. and Volpi, G. A. J. Chem. Phys. **27**, 1141 (1957).
13. Strong, R. L., Chien, J. C., Graff, P. E., and Wellard, J. E. J. Chem. Phys. **26**, 1287 (1957).
14. Christie, M. I., Harrison, A. J., Norrish, R. G. W., and Porter, G. Proc. Roy. Soc. (London), A, **231**, 446 (1955).
15. Bunker, D. L. and Davidson, N. J. Am. Chem. Soc. **80**, 5085, 5090 (1958).
16. Britton, D. and Davidson, N. J. Chem. Phys. **25**, 810 (1956).
17. Herron, J. T., Franklin, J. L., Bradt, P., and Dibeler, V. H. J. Chem. Phys. **29**, 230 (1958).
18. Wentinck, T., Sullivan, J. O., and Wray, K. L. J. Chem. Phys. **29**, 231 (1956).
19. Careri, G. J. Chem. Phys. **21**, 749 (1953).
20. Keck, J. C. J. Chem. Phys. **29**, 410 (1958).
21. Rabinowich, E. Trans. Faraday Soc. **33**, 283 (1937).

THE REACTION OF OXYGEN ATOMS WITH NO[1, 2]

E. A. OGRYZLO[3] AND H. I. SCHIFF

ABSTRACT

In the reaction between NO and O-atoms, the concentration of NO remains essentially unaltered. The reaction can therefore be considered as a NO-catalyzed recombination of O-atoms. Its rate can be conveniently studied by following the disappearance of O-atoms by an isothermal calorimetric technique. The reaction was found to be third order, first order in the concentrations of O, NO, and M, where M is some third body. The third-order rate constant was found to be 1.85×10^{16} cc^2 mole^{-2} sec^{-1} when M = O_2, A, or He and 2.0×10^{16} cc^2 mole^{-2} sec^{-1} when M = CO_2. The rate constant was found to have a slight negative temperature coefficient which corresponded to a negative Arrhenius activation energy of about 0.2 kcal/mole. A detailed mechanism for the reaction has been proposed.

INTRODUCTION

The preceding paper (1) described an isothermal calorimetric technique for following the rate of disappearance of oxygen atoms. The present section describes the application of this technique to the study of the reaction of O-atoms with nitric oxide. This reaction proceeds by the sequence:

$$O + NO + M \rightarrow NO_2 + M \quad [1]$$

$$O + NO_2 \rightarrow NO + O_2 \quad [2]$$

where M represents some third body. Since reaction [2] is much more rapid than reaction [1] at the pressures used in this study (2, 3), the NO concentration is essentially constant, and the entire reaction may be considered as a NO-catalyzed recombination of O-atoms. It can therefore be studied conveniently by the isothermal calorimetric method.

The purpose of the study was to determine the rate constant for the reaction, and to attempt to learn something of the detailed mechanism.

EXPERIMENTAL

The apparatus, the method of purification of the materials, and the method used to measure the atom concentration have been described in the previous paper (1). The reaction was studied over a total pressure range from 1.21 to 3.05 mm Hg. Helium, argon, and CO_2 were used in addition to O_2 as third bodies; the partial pressures of these gases were varied by a factor of 5. Argon and helium were added with the oxygen through the discharge, while the CO_2 was added through a separate jet in the reaction vessel.

The O-atom concentration was first measured along the reaction tube, in the absence of NO, with a silver oxide detector. NO was then added through the multiple jet inlet and, after steady conditions had been established, the atom concentration was again determined as a function of position in the reaction tube. Finally, the discharge was extinguished and the detector readings again taken to give the "i_0" readings for the conditions obtaining while NO was flowing through the tube.

In the preceding paper (1), evidence was presented to indicate that a freshly prepared silver oxide surface detected O-atoms only and did not detect any excited molecules.

[1]*Manuscript received June 18, 1959.*
Contribution from the Department of Chemistry, McGill University, Montreal, Quebec.
[2]*This work has been supported in part by the Air Force Cambridge Research Center under Contract No. AF19(604)-1488, and in part by the Defence Research Board of Canada.*
[3]*Holder, National Research Council Fellowship 1956–58.*

Since such a detector is imperative for the present work, it was frequently tested by introducing a large excess of NO, sufficient to destroy all the atoms. Under these conditions a satisfactory detector registered no heat effect below the reaction zone (as delineated by the glow). Since studies made with a cobalt oxide detector indicated that NO does not deactivate excited molecules, it can be concluded that the silver oxide detector measures atoms only. Further support for this conclusion will be presented in the following discussion.

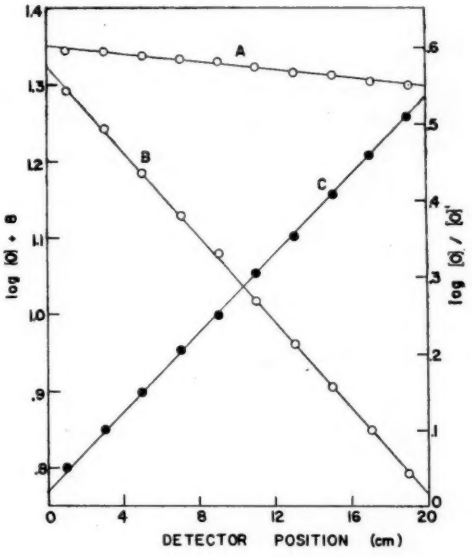

FIG. 1. Oxygen atom decay curves: A, in the absence of NO; B, in the presence of NO; C, the difference between A and B.

RESULTS AND DISCUSSION

Figure 1 shows the O-atom decay curves obtained for a typical experiment. Curve A shows the decrease in O-atom concentration obtained in the absence of NO; curve B shows the more rapid decay of O-atoms in the presence of NO. This decay also appears to be first order in the atom concentration.

It has been shown that, in the absence of NO, the first-order decay of O-atoms is consistent with the mechanism

$$O + W \rightarrow \tfrac{1}{2}O_2 + W \qquad [3]$$

$$O + O_2 + M \rightarrow O_3 + M \qquad [4]$$

$$O + O_3 \rightarrow 2O_2 \qquad [5]$$

where W represents the wall of the reaction vessel.

The integrated rate equation is

$$[i] \qquad \frac{1}{t}\log\frac{[O_0]}{[O]} = k_3[W] + 2k_4[O_2][M]$$

where $[O] = [O_0]$ at $t = 0$.

When NO is introduced, the following additional reactions may be considered:

$$O + NO + M \rightarrow NO_2 + M \quad [1]$$

$$O + NO_2 \rightarrow NO + O_2 \quad [2]$$

$$O_3 + NO \rightarrow NO_2 + O_2. \quad [6]$$

The reaction of O_3 with NO_2 need not be considered, since it is a relatively slow reaction (4) and the steady-state concentrations of both these species are low.[4]

If steady-state conditions are assumed for both O_3 and NO (or NO_2), the integrated rate equation for O-atom disappearance becomes:

$$[ii] \qquad \frac{1}{t}\log\frac{[O_0]'}{[O]'} = k_3[W]+2k_4[O_2][M]+2k_1[NO][M].$$

Since the flow rate of NO was always kept below 10% of the total flow rate, the values of t and $[O_2]$ in equations $[i]$ and $[ii]$ can be assumed to be identical for the same detector position. The equations can then be subtracted to yield

$$[iii] \qquad \log\frac{[O]}{[O]'} = \log\frac{[O_0]}{[O_0]'}+2tk_1[NO][M].$$

Thus, if the difference of the logarithms of the atom concentrations at a given detector position is plotted against the detector position, a straight line should be obtained with slope equal to $2k_1[NO][M]$. This plot is shown as curve C in Fig. 1. Similar straight line plots were obtained in all cases where the detector measured atoms only. If, however, the detector also measured excited molecules, the plots showed considerable curvature, as

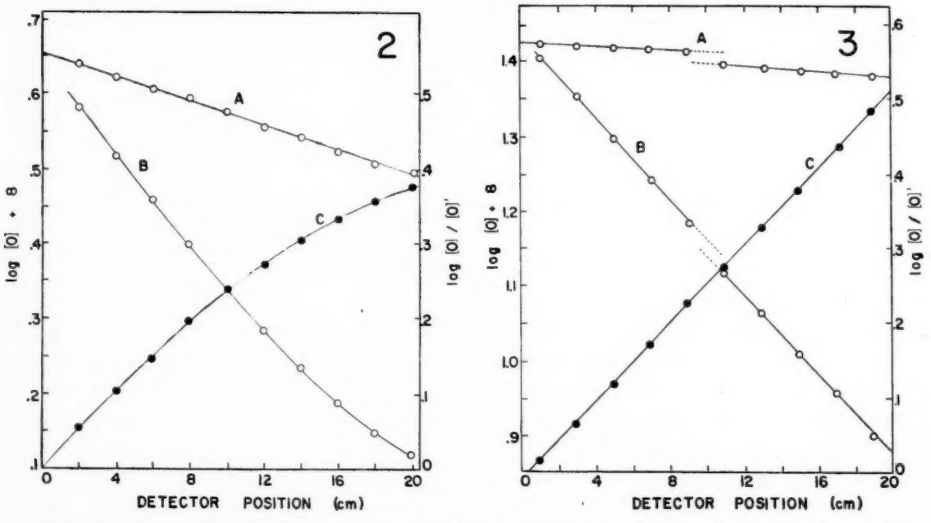

FIG. 2. Oxygen atom decay curves measured with a detector which also measured excited molecules: A, in the absence of NO; B, in the presence of NO; C, the difference between A and B.

FIG. 3. Oxygen atom decay curves showing the effect of a piece of silver placed half way down the reaction tube: A, in the absence of NO; B, in the presence of NO; C, the difference between A and B.

[4]*Similarly, the reactions*

$$NO_2 + O + M \rightarrow NO_3 + M$$

$$NO_3 + O \rightarrow NO + O_2$$

if they occur, can be shown, by using estimates of the rate constants (5), to have a negligible effect on the rate of O-atom disappearance.

shown in Fig. 2. A detector which gave such a curve always registered a heat effect when sufficient NO was added to consume all the atoms.

There remained the possibility that some reaction might be occurring on the detector. To test this, a piece of silver oxide was placed half way down the reaction tube. The discontinuities in curves A and B of Fig. 3 show that this silver oxide destroys some of the atoms. Nevertheless, the difference curve C shows no discontinuity at this position, which clearly indicates that the NO–O-atom reaction is occurring predominantly in the gas phase.

TABLE I

Expt. No.	Total pressure (mm Hg)	Temp. (° C)	O_2 flow (moles/sec $\times 10^6$)	NO flow (moles/sec $\times 10^6$)	Inert gas flow (moles/sec $\times 10^6$)	Slope (meter^{-1})	$k \times 10^{-16}$ cc^2 mole^{-2} sec^{-1}
A-1	2.14	293	99.0	3.20	—	1.73	1.78
A-2	2.68	293	133.4	3.20	—	1.86	1.73
A-3	2.08	293	95.0	6.87	—	3.44	1.79
A-4	2.08	293	98.0	2.04	—	1.00	1.68
F-3	2.23	293	88.3	3.43	—	2.45	1.97
F-4	2.15	293	88.3	3.43	—	2.72	1.99
E-3	3.27	279	160	3.50	—	2.98	1.75
E-4	1.38	279	55.8	3.50	—	1.91	1.90
					Argon		
D-1	2.87	279	23.4	3.5	107.9	2.61	1.65
D-2	2.36	279	16.3	3.5	92.7	3.25	2.38
D-3	2.12	279	15.0	3.5	82.3	2.06	2.40
D-4	3.05	279	23.4	3.5	122.5	3.72	2.23
D-5	3.16	279	23.4	3.5	131.6	3.34	2.05
D-6	1.84	280	20.0	3.5	61.4	2.56	2.25
D-7	3.34	279	23.4	3.5	146.5	3.43	2.12
F-1	2.72	296	49.1	3.43	67.6	2.70	1.80
F-2	2.23	296	49.1	3.43	43.2	2.52	1.95
F-5	2.71	293	49.1	3.77	67.6	2.45	1.96
					Helium		
E-1	3.21	279	23.4	3.5	131	3.28	1.90
E-2	1.21	279	23.4	3.5	20.0	2.22	2.09
F-6	2.88	293	49.1	3.77	73.6	3.58	1.86
F-7	3.05	279	81.9	1.92	52.7	2.12	1.90
					CO_2		
B-1	2.68	294	46.6	1.30	70.7	0.97	1.75
B-2	2.67	213	46.6	1.30	70.7	2.69	1.90
B-3	2.70	294	44.3	3.40	70.7	2.55	1.70
B-4	2.60	213	46.3	3.40	65.7	8.50	2.26
B-5	2.57	294	24.4	3.50	84.8	3.30	2.40
B-6	2.55	213	25.0	3.50	84.8	10.2	2.70
B-7	2.75	294	51.3	3.50	67.9	3.30	2.15
B-8	2.75	213	51.3	3.50	67.9	9.80	2.40

The results are shown in Table I. The capital letters prefixing the experiment numbers refer to separate series in which the same detector and reaction vessel were employed. Column 7 gives the slope of equation [*iii*].

Inspection of the data indicates that the over-all reaction is third order, first order in the concentrations of atomic oxygen, nitric oxide, and third body. Wall reactions cannot be significant since they would show zero or reciprocal pressure dependence. Helium, argon, and molecular oxygen appear to be equally efficient as third bodies within experimental error. The average value of the rate constant at 20° C is $1.85 \pm 0.10 \times 10^{16}$ cc^2 mole^{-2} sec^{-1} and $2.04 \pm 0.20 \times 10^{16}$ cc^2 mole^{-2} sec^{-1} at 6° C. Although the mean deviations in

these values would cause them to overlap, there does seem to be an indication of a small negative temperature coefficient. These values can be compared with the value of 1.8×10^{16} cc^2 mole^{-2} sec^{-1} obtained by Ford and Endow (5) at 25° C from a study of the photolysis of NO_2, and the value of 2.5×10^{16} cc^2 mole^{-2} sec^{-1} obtained by Kaufman (6) and the value of 2.7×10^{16} cc^2 mole^{-2} sec^{-1} obtained by Harteck *et al.* (7) from a study of the rate of decrease in the light intensity accompanying this reaction.

Carbon dioxide appears to be more efficient as a third body by about 10%. This is a somewhat smaller effect than found by Kaufman (6), who reported a rate constant for the reaction with CO_2 as third body of $4-5\times10^{16}$ cc^2 mole^{-2} sec^{-1}. An estimate of the temperature coefficient for the reaction can be obtained for the reactions in which CO_2 was introduced. Pairs of experiments in series B were performed in rapid succession with all conditions kept constant with the exception of the reaction tube temperature. The ratios of the rate constants for the pairs B-2 and B-1, B-4 and B-3, B-6 and B-5, B-8 and B-7, are 1.1, 1.3, 1.1, and 1.1 respectively. The average of these ratios corresponds to a negative Arrhenius activation energy of 0.24 kcal/mole.

Mechanism of the Reaction

A third-order association reaction can be analyzed in terms of successive bimolecular collisions. A collision between the two associating partners can be considered to produce a short-lived intermediate which will dissociate again unless it experiences a collision with a third body M, which removes sufficient energy to leave the product in a potential well. Thus, reaction [1] can be considered to be the result of the successive reactions

$$O + NO \rightarrow NO_2^* \qquad [7]$$

$$NO_2^* \rightarrow NO + O \qquad [8]$$

$$NO_2^* + M \rightarrow NO_2 + M. \qquad [9]$$

Reaction [8] must be much faster than reaction [9] if third-order kinetics is to be obtained. The over-all rate will depend mainly on the lifetime of NO_2^*, i.e. on the rate of reaction [8]. Due to its greater number of degrees of freedom, the NO_2^* complex may have a considerably longer lifetime than the complexes formed by collision of two atoms.

An additional fate for the excited NO_2^* must also be considered. The reaction is accompanied by the emission of radiation, in what appears to be a continuum, but might have a closely banded structure. This radiation could be produced in the reaction:

$$NO_2^* \rightarrow NO_2 + h\nu. \qquad [10]$$

Kaufman (6) has found that the rate of light emission is much slower than the rate of oxygen atom disappearance in the pressure range used here. This would correspond to the condition that $k_9[M] \gg k_{10}$. This condition, along with the assumption of steady-state concentrations for NO_2^* and NO, can be used to derive an expression for the rate of oxygen atom disappearance in the form:

$$-\frac{d[O]}{dt} = 2\frac{k_7}{k_8}k_9[O][NO][M]$$

in agreement with the empirical rate equation.

Furthermore, it can be readily shown that the rate of light emission is

$$I = \frac{d[h\nu]}{dt} = \frac{k_7}{k_8}k_{10}[NO][O]$$

in agreement with the second-order dependence found by Kaufman. However, recent studies of the recombination of iodine atoms (8, 9, 10) suggests that an alternate mechanism might be proposed in which M participates in the initial step:

$$O + M \rightarrow OM^* \quad [11]$$

$$OM^* \rightarrow O + M \quad [12]$$

$$OM^* + NO \rightarrow NO_2^* + M \quad [13]$$

$$NO_2^* \rightarrow NO_2 + h\nu \quad [14]$$

$$NO_2^* + M \rightarrow NO_2 + M. \quad [15]$$

This mechanism is also capable of explaining a third-order rate for atom disappearance and a second-order rate for light emission.

The relative importance of the two mechanisms will depend on the relative lifetimes of NO_2^* and OM^*. It might be expected that the second mechanism would be much more sensitive to the nature of the third body. For example, one would expect quite different lifetimes for O_3^* and OA^*. The observation that O_2 and A seem to be equally efficient as third bodies might therefore be considered to favor the first mechanism. Furthermore, if O_3^* is the excited molecule formed in the first step when O_2 is the third body, one would expect the rate of oxygen atom disappearance to be similar in the presence and in the absence of NO, i.e. the rate of reaction [13] should not change appreciably if O is substituted for NO. However, the presence of NO increased the rate of atom disappearance by at least an order of magnitude.[5]

It might also be argued that the reaction [14] in the second mechanism seems less likely to give rise to a continuum than does reaction [10] since $NO_2^{\mp}$ will be more stabilized than NO_2^*. However, Neuberger and Duncan (11) found a "pseudo" continuum emitted when NO_2 was irradiated with light of energies insufficient to cause dissociation, although there may be some doubt as to whether the excited state of NO_2 reached in this way has any connection with the one reached by the NO–O reaction. The data available at present do not permit an unequivocal choice between these two mechanisms. It is hoped that some work currently in progress in these laboratories on the light-emitting step will help in a decision.

REFERENCES

1. ELIAS, L., OGRYZLO, E. A., and SCHIFF, H. I. Can J. Chem. **37**, 1680 (1959).
2. HERRON, J. T. and SCHIFF, H. I. Can. J. Chem. **36**, 1159 (1958).
3. FORD, H. W. and ENDOW, N. J. Chem. Phys. **27**, 1277 (1957).
4. FORD, H. W., DOYLE, G. J., and ENDOW, N. J. Chem. Phys. **26**, 1336 (1957).
5. FORD, H. W. and ENDOW, N. J. Chem. Phys. **27**, 1156 (1957).
6. KAUFMAN, F. Proc. Roy. Soc. (London), A, **247**, 123 (1958).
7. HARTECK, P., REEVES, R. R., and MANNELLA, G. J. Chem. Phys. **29**, 1333 (1958).
8. STRONG, R. L., CHIEN, J. C., GRAFF, P. E., and WELLARD, J. E. J. Chem. Phys. **26**, 1287 (1957).
9. CHRISTIE, M. I., HARRISON, A. J., NORRISH, R. G. W., and PORTER, G. Proc. Roy. Soc. (London), A, **231**, 446 (1955).
10. BUTLER, D. and DAVIDSON, N. J. Chem. Phys. **25**, 810 (1956).
11. NEUBERGER, D. and DUNCAN, A. B. J. Chem. Phys. **22**, 1693 (1954).

[5]*The occurrence of reaction [2] simply doubles the rate of atom consumption.*

THE MERCURY-PHOTOSENSITIZED DECOMPOSITION OF BENZALDEHYDE, ACROLEIN, AND CROTONALDEHYDE[1]

A. G. HARRISON[2] AND F. P. LOSSING

ABSTRACT

The Hg^3P_1-photosensitized decomposition of benzaldehyde at low pressure and high radiation intensity forms predominantly a polymeric material. In the fraction of the reaction which forms the identifiable final products benzene and carbon monoxide, both a direct molecular rearrangement and a free radical split to phenyl and formyl radicals occur. The decomposition reactions of acrolein and crotonaldehyde involve the three primary processes:

$$\begin{aligned} RCHO + Hg^* &\rightarrow RH + CO + Hg \\ &\rightarrow R + CHO + Hg \\ &\rightarrow RCO + H + Hg. \end{aligned}$$

INTRODUCTION

In the photolytic and mercury-photosensitized decompositions of aldehydes three possible primary processes can occur:

$$RCHO \rightarrow R + CHO \quad [1]$$

$$RCHO \rightarrow RH + CO \quad [2]$$

$$RCHO \rightarrow RCO + H. \quad [3]$$

Where R is an alkyl group other than methyl, further primary processes involving rearrangements and bond splitting in this group are possible, and the course of the reaction may become quite complicated.

The direct photolysis and the mercury-photosensitized decomposition of acetaldehyde have both been studied in some detail. In the direct photolysis at 2537 to 3130 Å the main primary process is reaction [1], although part of the reaction appears to proceed by reaction [2] (1). In the reaction of acetaldehyde with $Hg(^3P_1)$ atoms (2) the primary decomposition is almost exclusively to form methyl and formyl radicals, although the experimental results could not rule out the possibility that 5% of the reaction proceeded by reaction [2]. There was no evidence for the occurrence of reaction [3].

Very little work has been done on the relative importance of these primary processes when R is an unsaturated group capable of conjugating with the aldehydic function. In this case it might be expected that the proportions of the three possible steps would change. Blacet and Roof (3) studied the photolysis of crotonaldehyde in the 2400–2600 Å region and found no decomposition; however, Volman, Leighton, Blacet, and Brinton (4) found that during the photolysis of crotonaldehyde at 2537 Å tellurium mirrors were removed, indicating the presence of radicals. They postulated the following reaction:

$$CH_3{-}CH{=}CH{-}CHO + h\nu \rightarrow CH_3{-}CH{=}CH + CHO. \quad [4]$$

Blacet, Fielding, and Roof (5) studied the direct photolysis of acrolein and postulated that the primary process was to some extent the following:

$$CH_2{=}CH{-}CHO + h\nu \rightarrow CH_2{=}CH + CHO. \quad [5]$$

[1]*Manuscript received June 18, 1959.*
Contribution from the Division of Pure Chemistry, National Research Council, Ottawa, Canada.
Issued as N.R.C. No. 5324.
[2]*National Research Council of Canada Postdoctorate Fellow 1957–59.*

By mirror-removal experiments Volman and co-workers (4) showed that radicals were produced at 2537 and 2810 Å.

No work has been reported on the direct photolysis of benzaldehyde or on the mercury-photosensitized decomposition of any of the three conjugated aldehydes: crotonaldehyde, acrolein, and benzaldehyde. In view of the few results available it was thought that some information on the relative importance of the three primary processes in the mercury-photosensitized decomposition of these aldehydes would be of interest.

EXPERIMENTAL

The reactions were studied by passing the reactant at a few microns pressure, together with mercury vapor, in a stream of helium through a photochemical reactor attached to a mass spectrometer. The apparatus and procedure have been described previously (2, 6, 7).

In recent work (7, 8) the addition of methyl radicals, produced by the photosensitized decomposition of dimethyl mercury, to the reaction products has been found to be a convenient method of detecting free radicals, particularly those which are difficult to detect directly with low energy electrons. This method of detection of a radical R depends on the occurrence of the combination reaction

$$R + CH_3 \rightarrow RCH_3. \qquad [6]$$

It is worth while to consider briefly the conditions upon which the success of this method of radical detection and identification depends. The method will work only if conditions are such that radical recombination reactions predominate over radical attack on stable molecules. Although radical–radical reactions are several orders of magnitude faster than radical–substrate reactions, the concentration of radicals in conventional photochemical work is usually so small that radical–substrate reactions nevertheless predominate. However, as has been pointed out previously (7), conditions in the present reactor are considerably different. In the present system some 10–20% of the parent compound is decomposed in the order of 10^{-3} second with the result that the concentrations of radicals can be relatively high. In the case of acetone (2) the concentration of methyl radicals was approximately 1/10 that of the parent compound for most of the contact time. Under such conditions radical–radical reactions would be expected to predominate.

Of course, as the fraction of the reaction proceeding by a free radical mechanism decreases the occurrence of radical–radical reactions will also decrease. However, when using methyl radicals as a radical detector this effect can be counterbalanced by increasing the amount of methyl radicals added to the system.

The sensitivity of this method for the detection of a radical R is dependent on many variables: among others, the rate of recombination, the ratio of recombination to disproportionation, and the sensitivity of the mass spectrometer to the product RCH_3. It is therefore impossible to put the limits of radical detection by this method on an absolute scale.

Materials

The benzaldehyde, acrolein, and crotonaldehyde were all Eastman-Kodak "White-Label" materials purified by bulb-to-bulb distillation and degassed before use. The benzaldehyde-d_6 was prepared by Dr. L. C. Leitch and was 94.7% pure. The impurity was chiefly benzaldehyde-d_5.

RESULTS AND DISCUSSION

Benzaldehyde

The only identifiable products found in the mercury-photosensitized decomposition of benzaldehyde were benzene and carbon monoxide. The major part of the reaction ($\sim 80\%$) appeared to proceed to the formation of a yellowish polymer which deposited on the walls of the reactor and rapidly caused a reduction in the amount of light transmitted. As the results in Table I show, the amounts of benzene and carbon monoxide produced were equal, suggesting that the deposit was a polymer of benzaldehyde and not of one of the reaction products.

TABLE I

Benzaldehyde decomposition

Benzaldehyde decomposed		Products		Yield (%)	
(μ)	(%)	C_6H_6	CO	C_6H_6	CO
0.92	11.7	0.166	0.172	18.1	18.8

No radicals could be detected at low electron energies. A search was therefore made for radicals by the addition of methyl radicals as previously discussed. Upon the addition of methyl radicals a peak at mass 92 of approximately 7 mm was produced. A peak was also produced at mass 91, the intensities at mass 92 and 91 being in the correct ratio for toluene. These results demonstrate the presence of the phenyl radical in the system, suggesting as a primary step the reaction:

$$C_6H_5CHO + Hg^* \rightarrow C_6H_5 + CHO + Hg. \qquad [7]$$

However, one cannot rule out the possibility that the primary reaction proceeds by the formation of the benzoyl radical, which then rapidly decomposes to form a phenyl radical and carbon monoxide.

$$C_6H_5CHO + Hg^* \rightarrow C_6H_5CO + H + Hg \qquad [8]$$

$$C_6H_5CO \rightarrow C_6H_5 + CO \qquad [9]$$

No formation of acetophenone, the addition product of C_6H_5CO and CH_3, was observed, indicating that the C_6H_5CO concentration was very small. An estimate of the bond dissociation energy $D(C_6H_5—CO)$ can be made from the heat of formation of CO and recent estimates of the heat of formation of the phenyl radical (ΔH_f = 70 kcal/mole) (9) and the benzoyl radical (ΔH_f = 15.6 kcal/mole) (10). These values lead to $D(C_6H_5—CO)$ = 28 kcal/mole. Since the benzoyl radical should therefore be stable at 55° C, the failure to detect it either directly or by CH_3 addition must be taken as evidence that reaction [8] does not occur to a significant extent.

Reaction [7] undoubtedly occurs to some extent, the observed products benzene and carbon monoxide being formed by the subsequent reaction:

$$C_6H_5 + CHO \rightarrow C_6H_6 + CO. \qquad [10]$$

To determine the importance of reactions [7] and [10] relative to a possible direct molecular rearrangement to benzene and carbon monoxide:

$$C_6H_5CHO + Hg^* \rightarrow C_6H_6 + CO + Hg \qquad [11]$$

experiments were carried out with C_6H_5CHO–C_6D_5CDO mixtures. In the absence of the free radical processes [7] and [10] all the benzene produced in such mixtures should be

either C_6H_6 or C_6D_6. The amount of isotopically mixed benzenes relative to the C_6H_6 and C_6D_6 benzenes should therefore provide an index of the amount of benzene formed by reaction [11].

TABLE II

Decomposition of C_6D_5CDO–C_6H_5CHO mixtures

Aldehyde decomposed (μ)		Product benzenes (μ)				% free radical reaction
C_6D_5CDO	C_6H_5CHO	C_6D_6	C_6D_5H	C_6H_5D	C_6H_6	
1.46	—	0.257_0	0.026_6	—	—	—
0.599	1.36	0.078_7	0.031_4	0.016_3	0.190	34.0
0.646	0.569	0.090_7	0.017_9	0.013_6	0.075_4	32.0

In Table II are recorded the results obtained in the decomposition of benzaldehyde-d_6 and of two mixtures of benzaldehyde-d_6 and ordinary benzaldehyde. Because of the formation of polymer it was necessary to keep the period of illumination as short as possible, therefore the yield of carbon monoxide was not measured in these experiments. The small amount of C_6D_5H formed in the decomposition of benzaldehyde-d_6 alone arises from the small percentage of benzaldehyde-d_5 present in the original material. The results given for the two mixtures were corrected by this factor.

Assuming that for the isotopic aldehydes the same fraction of the total reaction proceeds by formation of free radicals, and similarily that the rate of reaction [10] is the same for all isotopic species, it is possible to calculate from the results of the two experiments the fraction proceeding by steps [7] and [10]. If these assumptions are valid the amount of the mixed benzenes, C_6D_5H and C_6H_5D, formed in each experiment should be equal. The observed agreement was not too satisfactory, presumably because the amounts formed were quite small compared to the experimental error. For purposes of calculation the amounts of C_6H_5D and C_6D_5H were averaged. The final column of Table II shows that of that fraction of the total reaction which produced benzene, 33% did so by a free radical mechanism. There was no evidence for the formation of mixed aldehydes suggesting that the recombination reaction

$$C_6H_5 + CHO \rightarrow C_6H_5CHO \qquad [12]$$

must be much slower than the disproportionation reaction [10].

Acrolein

Using low energy electrons no free radicals could be detected in the photosensitized decomposition of acrolein. From a comparison of the 50-v spectra with and without illumination the principal products were found to be ethylene, acetylene, carbon monoxide, and a small amount of hydrogen. At higher partial pressures of aldehyde a substance of mass 54 was formed. This was identified as 1,3-butadiene, presumably formed by the dimerization of vinyl radicals.

On the addition of methyl radicals to the system a compound of parent mass 42 was formed. This compound was identified as propylene and confirms the presence of the vinyl radical. This suggests the primary step:

$$CH_2{=}CH{-}CHO + Hg^* \rightarrow CH_2{=}CH + CHO + Hg. \qquad [13]$$

In addition, a small amount of product of mass 70 was also formed. This compound was probably vinyl methyl ketone, suggesting the occurrence to some extent of the additional

primary step:

$$CH_2{=}CH{-}CHO + Hg^* \rightarrow CH_2{=}CH{-}CO + H + Hg. \quad [14]$$

The product yields obtained by varying the length of the illuminated zone are given in Table III and shown graphically in Fig. 1. The carbon and oxygen balances were low,

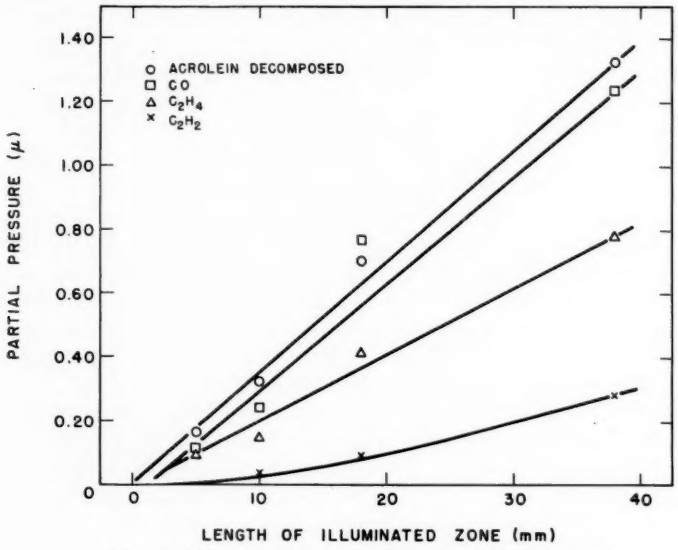

FIG. 1. Mercury-photosensitized decomposition of acrolein.

TABLE III

Acrolein decomposition (partial pressure acrolein 4.85 μ)

Length of illuminated zone (mm)	Acrolein decomposed		Products (μ)			Product balance	
	(μ)	(%)	CO	C_2H_4	C_2H_2	% C	% O
38	1.33	27.4	1.23	0.783	0.282	84.5	92.9
18	0.700	14.4	0.768	0.417	0.095	68.9	(109.7)
10	0.320	6.58	0.244	0.152	0.037	64.8	76.3
5	0.165	3.38	0.114	0.095	0.00	61.4	69.1

probably as a result of the presence of radicals which were not included in the material balances. The curved nature of the plot of the acetylene yield versus the length of illuminated zone suggests that acetylene was not produced in a primary step. The only primary step producing acetylene which would be energetically possible is the reaction:

$$CH_2{=}CH{-}CHO + Hg^* \rightarrow C_2H_2 + CH_2O + Hg. \quad [15]$$

The absence of formaldehyde as a product indicates that this reaction does not occur. Several secondary reactions can be postulated to explain the formation of acetylene

$$C_2H_3 + Hg^* \rightarrow C_2H_2 + H + Hg \quad [16]$$

$$C_2H_3 \rightarrow C_2H_2 + H \quad [17]$$

$$2C_2H_3 \rightarrow C_2H_2 + C_2H_4 \quad [18]$$

$$C_2H_4 + Hg^* \rightarrow C_2H_2 + H_2 + Hg. \quad [19]$$

From heats of formation, assuming $D(C_2H_3—H) \leqslant 110$ kcal/mole, $D(H—C_2H_2)$ can be calculated to be $\geqslant 36$ kcal/mole; therefore the decomposition reaction [17] should be very slow at the temperature of the reactor (55° C). It is possible that the acetylene could be produced by reaction [18]. However, most of the ethylene must arise by some other mechanism since in all cases more ethylene was produced than acetylene. The relatively large yield of ethylene, the apparent low concentration of vinyl radicals, and the absence of products containing the CHO group all suggest that a large proportion of the reaction proceeds by a molecular rearrangement mechanism:

$$CH_2{=}CH—CHO + Hg^* \rightarrow CH_2{=}CH_2 + CO + Hg. \qquad [20]$$

The presence of the vinyl and acrylyl radical, as shown by the methyl addition products propylene and vinyl methyl ketone, strongly suggest the occurrence of two other primary processes:

$$CH_2{=}CH—CHO + Hg^* \rightarrow CH_2{=}CH + CHO + Hg \qquad [13]$$

$$CH_2{=}CH—CHO + Hg^* \rightarrow CH_2{=}CH—CO + H + Hg. \qquad [14]$$

From the present experiments it is not possible to determine the relative importance of the three primary processes.

Crotonaldehyde

Difficulties were encountered in identifying the products formed in the mercury-photosensitized decomposition of crotonaldehyde. For this reason an identification of all primary reactions and an estimate of their relative importance could not be made. The main products detected were carbon monoxide, propylene, a product of mass 40, a small amount of acetylene, and a very small amount of a product of mass 56. Use of low energy electrons led to detection of a radical mass 41. The addition of methyl radicals caused a small but definite increase at mass 84 indicating the presence of the crotonyl radical in small amounts and thus suggesting the occurrence of the primary reaction:

$$CH_3—CH{=}CH—CHO + Hg^* \rightarrow CH_3—CH{=}CH—CO + H + Hg. \qquad [21]$$

The large amount of propylene produced suggested that the main primary step was the molecular rearrangement:

$$CH_3—CH{=}CH—CHO + Hg^* \rightarrow CH_3—CH{=}CH_2 + CO + Hg. \qquad [22]$$

It was not possible to determine whether the radical of mass 41 was formed by the primary reaction:

$$CH_2—CH{=}CH—CHO + Hg^* \rightarrow CH_3—CH{=}CH + CHO + Hg \qquad [23]$$

or by the reaction of Hg^* with propylene produced in reaction [22] as follows:

$$CH_2{=}CH—CH_3 + Hg^* \rightarrow CH_2{=}CH—CH_2 + H + Hg. \qquad [24]$$

Since a considerable amount of propylene was present, and since propylene has a large cross section for reaction with excited Hg atoms (6), the latter alternative appears more probable.

CONCLUSIONS

The mercury-photosensitized decomposition of benzaldehyde under the present conditions leads primarily to the formation of a polymeric material. However, that portion of the reaction which results in identifiable products has been shown to involve two primary processes, a molecular rearrangement to form benzene and carbon monoxide

and a free radical split to form phenyl and presumably formyl radicals, with 33% of the reaction occurring by the free radical mechanism. No evidence was found for the formation of benzoyl radicals and hydrogen atoms. This mode of decomposition is quite different from that of acetaldehyde, in which no molecular rearrangement was found to occur, and free radicals only were formed.

The reactions of both acrolein and crotonaldehyde appear to involve three primary processes

$$RCHO + Hg\,^3P_1 \rightarrow RH + CO + Hg \quad [25]$$

$$\rightarrow R + HCO + Hg \quad [26]$$

$$\rightarrow RCO + H + Hg. \quad [27]$$

For both these compounds the results suggest that the main reaction is the molecular rearrangement [25], with reaction [26] occurring to a lesser extent and reaction [27] only to a very slight extent. The results for acrolein and crotonaldehyde do not permit quantitative determinations of the relative importance of the three steps.

REFERENCES

1. Steacie, E. W. R. Atomic and free radical reactions. 2nd ed. Reinhold Publishing Corp., New York. 1954.
2. Lossing, F. P. Can. J. Chem. **35**, 305 (1957).
3. Blacet, F. E. and Roof, J. G. J. Am. Chem. Soc. **58**, 73 (1936).
4. Volman, D. H., Leighton, P. A., Blacet, F. E., and Brinton, R. K. J. Chem. Phys. **18**, 203 (1950).
5. Blacet, F. E., Fielding, G. H., and Roof, J. G. J. Am. Chem. Soc. **59**, 2375 (1937).
6. Lossing, F. P., Marsden, D. G. H., and Farmer, J. B. Can. J. Chem. **34**, 701 (1956).
7. Kebarle, P. and Lossing, F. P. Can. J. Chem. **37**, 389 (1959).
8. Collin, J. and Lossing, F. P. Can. J. Chem. **35**, 778 (1957).
9. Szwarc, M. and Williams, D. J. Chem. Phys. **20**, 1171 (1952).
10. Szwarc, M. and Taylor, J. W. J. Chem. Phys. **22**, 270 (1954).

THE POLYOXYPHENOLS OF WESTERN RED CEDAR (THUJA PLICATA DONN.)

I. ISOLATION AND PRELIMINARY CHARACTERIZATION OF PLICATIC ACID[1]

J. A. F. GARDNER, G. M. BARTON, AND HAROLD MACLEAN

ABSTRACT

An amorphous, optically active, heat and light sensitive, polyoxyphenolic acid ($pK_a = 3$) has been isolated from the mixture of polyoxyphenols present in the aqueous extractive of western red cedar. Analyses of crystalline derivatives are consistent with a molecular formula of $C_{20}H_{22}O_{10}$. Color tests, spectra, methylation, and alkaline nitrobenzene oxidation results indicate it to be a propylphenol dimer, a lignan acid, in which one aromatic ring is 3-methoxy-4-hydroxyphenyl and the other is 3,4-dihydroxy-5-methoxyphenyl. Acetylation results and lactone formation require the presence of three alcoholic hydroxyls, one of which is in the γ position to the carboxyl.

In a previous paper (1), the presence in the acetone extractive of western red cedar of several water-soluble polyoxyphenols was reported. This phenolic mixture constituted 4 to 5% of wood samples having acetone solubilities of 10 to 14%. These substances were also extracted with water and accounted for the main portion (85–95%) of the hot-water extractive of butt outer heartwood which was found to have hot-water solubilities ranging from 10 to 23% (2). This indicated high content of natural phenolic substances together with the availability of large volumes of western red cedar wood as mill and forest residue in British Columbia prompted a detailed investigation of the chemistry of the phenolic constituents.

Paper chromatography of the aqueous extractive, a brown resin, showed the presence of at least seven different phenols and arabinose. By steaming the mixture during aqueous extraction of the wood, the steam-volatile tropolones, thujic acid and methyl thujate, were virtually eliminated. The arabinose and other non-phenols in the extractive were removed by treatment with lead acetate solution and regeneration of the phenols from the precipitated lead salts. Attempts to fractionate the regenerated phenols with a variety of solvents were made, and the separation efficiency was checked by means of paper chromatography of the fractions. In this manner it was established that a major component ($R_f = 0.9$, carbon dioxide – water) was very soluble in water and, compared with the others, practically insoluble in ethyl acetate. Thus, thorough extraction of the phenolic mixture with ethyl acetate gave a residue which was paper chromatographically pure in respect to carbohydrates and other phenols. This product was an amorphous brown powder which gave positive tests for pyrocatechol, methoxyl, and carboxyl groups. In view of its acidity and source, this substance was termed plicatic acid.

Additional quantities of plicatic acid were isolated simply by extracting it from the mixture of phenols in methyl ethyl ketone with sodium bicarbonate solution. The yield was 40% of the aqueous extractive, but since the product was brown in color and failed to crystallize or give crystalline methyl ethers with diazomethane, milder methods of isolation not involving the use of acids and alkalis were investigated.

Column chromatography with a variety of packings including cellulose, magnesol–

[1]*Manuscript received June 15, 1959.*
Contribution from the Vancouver Laboratory, Forest Products Laboratories of Canada, a Division of the Forestry Branch, Department of Northern Affairs and National Resources. Paper presented at the 133rd National Meeting, American Chemical Society, San Francisco, California, April 13–18, 1958.

celite, alumina, and ion-exchange resins was examined. The low solubility of the aqueous extractive in most solvents limited the loading of most columns to very small quantities. Also, although weakly basic ion-exchange resins separated plicatic acid from the other phenols, acid was required to elute the plicatic. The most successful column separation of the phenols was obtained with a weakly acid (carboxylic) cation-exchange resin which is also useful in the separation of flavonoids (3). Elution with water of a column loaded with the aqueous extractive yielded plicatic acid and the phenols, R_f .7 and .5 (carbon dioxide – water), in that order with some overlapping. Subsequent graded elution with water–ethanol gave the phenols of R_f .52 and .03 and finally a mixture of the remainder, R_f .03, .06, and .1. Paper chromatography showed that the first plicatic acid eluted from the column was contaminated with arabinose. Subsequent fractions showing no contamination were combined and lyophilized to provide amorphous plicatic acid in small quantities (1 g or less).

Consideration of the high solubility of plicatic acid in water and very poor solubility in ethyl acetate together with the poor solubility of the other phenols in water and their good solubility in ethyl acetate led to isolations on a larger scale by a six-stage countercurrent distribution of the aqueous extractive between these two solvents. This procedure provided almost equal quantities of chromatographically pure plicatic acid and plicatic acid contaminated with 5–6% of arabinose and traces of other sugars in a combined yield of 40% on the aqueous extractive.

As obtained by the column or countercurrent distribution technique, the plicatic acid was a very light tan-colored, amorphous, optically active powder, very soluble in water, soluble in absolute acetone and ethanol, and very slightly soluble in ethyl acetate and ether.

The color reaction with aqueous ferric chloride was pinkish purple shifting to blue-green at neutrality and thence to deep red in sodium carbonate solution. This indication of the presence of adjacent phenolic hydroxyls was confirmed by positive tests with ferrous sulphate, ammonium molybdate, titanium chloride, and bromine solutions. A test for three vicinal phenolic hydroxyls with ferrous sulphate – potassium tartrate solution was negative, but the chlorine – sodium sulphite test for pyrogallol derivatives was positive. Alkaline nitrobenzene oxidation gave a 4% yield of vanillin. A test for methylenedioxy groups was negative.

Solutions of plicatic acid were unstable to sunlight, rapidly turning dark red-brown in color. Heating the solid or an aqueous solution caused a gradual conversion to another phenol of R_f 0.7 (carbon dioxide – water) having an infrared absorption characteristic of a γ-lactone. This substance, according to paper chromatography, was identical with one of the other phenols occurring with plicatic acid in the cedar extractive. Acidification of an alkaline solution regenerated plicatic acid.

Elementary analyses and molecular weight determinations indicated an empirical formula for plicatic acid of $C_{20}H_{24}O_{10}$. For two methoxyl groups and one carboxyl group per molecule, this requires a methoxyl content of 14.6% and a neutral equivalent of 424. The best values found were 13.7% and 432 respectively. The heating (65–100° C) necessary for moisture removal prior to analyses also caused some decomposition making analytical results on plicatic acid itself subject to question.

Methylation of plicatic acid with dimethyl sulphate and alkali in aqueous acetone solution followed by diazomethane in dioxane gave a crystalline product which could also be obtained in poorer yield directly from plicatic with diazomethane. Analytical values for carbon, hydrogen, and methoxyl content and molecular weight fitted an empirical

formula of $C_{24}H_{30}O_{10}$. This corresponds to the methyl ester of the trimethyl ether of a plicatic acid containing two fewer hydrogens per molecule than the formula above. Since dehydrogenation during diazomethane methylation is unlikely and the analytical values for plicatic are based on amorphous heat-labile material, the $C_{20}H_{22}O_{10}$ formula for plicatic acid is favored.

The methyl ester of the trimethyl ether effervesced when heated above its melting point, evolving methanol and yielding a crystalline product which analyzed as the trimethyl ether lactone, $C_{23}H_{26}O_9$. The lactone character was confirmed by the appearance of a strong band in the infrared absorption spectrum at 1784 cm^{-1}, the region assignable to the carbonyl group of five-membered lactones (4) and disappearance of the band at 1716 cm^{-1} assignable to the carbonyl group in the ester (5). The infrared absorption spectrum of the lactone also indicated additional hydroxyl group content.

Acetylation of plicatic acid in acetic anhydride and pyridine gave an amorphous product analyzing for methoxyl content as a hexaacetate.

The neutralization curve for plicatic acid disclosed it to be a strong acid, $pK_a = 3$, comparable to orthohydroxybenzoic acids. However, in acids of this type having strong intramolecular hydrogen bonding the absorption band in the infrared spectrum assignable to the carbonyl occurs below 1680 cm^{-1} (5), whereas for plicatic acid the band assignable to the carbonyl is at 1713 cm^{-1}, a frequency normal for monobasic aliphatic acids.

The high acidity of plicatic acid indicated it would displace acetic acid from its salts. Treatment of an alcoholic solution with alcoholic potassium acetate precipitated a crystalline monopotassium salt, $C_{20}H_{21}O_{10}K$, in high yield. Therefore the possibility of isolating and purifying plicatic acid directly from the aqueous extractive by precipitation as the potassium salt is now being examined.

The analytical and molecular weight results on plicatic acid and its crystalline derivatives indicate it to be a propylphenol dimer of the lignan type and, pending completion of degradative studies, some deductions may be made as to the nature of the aromatic nuclei. The formation of some vanillin by oxidation indicates one aromatic ring to be 3-methoxy-4-hydroxyphenyl. The presence of two additional phenolic hydroxyls adjacent to one another is shown by the methylation data and the color tests. This together with the positive test for pyrogallol derivatives indicates a vicinal arrangement of these two phenolic hydroxyls with the other methoxyl on the other aromatic ring. In addition to the three phenolic hydroxyls and one carboxylic hydroxyl which, with two methoxyls, account for seven of the 10 oxygens required by the empirical formula, $C_{20}H_{22}O_{10}$, there are three alcoholic hydroxyls as shown by formation of a hexaacetate. One of these is used in γ-lactone formation by the methyl ester of the trimethyl ether, and the other two account for the hydroxyl band remaining in the infrared absorption spectrum of the lactone. Thus the formula for plicatic acid can be provisionally written: $C_6H_3(OH)(OCH_3).C_6H_4(OH)_3(COOH).C_6H_2(OH)_2(OCH_3)$, and it is reasonable to conclude that it is a highly hydroxylated lignan acid. Structural investigations are continuing.

While no lignan acids have been isolated from plant material heretofore, many of the lactones have (6), and it is significant that the infrared absorption spectrum of the lactone of methylated plicatic acid is similar to those published for the podophyllotoxin series (4).

The presence in plicatic acid of unetherified neighboring phenolic hydroxyls as in another lignan, nordihydroguaiaretic acid, a well-known commercial antioxidant, justifies its testing as an antioxidant. Similarly, biological testing of it and its lactone derivatives is in order in view of the fact that many lactones have marked physiological activity and some are valuable medicinals (7).

EXPERIMENTAL

Evaporations were conducted under reduced pressure at 40° C. Melting points were determined on a Fisher–Johns apparatus and are uncorrected. Carbon and hydrogen analyses were by Clark Microanalytical Laboratory, Urbana, Illinois. Infrared absorption spectra were determined on a Baird Atomic KM-1 spectrophotometer. Solvent mixtures for paper chromatography were carbon dioxide – water and butanol – acetic acid – water (40–10–50) for phenols and the latter and butanol–pyridine–water (10–3–3) for sugars.

Preparation of the Aqueous Extractive of Western Red Cedar

Straw-colored shingle mill spalts were ground in a Wiley mill to pass a 20-mesh screen. The wood meal (1.49 kg moisture-free basis, TAPPI hot-water solubility, 14.5%) was leached with four batches of hot water in an earthenware crock. The temperature was maintained at 100° C and agitation achieved by passing steam into the mixture. Results were as follows:

Extraction time (hours)	Volume of extract (liters)	Solids content (g)
2	14.3	84.4
1	7.7	27.1
1	7.0	13.4
1/2	9.3	11.8
Totals	38.3	136.7

After the solution was cooled, the combined extract was decanted from settled solids (10 g) and evaporated at reduced pressure to a viscous brown syrup, (168 g, 25% moisture). Yield based on the wood, 8.5% or 59% of the TAPPI hot-water solubility. Paper chromatograms (carbon dioxide – water) showed spots for phenols at R_f 0, .03, .07, .12, .16, .50, .70, .90. Color tests for thujaplicins were negative. Paper chromatograms showed arabinose and traces of other sugars.

Isolation of Plicatic Acid from Aqueous Extractive

(*a*) *By Sodium Bicarbonate Extraction of Lead-precipitated Phenols*

Aqueous extractive (331 g, moisture-free basis) in water solution was treated with lead acetate solution (900 g in 2 l.) and the precipitated white lead salts (427 g) removed by filtration. A portion (273 g) of the lead salt was agitated with 2-butanone (2 l.) containing excess sulphuric acid (6 *N*). After filtration, the 2-butanone solution was extracted with 5% sodium bicarbonate solution (500 ml, 3×250 ml). The bicarbonate solution after back extraction with 2-butanone was saturated with sodium chloride, acidified with dilute sulphuric acid (12 *N*), and extracted with 2-butanone (2×500 ml, 2×100 ml). The 2-butanone solution was dried over sodium sulphate and evaporated to yield brown amorphous plicatic acid (119 g), which in paper chromatography showed no contamination with sugars or other phenols.

(*b*) *By Column Chromatography*

Aqueous extractive (2.6 g, moisture-free basis) in warm water (400 ml) was added to a column bed (5 cm × 30 cm) of Amberlite IRC-50 (H) (Rohm and Haas, Philadelphia, Penn.) at a rate of 1.5 ml/minute. The column was eluted at the same rate, first with water and then with graded ethanol–water using a fraction collector loaded with 15-ml tubes. The contents of each fifth tube were checked by paper chromatography. The water

eluted arabinose and phenols of R_f .9, .7, and .5 in that order with partial overlapping. The ethanol–water eluted phenols of R_f .52, .03, and a mixture of R_f .03, .06, and .1 in that order. Fractions which were pure by paper chromatography were combined and lyophilized. Total yields were estimated from the pure yields and paper chromatographic data on fractions showing overlapping as follows:

Tube No.	Eluant	R_f of phenols	Yield of pure material (mg)	Total yield estimated (mg)
0–40	H_2O	—	—	—
40–80	H_2O	.90	650	1250
65–140	H_2O	.70	—	200
80–200	H_2O	.50	215	525
200–320	5–20% EtOH	.52	110	225
310–330	20–25% EtOH	.03	30	100
330–340	25–30% EtOH	.03		
		.06	200	200
		.10		
	Totals		1105	2500

The plicatic acid (R_f 0.9) obtained was a light tan, amorphous powder.

(*c*) *By Countercurrent Distribution with Ethyl Acetate – Water*

Aqueous extractive solids (12 g) were added to a 1-liter separatory funnel containing water-saturated ethyl acetate (400 ml) and ethyl-acetate-saturated water (400 ml) and the mixture shaken 5 minutes before separation. The water layer was transferred to a second funnel and similarly treated with fresh ethyl acetate while the ethyl acetate layer was treated with fresh water in the first funnel. This procedure was repeated through six stages involving six funnels until the original water was in funnel six in contact with the last added ethyl acetate and the original ethyl acetate was in funnel one in contact with the last added water. The water layer in funnel six on lyophilization yielded plicatic acid (2.5 g) contaminated with 7–9% arabinose (as determined by quantitative paper chromatography). The combined water layers from funnels four and five with the ethyl acetate layers from five and six yielded paper chromatographically pure plicatic acid (2.3 g), R_f in carbon dioxide – water, 0.9; in butanol – acetic acid – water, 0.4, a light tan-colored powder; $[\alpha]_D^{21}$ −9.99 (water). Ultraviolet absorption in water: min. 256 mμ (log ϵ = 3.23); max. 281 mμ (log ϵ = 3.58); shoulder, 307 mμ (log ϵ = 2.42). Infrared absorption, ν_{max}^{KBr} in cm^{-1}: 3340, 1713, 1611, 1518, 1200, 1088. Calc. for $C_{20}H_{24}O_{10}$: C, 56.6; H, 5.71; OCH_3, 14.6; mol. wt. and neutral equivalent, 424.2; for $C_{20}H_{22}O_{10}$: C, 56.9; H, 5.26; OCH_3, 14.67; mol. wt. and neutral equivalent, 422.2. Found: C, 56.24; H, 5.84; OCH_3, 13.7; mol. wt. (Rast), 433; neutral equivalent, 432. Approximate pK_a from pH at half-neutralization, 3.0.

Color tests with aqueous solutions of plicatic acid were as follows: aqueous ferric chloride, pinkish purple shifting to blue and then red on addition of sodium carbonate; ammonium molybdate and acetic acid (8), reddish brown; with Folin–Denis reagent (9) blue; ferrous sulphate – sodium potassium tartrate at pH 5.6 (10), negative; titanium chloride, yellow; chlorine – sodium sulphite (11), red; Gaebel test for methylenedioxy groups (12), negative.

A quantitative alkaline–nitrobenzene oxidation test, using the technique of Stone and Blundell (13) showed 4% vanillin formation.

Repeated attempts to obtain a crystalline acetate or benzoate of plicatic acid were

unsuccessful. The amorphous product of treatment with acetic anhydride and pyridine in benzene solution was precipitated in fractions by stepwise addition of ligroin. The last most soluble fraction had a methoxyl content of 9.1; calculated for a hexaacetate, $C_{32}H_{34}O_{16}$, 9.17.

Plicatic Acid Trimethyl Ether Methyl Ester

Plicatic acid (5 g) in a mixture of water (5 ml) and acetone (9 ml) was treated with dimethyl sulphate (4 ml) and 5 *N* sodium hydroxide dropwise at reflux for 2 hours while maintaining the pH at 8–9. The methylated plicatic precipitated as the white sodium salt during the latter stages of the reaction. The reaction mixture was acidified to pH 3, the acetone removed, and the mixture extracted with chloroform. The residue from evaporation of the chloroform solution was methylated in dioxane with excess diazomethane to yield a product which crystallized from benzene in 42% yield. Melting point after recrystallization from benzene 204–205° C $[\alpha]_D^{22}$ −29.9 ($CHCl_3$).

A methylation of plicatic acid in methanol directly with diazomethane gave the same product contaminated with large amounts of black ether-soluble tar which complicated the purification and reduced the yield of pure product to 23%.

The product, recrystallized from benzene, contained benzene of crystallization. Recrystallization from ethanol gave colorless crystals m.p. 203–204° C. Calc. for $C_{24}H_{30}O_{10}$: C, 60.24; H, 6.32; OCH_3, 38.9; mol. wt., 478.6. Found: C, 59.91; H, 6.02; OCH_3, 38.7; mol. wt. (Rast), 478. Infrared spectrum, ν_{max}^{KBr} in cm^{-1}: 3460, 1716, 1588, 1522, 1511, 1451, 1422, 1256, 1235, 1215, 1128, 1002, 861.

Plicatic Acid Trimethyl Ether Lactone

The trimethyl ether methyl ester on the melting point stage was observed to evolve a gas after melting and then recrystallize. The material evolved was condensed and found to be methanol and the solid, m.p. 252–255° C had an infrared absorption characteristic of a γ-lactone. Accordingly the ester (0.1 g) was heated under nitrogen at 220° C until evolution of gas had ceased and the material had resolidified. Recrystallization from ethanol gave colorless crystals, m.p. 257° C. Calc. for $C_{23}H_{26}O_9$: C, 61.93; H, 5.88; OCH_3, 34.72. Found: C, 61.82; H, 5.99; OCH_3, 34.66. Infrared spectrum, ν_{max}^{KBr} in cm^{-1}: 3450, 1784, 1593, 1518, 1465, 1425, 1322, 1255, 1220, 1126, 992, 862.

Potassium Plicatate

Plicatic acid (2 g) in anhydrous ethanol (50 ml) was treated with anhydrous potassium acetate (0.6 g) in ethanol (10 ml). The white salt which precipitated immediately was separated on the centrifuge and washed well with ethanol (70 ml) before drying under pressure at 65° C. Yield 1.5 g (68.5% of theory). The product was quite soluble in methanol and could be reprecipitated by addition of ethanol. Calc. for $C_{20}H_{21}O_{10}K$: C, 52.16; H, 4.60; OCH_3, 13.45; K as sulphated ash, 18.82. Found: C, 52.17; H, 5.11; OCH_3, 13.39; K as sulphated ash, 18.7. The infrared absorption spectrum was characteristic of the salt of an organic acid (5), ν_{max}^{KBr} in cm^{-1}: 3340, 1610 and 1600 (broad doublet), 1515, 1350–1320 (broad), 1205, 1090, 872.

ACKNOWLEDGMENT

The authors are indebted to Canadian Forest Products Limited for supplying cedar wood samples.

REFERENCES

1. BARTON, G. M. and GARDNER, J. A. F. Pulp Paper Mag. Can. **55** (10), 132 (1954).
2. MACLEAN, H. and GARDNER, J. A. F. Forest Prods. J. **6**, 510 (1956).
3. GAGE, T. B., MORRIS, Q. L., DETTY, W. E., and WENDER, S. H. Science, **113**, 522 (1951).
4. SCHRECKER, H. W. and HARTWELL, J. L. J. Am. Chem. Soc. **75**, 5916 (1953).
5. BELLAMY, L. J. The infrared spectra of complex molecules. Methuen & Co. Ltd., London. 1954.
6. HEARON, W. M. and MACGREGOR, W. S. Chem. Revs. **55**, 957 (1955).
7. HAYNES, L. J. Modern methods of plant analysis. Vol. II. Springer-Verlag, Berlin. 1955. p. 584.
8. QUASTEL, J. H. Analyst, **56**, 311 (1931).
9. FOLIN, O. and DENIS, W. J. Biol. Chem. **12**, 239 (1912).
10. KURSANOV, A. L. and ZAPROMETOV, M. N. Biokhimiya, **14**, 467 (1949).
11. CAMPBELL, W. G., MACGOWAN, J. G., and BRYANT, S. A. Biochem. J. **32**, 2138 (1938).
12. GAEBEL, G. O. Arch. Pharm. **248**, 225 (1910).
13. STONE, J. E. and BLUNDELL, M. J. Anal. Chem. **23**, 771 (1951).

INFRARED SPECTRA AND STRUCTURE OF POLYALDEHYDES

III. POLYACETALDEHYDE AND POLYPROPIONALDEHYDE[1]

A. NOVAK[2] AND E. WHALLEY

ABSTRACT

Acetaldehyde and propionaldehyde have been polymerized at room temperature and pressures of about 10 kb. The infrared spectra of the polymers have been investigated and it is shown that the polymers have the formula $HO(CHR.O)_nH$. The spectra are too complicated to be understood if there is only one monomer unit in the repeating unit of the chain; there are at least two units.

1. INTRODUCTION

Polyacetaldehyde was first made approximately simultaneously by Letort (1) and by Travers (2) by cooling acetaldehyde in liquid nitrogen. The molecular weight of a sample was about a half-million (3). A note (4) describes briefly its infrared spectrum, which indicates that its structure is $(CHCH_3.O)_n$, confirming Staudinger's suggestion (5). Attempts to polymerize propionaldehyde by this method failed (6). The higher aliphatic aldehydes, butyraldehyde and higher homologues, polymerize under pressures of about 10 kb (7, 8) to give compounds that are presumed to have the structure $(CHR.O)_n$, but an attempt to polymerize acetaldehyde by subjecting it to a pressure of 9 kb and 40° C failed (9). Low-molecular-weight polymers of acetaldehyde have been made (10) by treating mixtures of acetaldehyde and acetaldehyde diethylacetal with a small amount of concentrated sulphuric acid at −40 to +20° C, and the structure C_2H_5O-$(CHCH_3.O)_nC_2H_5$ was suggested. Propionaldehyde has apparently not been polymerized previously except by the aldol condensation.

In this paper we describe the preparation of polymers of acetaldehyde and propionaldehyde by subjecting the monomers to pressures of about 9 kb at room temperature. The infrared spectra and X-ray diffraction patterns of these polymers, of low-temperature polyacetaldehyde, and of the polymer from acetaldehyde and acetal have been obtained in order to help elucidate the structures.

2. EXPERIMENTAL METHODS AND RESULTS

Eastman-Kodak White-Label acetaldehyde, acetal, and propionaldehyde were used. They were dried with Drierite and distilled before use in a fractionating column in an atmosphere of dry air. Acetaldehyde-d_1 (CH_3CDO) and propionaldehyde-d_1 (C_2H_5CDO) were prepared from nitroethane and nitropropane respectively by the method described by Leitch (11).

High-pressure Polymerization

The monomers were subjected to pressures of about 9 kb for 1–2 days at room temperature. The reaction vessel was a 1-cm³ stainless-steel test tube closed by a piston that was fitted with an *o*-ring. The vessel was filled with aldehyde, stoppered, and put into the high-pressure end of an intensifier which was then pressurized. When the monomers were almost free of water the polymerization was almost complete in 1–2 days and the

[1]*Manuscript received March 25, 1959.*
Contribution from the Division of Applied Chemistry, National Research Council, Ottawa, Canada.
Issued as N.R.C. No. 5309.
[2]*N.R.C. Postdoctorate Fellow, 1956–58.*

polymers were tacky solids. The proportion polymerized and the viscosity of the product decreased rapidly when small amounts of water were added to the monomer. For example, the azeotropic mixture of propionaldehyde and water, which contains about 1.9% of water in the form of the hydrate (12), polymerized under pressure only to the extent of about 30%, as estimated from the intensity of the C=O stretching band in a solution of the mixture in carbon tetrachloride, and after evaporation of the monomer the polymer remained as a liquid probably of low molecular weight as estimated from the intensity of the OH end group stretching band (see below). If we can anticipate our conclusions about structure, this is probably due to the equilibrium

$$\frac{1}{n}H_2O + RCHO \rightleftharpoons \frac{1}{n}HO(CHR.O)_nH$$

being dependent upon the amount of water present. At 1 atm pressure and room temperature the polymers depolymerized spontaneously to the parent aldehyde. The depolymerization of the solid polymer was rather slow and took several weeks at room temperature if it was exposed to the atmosphere so that the monomer could evaporate. If the monomer was not allowed to evaporate, or if the polymer was liquid, or if it was dissolved in carbon tetrachloride, depolymerization was complete, as determined by the infrared spectrum, in a few days. Presumably depolymerization occurs faster in a less viscous medium.

Low-pressure Polymerization of Acetaldehyde

The low-temperature polymer was made by condensing the vapor at liquid-nitrogen temperatures as described by Bevington and Norrish (13). A polymer of low molecular weight was prepared by treating a mixture of acetaldehyde and acetal in molar ratio 6:1 at −40° C with a drop of concentrated sulphuric acid (10). After 2 hours the acid was neutralized with sodium bicarbonate and the mixture dried with Drierite and filtered. The dimer and trimer were distilled off under reduced pressure; an oily liquid remained.

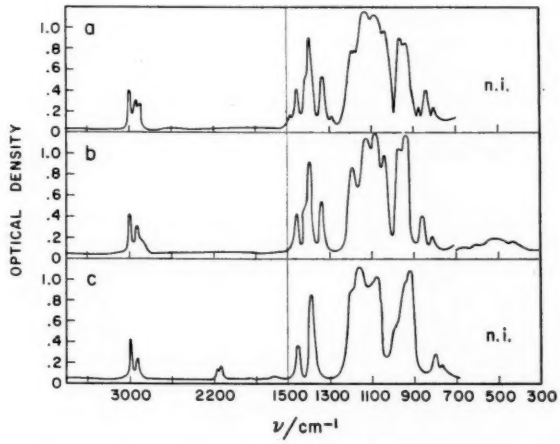

FIG. 1. Infrared spectrum of polyacetaldehyde: (*a*) low-molecular-weight polymer from acetaldehyde and acetal, (*b*) high-pressure polyacetaldehyde, (*c*) high-pressure polyacetaldehyde-d_1.

The polymers were examined spectroscopically as thin films pressed between sodium chloride or cesium bromide windows and as solutions in carbon tetrachloride. The spectra were recorded between 4000 and 700 cm^{-1} using a Perkin–Elmer Model-21 infrared spectrophotometer equipped with a rock salt prism, and between 700 and 300 cm^{-1} with a Beckmann IR-4 spectrophotometer equipped with a cesium bromide prism. The infrared spectra of polyacetaldehyde and polypropionaldehyde are shown in Figs. 1 and 2, and the wave numbers and relative intensities of the bands are given in Tables I and II.

X-ray diffraction photographs of films were taken with a Debye–Scherrer powder-camera, diameter 114.7 mm, using nickel-filtered copper radiation. Polyacetaldehyde gave two diffuse rings corresponding to interplanar spacings of 3.9 and 7.2 Å; polypropionaldehyde gave three diffuse rings corresponding to interplanar spacings of 2.1, 4.1, and 9.0 Å.

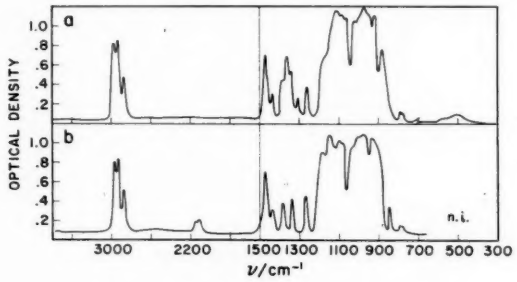

FIG. 2. Infrared spectrum of: (*a*) polypropionaldehyde, and (*b*) polypropionaldehyde-d_1.

TABLE I

Infrared spectra of polyacetaldehyde and polyacetaldehyde-d_1

$(-CHCH_3-O-)_n$			$(-CDCH_3-O-)_n$		
Wave No. cm^{-1}	Intensity	Tentative approximate description	Wave No. cm^{-1}	Intensity	Tentative approximate description
3440	Variable, w	OH stretching	3440	Variable, w	OH stretching
2980	m	CH_3 asym. stretching	2980	m	CH_3 asym. stretching
2920	m	CH_3 sym. stretching	2920	m	CH_3 sym. stretching
2860	sh	CH stretching	2160	w	CD stretching
			2140	w	
1445	m	CH_3 asym. bending	1445	m	CH_3 asym. bending
1400	sh	CH bending			
1380	s	CH_3 sym. bending	1380	s	CH_3 sym. bending
1335	m	CH bending			
1187	s	CH_3 rocking	1195	sh	CH_3 rocking, C—O and C—C stretching, and C—D bending
1130	vs	C—O and C—C stretching	1165	vs	
1085	vs		1100	sh	
1040	vs		1078	vs	
970	vs		990	sh	
			950	vs	
935	vs		925	vs	
845	m	C—H bending	787	m	C—D bending
810	w		760	w	
620	sh	C—O and C—C bending			
490	w				
450	sh				

TABLE II

Infrared spectra of polypropionaldehyde and polypropionaldehyde-d_1

$(-CHC_2H_5-O-)_n$			$(-CDC_2H_5-O-)_n$		
Wave No. cm^{-1}	Intensity	Tentative approximate description	Wave No. cm^{-1}	Intensity	Tentative approximate description
3460	Variable, w	OH stretching	3460	Variable, w	OH stretching
2960	s	C—H stretching	2960	s	CH_3, CH_2, and C—H stretching
2925	s		2925	s	
2870	m		2870	m	
			2150	w	C—D stretching
			2125	w	
1468	s	CH_2 bending	1468	s	CH_2 bending
1443	m	CH_3 asym. bending	1443	m	CH_3 asym. bending
1380	sh	CH_3 sym. bending	1380	m	CH_3 sym. bending
1360	s	C—H bending			
1345	m	CH_2 wagging	1342	m	CH_2 wagging
1305	m	C—H bending			
1265	m	CH_2 twisting	1270	m	CH_2 twisting
1175	sh	CH_3 rocking	1182	vs	CH_3 rocking, C—O and C—C stretching, and C—D bending
1120	vs	C—O and C—C stretching	1150	vs	
1085	vs		1108	vs	
1050	sh		1092	vs	
1020	vs		1045	sh	
1010	sh		1007	vs	
975	vs		980	vs	
960	sh		940	vs	
925	vs		920	sh	
895	m	C—H bending	855	m	C—D bending
795	w	CH_2 rocking?	790	w	CH_2 rocking
780	w		773	w	
520	sh	C—O and C—C bending	n.i.		
480	w				

3. DISCUSSION

(*i*) *Polyacetaldehyde*

The infrared spectra of low-temperature and high-pressure polyacetaldehyde were identical, except for the intensity of the minor bands in some samples in the region of 3300 cm^{-1} which we ascribe to end groups (see below). Chemical evidence (14) and previous spectroscopic evidence (4) show that the low-temperature polymer has the structure $(CHCH_3.O)_n$. Detailed examination of the spectra, which is described below, fully agrees with this. Hence, the low-temperature and high-pressure polymers are identical, except perhaps for molecular weight. There is a weak band at 3440 cm^{-1} which varies in intensity from sample to sample. It is probably due to OH end groups; the formula is thus $HO(CHCH_3.O)_nH$.

The X-ray diffraction patterns of thin films of both low-temperature and high-pressure polymer show only two diffuse rings which correspond to spacings of about 3.9 and 7.2 Å, in agreement with the spacings reported for the low-temperature polymer (14). Filaments were drawn from the polymers, but X-ray diffraction photographs of them showed no orientation. It has been suggested (14) that the broad rings are due to intrachain spacings. However, the corresponding spacings of other polyaldehydes are greater than those of polyacetaldehyde by an amount that increases as the bulk of the side chain increases (15). It seems more likely, therefore, that these broad bands are due to interchain and not to intrachain distances.

The infrared spectrum of the polymer obtained from acetaldehyde and acetal is similar

to that of polyacetaldehyde and confirms the proposed structure (10) $C_2H_5O(CHCH_3.O)_n$-C_2H_5. The bands in the skeletal stretching region (1200–900 cm^{-1}) are slightly displaced from, and their relative intensities are somewhat different from, those of high-molecular-weight polyacetaldehyde. In addition, a few weak bands or shoulders appear near 2880, 1470, 1295, 1170, and 870 cm^{-1}; they are probably due to the ethyl end groups.

The infrared spectra of high-pressure polyacetaldehyde and polyacetaldehyde-d_1 are shown in Fig. 1. The bands in the skeletal stretching and skeletal bending regions are broad, in contrast to those of polychloral (15), probably because there are many rotational isomers present. However, if, as seems likely, the polymer chain is kinked at a small proportion of the C—O bonds and the interaction between the chains is small, the spectrum will resemble that of the isolated regular (i.e. repeating) chain. In particular, the number of strong bands observed should be close to the number expected for an isolated regular chain, and the bands will be broader than for the regular chain because rotational isomers are present. Similar assumptions about other polymers have been made by others (16, 17), and we tentatively assume that they are true for polyacetaldehyde and polypropionaldehyde. The observation that the infrared spectrum of polyacetaldehyde in solution is similar, except that the bands are broader, to the spectrum of the pure polymer verifies that interaction between chains does not produce major changes in the number of strong bands. Davison (18) has shown that the presence of rotational isomers causes broadening of the bands in polyesters and related compounds. The assumption that the number of strong bands in a moderately kinked chain is close to the number expected for a regular chain allows us to obtain some tentative information about the structure of the polymer chain. Unfortunately, there appears to be no simple way of counting the number of kinks and so of verifying our assumption directly. We were not able to obtain oriented specimens of polyacetaldehyde or polypropionaldehyde and so could not obtain the dichroisms, probably because the melting point is below room temperature.

If there is one monomer unit in the repeat of polyacetaldehyde there are $3\times7-4 = 17$ fundamental frequencies that may be optically active, because only those vibrations that are in phase in all repeat units can be active in a perfect chain. These frequencies may be approximately divided as follows. Between 3000 and 2700 cm^{-1} two asymmetrical (which are probably not resolvable) and one symmetrical CH_3 stretching frequency and one CH stretching frequency are expected. Between 1500 and 1300 cm^{-1} two asymmetrical (which may not be resolvable) and one symmetrical CH_3 bending frequency are expected. Only one CH bending frequency is expected in this region, the other being probably below 1200 cm^{-1}, because deuterated chloral hydrate (19) has only one band in this region, and a band near 1100 cm^{-1} that is present in acetals and absent in ketals has been ascribed (20) to the CH bending mode. Between 1300 and 700 cm^{-1} two CH_3 rocking (which may not be resolved), one CH bending, and three skeletal (CO and CC) stretching bands are expected.

In the spectrum of polyacetaldehyde there are three bands in the 3-μ region, 2980, 2920, and 2860 cm^{-1}. The 2860-cm^{-1} shoulder disappears on deuteration and is replaced by two bands at 2160 and 2140 cm^{-1}. The 2860-cm^{-1} shoulder is thus a CH stretching band and the 2980- and 2920-cm^{-1} bands are the CH_3 asymmetrical and symmetrical stretching bands respectively. The two bands at 2160 and 2140 cm^{-1} may both be CD stretching fundamentals of the regular chain or one may be a band characteristic of the non-crystalline polymer, as occurs in the CH stretching region in polychloral (15), or one may be an overtone whose intensity is increased by Fermi resonance.

In the range 1500–1300 cm^{-1} there are three medium or strong bands, 1445, 1380, and 1335 cm^{-1}, and a shoulder, 1400 cm^{-1}. The 1400- and 1335-cm^{-1} bands disappear on deuteration and are thus CH bending bands; two CH bending bands are also present in polychloral (15) at 1360 and 1325 cm^{-1}. The bands at 1445 and 1380 cm^{-1} do not shift on deuteration and are straightforwardly assigned to the asymmetrical and symmetrical CH_3 bending modes, respectively.

The bands below 1200 cm^{-1} are not so easily identified. There are very intense and broad bands at 1187, 1130, 1085, 1040, 970, and 935 cm^{-1}. No band similar to the 1187-cm^{-1} band is observed in the spectra of the polyaldehydes which do not contain methyl groups, such as polymers of formaldehyde (21), chloral (15), and mono- and di-chloroacetaldehyde (22), and it might be due to the CH_3 rocking vibrations which are expected in this region (23). This mode involves appreciable skeletal stretching motion (23) and so may absorb strongly. The remaining bands in the 1200–900 cm^{-1} region are likely to be due to C—O and C—C stretching vibrations; they are similar to bands in the spectra of acetals and of other polyaldehydes. The changes in this region on deuteration are difficult to interpret because the bands overlap and are broad. Two CD bending bands, corresponding to the CH bending bands 1400 and 1335 cm^{-1}, should be here.

There is a medium band at 845 cm^{-1} and a weak band at 810 cm^{-1} which are replaced on deuteration by bands at 787 and 760 cm^{-1}. They might be associated with the low-frequency C—H bending mode. The shifts, however, are small and if they are CH bending bands they must be strongly coupled with skeletal motions; presumably other bands in the region 1200–1000 cm^{-1} shift but the shifts are masked by the overlapping of bands.

In the remaining part of the spectrum there occurs only one very broad weak band at 490 cm^{-1} with shoulders at 510 and 450 cm^{-1}. Similar bands occur in the spectra of acetals (20) and other polyaldehydes (15, 21, 22, 25) and are probably due to skeletal bending motions.

It is not easy to interpret the spectrum on the grounds of one monomer unit in the repeat unit. Thus, there are two higher-frequency C—H bending bands where only one is expected; there are eight bands in the region 1250–700 cm^{-1} where there are only six expected if the two CH_3 rocking modes are resolved and only five if, as seems very likely, they are not. If the assumption that we have made, that the kinking of the chain does not greatly effect the number of strong bands, is true then there are at least two monomer units in the repeat unit of the polymer chain.

(ii) Polypropionaldehyde

Polypropionaldehyde is very similar to polyacetaldehyde in chemical properties and in infrared spectrum. It is therefore a substituted polyoxymethylene and has the monomer unit ($CHC_2H_5.O$), as expected from the ease of polymerization and depolymerization. A broad weak band at 3460 cm^{-1} occurs in some samples; it is probably an OH stretching band due to the end groups. The polymer is therefore $HO(CHC_2H_5.O)_nH$. The X-ray powder diagram has two diffuse rings that correspond to spacings of about 9.0 and 4.1 Å. This and the broadness of the skeletal stretching and bending bands show (see below) that the polymer is amorphous. The broad rings on the X-ray diagram probably relate to interchain rather than to intrachain distances, as argued above for polyacetaldehyde. The infrared spectra can be analyzed, as was that of polyacetaldehyde, to show that there is probably more than one monomer unit in the repeat. The assumptions made are the same as those made for polyacetaldehyde, i.e. that rotational

isomerism and interaction between chains broadens the infrared bands but does not produce much change in the number of strong bands. By analogy with polyacetaldehyde and polychloral it is likely that only the CH bending and skeletal stretching and possibly the CH stretching modes will give information about the structure. If there is one monomer in the repeat unit then one CH stretching, one CH bending, and four skeletal stretching bands are expected.

There are three strong bands in the 3-μ region, at 2960, 2925, and 2870 cm^{-1}. They do not shift on deuteration, and so are due mainly to methyl and methylene groups. Though no shifts are observed on deuteration, two bands, 2150 and 2125 cm^{-1}, appear in the spectrum of polypropionaldehyde-d_1. At least one band is CD bending and, as with polyacetaldehyde, both may be fundamentals of the crystalline polymer, one may be a band characteristic of the disordered regions of the polymer, or one may be an overtone in resonance with the fundamental.

In the region 1500–1200 cm^{-1} there are medium or strong bands at 1468, 1443, 1380, 1345, 1305, and 1265 cm^{-1}. The 1360- and 1305-cm^{-1} bands disappear on deuteration and, as we argued for similar bands in polyacetaldehyde, are probably higher-frequency CH bending bands. The 1443- and 1380-cm^{-1} bands are close to those of polyacetaldehyde and are therefore probably respectively asymmetrical and symmetrical CH_3 bending bands. The remaining three bands, 1468, 1345, and 1265 cm^{-1}, are not present in polyacetaldehyde and shift but slightly on deuteration. They are therefore probably CH_2 bending modes and, on grounds of frequency by comparison with small molecules, are probably the bending, wagging, and twisting modes respectively.

The 1200–900 cm^{-1} region is less straightforward. There are about nine strong or very strong bands. A shoulder at 1175 cm^{-1} might, by analogy with polyacetaldehyde and smaller molecules, be due to the CH_3 rocking modes. The remaining are probably skeletal stretching bands. There are therefore about eight skeletal stretching bands. If there is one monomer unit in the repeating unit only four are expected. This together with the two CH bending bands at 1400–1300 cm^{-1} shows that, if kinking does not cause many new strong bands, then there is probably more than one monomer unit in the repeating unit of the chain. In the spectrum of polypropionaldehyde-d_1 the bands in this region are shifted and their intensities changed. The interpretation of this is uncertain because CD bending bands are expected here.

In the remaining part of the spectrum there are medium or weak bands at 895, 795, 780, and 480 cm^{-1}. The 895-cm^{-1} band is replaced on deuteration by a band at 855 cm^{-1}. It is likely that CH bending is an important contributor to this mode. The bands at 795 and 780 cm^{-1} shift little on deuteration and are not observed in polyacetaldehyde. They may be CH_2 rocking modes, which are expected about here. The very broad weak band at 480 cm^{-1} accompanied by a shoulder at about 590 cm^{-1} is due to skeletal bending vibrations.

We have seen that the spectra of polyacetaldehyde and polypropionaldehyde are considerably more complicated than they would be if there was only one monomer unit in the repeat unit. In particular, there are twice as many high-frequency CH bending and somewhat less than twice as many skeletal stretching bands as are expected for one monomer unit. No further information is obtainable from the infrared spectrum at present. It is interesting to note, however, that polyformaldehyde has a helical configuration (24) which is probably formed from gauche conformations of the C—O bonds (25). The stable conformation of the smallest molecules derived from polyformaldehyde dimethoxymethane, is the double gauche form (26, 27). It seems not unlikely that the

higher homologues of dimethoxymethane, i.e. 1,1-dimethoxyethane and 1,1-dimethoxypropane, have a stable conformation similar to that of dimethoxymethane. If this is so then a chain of such units, such as are polyacetaldehyde and polypropionaldehyde, would be expected to have at equilibrium at low temperatures a spiral structure similar to that of polyformaldehyde. The infrared spectra are certainly consistent with a spiral structure, but do not prove it. As outlined previously (21), for all cyclic structures but the trivial plane zigzag, each mode of vibration of the monomer splits into two infrared-active modes, of species A and E_1 (E in some of the simpler spirals). Consequently, if the spiral were perfect, then two high-frequency CH bending and six (polyacetaldehyde) and eight (polypropionaldehyde) skeletal stretching modes would be expected to be active. These are approximately the number of strong bands found in the spectra, and so, if rotational isomerism does not cause many new strong bands, the spectra are consistent with the structures' being spirals.

ACKNOWLEDGMENTS

The authors are very grateful to Dr. L. D. Calvert for taking the X-ray diffraction photographs and to Mr. A. Lavergne for help with the high-pressure equipment.

REFERENCES

1. LETORT, M. Compt. rend. **202**, 767 (1936).
2. TRAVERS, M. Trans. Faraday Soc. **32**, 246 (1936).
3. MUTHANA, M. S. and MARK, H. J. Polymer Sci. **4**, 91 (1949).
4. SUTHERLAND, G. B. B. M., PHILPOTTS, A. R., and TWIGG, G. H. Nature, **157**, 267 (1946).
5. STAUDINGER, H. Trans. Faraday Soc. **32**, 246 (1936).
6. LETORT, M. and DUVAL, X. Compt. rend. **216**, 58 (1943).
7. BRIDGMAN, P. W. and CONANT, J. B. Proc. Nat. Acad. Sci. **15**, 680 (1929).
8. CONANT, J. B. and TONGBERG, C. O. J. Am. Chem. Soc. **52**, 1659 (1930).
9. FAWCETT, E. W. and GIBSON, R. O. J. Chem. Soc. 386 (1934).
10. FENNE, D. J. and MUGDAN, M. U.S. Pat. No. 2,607,804 (1952).
11. LEITCH, L. C. Can. J. Chem. **33**, 400 (1955).
12. SMITH, T. E. and BONNER, R. F. Ind. Eng. Chem. **43**, 1169 (1951).
13. BEVINGTON, J. C. and NORRISH, R. G. W. Proc. Roy. Soc. (London), A, **196**, 363 (1949).
14. RIGBY, H. A., DANBY, C. J., and HINSHELWOOD, C. N. J. Chem. Soc. 234 (1948).
15. NOVAK, A. and WHALLEY, E. Trans. Faraday Soc. In press.
16. TOBIN, M. C. J. Chem. Phys. **23**, 891 (1955).
17. LIANG, C. Y., KRIMM, S., and SUTHERLAND, G. B. B. M. J. Chem. Phys. **25**, 543 (1957), and later papers.
18. DAVISON, W. H. T. J. Chem. Soc. 3270 (1955).
19. NOVAK, A. and WHALLEY, E. Unpublished work.
20. BERGMANN, E. D. and PINCHAS, S. Rec. trav. chim. **71**, 161 (1952).
21. NOVAK, A. and WHALLEY, E. Trans. Faraday Soc. In press.
22. NOVAK, A. and WHALLEY, E. Can. J. Chem. **37**, 1722 (1959).
23. JONES, R. N. and SANDORFY, C. In A. WEISSBERGER. *Editor*. Technique of organic chemistry. Vol. IX. Interscience Publishers, Inc., New York. 1956. p. 342.
24. WILMSHURST, J. K. Can. J. Chem. **36**, 285 (1958).
25. NOVAK, A. and WHALLEY, E. Can. J. Chem. **37**, 1718 (1959).
26. SAUTER, E. Z. physik. Chem. B, **21**, 161 (1933).
27. SHIMANOUCHI, T. and MIZUSHIMA, S. J. Chem. Phys. **23**, 707 (1955).
28. MIZUSHIMA, S., MORINO, Y., and KUBO, M. Physik. Z. **38**, 459 (1937).
29. AOKI, K. J. Chem. Soc. Japan, Pure Chem. Sect. **74**, 110 (1953).

THE INFRARED SPECTRA AND STRUCTURE OF POLYALDEHYDES

IV. THE HIGHER POLYALDEHYDES[1]

A. NOVAK[2] AND E. WHALLEY

ABSTRACT

The polymers of *n*- and iso-butyraldehyde and *n*-valeraldehyde, which were made by subjecting the aldehydes to pressures of about 8 kb, have been examined by infrared spectroscopy. They are homologues of polyformaldehyde, having the formula $HO(CHR.O)_nH$.

1. INTRODUCTION

The polymerization under pressure of aliphatic aldehydes was first observed by Bridgman and Conant (1) and by Conant and Tongberg (2). The polymers were quite different from those obtained by the aldol condensation, and they readily reverted to the monomers at normal temperature and pressure. Conant and Peterson (3) suggested that they were homologues of polyformaldehyde on the grounds that polymerization and depolymerization was relatively easy and was not catalyzed by bases.

We have investigated the infrared spectra of polymers of *n*- and iso-butyraldehyde, *n*-valeraldehyde, and *n*-heptaldehyde and confirm the structure suggested by Conant and Peterson. This paper reports this work.

2. EXPERIMENTAL METHODS AND RESULTS

The aldehydes were Eastman Kodak White-Label products; they were dried with Drierite several times and were fractionated in an atmosphere of dry air before use. Their infrared spectra were recorded for comparison purposes and to check the substantial absence of water and hydrates. The polymers were prepared by subjecting the monomers to pressures of about 9 kb at room temperature for about one day; this was done by placing them in 1-cm^3 stainless-steel test tubes which were sealed with a plug carrying an *o*-ring and put into the high-pressure end of a pressure intensifier of standard design. Polymerization was usually almost complete; monomer and lower polymers were removed if necessary by extraction with ethanol. Poly-*n*-butyraldehyde was a waxy solid, poly-*n*-valeraldehyde was a viscous liquid, and poly-*n*-heptaldehyde was a solid; all were soluble in ether and carbon tetrachloride and insoluble in ethanol. Poly-isobutyraldehyde was a hard transparent solid that was insoluble in the commoner solvents.

At room temperature all the polymers reverted to monomer. The depolymerization of poly-*n*-butyraldehyde in carbon tetrachloride solution was followed by infrared spectroscopy; depolymerization was complete in about 30 hours at room temperature. Poly-*n*-butyraldehyde was stored for several months in ethanol at about $-10°$ C without apparent depolymerization. No attempt was made to store the other polymers.

The polymers were investigated spectroscopically as films or as suspensions in nujol and hexachlorobutadiene. The spectra were recorded between 4000 and 700 cm^{-1} using a Perkin–Elmer infrared spectrophotometer, Model 21, with a sodium chloride prism, and between 700 and 300 cm^{-1} using a Beckmann IR-4 spectrophotometer with a cesium bromide prism. The spectra are shown in Fig. 1, and the wave numbers and relative intensities of the bands are listed in Table I.

[1]*Manuscript received March 25, 1959.*
Contribution from the Division of Applied Chemistry, National Research Council, Ottawa, Canada.
Issued as N.R.C. No. 5308.
[2]*N.R.C. Postdoctorate Fellow, 1956–58.*

TABLE I

Infrared spectra of polyaldehydes, $(CHR—O—)_n$

$R = CH_3(CH_2)_2$		$R = CH_3(CH_2)_3$		$R = CH_3(CH_2)_5$		$R = (CH_3)_2CH$	
Wave No. cm^{-1}	Intensity	Wave No. cm^{-1}	Intensity	Wave No. cm^{-1}	Intensity	Wave No. cm^{-1}	Intensity
		3440	Variable, w	3440	Variable, w		
2940	vs			2940	vs	2940	vs
2920	vs	2920	vs	2920	vs	2920	vs
2860	s	2860	vs	2850	vs	2860	s
1470	s	1470	s	1470	s	1475	s
1460	s	1460	sh	1460	sh	1463	sh
1436	m	1436	m	1436	m		
1372	s	1380	s, b	1374	s	1382	s
1345	s	1355	s	1355	s	1368	s
		1342	sh	1345	sh	1353	s
				1325	m	1335	m
1295	w	1285	w	1300	w	1304	m
1270	w	1250	w	1276	w		
1238	m	1220	m	1255	w		
				1225	m		
				1200	m		
						1190	s
1165	sh	1140	sh	1150	sh	1158	s
1125	vs, b			1130	vs	1130	s
1105	vs, b	1095	vs, vb	1102	vs	1060	vs
1090	vs, b			1050	s	1025	vs
1050	s	1050	sh	1036	vs	1008	vs
1007	vs, b	1005	vs, vb	1025	vs		
982	vs, b			1015	s	990	s
960	sh	960	sh	990	s	968	vs
914	vs	935	vs, vb	948	m	918	sh
				905	m	908	vs
840	w	875	sh	870	w	845	m
825	w			785	w	840	m
755	sh	780	w, b	760	w		
740	w	730	w	722	m	676	w
				610	w	628	vw
				544	m	519	m
530	w, vb	530	w, vb	455	w	495	sh
				390	w	456	m

NOTE: b=broad, vb=very broad.

X-ray diffraction photographs were taken on a Debye–Scherrer powder-camera using Ni-filtered Cu radiation. The lattice spacings are listed in Table II.

3. DISCUSSION

The infrared spectra (Fig. 1 and Table I) confirm Conant and Peterson's suggestion (3) that the polymers are substituted polyoxymethylenes. Thus, there are strong bands in the region 1200–900 cm^{-1}; i.e. in the region of C—O stretching bands, and there are no very strong broad bands near 3400 cm^{-1}, showing that OH groups in quantity are absent. Broad weak bands at about 3440 cm^{-1} occur in the spectra of some samples and are probably due to OH end groups; those samples in which the band is missing are probably of higher molecular weight. The chemical formula of the polyaldehydes is thus $HO(CHR.O)_nH$ and they are analogues of polyformaldehyde (4–6), polychloral (7), polyacetaldehyde (8), and polypropionaldehyde (8). The polymerization can be represented thus,

$$RCHO + \frac{1}{n}H_2O \rightleftharpoons \frac{1}{n}HO(CHR.O)_nH,$$

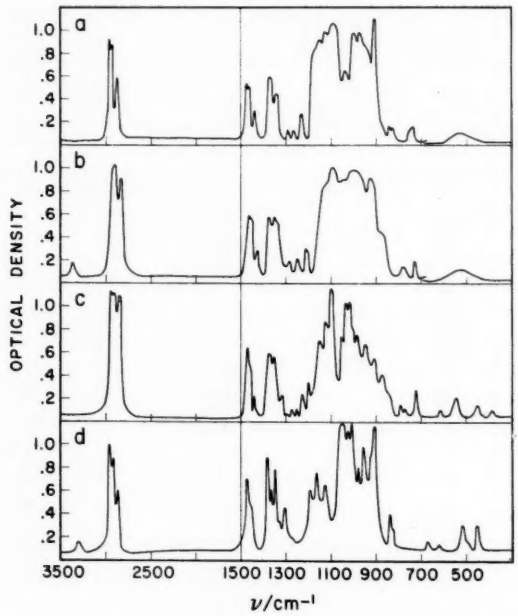

FIG. 1. Infrared spectra of polyaldehydes: (*a*) poly-*n*-butyraldehyde film; (*b*) poly-*n*-valeraldehyde film; (*c*) poly-*n*-heptaldehyde mull in nujol and hexachlorobutadiene; (*d*) poly-isobutyraldehyde mull in nujol and hexachlorobutadiene.

and the position of equilibrium is evidently displaced from almost completely on the left to nearly completely on the right by pressures of about 9 kb.

It is not possible to identify the infrared bands in detail. Undoubtedly C—H stretching modes are in the region 3000–2700 cm^{-1}, C—H bending modes in the region 1500–1200 cm^{-1}, skeletal stretching modes in the region 1200–700 cm^{-1}, with probably some of the lower-frequency C—H bending modes, and skeletal bending modes in the region 700–300 cm^{-1}. The spectra are too complicated to analyze in more detail at the present time.

It should be noted that the bands in the skeletal bending and stretching regions are broad in poly-*n*-butyraldehyde and poly-*n*-valeraldehyde and that the X-ray diagram of poly-*n*-butyraldehyde shows only a few diffuse halos. The X-ray diffraction diagram of poly-*n*-valeraldehyde could not be taken because it decomposed rapidly; since it is a viscous liquid it is likely to be amorphous. On the other hand, the infrared spectra of poly-isobutyraldehyde and poly-*n*-heptaldehyde in the skeletal bending and stretching regions are sharp and the X-ray diagrams for these polymers have relatively sharp rings. We conclude from this evidence that the polymers of *n*-butyraldehyde and *n*-valeraldehyde are amorphous and that the broadness of the infrared bands is caused by the presence of rotational isomers. It is unlikely that the broadness is due to intermolecular effects because the spectrum of poly-*n*-butyraldehyde in carbon tetrachloride solution is similar to that of the film. The polymers of isobutyraldehyde and *n*-heptaldehyde are relatively crystalline, and the sharpness of the infrared bands confirms that they contain relatively few rotational isomers.

TABLE II

Interplanar spacings of polyaldehydes, $(CHR.O)_n$

$R = CH_3(CH_2)_5$		$R = CH_3CH_2CH_2$		$R = (CH_3)_2CH$	
Spacing Å	Intensity	Spacing Å	Intensity	Spacing Å	Intensity
13.1	100	12.0	Halo 100	9.3	100 vb
11.5	100	9.0			
7.44	30			7.9	60 vb
6.53	50				
5.87	50			5.5	10
5.00	40	4.8	Halo 100		
4.66	50	4.0		4.6	60 b
4.18	90 b			3.95	20
3.65	50				
3.46	25			3.5	40 b
3.09	25				
2.87	25			2.65	5
2.67	25				
2.50	25 b			2.40	10 b
2.29	25			2.25	2 b
2.23	25				
2.17	30	2.05	20	2.04	5

The lattice spacings corresponding to the rings of the most intense lines of the X-ray diffraction photographs (Table II) increase with increasing length of the side groups. As we have pointed out before (8), it is likely because of this increase that these spacings are related to interchain rather than to intrachain distances.

REFERENCES

1. BRIDGMAN, P. W. and CONANT, J. B. Proc. Nat. Acad. Sci. **15**, 680 (1929).
2. CONANT, J. B. and TONGBERG, C. O. J. Am. Chem. Soc. **52**, 1659 (1930).
3. CONANT, J. B. and PETERSON, W. R. J. Am. Chem. Soc. **54**, 628 (1932).
4. STAUDINGER, H. Die hochmolekularen organischen Verbindungen. Springer-Verlag, Berlin. 1932.
5. PHILPOTTS, A. R., EVANS, D. O., and SHEPPARD, N. Trans. Faraday Soc. **51**, 1051 (1955).
6. NOVAK, A. and WHALLEY, E. Trans. Faraday Soc. In press.
7. NOVAK, A. and WHALLEY, E. Trans. Faraday Soc. In press.
8. NOVAK, A. and WHALLEY, E. Can. J. Chem. **37**, 1710 (1959).

INFRARED SPECTRA AND STRUCTURE OF POLYALDEHYDES

V. POLYMONOCHLOROACETALDEHYDE AND POLYDICHLOROACETALDEHYDE[1]

A. NOVAK[2] AND E. WHALLEY

ABSTRACT

The polymers of monochloroacetaldehyde and dichloroacetaldehyde have been examined by infrared spectroscopy. They are homologues of polyformaldehyde, having the formula $HO(CHR.O)_nH$. X-ray-diffraction powder photographs show that they are fairly crystalline.

1. INTRODUCTION

It has been known for some time that mono- and di-chloroacetaldehyde form trimers and polymers (1–3). Trimers are produced when the aldehydes are treated with concentrated sulphuric acid; they are crystalline substances with well-defined melting points (1–3) and are probably analogous to paraldehyde. Monochloroacetaldehyde polymerizes fast when allowed to stand in sealed tubes to give a substance described as amorphous (1) which has the same empirical formula as the aldehyde. Dichloroacetaldehyde, when purified, rapidly forms a similar substance that has the same empirical formula as the aldehyde. Both polymers are insoluble in water and alcohol, and that derived from monochloroacetaldehyde is insoluble also in ether and chloroform. They have no sharp melting points and they decompose to the parent aldehyde when heated to above 120° C. No work on the nature of these substances has been reported.

As part of our program of investigation of the structures of polyaldehydes (4–7) we have investigated the infrared spectra and X-ray powder diagrams of these polymers in order to elucidate their structure. This paper reports the results of this work.

2. EXPERIMENTAL AND RESULTS

Monochloroacetaldehyde (40% water solution) and dichloroacetaldehyde were commercial samples. Monochloroacetaldehyde solution was treated with concentrated sulphuric acid and distilled. The distillate formed a crystalline substance of melting point about 40–50° C which is probably the hydrate (1); this was treated again with concentrated sulphuric acid, and the vapor of the aldehyde which was obtained was dried by being passed through a tube containing calcium chloride heated at 100° C. The vapors when condensed polymerized rapidly to a solid which had similar properties to the polymer previously described (1). The commercial dichloroacetaldehyde was a rather viscous substance whose infrared spectrum indicates that it is a mixture mainly of a polymer whose structure is described below, aldehyde, and water. A small amount of concentrated sulphuric acid was added to this mixture and it was then distilled, and the vapor was dried in a similar manner to that used for monochloroacetaldehyde. The distillate polymerized into a block of translucent soft solid. The polymer was dissolved in acetone and precipitated with methanol. The precipitate was filtered and dried under reduced pressure.

The samples were examined as mulls in nujol and hexachlorobutadiene; the polymer of dichloroacetaldehyde was examined also in chloroform solution and as a film that was obtained by evaporating a solution of the polymer in acetone. The spectra were recorded

[1]*Manuscript received March 25, 1959.*
Contribution from the Division of Applied Chemistry, National Research Council, Ottawa, Canada.
Issued as N.R.C. No. 5307.
[2]*N.R.C. Postdoctorate Fellow 1956–58.*

between 4000 and 700 cm^{-1} using a Perkin–Elmer infrared spectrophotometer, Model 21, with a rock salt prism and a Beckmann IR-4 spectrophotometer with a cesium bromide prism. The infrared spectra of the polymers are shown in Fig. 1 and the wave numbers and relative intensities of the bands are listed in Table I.

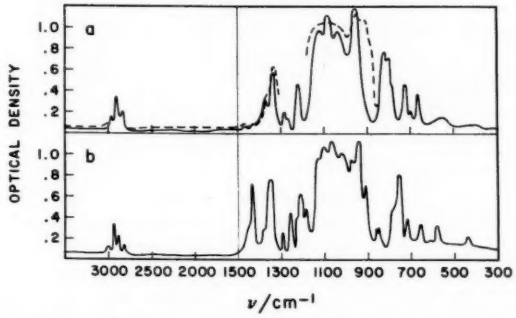

FIG. 1. Infrared spectra. (*a*) Polydichloroacetaldehyde: solid line, film: dotted line, in solution in $CHCl_3$. (*b*) Polymonochloroacetaldehyde: suspensions in nujol and hexachlorobutadiene.

TABLE I

Infrared spectra of polymers of mono- and di-chloroacetaldehyde

$(CHCH_2Cl—O—)_n$			$(CHCHCl_2—O—)_n$		
Wave No. cm^{-1}	Intensity	Approximate description	Wave No. cm^{-1}	Intensity	Approximate description
3460	Variable, w	OH stretching	3420	Variable, w	OH stretching
3000	w	CH stretching	3005	m	CH stretching
2935	m		2940	m	
2890	m		2870	m	
2820	w				
			1460	w	Combinations
1445	sh	CH_2 bending	1430	w	
1434	s				
			1370	m	CH bending
1375	sh		1338	s	
1350	s				
1298	m	CH bending, CH_2 wagging, and CH_2 twisting	1287	m	$CHCl_2$ bending
1265	m		1265	m	
1230	sh		1217	s	
1216	s		1132	vs	C—O stretching
1192	m		1087	vs	
			1040	vs	
1135	vs, b		955	vs	
1105	vs				
1065	vs		815	vs	C—C and C—Cl stretching
1025	vs		800	vs	
975	vs		775	sh	
942	vs	C—O, C—C, and C—Cl stretching, CH_2 rocking, and CH bending	725	s	
915	s		710	w	
862	m		675	m	
852	m				
790	s		550	m, b	Skeletal bending
762	s				
730	m				
716	w				
660	m				
620	w	Skeletal bending			
580	m				
440	w				

The X-ray powder photographs were taken with a Debye–Scherrer camera using nickel-filtered copper radiation. The lattice spacings calculated from the X-ray photographs are given in Table II.

TABLE II

X-Ray powder diagrams of polymers of mono- and di-chloroacetaldehyde

$(CHCH_2Cl—O—)_n$		$(CHCHCl_2—O—)_n$	
Spacing Å	Intensity	Spacing Å	Intensity
7.76	100	8.32	100
5.45	50	4.99 to 4.41	30
4.35 to 3.63	75 Halo	4.41 to 3.62	75
3.85	90	3.42	40
3.45	90	3.13	50
3.06	30	2.83	50
2.93	30	2.32	30
2.74	50	2.01	25
2.60	40		
2.44	60		
2.14	40		
2.00	25		

3. DISCUSSION

The infrared spectra have very strong bands in the region 1200–900 cm^{-1} that must involve C—O stretching motions. There are no carbonyl stretching bands and only very weak bands in the region of the OH stretching band. This evidence together with the ease of polymerization and depolymerization shows that the structure of the polymers is $(CHR.O)_n$ where R is either the monochloromethyl or dichloromethyl group. There are weak bands in the spectra of some samples in the region of 3400 cm^{-1} which are probably due to OH stretching vibrations. It is likely that the OH groups are at the ends of the chains, and so the formulas are $HO(CHR.O)_nH$. The polymers are thus substituted polyoxymethylene glycols, entirely analogous to the other polymers discussed in this series of papers.

The X-ray diffraction photographs have relatively sharp rings, indicating that the polymers are fairly crystalline, as we found also for polychloral. The bands in the skeletal stretching region of the spectra are broader than those of polychloral and narrower than those of polyacetaldehyde and polypropionaldehyde. It seems likely that the broadness is due, at least partly, to the presence of rotational isomers in the non-crystalline parts of the spectrum. This is supported by the skeletal stretching bands in the spectrum of polydichloroacetaldehyde in chloroform solution, which probably contains more rotational isomers than the solid, being much broader than those of the solid.

We have seen previously (4–7) that the spectra of the simpler polyaldehydes have more bands than they would have if there were only one monomer unit in the repeating unit, and it is pertinent to inquire if this is so also for polymonochloroacetaldehyde and polydichloroacetaldehyde. We make the same assumption that we have made previously, viz. that the amorphous regions of the polymers cause the infrared bands to broaden but do not cause many new bands.

Polydichloroacetaldehyde

If there is one monomer unit in the repeating unit then there are $3\times7-4 = 17$ potentially active fundamentals, which can be approximately divided into 6 CH and 11 skeletal vibrations, though there may, of course, be strong interaction between the lower-frequency CH and the skeletal vibrations. There are two kinds of CH group $CC(O—)_2H$ and $CCCl_2H$. The two CH bending frequencies of the $CC(O—)_2H$ group are expected, according to arguments presented in reference 5, to be one above 1300 cm^{-1} and one below 1200 cm^{-1}. The two CH bending frequencies of the $CCCl_2H$ group are expected to be between 1300 and 1200 cm^{-1} by analogy with smaller molecules containing a similar group (8). Thus, the bands expected are summarized as follows: 3000–2700 cm^{-1}, two C—H stretching bands; 1500–1200 cm^{-1}, three C—H bending bands; 1200–600 cm^{-1}, one C—H bending and five skeletal stretching bands.

In the observed spectrum there are three medium bands near 3005, 2950, and 2870 cm^{-1}; they are probably all fundamentals, being strong for ternary combinations, but one may be characteristic of the amorphous polymer, as we found with polychloral.

In the region 1500–1200 cm^{-1}, there are weak bands at 1460 and 1430 cm^{-1} and medium or strong bands at 1370, 1339, 1287, 1265, and 1217 cm^{-1}. The weak 1460- and 1430-cm^{-1} bands are probably combination bands; CCl vibrations frequently give bands about here. The others are likely to be all CH fundamentals.

In the region 1200–600 cm^{-1} there are 10 bands, at 1132, 1087, 1040, 955, 815, 800, 775, 725, 710, and 675 cm^{-1}. Most are very strong and they are probably all fundamentals, mostly skeletal stretching bands. The 1132-, 1087-, 1040-, and 955-cm^{-1} bands are, by analogy with other polyaldehydes, probably due mainly to C—O stretching modes.

There are many more bands than expected for a one-monomer-unit repeat. Thus, there are five C—H bending bands, where only three are expected; there are nine bands in the skeletal stretching region, where only six are expected. We conclude, therefore, that there are at least two monomer units in the repeat.

Polymonochloroacetaldehyde

If there is one monomer unit in the repeating unit the number of bands expected in the different regions are as follows: 3000–2700 cm^{-1}, one CH and two CH_2 stretching bands; 1500–1200 cm^{-1}, one CH bending and CH_2 bending, wagging, and twisting bands; 1200–600 cm^{-1}, one CH bending, one CH_2 rocking, and four skeletal (C—O, C—C, and C—Cl) stretching bands.

In the region 3000–2700 cm^{-1} there are four bands, 3000, 2935, 2890, and 2820 cm^{-1}; as with polychloral, they may not all be fundamentals of the crystalline polymer.

In the region 1500–1200 cm^{-1} there are bands at 1445, 1434, 1375, 1350, 1298, 1265, 1230, 1216, and 1192 cm^{-1}. Allowing for the possibility that some of these are overtone or combination bands, or bands due to non-crystalline regions, there are many more than the four expected for a one-monomer repeat.

In the region 1200–600 cm^{-1} there are bands at 1135, 1105, 1065, 1025, 975, 942, 915, 862, 852, 790, 762, 730, 716, 660, and 610 cm^{-1}. Again, allowing for the possibility of overtones and combination bands, and the possibility that a few may be due to amorphous regions (cf. the 630-cm^{-1} band in polychloral) there are many more than the six bands expected for a one-monomer repeat.

We conclude, therefore, that there is more than one monomer unit in the repeating unit.

ACKNOWLEDGMENT

We are very grateful to Dr. L. D. Calvert for taking the X-ray diffraction photographs.

REFERENCES

1. NATTERER, K. Monatsh. Chem. **3**, 442 (1882).
2. FRIEDRICH, R. Ann. **206**, 251 (1881).
3. JACOBSEN, O. Ber. **8**, 87 (1875).
4. NOVAK, A. and WHALLEY, E. Trans. Faraday Soc. In press.
5. NOVAK, A. and WHALLEY, E. Trans. Faraday Soc. In press.
6. NOVAK, A. and WHALLEY, E. Can. J. Chem. **37**, 1710 (1959).
7. NOVAK, A. and WHALLEY, E. Can. J. Chem. **37**, 1718 (1959).
8. DAASCH, L. W., LIANG, C. Y., and NIELSEN, J. R. J. Chem. Phys. **22**, 1293 (1954).

INTERACTION BETWEEN KETONE AND TERTIARY AMINE GROUPS[1]

OWEN H. WHEELER[2] AND ERIC M. LEVY[3]

ABSTRACT

Vapor pressure studies of trimethylamine and ketones in heptane solution have shown that unstable complexes are formed with cyclohexanone at 0° and with cyclohexanone and cyclopentanone at −40°. No complex formation was observed with methylethyl ketone, diethyl ketone, or cyclopentanone at 0°.

Robinson and co-workers (1, 2) originally suggested that there was some type of interaction between a keto group and a tertiary amine group in certain alkaloids having these groups in a large-membered ring, to explain the masked reactivity of the keto group (1) and the large displacement of its infrared stretching frequency from its normal value (2). Later Leonard and co-workers (3, 4, 5) prepared a series of cyclic aza-acyloins and found evidence for transannular interaction in 8- (3, 5), 9- (4), and 10- (5) membered rings between the ketone and tertiary amine group. This was demonstrated by infrared and ultraviolet absorption (6) studies.

Anet, Bailey, and Robinson (2) found no evidence for interaction between acetone and triethylamine or between cyclopentanone and N-methyl piperidine by infrared measurements in chloroform solution. However, the amine would preferentially interact with the chloroform (7) and hinder association between the amine and ketone, and the evidence of these workers cannot be considered conclusive. Thus, though interaction between keto and amine groups within the same ring has been amply proved, no sound evidence has been published concerning possible interaction between ketone and amine groups in separate molecules.

Infrared and ultraviolet measurements are probably not the best method of observing weak interactions resulting in unstable complex formation, since such measurements must be carried out in dilute solution and cannot readily be made at low temperatures. Moreover these measurements will only detect interactions which result in a change in the electron density of the keto group. Vapor pressure studies, however, are usually made with solutions of moderate concentration, and the lower limit of temperature is only governed by the measurable vapor pressure of one (or more) component, and the method is not limited to specific types of interaction. In this study the vapor pressure of trimethylamine above a *n*-heptane solution and above solutions of the ketones, methylethyl ketone, diethyl ketone, cyclohexanone, and cyclopentanone in *n*-heptane has been measured. Trimethylamine was chosen as a conveniently volatile, non-sterically hindered amine and methylethyl ketone and diethyl ketone as examples of reactive and unreactive acyclic ketones, and cyclohexanone and cyclopentanone as examples of a very reactive and a moderately reactive cyclic ketone. The results are expressed in terms of Henry's law (8) (P solute $= K.N$ solute) and negative deviations are assumed to be due to complex formation (8) caused by interaction between the ketones and the amine.

[1]*Manuscript received March 31, 1959.*
Contribution from the Departments of Chemistry of the College of Agriculture and Mechanic Arts, University of Puerto Rico, Mayaguez, Puerto Rico, and Dalhousie University, Halifax, N.S. Published as Part XII of Structure and Properties of Cyclic Compounds. Part XI, Can. J. Chem. **36**, *656 (1958).*
[2]*Present address: College of Agriculture and Mechanic Arts, Mayaguez, Puerto Rico.*
[3]*Present address: Dalhousie University, Halifax, N.S.*

EXPERIMENTAL

n-Heptane

This was a sample from Matheson, Coleman, and Bell and was distilled over sodium (see Table I).

TABLE I

Physical constants*

	B.p. (° C)	n_D^{20}
n-Heptane	98.3 (98.43)	1.3884 (1.3879)
Methylethyl ketone	79.5 (79.50)	1.3786 (1.3784)
Diethyl ketone	101.6 (101.70)	1.3929 (1.3929)
Cyclopentanone	129.5 (130.6)	1.4369 (1.4366)
Cyclohexanone	155.7 (155.65)	1.4506 (1.4510)

*Values from International Critical Tables in parenthesis.

Trimethylamine

Eastman-Kodak white-label grade was dried over calcium hydride as described below.

Ketones

Eastman-Kodak white-label samples were dried over anhydrous calcium sulphate and fractionally distilled before use (see Table I).

Apparatus

The apparatus was similar to that used by Brown and Brady (9) and consisted of a flat-bottomed reaction flask of known volume (65.00 ml) joined by narrow-bore glass tubing to a differential mercury barometer, connected by a narrow-bore stopcock to a storage vessel of known capacity (534.0 ml), itself joined to another differential mercury barometer. The whole was attached to a conventional high-vacuum line which incorporated bulbs for the purification and storage of trimethylamine.

Method

A sample of 10 ml of purified *n*-heptane was introduced into the reaction flask together with two small Teflon-covered magnetic stirring bars, and was frozen and pumped out several times to remove dissolved air. Trimethylamine, which had been dried with calcium hydride, and freed from non-condensable gases, was distilled into the storage vessel. Small quantities were introduced into the reaction vessel and the amount admitted obtained from the known volume of the storage vessel and the pressure decrease on its manometer. The reaction vessel was immersed in a constant temperature bath (at 0° of ice; at −39.50° a slush bath of diethyl ketone (10), and at −63.55° of chloroform (11), and stirred by a strong permanent bar magnet mounted externally on a slow-speed motor. The reaction vessel was stirred continuously for about 10 to 15 minutes when the pressure ceased to drop and the residual pressure was noted. This process was repeated a number of times with pressures up to 160 mm of mercury, taking about 15 readings. All pressure readings were taken at constant volume by adjusting the amount of mercury in the barometers to a fixed mark on one limb.

The experiments were repeated with 10-ml samples of 1.0 *M* solutions of the ketones in *n*-heptane.

The amount of trimethylamine in solution is the difference between the amount added from the storage vessel and the amount remaining in the gas phase above the reaction vessel (this was usually $< 3\%$ the total amount; see Table II for typical data).

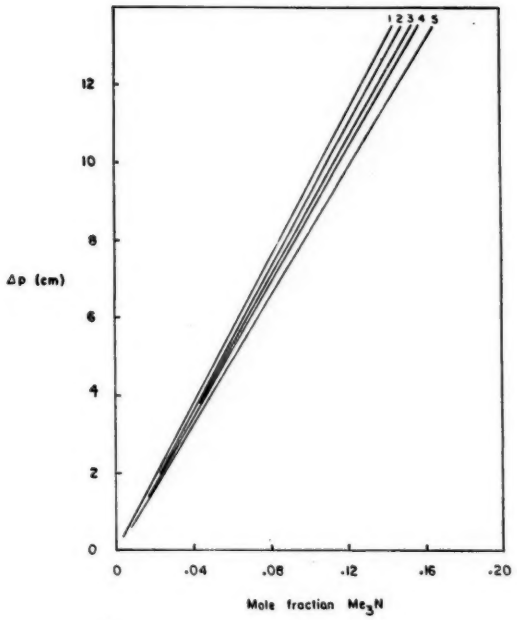

FIG. 1. Henry's law plot at 0° C. 1. Methylethyl ketone. 2. Diethyl ketone. 3. Cyclopentanone. 4. *n*-Heptane (pure). 5. Cyclohexanone.

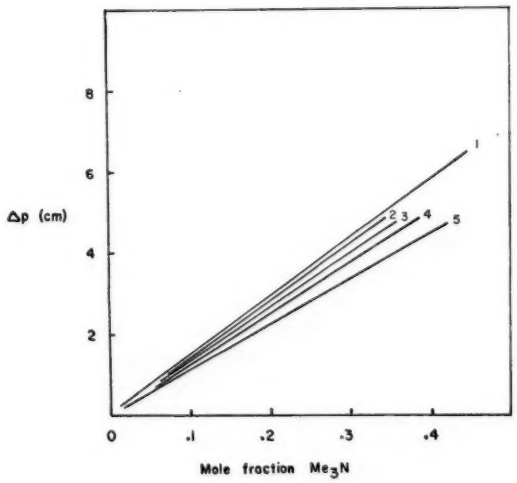

FIG. 2. Henry's law plots at −40° C. 1. Pure *n*-heptane. 2. Methylethyl ketone. 3. Diethyl ketone. 4. Cyclopentanone. 5. Cyclohexanone.

TABLE II

Typical data for cyclohexanone at 0° C*

Δp† (mm)	n_{Me_3N} added $\times 10^4$	$P_{equil.}$ soln. (mm)	n_{Me_3N} gas phase $\times 10^4$	n_{Me_3N} soln. $\times 10^4$	N_{Me_3N} soln.
5.34	15.5	0.56	0.181	15.3	0.0212
13.43	39.1	4.11	1.33	37.8	.0506
25.24	73.5	7.36	2.38	71.1	.0914
42.18	123	12.03	3.88	119	.144
54.92	160	14.52	4.68	155	.180
66.62	194	17.11	5.53	189	.211

*1 *M* in *n*-heptane (10 ml).
†Pressure difference on "storage" manometer.

The amount of trimethylamine was converted to its mole fraction and these values are plotted against the pressure of trimethylamine above the solution (corrected for the small vapor pressure of the solvent) in Figs. 1 and 2. The Henry's law constants (K in $P = K.N$) were determined from the slope of the straight lines and are given in Table III.

DISCUSSION

The slopes of the graphs at both 0° C (Fig. 1) and −40° C (Fig. 2) for solutions containing the ketones are little different from the slopes of the graphs for pure *n*-heptane, showing that no very stable complex is formed. The vapor pressures at −63.55° were too small to obtain reliable data.

The graphs of methylethyl ketone, diethyl ketone, and cyclopentanone at 0° (Fig. 1 and Table III) all lie above that of *n*-heptane itself. Such positive deviations from Henry's law can be attributed to a decrease in the association (8) of the solute ketone molecules in the presence of trimethylamine. Cyclohexanone, however, shows a small but definite negative deviation and this must be due to association (8) between the ketone and trimethylamine. Assuming that a 1:1 complex is formed the dissociation constant

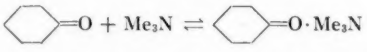

of the complex will be given (9) by $K_D = N\text{(ketone)} \times P(Me_3N)/N\text{(complex)}$. At any given pressure of trimethylamine above the solution the difference between the mole fraction of trimethylamine in the cyclohexanone solution and in pure *n*-heptane must be the amount which has reacted with the cyclohexanone. The mean of three values of the dissociation constant so calculated is 1550 mm, which corresponds to a very unstable complex with a dissociation pressure of some 2 atmospheres. This result neglects any possible positive deviation from Henry's law, resulting from decreased association of the ketone itself, which will be masked by the negative deviation produced by association of the ketone and amine. If the graph of cyclohexanone is compared with that of diethyl ketone, for which complex formation is very unlikely, then the value of K_D is 1010 mm, which still corresponds to a very unstable complex.

The results at −40° (Fig. 2 and Table III) show small negative deviations from Henry's law in the cases of methylethyl and diethyl ketone and larger negative deviations for cyclohexanone and cyclopentanone. These larger deviations must be due to complex formation and give values of K_D for cyclohexanone of 95 mm and only 165 mm for cyclopentanone.

TABLE III

Henry's law constants*

	0° C	−40° C
n-Heptane	86.4	14.8
Cyclohexanone	81.4	11.1
Cyclopentanone	88.4	12.3
Diethyl ketone	90.8	13.3
Methylethyl ketone	94.4	13.8

*In cm of Hg.

The data for cyclohexanone may be treated in another manner. In general the reaction may be expressed by

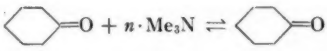

where n is the number of moles of trimethylamine reacting with 1 mole of cyclohexanone. If a is the original concentration of ketone and b and c are the equilibrium concentrations of trimethylamine and the complex, respectively, then

$$K_D = (a-c).b^n/c.$$

The concentration of the complex c is measured by the amount of trimethylamine which has reacted (say d) and $c = d/n$. Since the concentration of complex is very small compared to the initial concentration of the ketone, then

$$a-c = a-d/n = a.$$

The equation thus reduces to

$$K_D = nab^n/d$$

or

$$\log d = n \log b + \log na - \log K_D.$$

In any experimental run b and d are the only variables and thus a graph of log d against log b will be linear with slope of n and an intercept of (log na − log K_D). The results of cyclohexanone at 0° give a straight line through nine points which has a slope of 1.02 (see Fig. 3), corresponding to the formation of a 1:1 complex, and a value of K_D of 14.3 moles $l.^{-1}$. A similar graph for the data at −40° gives $n = 1.04$ and $K_D = 13.1$ moles $l.^{-1}$. These values should be compared to the very high reactivity of cyclohexanone in equilibrium reactions involving addition to the ketone group, such as cyanohydrin formation with $K_D = 0.00059$ in 95% ethanol (12) and $K_D = 0.060$ mole $l.^{-1}$ in 80% dioxane (13) (both at 25° C). The small difference (if real) between the dissociation constants of complex formation at 0° and −40° C corresponds to a heat of formation (ΔH) of only +0.27 kcal mole.

While the non-reactivity of methylethyl and diethyl ketones towards trimethylamine is not surprising, since these ketones are known to be unreactive (14), the low reactivity of cyclohexanone is surprising, and must be contrasted with the ready interaction of ketone and amine groups in the same ring. The interaction in ring compounds, however, occurs more readily in 8- (3, 5), 9- (4, 15), and 10- (5, 16, 17) membered rings, in which the bridged product will have fused 5- or 6-membered rings, and may have a favorable free energy or entropy difference (18) with respect to the monocyclic compound.

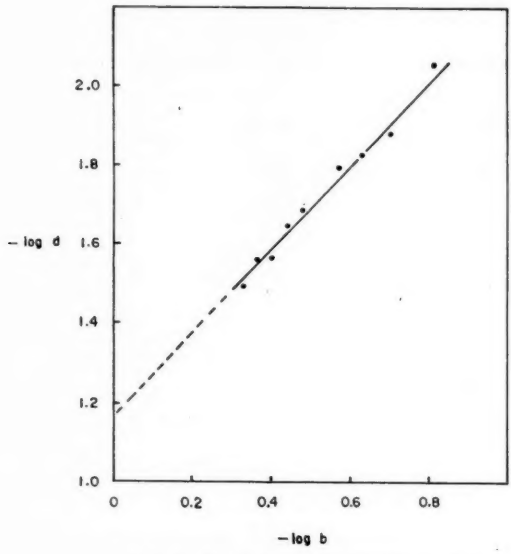

FIG. 3. Data for cyclohexanone at 0° C.

ACKNOWLEDGMENTS

One of the authors (E.M.L.) wishes to acknowledge financial support in the form of a bursary from the National Research Council of Canada. The helpful comments of the referee are also acknowledged.

REFERENCES

1. KERMACK, W. O. and ROBINSON, R. J. Chem. Soc. **121**, 427 (1922).
2. ANET, F. A. L., BAILEY, A. S., and ROBINSON, R. Chem. & Ind. (London), **36**, 944 (1953).
3. LEONARD, N. J., FOX, R. C., ŌKI, M., and CHIAVARELLI, S. J. Am. Chem. Soc. **76**, 630 (1954).
4. LEONARD, N. J., FOX, R. C., and ŌKI, M. J. Am. Chem. Soc. **76**, 5708 (1954).
5. LEONARD, N. J., ŌKI, M., and CHIAVARELLI, S. J. Am. Chem. Soc. **77**, 6234 (1955).
6. LEONARD, N. J. and ŌKI, M. J. Am. Chem. Soc. **77**, 6239 (1955).
7. KORINEK, G. J. and SCHNEIDER, W. G. Can. J. Chem. **35**, 1157 (1957).
8. HILDEBRAND, J. H. and SCOTT, R. L. The solubility of non-electrolytes. Reinhold Publishing Corp., New York. 1950.
9. BROWN, H. C. and BRADY, J. D. J. Am. Chem. Soc. **74**, 3570 (1952).
10. DREISBACH, R. R. and MARTIN, R. A. Ind. Eng. Chem. **41**, 2875 (1949).
11. STULL, D. K. J. Am. Chem. Soc. **59**, 2726 (1937).
12. WHEELER, O. H. and ZABICKY, J. Z. Can. J. Chem. **36**, 656 (1958).
13. WHEELER, O. H. and MATEOS, J. L. Can. J. Chem. **36**, 712 (1958).
14. EVANS, D. P. and YOUNG, J. R. J. Chem. Soc. 1310 (1954).
15. LEONARD, N. J., ŌKI, M., BRADER, J., and BOAZ, H. J. Am. Chem. Soc. **77**, 6237 (1955).
16. MOTTUS, E. H., SCHWARZ, H., and MARION, L. Can. J. Chem. **31**, 1144 (1953).
17. ANET, F. A. L. and MARION, L. Can. J. Chem. **32**, 452 (1954).
18. ALLINGER, N. J. Org. Chem. **21**, 915 (1956).

A SHORTER SYNTHESIS OF GLUTATHIONE[1]

CASIMIR BERSE, ROGER BOUCHER, AND LUCIEN PICHÉ

ABSTRACT

A preparation of glutathione is proposed, in which the cystinyl residue is at one stage only partially reduced, to uncover the basic groups necessary for ensuing condensation, but without cleavage of the disulphide linkage. This affords an economy of intermediate steps but it does not provide a substantial increase in over-all yield of the hormone.

Synthesis of glutathione was accomplished with difficulty and in low over-all yields (1–5). The latest preparations (6, 7) report yields of 4 to 6% and the peptide is still prepared from yeast (8, 9). New synthetical methods are of potential value for its production and also to the study of analogues of glutathione.

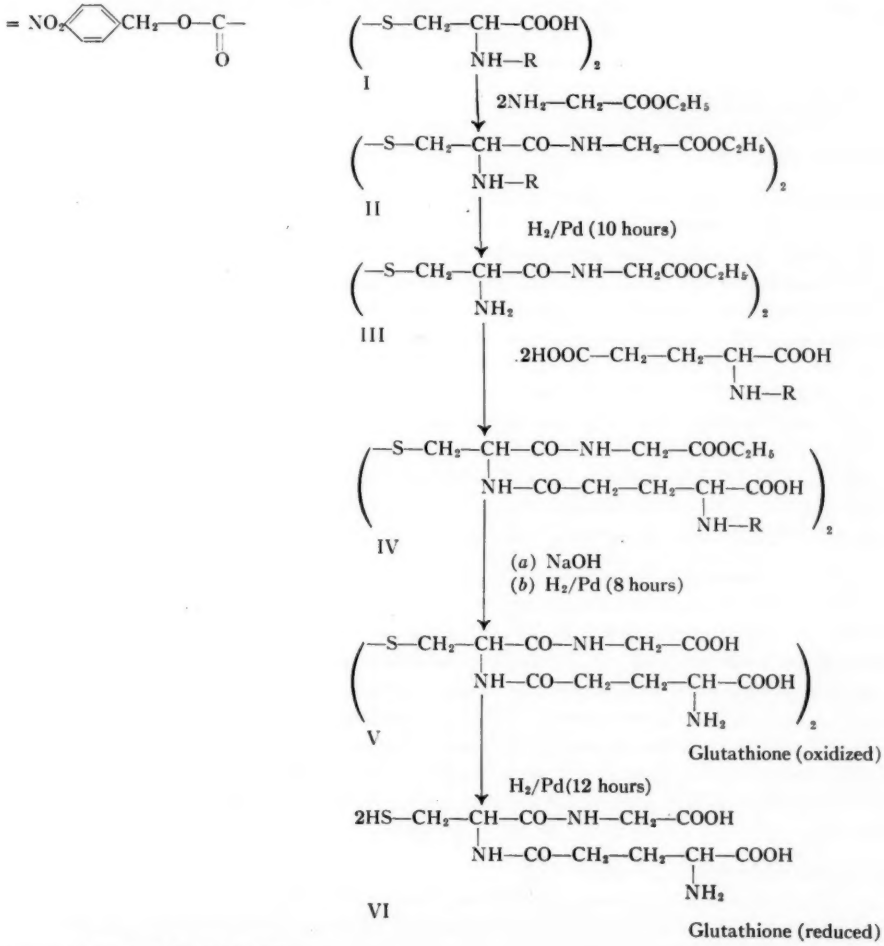

[1]*Manuscript received April 22, 1959.*
Contribution from the Department of Chemistry, Faculty of Science, Université de Montréal, Montreal, Quebec.

In a previous publication (10), we have shown the possibility of reducing peptidic derivatives of di-(N-*p*-nitrocarbobenzoxy)-L-cystine either partially to L-cystinyl peptides or completely to L-cysteinyl derivatives by appropriately controlled hydrogenation on palladium catalyst. This has afforded a favorable short route to glutathione through the following steps: di-(N-*p*-nitrocarbobenzoxy)-L-cystine I was condensed with glycine ethyl ester in the presence of N,N′-dicyclohexylcarbodiimide (11); the intermediate ester II was partially reduced to uncover the amino groups of the L-cystine residue without cleaving its disulphide linkage. The resulting diethyl L-cystinyldiglycinate III was condensed with 2 equivalents of *p*-nitrocarbobenzoxy-L-glutamic acid to provide an ester IV in which the glutathione structure has been assembled. Saponification (*a*) and partial reduction (*b*) of IV lead to oxidized glutathione V. Complete hydrogenation on palladium catalyst leads to glutathione VI.

This procedure, involving fewer steps to oxidized glutathione, affords an over-all yield of 10% on cystine; the reduced form of the hormone is provided in 6.6% yield.

EXPERIMENTAL

Melting points, unless otherwise indicated, have been determined in semicapillary tubes and are uncorrected. In some cases where the materials decomposed, instantaneous melting points have been determined on the Maquenne block.

Diethyl di-(N-*p-nitrocarbobenzoxy*)-L-*cystinyldiglycinate* II

To a solution of glycine ethyl ester hydrochloride (5.6 g, 0.04 mole) in 50 ml of dimethylformamide and 10 ml of acetonitrile, 9.5 ml of tri-*n*-butylamine and di-(N-*p*-nitrocarbobenzoxy)-L-cystine (12 g, 0.02 mole) were added. After cooling of the solution to −5°, dicyclohexylcarbodiimide (9 g) was added and the mixture was kept at this temperature for 30 minutes. The reaction mixture was allowed to come to room temperature and set aside for 1 day. It was acidified with 5 ml of glacial acetic acid (to decompose excess reagent). The insoluble urea was removed; 200 ml of chloroform and 350 ml of water were added. The chloroformic solution was washed with *N* HCl, 5% aqueous sodium bicarbonate, and dried over anhydrous sodium sulphate. The solvent was evaporated *in vacuo* and the residue was recrystallized from nitromethane. Yield: 12.3 g (80%). Identity was ascertained through comparison by melting point, mixed melting point, and optical rotation with the product described in a previous publication (10).

*Diethyl-*L-*cystinyldiglycinate Dihydrochloride* III

Diethyl di-(N-*p*-nitrocarbobenzoxy)-L-cystinyldiglycinate (6 g, 0.08 mole) was dissolved in a mixture of dimethylformamide (25 ml) and ethanol 80% (50 ml). The compound was hydrogenated for 10 hours at room temperature and at atmospheric pressure over 10% palladium on carbon (2 g). The catalyst was removed by filtration and the solvent was evaporated *in vacuo* at 50°. The resulting syrup was triturated with *N* HCl (30 ml) and the filtrate evaporated *in vacuo*. The residue after treatment with water and Norit gave a white amorphous hygroscopic powder. Yield: 2.5 g (70%). Anal. Calc. for $C_{14}H_{26}N_4O_6S_2.2HCl$: C, 34.78; H, 5.84; N, 11.59%. Found: C, 34.79; H, 5.82; N, 11.70%.

*p-Nitrocarbobenzoxy-*L-*glutamic Acid*

L-Glutamic acid (12.3 g) was dissolved in 42 ml of 4 *N* NaOH; 20 ml of purified dioxane were added. The solution was stirred vigorously and cooled to 0°; *p*-nitrocarbobenzoxyl chloride (19 g) dissolved in 50 ml of dioxane was added in 5 portions (30 minutes). During

reaction, the pH was maintained at 11 with 2 *N* NaOH. Stirring was continued for 0.5 hour after the addition of all reactants. The mixture was allowed to come to room temperature and 300 ml of water were added. The resulting alkaline solution was washed twice with ethyl acetate and acidified to Congo red with 1 *N* HCl. The precipitate was collected and recrystallized from a mixture of ethanol and water. Yield: 21 g (77%); m.p. 157–158°; $[\alpha]_D^{25}$ −8.0 (*c*, 0.9 in ethanol, 95%). Anal. Calc. for $C_{13}H_{14}O_8N_2$: C, 47.85; H, 4.32; N, 8.58%. Found: C, 47.68; H, 4.32; N, 8.55%.

Diethyl di-(N-*p-nitrocarbobenzoxy-*γ-L-*glutamyl*)-L-*cystinyldiglycinate* IV

To a solution of diethyl L-cystinyldiglycinate dihydrochloride (2.2 g, 4.5 mmole) in 30 ml of dimethylformamide and 5 ml of acetonitrile, 2 ml of tri-*n*-butylamine and *p*-nitrocarbobenzoxy-L-glutamic acid (2.7 g, 8 mmole) were added. After the solution had been cooled to −5°, dicyclohexylcarbodiimide (2 g) was added and the mixture was kept at this temperature for 30 minutes. The reaction mixture was allowed to come to room temperature and allowed to stand for 1 day. It was acidified with 1 ml glacial acetic acid. The insoluble urea was removed and 200 ml of ethyl acetate and 300 ml of water were added. The ethyl acetate solution was washed with *N* HCl and water, then dried over anhydrous sodium sulphate. The solvent was evaporated *in vacuo*. Yield: 2.8 g (60%).

Di-(N-*p-nitrocarbobenzoxy-*γ-L-*glutamyl*)-L-*cystinyldiglycine*

The crude product obtained above (2.7 g) was dissolved in methanol (20 ml), and *N* NaOH (2% excess) was added in two portions. The mixture was stirred at 0–5° for a first hour and at room temperature for another. It was acidified with HCl. The crude product, an oil, was dissolved in ethanol. The solvent was evaporated *in vacuo* and the residue was dissolved in dioxane; precipitation with ether yielded 1.9 g of product (74%).

Glutathione (*Oxidized*) V

Di-(N-*p*-nitrocarbobenzoxy)-γ-L-glutamyl-L-cystinyldiglycine (2 g) was dissolved in 80% ethanol (25 ml). The compound was hydrogenated for 8 hours at room temperature and at atmospheric pressure over 10% palladium on carbon (1 g). After filtration, the catalyst was washed with water and the washings were combined with the first filtrate. The solvent was evaporated *in vacuo* and the residue was triturated with water. The filtrate was concentrated and glutathione (oxidized) was precipitated by addition of absolute ethanol. Yield: 0.7 g (55%); m.p. 175–195°; $[\alpha]_D^{25}$ −92.8 (*c*, 1.2 in water). Literature (12, 13) m.p. 170–195°; $[\alpha]_D^{27}$ −93.9 (*c*, 1.0 in water).

Glutathione VI

Glutathione (oxidized) (0.4 g) was dissolved in 25 ml of water. The compound was hydrogenated for 12 hours at room temperature and at atmospheric pressure over palladium (13) (200 mg). The catalyst was removed by filtration and the filtrate was concentrated *in vacuo*. By addition of ethanol (95%) to the syrupy residue, the glutathione precipitated. Yield: 0.26 g (65%); m.p. 190° decomp., $[\alpha]_D^{25}$ −20.6 (*c* 1.5 in water). (Literature (2) m.p. 190°; $[\alpha]_D^{27}$ −21.3 (*c*, 2% in water).) Anal. Calc. for $C_{10}H_{17}N_3O_6S$: C, 39.08; H, 5.58; N, 13.67. Found: C, 39.00; H, 5.48; N, 13.62%.

ACKNOWLEDGMENTS

This research was supported by a National Research Council grant. One of us (R.B.) is also indebted to the Quebec Bureau of Research for a bursary.

REFERENCES

1. HARINGTON, C. A. and MEAD, T. H. Biochem. J. **29**, 1602 (1935).
2. DU VIGNEAUD, V. and MILLER, G. L. J. Biol. Chem. **116**, 469 (1936).
3. HEGEDÜS, B. Helv. Chim. Acta, **31**, 737 (1948).
4. RUDINGER, J. and SORM, F. Collection Czechoslovak Chem. Commun. **16**, 214 (1951).
5. GOLDSCHMIDT, S. and JUTZ, C. Chem. Ber. **86**, 1116 (1953).
6. AMIAR, G., HEYMES, R., and VELLUZ, L. Bull. soc. chim. France, 698 (1956).
7. KING, F. E., CLARK-LEWIS, S. W., and WADE, R. J. Chem. Soc. 880 (1957).
8. HOPKINS, F. G. J. Biol. Chem. **84**, 269 (1929).
9. KENDALL, E. C., MCKENZIE, B. F., and MASON, H. L. J. Biol Chem. **84**, 657 (1929).
10. BERSE, C., BOUCHER, R., and PICHÉ, L. J. Org. Chem. **22**, 805 (1957).
11. SHEEHAN, J. C., and HESS, G. P. J. Am. Chem. Soc. **77**, 1067 (1955).
12. HUNTER, G. and EAGLES, B. A. J. Biol. Chem. **72**, 165 (1927).
13. JOHNSON, J. M. and VOEGTLIN, C. J. Biol. Chem. **75**, 710 (1927).

THE PHOTOLYSIS OF TRIFLUOROMETHYL CYANIDE[1]

A. Bruce King[2] and E. W. R. Steacie

ABSTRACT

The photolysis of CF_3CN at 1849 Å has been studied. The major products are hexafluoroethane, cyanogen, and perfluoro-3-methyl-2-aza-2-butene.

The experimental value for $k_3/k_2^{\frac{1}{2}}$ is:

$$10^{-9.08\pm.13}\, e^{-5.00\pm.21 \text{ kcal mole}^{-1}/RT} \text{ molecule}^{-\frac{1}{2}} \text{ cc}^{\frac{1}{2}} \text{ sec}^{-\frac{1}{2}},$$

where:

$$CF_3 + CF_3 \rightarrow C_2F_6, \qquad [2]$$

$$CF_3 + CF_3CN \rightarrow (CF_3)_2CN. \qquad [3]$$

Another product was isolated in smaller amounts and has been tentatively identified as perfluorotrimethyl-aza-2-pentene.

INTRODUCTION

Earlier work on the photolysis of CH_3CN (1) showed the mechanism to be so complex that a unique interpretation was difficult. It was felt that the vulnerability of the C—H bond, both to break in the primary step and to subsequent abstraction, led to the wide variety of reaction paths and products. It was thus hoped that a study of the photolysis of CF_3CN would give information for the interpretation of the CH_3CN studies. In particular the importance of reaction [8]:

$$CN + CF_3CN \rightarrow C_2N_2 + CF_3 \qquad [8]$$

was sought.

EXPERIMENTAL

Photolyses were carried out in a cylindrical quartz reaction vessel 4.8 cm long and 4.7 cm in diameter, which was connected to a mercury-free system with a Hoke No. 413 high-vacuum stainless-steel valve. The windows of the cell were 1.00-mm-thick quartz, each of which transmitted about 75% of the 1849 Å radiation used in this work. The initial pressure in the reaction cell was measured with a quartz spiral Bourdon gauge nulled with a mercury manometer. When a mixture of gases was desired in the reaction cell, the appropriate amounts of the gases were premixed in a 125-cc bulb with a magnetically driven stirrer and then expanded into the reaction cell. The techniques described by McElcheran *et al.* (1) were used; the reaction products were transferred to the analytical system through a silicone oil diffusion pump, a stopcock, and two liquid nitrogen traps to keep the mercury vapor in the analytical system out of the reaction cell.

The cell was placed inside a cylindrical furnace which was mounted on an optical bench. The quartz spiral low-pressure mercury lamp and the platinum photocell were also mounted on the optical bench as part of an airtight system with the furnace tube. This permitted nitrogen to flow through the light path and yet allowed the lamp and photocell to be easily moved for heating the windows of the reaction cell with a torch.

[1]*Manuscript received June 18, 1959.*
Contribution from the Division of Pure Chemistry, National Research Council, Ottawa, Canada.
Issued as N.R.C. No. 5332.

[2]*National Research Council Postdoctorate Fellow 1956–58. Present address: Chemical Physics Department, Stanford Research Institute, Menlo Park, California, U.S.A.*

The nitrogen was passed through the system at approximately 200 cc min^{-1} by means of a small heater in a Dewar of fresh liquid nitrogen. Provision was also made to introduce glass plates between the lamp and the reaction cell. A Vycor plate (Corning No. 7910) was inserted when only 2537 Å radiation was desired and several 3-mm-thick quartz plates were inserted to reduce the 1849 Å intensity to about 20% of the usual value.

Because of polymer formation during the photolysis it was necessary at the end of each run to fill the cell with an atmosphere of oxygen and flame both windows to red heat. This removed the polymer from the windows and ends of the cylindrical walls, but after a number of runs some polymer was built up on the walls of the central section of the cell. The relative amount of polymer was determined for each run by the drop in transmitted 1849 Å radiation during the photolysis and this intensity decrease was as high as 50% for some of the higher-pressure experiments.

The photocell consisted of a semicylindrical cathode of platinum (2) mounted in a quartz envelope that had been thinned slightly in front of the cathode to decrease the light absorption by the envelope. Before the photocell was sealed off, it was evacuated overnight at 10^{-6} mm of Hg with the envelope heated to 500° C, and then the cathode was heated with an induction heater (two thin strips of platinum had been spot-welded to the top and bottom of the cathode to complete the loop and give more effective coupling) until the cathode was no longer sensitive to 2537 Å light. This was determined by measuring the photocurrent produced by a low-pressure Hg lamp with a Vycor plate in front of the photocell. The effective area of the photocell was about 4 cm^2 and the operating anode potential was 135 v. Photocurrents of the order of 10^{-9} amp were obtained in this work and were measured with a Keithley electrometer and decade resistance attachment. After more than a year of use, the photocell remained completely insensitive to the 2537 Å radiation of the mercury lamp.

The volatile products were condensed at −195° C and then separated by distillation from a Ward–Leroy still (3). The C_2F_6 and the bulk of the CF_3CN were removed at −150° C and condensed in a liquid nitrogen trap until the distillation pressure had dropped to approximately half the value of the equilibrium pressure during the bulk of the distillation. This procedure removed at least 95% of the CF_3CN, but none of the higher-boiling products. The CF_3CN–C_2F_6 mixture was then reacted in a micro-hydrogenation tube with about 500 mm of hydrogen over a nickel–kieselguhr catalyst (4) at 85° C for 1 to 2 hours. This converted about 95% of the CF_3CN, principally to higher-boiling amines. The excess hydrogen was pumped off at liquid nitrogen temperature, and the products of the hydrogenation were distilled from −140° C to a liquid nitrogen trap. The quantity of this fraction (cut No. 4) was measured in a gas burette and sealed off in a sample tube for mass spectrometric analysis. This cut consisted mainly of the unreacted CF_3CN, the C_2F_6 (from the photolysis only; none was found in a blank hydrogenation), and some ammonia. This procedure thus served to concentrate the C_2F_6 from about 1% of the original fraction to an appreciable component that could readily be measured by mass spectrometry.

Other fractions of the photolysis reaction products were taken at −130° C (cut No. 1), −115° C (cut No. 2), and the residual higher boiling compounds that remained condensed at −115° C were collected as cut No. 3. The total quantity of each of the samples was measured on a gas burette and then the sample was sealed in a tube for mass spectrometric analysis. The total volume of the inlet system of the mass spectrometer was calibrated by expanding samples of known quantities of pure nitrogen (similar sample size to the unknown samples) into the spectrometer, measuring the

m/e 28 peak height, and comparing with the nitrogen sensitivity. Calculation of analyses for two component samples where standards were not available is described in the Appendix.

The CF_3CN was obtained from Peninsular Chemresearch Inc., practical grade, and was purified by several fractionations from −80° C to −195° C. The hexafluoroacetone was obtained by reacting the hydrate (Merck Chemical) with phosphorus pentoxide, followed by several vacuum fractionations. This gas was stored in a blackened bulb until used.

RESULTS

Mass spectrometric analyses indicated that cut No. 1 contained the remaining CF_3CN (pattern given in Table I) and some of the C_2N_2, while cut No. 2 contained the remainder of the C_2N_2 and a fluorinated product. The pattern for this product is listed in Table I and is consistent with the pattern to be expected for perfluoro-3-methyl-2-aza-2-butene ($(CF_3)_2C{=}NCF_3$, hereafter called MAB). This type of compound gives mass spectral patterns with a small parent peak (m/e 233), medium-sized peaks corresponding to loss of one or two fluorine atoms (m/e 214 and 195), a large peak for loss of a CF_3 group (m/e 164), and a large m/e 69 peak. All other peaks are also consistent with the structure of MAB. Further evidence of consistency with the proposed structure is indicated by the metastable transitions observed which are also listed in Table I. In every case they correspond to transitions of the important ions in the spectrum by typical reaction paths found in mass spectral fragmentation patterns, e.g. references 5 and 6.

TABLE I

Mass spectral patterns for CF_3CN and MAB

m/e	CF_3CN	MAB	m/e	CF_3CN	MAB	
12	5.3		131		0.2	
24	0.5		145		5.2	
26	11.6		164		(100.)	
27	1.7		165		3.7	
31	25.8	9.8	169		0.3	
38	4.2		171		0.2	
50	50.2	12.8	176		2.1	
51	0.6		195		4.3	
57	2.5		214		35.7	
69	311.	242.	233		0.8	
70	3.5	2.8		Metastable ions observed and suggested transition		
76	(100.)	11.8		None observed	m/e	Transition
77	2.5					
81		0.7			29.	164 → 69
93		1.1			32.8	76 → 50
95	5.1	1.2			60.9	214 → 114
100		1.8			79.	164 → 114
114		16.7			115.5	233 → 164
119		1.3			125.9	214 → 164
126 + m^+		2.6				

Because of lack of mass spectral standards for MAB and because of troubles in obtaining a reproducible cyanogen standard (apparently due to absorption problems), the effective sensitivities of the cyanogen m/e 52 peak and the MAB m/e 164 peak were determined by the method described in the Appendix. A typical plot of equation [*A*-3] for a set of analyses performed on the same day is shown in Fig. 1 with the sensitivities of C_2N_2 and MAB being determined from the slope and the intercept, respectively, of the straight

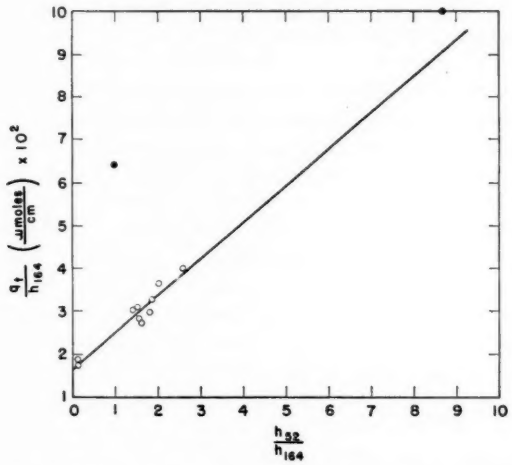

FIG. 1. Plot of equation [*A*-3] for a typical group of cut No. 2 analyses. Open circles used to determine linear plot and closed circles are for points above the line that indicate an additional component present.

line. These sensitivities were used to calculate the absolute amounts of C_2N_2 and MAB in the samples of cut No. 2 as well as samples of cut No. 1 that were analyzed at the same time.

Cut No. 4 was analyzed for C_2F_6 by using the *m/e* 119 peak. Because of absorption of the ammonia and amines in the sample, a complete analysis of the sample was not undertaken. Rather, by expanding the total sample into the calibrated volume on the inlet system of the mass spectrometer, one could relate the partial pressure of C_2F_6 (from the *m/e* 119 peak height) directly to the absolute amount of C_2F_6 in the sample.

The small amount of high-boiling products (cut No. 3) was analyzed on the mass spectrometer and found to contain two major components. One component was distinguished by peaks at *m/e* 96 and 97 (as well as 77, 76, 69, etc.) and is tentatively identified as 2,2,2-trifluoroethylideneimine ($CF_3CH{=}NH$) or a similar partially hydrogenated compound. This compound must arise from reaction of photolytic species or photolysis products with adsorbed water on the walls or with the silicone oil in the diffusion pump, because this compound was not found after a similar fractionation procedure on a sample of CF_3CN that had not been photolysed.

The pattern assigned to the major component of cut No. 3 is shown in Table II. Because of the small quantity of this product in any of the samples, the smaller-sized peaks are subject to considerable scatter and only the major peaks are listed. Many of the lower mass peaks are also omitted because of interference from the other component. The higher mass peaks are consistent with a molecular weight of 383 (loss of one fluorine atom gives *m/e* 364; loss of CF_3 gives *m/e* 314, which is a major peak, etc.). This would indicate a formula of $C_7F_{15}N$ and would probably be either perfluoro-3,4,4-trimethyl-2-aza-2-pentene ($CF_3C(CF_3)_2C(CF_3){=}NCF_3$) or perfluoro-2,4,4-trimethyl-3-aza-2-pentene ($CF_3C(CF_3)_2N{=}C(CF_3)_2$), hereafter called TAP. A plot of equation [*A*-3] for cut No. 3 (Fig. 2) indicates that the amounts of the two major components present are proportional to the *m/e* 314 and 96 peak heights and that there are no other compounds consistently present in significant quantity in these samples (see Appendix).

TABLE II

Mass spectrum of TAP

m/e	Relative peak height	m/e	Relative peak height
31	5.0	196	2.1
50	4.5	214	9.
69	270.	221	2.3
76	4.7	226	11.7
112	3.5	245 and 246	12.
114	2.	259	11.2
131	4.0	264	22.6
138	1.5	271	2.3
145	2.	295	1.4
146	1.	303	0.8
150	2.1	310	3.9
159	3.	314	(100.)
164	9.	322	1.
169	4.3	328	3.
176	3.6	342	4.6
192	2.6	354	1.
195	1.6	364	5.5

The sensitivities for these two components were determined from the graph and were used to calculate the absolute amount of TAP formed.

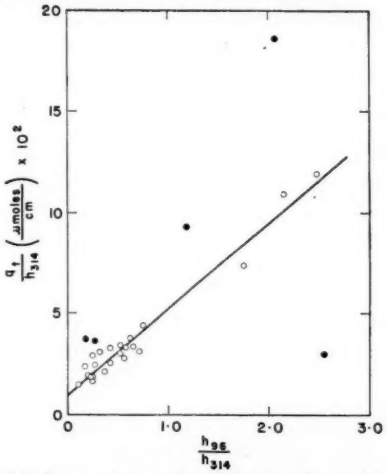

FIG. 2. Plot of equation [*A*-3] for a group of cut No. 3 analyses. Open circles used to determine linear plot and closed circles are for points above the line that indicate an additional component present.

On the basis of the reaction mechanism one might expect perfluorodiisopropylidene hydrazine ($(CF_3)_2C{=}N{-}N{=}C(CF_3)_2$(PDH)), or its isomer perfluoro-3,4-dimethyl-2,5-diaza-2,4-hexadiene ($CF_3N{=}C(CF_3)C(CF_3){=}NCF_3$), as a product. This compound would have a parent peak at *m/e* 328 and significant peaks at *m/e* 309, 290, and 259. Peaks are observed at *m/e* 328, 310, and 259, but the ratio of these peak heights to the *m/e* 314 peak height is reasonably constant (although with more scatter than some of the other peaks in the spectrum of TAP), indicating that traces of PDH may be present, but that the major contribution to these peaks comes from the same compound that gives the *m/e* 314 peak. (A coincidental proportionality between the yields of two different products for all runs under the variety of conditions studied is very unlikely.)

The polymer formation (measured as the decrease in the logarithm of the 1849 Å light transmitted) as a function of irradiation time was found to be linear after an initial induction period. The slope of the linear region was found to be proportional to the square root of the CF_3CN pressure at constant light input (uncorrected for the change in optical density of the CF_3CN) and approximately proportional to the incident intensity at constant pressure. One photolysis was carried out on a mixture of CF_3CN and CF_3COCF_3 with 2537 Å light so that only CF_3COCF_3 would undergo photolysis. No polymer formation was detected with 1849 Å light after the run, although a 20–30% decrease in intensity was observed for runs on CF_3CN alone at 1849 Å at the same pressure and temperature. This indicated that the formation of polymer required reactants in addition to the $CF_3\cdot$ radical and CF_3CN. This fact, and the induction period observed, indicate that the polymer must arise from polymerization of the cyanogen formed during the photolysis.

A blank photolysis of CF_3COCF_3 at 2537 Å in the reaction cell that was partially coated with paracyanogen gave a C_2F_6/CO ratio of about 0.6, indicating an appreciable loss of $CF_3\cdot$ radicals by addition to the unsaturated paracyanogen. This is also confirmed by the observation of the evolution of C_2F_6 on heating the polymer formed in the photolysis of CF_3CN. Because of loss of some of the C_2N_2 product by polymerization and some of the $CF_3\cdot$ radicals by reaction with the polymer, attempts at absolute quantum measurements in order to test the existence of reaction [8] are useless.

The absorption coefficient of CF_3CN at 1849 Å was found to vary with temperature and a statistical analysis of the data taken during the course of this work yielded:

$$\epsilon = 10^{1.483\pm.045}\, e^{-1620\pm70 \text{ cal mole}^{-1}/RT} \text{ mole}^{-1} \text{ l. cm}^{-1}.$$

This rather significant dependence on temperature would seem to indicate that the 1849 Å line coincides with the edge of an absorption band. The same situation occurs for CH_3CN (7), and thus it would appear that the substitution of fluorine atoms on the methyl group of CH_3CN does not shift the absorption band edge very much.

DISCUSSION

The experimental data are summarized in Table III. On the basis of these data and the other results discussed above, the following mechanism is proposed:

$$CF_3CN + h\nu \rightarrow CF_3 + CN, \quad [1]$$

$$CF_3 + CF_3 \rightarrow C_2F_6, \quad [2]$$

$$CF_3 + CF_3CN \rightarrow (CF_3)_2C{=}N\cdot, \quad [3]$$

$$CF_3 + (CF_3)_2CN\cdot \rightarrow (CF_3)_2C{=}NCF_3\,(\text{MAB}), \quad [4]$$

$$CF_3 + \text{MAB} \rightarrow \rightarrow \rightarrow \text{TAP}, \quad [5]$$

$$CN + CN + M \rightarrow C_2N_2 + M, \quad [6]$$

$$C_2N_2 + R(CN?) \xrightarrow{\text{wall?}} \text{paracyanogen}. \quad [7]$$

The formation of MAB proceeds through reactions [3] and [4] with reaction [3] the rate-determining step. An Arrhenius plot of $R_{MAB}/R_{C_2F_6}^{\frac{1}{2}}[CF_3CN]$ is shown in Fig. 3 and gives

$$k_3/k_2^{\frac{1}{2}} = 10^{-9.09\pm.11}\, e^{-5.05\pm.17 \text{ kcal mole}^{-1}/RT} \text{ molecule}^{-\frac{1}{2}} \text{ cc}^{\frac{1}{2}} \text{ sec}^{-\frac{1}{2}}.$$

The mechanism for the formation of TAP is subject to some doubt, but the best kinetic agreement has been found for $R_{TAP}/R_{MAB}R_{C_2F_6}^{\frac{1}{2}}t$ (where t is the reaction time),

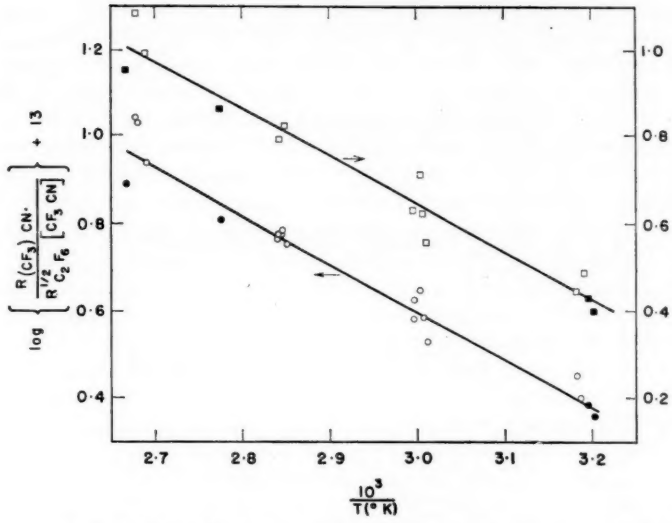

FIG. 3. Arrhenius plot of $k_3/k_2^{\frac{1}{2}}$. Circles (lower plot) represent $R_{(CF_3)_2CN\cdot} = R_{MAB}$. Squares (upper plot) represent $R_{(CF_3)_2CN\cdot} = R_{MAB} + 2R_{TAP}$. Solid circles and squares indicate low-intensity runs.

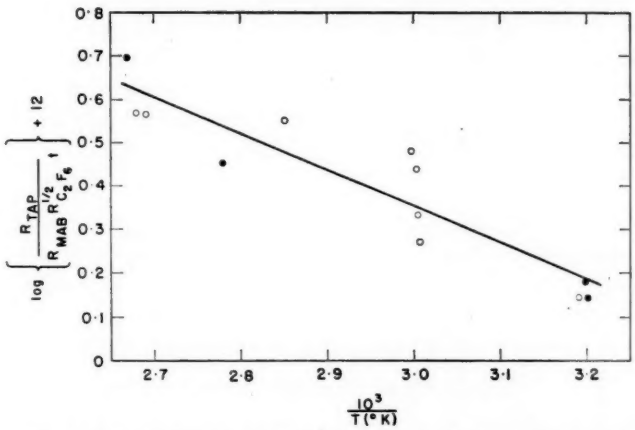

FIG. 4. Arrhenius plot of $k_5/k_2^{\frac{1}{2}}$. Solid circles indicate low-intensity runs.

indicating the rate-determining step for the formation of TAP is the addition of $CF_3\cdot$ to MAB. An Arrhenius plot of this function is shown in Fig. 4 and the lack of effect of intensity on the plot indicates this function represents the rate-determining step for the formation of TAP. From Fig. 4 and assuming the average concentration of MAB is $\frac{1}{2}R_{MAB}t$, one obtains:

$$k_5/k_2^{\frac{1}{2}} = 10^{-8.81\pm.22}\, e^{-3.87\pm.33 \text{ kcal mole}^{-1}/RT} \text{ molecule}^{-\frac{1}{2}} \text{ cc}^{\frac{1}{2}} \text{ sec}^{-\frac{1}{2}}.$$

It is difficult to decide what additional reaction steps following reaction [5] must be involved to explain the formation of TAP. The difficult part is the origin of the perfluoro-

TABLE III

Summary of experimental results

Run No.	Concn. of CF_3CN (molecule $cc^{-1} \times 10^{-18}$)	Temp. (° K)	Rel. initial incident intensity	Time (sec $\times 10^{-4}$)	Molecule cc^{-1} sec^{-1} $\times 10^{-11}$ of:				R_{MAB}	R_{TAP}	$R_{MAB}+2R_{TA}$
					$R_{C_2F_6}$	R_{MAB}	$R_{C_2N_2}$	R_{TAP}	$R_{C_2F_6}{}^{\frac{1}{2}}[CF_3CN]$ (molecule$^{-\frac{1}{2}}$ $cc^{\frac{1}{2}}$ $sec^{-\frac{1}{2}}$ $\times 10^{13}$)	$R_{MAB}-R_{C_2F_6}{}^{\frac{1}{2}}t$ (molecule$^{-\frac{1}{2}}$ $cc^{\frac{1}{2}}$ $sec^{-\frac{1}{2}}$ $\times 10^{12}$	$R_{C_2F_6}{}^{\frac{1}{2}}[CF_3CN]$ (molecule$^{-\frac{1}{2}}$ $cc^{\frac{1}{2}}$ $sec^{-\frac{1}{2}}$ $\times 10^{13}$)
59	1.826	314.2	2.38	6.06	1.24	0.687	2.01	0.037	2.50	(2.52)†	2.78
61	2.40	313.4	2.40	6.48	2.34	3.29	5.18	0.144	2.83	1.39	3.08
64	1.597	312.8	0.400	30.40	0.113	0.411	0.514	0.0200	2.42	1.51	2.68
65	3.124	312.2	0.418	24.55	0.193	0.987	0.978	0.0480	2.27	1.39	2.49
52	0.599	332.0	1.84	6.13	0.783	0.564	2.23	0.018	3.36	1.86	3.58
54	1.130	333.8	1.88	6.32	0.977	1.33	3.73	0.080	3.78	3.04	4.24
51	1.717	332.4	1.86	6.64	1.188	2.25	5.59	0.112	3.81	2.16	4.19
56	2.36	332.6	2.38	6.42	1.548	4.13	3.75	0.289	4.45	2.76	5.09
55	2.97	333.8	2.44	6.18	1.71	5.16	5.02	n.d.*	4.21	—	—
46	0.482	351.8	1.96	6.20	0.294	0.482	1.95	0.010	5.85	(1.94)†	6.10
50	1.610	351.8	1.87	6.65	0.850	2.80	4.29	n.d.*	5.98	—	—
63	2.15	351.2	2.04	7.60	1.065	4.23	4.07	n.d.*	6.00	—	—
49	2.74	350.8	2.40	6.82	1.170	5.31	9.80	0.443	5.68	3.56	6.60
66	1.045	360.2	0.382	32.76	0.049	0.469	0.049	0.0305	6.41	2.84	7.26
70	1.007	371.6	2.32	7.01	0.737	2.35	3.43	0.165	8.58	3.68	9.79
69	1.566	373.0	2.10	6.26	0.731	4.49	4.47	0.283	10.60	3.71	11.99
68	2.083	373.3	2.20	6.46	0.727	6.09	5.72	n.d.*	10.85	—	—
71	2.103	374.7	0.320	23.8	0.0404	1.030	0.957	0.0800	7.70	4.95	8.90

NOTE: *n.d., not determined.
†Outside 2.5 × standard deviation.

t-butyl group. This may have required breaking a C—N bond, possibly by addition of two CF_3 radicals to MAB and then breaking of the C—N bond due to steric repulsion. If the *t*-butyl radical is an intermediate, one would expect perfluoroneopentane as a detectable product. From the boiling point of this compound (8), one would expect it to appear in cut No. 2 and to give a large m/e 219 peak, but none is observed.

Another possibility is that the C—N bond does not break until after 2 molecules of the original CF_3CN are associated in some intermediate compound that contains a number of additional CF_3 groups. This would not require the *t*-butyl radical as an intermediate, but again the absence of any other obvious intermediate is difficult to explain. Still another possibility is that TAP is not the actual product, but rather none of the higher mass peaks (above m/e 364) in the pattern of the actual product is stable. Thus the C—N bond has been broken on electron impact of the compound in the mass spectrometer to give a pattern resembling TAP. (It should be emphasized that the kinetic dependence for the formation of the compound giving the m/e 314 peak is much better understood from the data available than the structure of the compound.)

If TAP is formed by the reaction of MAB, then $k_3/k_2^{\frac{1}{2}}$ should be corrected for the number of $(CF_3)_2CN\cdot$ radicals or MAB molecules that are consumed in the formation of TAP. If two $(CF_3)_2CN\cdot$ radicals are assumed to be precursors for each molecule of TAP, $k_3/k_2^{\frac{1}{2}}$ would be determined from $(R_{MAB}+2R_{TAP})/R_{C_2F_6}{}^{\frac{1}{2}}[CF_3CN]$. A plot of this function (also shown in Fig. 3) results in a value for $(k_3/k_2^{\frac{1}{2}})_{corr}$ of:

$$10^{-9.08\pm.13}\, e^{-5.00\pm.21\ \text{kcal mole}^{-1}/RT}\ \text{molecule}^{-\frac{1}{2}}\ \text{cc}^{\frac{1}{2}}\ \text{sec}^{-\frac{1}{2}}.$$

It is seen that the uncertainty in the number of precursor $(CF_3)_2CN\cdot$ radicals in the formation of TAP will have only a small effect on the experimental value of k_3.

Using the latter value of $k_3/k_2^{\frac{1}{2}}$, assuming $E_2 = 0$, collision diameters for CF_3, CF_3CN, and MAB as 4.0, 7.0, and 8.0 Å, respectively, and a temperature of 343° K, one calculates $E_3 = 5.0\pm.2$ kcal mole^{-1}, $E_5 = 3.9\pm.3$ kcal mole^{-1}, $p_3/p_2^{\frac{1}{2}} = 2.2\times10^{-5}$, $p_5/p_2^{\frac{1}{2}} = 3.4\times10^{-5}$. If p_2 is taken to be unity, then p_3 and p_5 are about 2×10^{-5} and 3×10^{-5}, respectively.

Reactions [3] and [5] are similar to the addition of CH_3 radicals to simple olefins where the activation energies are about 5–7 kcal mole^{-1} and the steric factors are about 4×10^{-4} (9). The activation energies observed here are about the same, but the steric factors are lower by about a factor of 20. This decrease from the hydrocarbon case is presumably due to the increased size of the fluorinated groups.

ACKNOWLEDGMENTS

The authors wish to express their appreciation to Drs. K. O. Kutschke and F. P. Lossing for helpful discussions. They also wish to thank Miss B. Thornton for the mass spectrometric analyses and Mr. G. Ensel for making some of the glassware used in this work.

REFERENCES

1. McElcheran, D. E., Wijnen, M. H. J., and Steacie, E. W. R. Can. J. Chem. **36**, 321 (1958).
2. DuBridge, L. A. Phys. Rev. **29**, 451 (1927).
3. Leroy, D. J. Can. J. Research, B, **28**, 492 (1950).
4. Shepp, A. and Kutschke, K. O. Can. J. Chem. **32**, 1112 (1954).
5. Bloom, E. G., Mohler, F. J., Wise, C. E., and Wells, E. J. J. Research Nat. Bur. Standards, **43**, 65 (1949).
6. King, A. B. and Long, F. A. J. Chem. Phys. **29**, 374 (1958).
7. Platt, J. R. and Klevens, H. B. Rev. Modern Phys. **16**, 182 (1941).
8. Dresdner, R. D. J. Am. Chem. Soc. **78**, 876 (1956).
9. Mandelcorn, L. and Steacie, E. W. R. Can. J. Chem. **32**, 414 (1954).

APPENDIX

Consider the case of a mass spectral analysis on a two-component mixture where each of two peaks in the spectrum can be attributed solely to each component. The total pressure (p_t) is equal to the sum of the partial pressures of the two components and thus:

$$p_t = (h_1/S_1)+(h_2/S_2), \qquad [A\text{-}1]$$

where h refers to the peak height and S the sensitivity of the particular component.

If the total quantity of the sample (q_t) is known and the entire sample is expanded into a volume (V), then:

$$q_t/V = (h_1/S_1)+(h_2/S_2), \qquad [A\text{-}2]$$

and rearranging,

$$q_t/h_2 = (h_1/h_2)(V/S_1)+(V/S_2). \qquad [A\text{-}3]$$

A plot of q_t/h_2 vs. h_1/h_2 for a series of samples of varying relative composition will give the constants V/S_1 and V/S_2 from the slope and intercept, respectively. Since the absolute quantity of each component is:

$$q_1 = h_1(V/S_1), \qquad [A\text{-}4]$$

the absolute quantity can be calculated from the peak height in the individual samples and the constant determined from the plot of equation [A-3] for a set of analyses. No standards are therefore required and the volume (V) need not be known, merely that it is the same for all of the samples. If different volumes have to be used for different sample sizes, only the ratio of volumes needs to be known.

The presence of a third component in all of the samples will cause a scatter of the plot, but an occasional impurity in only a few samples will show up as a few points above the line with the remainder of the analyses giving a good linear plot. Figures 1 and 2 show this latter type of deviation, indicating that there are no significant additional components present in cuts No. 2 and No. 3.

This technique has the added advantage that if one of the components shows preferential absorption on the walls of the inlet system of the mass spectrometer, no effect on the linearity of equation [A-3] will be observed if the fraction of the component absorbed is independent of the total quantity of that component present. The V/S_1 thus obtained is an effective reciprocal sensitivity and the correct absolute quantities will still be obtained when the effective reciprocal sensitivity is used in equation [A-4].

AN ASYMMETRIC SYNTHESIS OF D- AND L-MANNOSAMINE[1]

A. N. O'NEILL[2]

ABSTRACT

The addition of ammonia to the ethylenic bond of D-arabo-tetraacetoxy-1-nitrohexene-1 was stereospecific and formed a crystalline product, 1-nitro-1-deoxy-N-acetyl-D-mannosaminol. Application of the Nef reaction to this compound gave 2-amino-2-deoxy-D-mannose, which was isolated as the crystalline pentaacetate and further characterized as the hydrochloride by deacetylation with hydrochloric acid. In the deacetylation of the pentaacetate with barium methoxide, however, an abnormal epimerization occurred to yield N-acetyl-D-glucosamine.

L-Mannosamine pentaacetate was synthesized in a similar manner from L-arabo-tetraacetoxy-1-nitrohexene-1.

The general chemistry of the simple α-nitroölefins has been investigated extensively. It has been found, in agreement with theoretical considerations, that the α-nitro group, by virtue of its powerful inductive and resonance effects, strongly activates the double bond, thereby facilitating attack in the β-position by nucleophilic reagents. Thus the addition of such reagents as ethyl malonate (7, 8), alcohols (10), thiols (5), ammonia and amines (6), nitroparaffins (11), hydrogen cyanide (2), Grignard reagents (9, 1), and arylacetonitriles (3) to α-nitrostyrene, nitroethylene, α-nitropropylene, etc. has been easily accomplished in the presence of basic catalysts.

Some of the more complex acetylated carbohydrate C-nitroölefins with an olefinic bond in conjugation with the nitro group have been prepared (16), but their reactivities have not been studied other than in the synthesis of 2-deoxy aldoses by selective hydrogenation of the double bond (16, 17). These compounds are readily obtained from the aldoses with one less carbon atom by condensation with nitromethane. This is followed by acetylation and elimination of 1 mole of acetic acid by treatment with a mild base under the conditions of the Schmidt and Rutz reaction (15). The resulting acetylated nitroölefins are obtained in good yield and in general are easily crystallized. As the primary C-nitro group can readily be converted into an aldehyde by the Nef reaction, these compounds should provide excellent starting materials for the synthesis of hexosamines by the addition of ammonia, and branched-chain carbohydrates by the addition of nitroparaffins, malonic ester, or other nucleophilic reagents.

The addition of amines and ammonia to the more simple α-nitroölefins has been studied by Heath and Rose (6), who found the reaction a general one. However the yields were variable, due partly to the instability of the resulting 2-nitroalkylamine in which the basic group caused rapid decomposition of the nitro compound, and partly to the tendency of the nitroölefins to polymerize under the influence of the amine.

In the present investigation both D- and L-arabo-tetraacetoxy-1-nitrohexene-1 were synthesized from D- and L-arabinose by the method of Sowden (16). The addition of ammonia to the olefinic bond was readily accomplished by adding the acetylated nitroölefin slowly to a saturated solution of ammonia in anhydrous methanol at 0°. The product, obtained in 82% yield, was a very stable, white, crystalline solid. Its aqueous solution was neutral. Microanalysis and the infrared spectrum indicated the presence of a N-acetyl group. The absorption spectrum showed the typical bands, types I and II,

[1]*Manuscript received June 8, 1959.*
Contribution of the National Research Council of Canada, Atlantic Regional Laboratory, Halifax, Nova Scotia.
Issued as N.R.C. No. 5333.
[2]*Deceased. Manuscript completed by B. A. Bolto.*

of a secondary amide at 1640 and 1550 cm^{-1} respectively. This compound would not undergo the rapid decomposition characteristic of the basic unsubstituted 2-nitroalkylamines because it contains a neutral amide group, which must result from an acyl migration from O to N during the concomitant addition and de-O-acetylation reactions.

From the addition reaction only one of the two possible diastereoisomers was isolated. A search for the second isomer in the mother liquors from the crystallization failed to reveal its presence. The compound isolated was shown to have the *erythro* configuration about carbon atoms two and three by its subsequent conversion into derivatives of mannosamine.

It is reasonable to assume that this addition reaction proceeds through a primary nucleophilic attack by the ammonia or amide ion on the β-carbon atom of the acetylated nitroölefin. If Cram's rule of "steric control of asymmetric induction" (4) can be applied, then the ammonia would enter preferably from the least-hindered side of the double bond when the rotational conformation of the C—C bond is such that the double bond is flanked by H and OAc, the two least bulky groups attached to the adjacent asymmetric center. This should lead to a predominance of the erythroisomer, as was actually obtained (Fig. 1). However, in this case, this simple interpretation is complicated by the possible interaction of the carbonyl carbon atom of the migrating acyl group with the incoming amino group. If the addition of ammonia at the double bond is complete before the

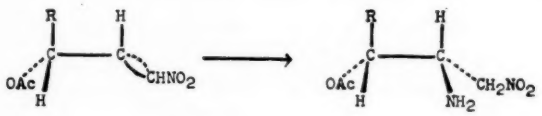

Fig. 1. R = $(CHOAc)_2.CH_2OAc$

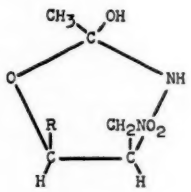

Fig. 2. R = $(CHOAc)_2.CH_2OAc$

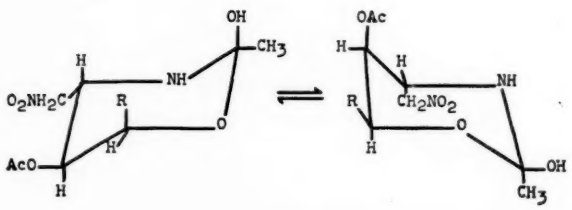

Fig. 3. R = $CHOAc.CH_2OAc$

acyl migration takes place, then the acyl group concerned could originate from C_3, with a planar five-membered ring as the intermediate (Fig. 2), or from C_4, with a non-planar six-membered ring as the intermediate (Fig. 3). In each case the nitrogen atom of the amino group can attack the carbonyl carbon atom of the migrating acyl group from either side. In Fig. 3, only one of the two possible configurations for the transient asymmetric center is given.

It is difficult to predict the most favored course of the rearrangement. In each of the above two cases, an intermediate is involved in which there is strong non-bonded repulsion

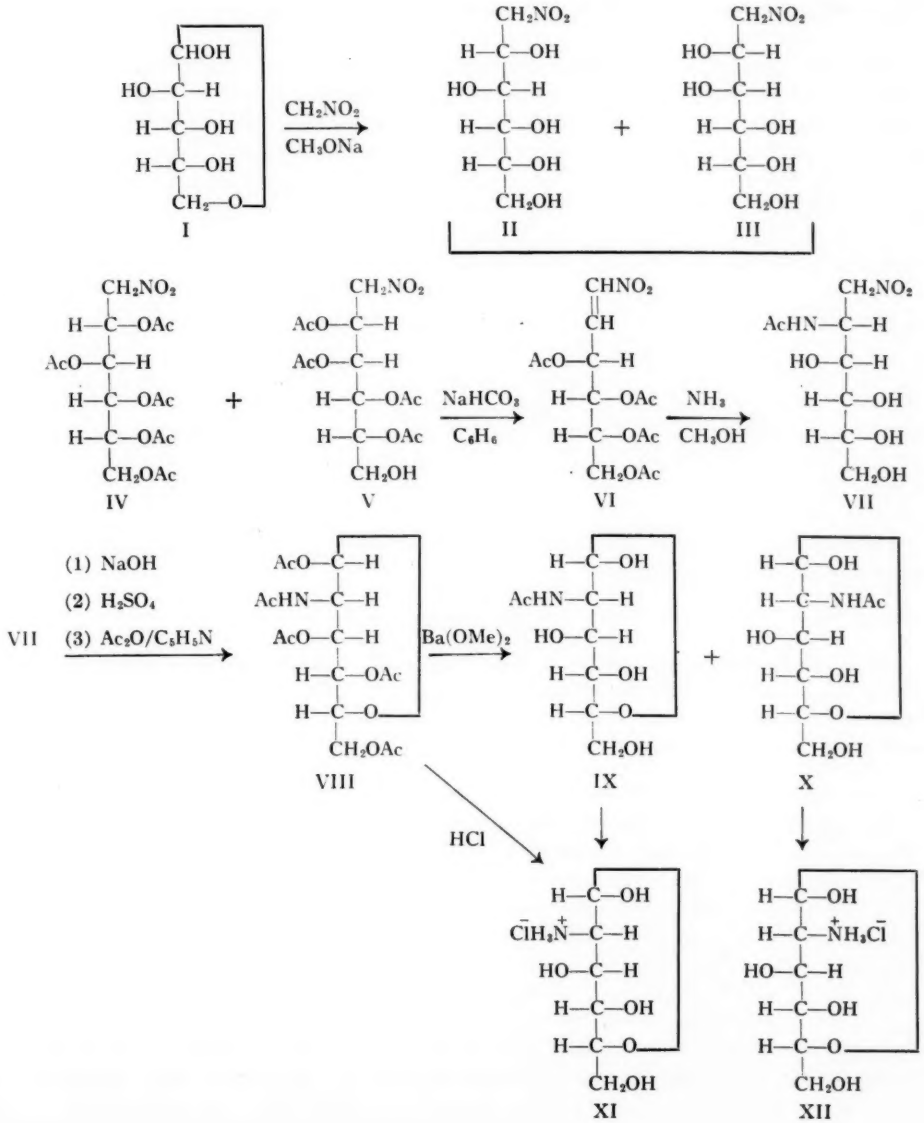

between fairly large groups, or in which bulky groups are in axial conformations. The addition product VII was treated with sodium hydroxide and the resulting sodium salt of the *aci*-nitro form treated with sulphuric acid under the conditions of the Nef reaction. Acetylation of the crude syrup so obtained yielded a crystalline pentaacetate of which the melting point and specific rotation agreed with values reported by Levene (13) for the β-pentaacetate of epichitosamine (β-D-mannosamine pentaacetate). The compound was further characterized as the hydrochloride by deacetylation with hydrochloric acid when agreement with the reported specific rotation was again obtained (13). Further evidence that XI was indeed D-mannosamine hydrochloride was obtained by a positive Elson–Morgan reaction, and by a degradation to D-arabinose with ninhydrin in pyridine (18).

However, deacetylation of the pentaacetate with barium methoxide gave 80–90% yields of N-acetyl-D-glucosamine (X) and only traces of N-acetyl-D-mannosamine (IX). These compounds were characterized as the hydrochlorides. This is evidence of an unusual epimerization during deacetylation in which a catalytic amount of barium methoxide was used, and is another example of the abnormal behavior of this compound. Thus, as the hydrochloride, it shows no mutarotation, nor is it oxidized by bromine or mercuric oxide. In fact treatment of D-mannosamine hydrochloride with mercuric oxide yields crystalline 2,5-anhydro-D-glucose (14).

For purposes of confirmation and for comparison of physical properties, derivatives of D-mannosamine were synthesized by a modification of Levene's original method (12). D-Glucosamine was oxidized to D-glucosaminic acid and epimerization accomplished in aqueous pyridine to form D-mannosaminic acid. After conversion to the lactone hydrochloride, reduction with sodium amalgam yielded D-mannosamine hydrochloride. The pentaacetate was formed in the usual manner and deacetylated with barium methoxide, when N-acetyl-D-glucosamine was again obtained with only traces of N-acetyl-D-mannosamine. But deacetylation of the pentaacetate with hydrochloric acid gave a quantitative yield of D-mannosamine hydrochloride.

The corresponding enantiomorphs of compounds II to VIII were synthesized by the same method from L-arabinose.

EXPERIMENTAL

All rotations were measured in a 2-dm tube with a Rudolph polarimeter. Melting points were observed on a Kofler micro-melting-point apparatus and are corrected. The infrared spectra were determined in nujol mulls with a Baird double-beam infrared spectrophotometer, model 4-55.

D-*Arabo-tetraacetoxy-1-nitrohexene-1* (VI)

This compound was synthesized from D-arabinose according to the method of Sowden (16), by condensation with nitromethane, acetylation, and elimination of 1 mole of acetic acid from the resulting mixture of acetylated C-nitroalcohols (IV and V). The yield of D-arabo-tetraacetoxy-1-nitrohexene-1 (VI) from 25 g of D-arabinose was 30 g; m.p. 115–116°, $[\alpha]_D^{24}$ +33° (c = 1.0 in chloroform). Main infrared absorption bands: 2900, 1740, 1667, 1530, 1460, 1379, 1220, 1122, 1078, 1050, 972, 953, and 853 cm^{-1}. Anal. Calc. for $C_{14}H_{19}O_{10}N$: C, 46.54; H, 5.30; N, 3.88. Found: C, 46.31; H, 4.87; N, 3.76%.

The corresponding L-arabo-tetraacetoxy-1-nitrohexene-1 prepared in the same manner from L-arabinose had m.p. 114–116°, $[\alpha]_D^{25}$ −34° (c = 1.0 in chloroform), and gave an identical infrared absorption spectrum.

*1-Nitro-1-deoxy-*N*-acetyl-*D*-mannosaminol* (VII)

Finely powdered D-arabo-tetraacetoxy-1-nitrohexene-1 was added slowly, in portions and with continuous shaking, to 500 ml of absolute methanol saturated with anhydrous ammonia at 0°. Each portion was allowed to dissolve before the next was added. When all of the acetylated nitroölefin was added the solution was left at 5° for 18 hours. Methanol and ammonia were removed by distillation under reduced pressure. This left a crystalline residue. It was recrystallized twice from methanol to give long needles; yield 16 g (82%), m.p. 172–173°, $[\alpha]_D^{24}$ −13.2° (c = 1.1 in water). Anal. Calc. for $C_8H_{16}O_7N_2$: C, 38.09; H, 6.40; N, 11.11. Found: C, 37.99; H, 6.14; N, 11.05%. Main infrared absorption bands: 3330, 2930, 1640, 1570, 1550, 1460, 1379, 1300, 1240, 1122, 1080, 1023, 943, 908, and 855 cm^{-1}.

The enantiomorphous 1-nitro-1-deoxy-N-acetyl-L-mannosaminol had m.p. 172–172.5° and $[\alpha]_D^{24}$ +14.9° (c = 1.5 in water). Its infrared absorption spectrum was identical with that of the D-isomer.

*2-Acetamido-2-deoxy-1,3,4,6-tetra-*O*-acetyl-β-*D*-mannose* (VIII)

An amount of 10 g of the above crystalline addition product was dissolved in 25 ml of 2 *N* sodium hydroxide at 5° and added dropwise with shaking to 12 ml of sulphuric acid in 15 ml of water also at 5°. During the addition the temperature was maintained at 10–15° by external cooling. The solution was neutralized with warm barium hydroxide solution and filtered. Two drops of acetic acid were added and the filtrate concentrated to a syrup under reduced pressure. It was further dried by the distillation of added ethanol, and finally over phosphorus pentoxide in a vacuum desiccator.

This syrupy material was acetylated for 3 days at 0° with acetic anhydride (125 ml) and pyridine (100 ml). The acetylation mixture was poured into 500 ml of ice and water and extracted with chloroform. The chloroform extract was washed twice with dilute sodium bicarbonate, four times with dilute copper sulphate, four times with water, and dried over anhydrous sodium sulphate. Distillation of the solvent under reduced pressure left a yellow syrup which was crystallized from absolute ethanol and recrystallized from ethanol–ether; yield 13 g (84% from VII), m.p. 162–163°, $[\alpha]_D^{24}$ −17.0° (c = 1.8 in chloroform). Anal. Calc. for $C_{16}H_{23}O_{10}N$: C, 49.35; H, 5.95; N, 3.60. Found: C, 49.44; H, 5.73; N, 3.50%. Levene (13) reported m.p. 158–159° and $[\alpha]_D^{20}$ −18° for his preparation of β-D-mannosamine pentaacetate.

The corresponding compound in the L-series had m.p. 162–163°, $[\alpha]_D^{25}$ +18.0° (c = 1.1 in chloroform).

*2-Amino-2-deoxy-α-*D*-mannose Hydrochloride* (XI)

β-D-Mannosamine pentaacetate was completely deacetylated by dissolving 200 mg in 4 ml of 2 *N* hydrochloric acid and heating on the steam bath for 4½ hours. After concentration under reduced pressure small amounts of residual water, hydrochloric acid, and acetic acid were removed by co-distillation with ethanol. The resulting dark brown crystalline material was dissolved in a small amount of water, decolorized with charcoal, and, after filtration through a cotton and asbestos plug, crystallized by the addition of ethanol; yield 107 mg. The product reduced Fehling's solution, and gave the characteristic Elson–Morgan reaction for hexosamine hydrochlorides. A small amount when degraded in a sealed tube with ninhydrin and pyridine by the method of Jeanloz (18) gave only D-arabinose as determined by paper chromatography. This compound had an indefinite melting point and showed no mutarotation; $[\alpha]_D^{25}$ −4° (c = 1.0 in 3% hydrochloric acid). Anal. Calc. for $C_6H_{14}O_5NCl$: C, 33.26; H, 6.48; N, 6.50; Cl, 16.44.

Found: C, 33.05; H, 6.36; N, 6.70; Cl, 16.40%. Levene (13) reported no mutarotation for his preparation of D-mannosamine hydrochloride, $[\alpha]_D$ −4.7° in 5% hydrochloric acid.

2-Acetamido-2-deoxy-D-glucose (X)

A portion (10 g) of the syrupy β-D-mannosamine pentaacetate was dissolved in 150 ml of absolute methanol, cooled to 0°, and treated at this temperature for 24 hours with 20 ml of 0.4 *N* barium methoxide. The solution was diluted with an equal volume of water, deionized by shaking with exchange resins Amberlite IR-120 and IR-45, filtered, and the filtrate concentrated to a syrup by distillation under reduced pressure. This was crystallized from ethanol–ether to yield 0.75 g of crystalline material and 5.0 g of syrup. The crystalline material, after recrystallization, had m.p. 193–196° with decomposition starting at 185°; $[\alpha]_D^{26}$ +75.0° (5 minutes), +69.0° (15 minutes), +58.2° (30 minutes), and +43.8° at equilibrium (4 hours); (c = 1.2 in water). Anal. Calc. for $C_8H_{15}O_6N$: C, 43.43; H, 6.84; N, 6.33. Found: C, 43.53; H, 6.79; N, 6.48%.

Both the crystalline material and the syrup gave the characteristic Elson–Morgan reaction for N-acetyl hexosamines. The crystalline material was further deacetylated with hydrochloric acid by dissolving 100 mg in 1 ml of 2 *N* hydrochloric, treating on the steam bath for 2 hours, and working up the material as described in the preceding preparation of D-mannosamine hydrochloride. It was recrystallized from aqueous ethanol; yield 93 mg. It reduced Fehling's solution and gave the Elson–Morgan color reaction for hexosamine hydrochlorides. An $[\alpha]_D^{25}$ of +82.4° at 5 minutes and +73° at 18 hours (c = 0.91 in water) established that the material was D-glucosamine hydrochloride, and that the crystalline N-acetyl hexosamine was N-acetyl-D-glucosamine and not N-acetyl-D-mannosamine.

However, when the syrupy material was treated with hydrochloric acid in the same manner, the product had $[\alpha]_D^{24}$ +18.0° changing to +15.5° after 26 hours (c = 2.2 in water). Fractional crystallization of some of this hydrochloride produced D-glucosamine hydrochloride ($[\alpha]_D^{25}$ +98° (5 minutes), +76° (17 hours; c = 1.1 in water)) and a small amount of D-mannosamine hydrochloride ($[\alpha]_D^{26}$ −4°; c = 1.0 in 2.5% hydrochloric acid). Thus the syrupy N-acetyl hexosamine was a mixture of N-acetyl-D-glucosamine and N-acetyl-D-mannosamine, while the crystalline material was pure N-acetyl-D-glucosamine. Of the total yield of N-acetyl derivative, 80–90% was estimated as N-acetyl-D-glucosamine.

Alternate Preparation of D-Mannosamine Hydrochloride

D-Mannosamine was synthesized by a modification of the method of Levene (12). D-Glucosamine hydrochloride (80 g) was first oxidized in aqueous solution with yellow mercuric oxide (200 g) to give D-glucosaminic acid in 50% yield, $[\alpha]_D^{25}$ −14° (c = 1.3 in 2.5% hydrochloric acid). Epimerization was accomplished by refluxing 40 g of D-glucosaminic acid dissolved in 400 ml water containing 40 ml pyridine on a steam bath for 24 hours. The D-mannosaminic acid was obtained by fractional crystallization from the large amount of starting material. The recovered D-glucosaminic acid was treated twice again with aqueous pyridine in the same manner. Each treatment yielded about 4 g of D-mannosaminic acid which was further purified by many recrystallizations from aqueous ethanol, $[\alpha]_D^{24}$ +10° (c = 1.5 in 2.5% hydrochloric acid). The D-mannosaminic acid was converted into its lactone hydrochloride by treatment with ethanolic hydrogen chloride containing a small amount of benzaldehyde; yield 75%, $[\alpha]_D^{24}$ +45° (c = 1.4 in water). Reduction of the lactone with 2.5% sodium amalgam yielded D-mannosamine hydrochloride; yield

60% from the lactone. Recrystallization from water containing a small amount of methanol gave pure material, $[\alpha]_D^{24}$ −4.0° (c = 2.0 in 2.5% hydrochloric acid).

Acetylation of the hydrochloride with pyridine and acetic anhydride in the usual manner gave β-D-mannosamine pentaacetate, m.p. 161–162°, $[\alpha]_D^{24}$ −18° (c = 1.5 in chloroform). Deacetylation with barium methoxide again yielded predominantly N-acetyl-D-glucosamine. But deacetylation with hydrochloric acid gave a quantitative yield of D-mannosamine hydrochloride.

REFERENCES

1. BUCKLEY, G. D. J. Chem. Soc. 1494 (1947).
2. BUCKLEY, G. D., HEATH, R. L., and ROSE, J. D. J. Chem. Soc. 1500 (1947).
3. BUCKLEY, G. D., HUNT, F. G., and LOWE, A. J. Chem. Soc. 1504 (1947).
4. CRAM, D. J. and ABD ELHAFEZ, F. A. J. Am. Chem. Soc. **74**, 5828 (1952).
5. HEATH, R. L. and LAMBERT, A. J. Chem. Soc. 1477 (1947).
6. HEATH, R. L. and ROSE, J. D. J. Chem. Soc. 1486 (1947).
7. KOHLER, E. P. and ENGELBRECHT, H. J. Am. Chem. Soc. **41**, 764 (1919).
8. KOHLER, E. P. and BARRETT, G. R. J. Am. Chem. Soc. **48**, 1770 (1928).
9. KOHLER, E. P. and STONE, J. F. J. Am. Chem. Soc. **52**, 761 (1930).
10. LAMBERT, A., SCAIFE, C. W., and WILDER-SMITH, A. E. J. Chem. Soc. 1474 (1947).
11. LAMBERT, A. and PIGGOTT, H. A. J. Chem. Soc. 1489 (1947).
12. LEVENE, P. A. J. Biol. Chem. **36**, 73 (1918).
13. LEVENE, P. A. Hexosamines and mucoproteins. Longmans, Green and Co., Ltd., London. 1925. p. 16.
14. LEVENE, P. A. J. Biol. Chem. **39**, 69 (1919).
15. SCHMIDT, E. and RUTZ, G. Ber. **61**, 2142 (1928).
16. SOWDEN, J. C. and FISCHER, H. O. L. J. Am. Chem. Soc. **69**, 1048 (1947).
17. SOWDEN, J. C. J. Am. Chem. Soc. **72**, 808 (1950).
18. STOFFYN, P. J. and JEANLOZ, R. W. Arch. Biochem. Biophys. **52**, 373 (1954).

SYNTHESIS OF SUGARS FROM SMALLER FRAGMENTS

PART XI. SYNTHESIS OF L-GALACTOHEPTULOSE[1]

J. K. N. JONES AND N. K. MATHESON[2]

ABSTRACT

1,3-Dihydroxy-2-propanone phosphate condenses with L-threose in the presence of the enzyme aldolase to yield L-galactoheptulose phosphate, from which the heptose was prepared.

Dihydroxyacetone phosphate (1,3-dihydroxy-2-propanone phosphate) which was formed from D-fructose 1,6-diphosphate has been shown to yield new sugar derivatives when its solution is incubated at pH 6.5 with aldehydes in the presence of crude pea aldolase or purified muscle aldolase (1). The reaction takes place between the aldehyde and an enzyme–substrate complex which involves aldolase and dihydroxyacetone phosphate (2). In particular three of the possible aldotetroses, D-erythrose (3), L-erythrose (4), and D-threose (5) have been shown to condense with dihydroxyacetone phosphate in the presence of aldolase and the resultant heptulose derivatives have the D-*threo* configuration on carbon atoms 3 and 4.

It was considered of interest to examine the behavior of the fourth aldotetrose, L-threose. At pH 6.5, L-threose and dihydroxyacetone phosphate (produced by the cleavage of fructose diphosphate with aldolase) in the presence of aldolase gave a low yield of L-galactoheptulose 1-phosphate which was converted to the crystalline sugar. No other heptulose could be detected chromatographically (an orcinol – trichloroacetic acid spray was used for the detection of heptuloses on chromatograms (6)). The ultraviolet absorption of the product formed on heating the heptulose with cysteine and sulphuric acid (7) was measured at 5080 Å, and its intensity indicated that 1 mole of L-threose had yielded 0.021 mole of heptulose. Thus all the aldotetroses condense with dihydroxyacetone phosphate in the presence of aldolase to yield heptulose derivatives which possess the D-*threo* configuration on carbon atoms 3 and 4.

In view of the results of other workers (8, 9) which indicated that these condensations take place without the intervention of enzymes a reaction mixture which was composed of dihydroxyacetone (1,3-dihydroxy-2-propanone), L-threose, and aldolase at pH 6.5 was studied. The presence of heptulose was determined colorimetrically by the method of Dische (7). The reaction products were also separated on paper chromatograms which were sprayed with orcinol–trichloroacetic acid (6). No heptulose was detected by either method. The formation of heptulose was therefore enzymic and involved dihydroxyacetone as its phosphate.

EXPERIMENTAL

Preparation of L-*Threose*

2,4-*O*-benzylidene-L-threose was prepared by the method of Neish (10). The *O*-benzylidene group was removed by heating the derivative in 10% acetic acid solution at 100° C for 1 hour. The solution was extracted three times with ether and the extracts were evaporated under diminished pressure to half their original volume. This concentration of aldotetrose was used in the enzymic experiments.

[1]*Manuscript received June 22, 1959.*
Contribution from the Department of Chemistry, Queen's University, Kingston, Ontario.
[2]*Present address: Tobacco Research Institute, P.O. Box 172, Mareeba, Queensland, Australia.*

D-*Fructose Sodium Diphosphate*

Commercial barium salt was deionized on a column of Amberlite ion-exchange resin IR-120, the acidity of the eluate was neutralized with sodium hydroxide, after which the solution was evaporated to a small volume and the concentrate was cooled to 0° C.

The efflorescent crystalline hydrate which separated was collected on a filter, washed with the cold water, and quickly transferred to a desiccator. The dried salt was a pale yellow powder.

The chromatographic behavior of this substance corresponded to that of authentic D-fructose 1,6-diphosphate.

Reaction of L-*Threose,* D-*Fructose Diphosphate, and Crystalline Muscle Aldolase*

A solution of L-threose (3.0 g) and the sodium salt of D-fructose diphosphate (3.0 g) was adjusted to pH 6.5 with dilute acetic acid. Twice-recrystallized muscle aldolase (50 mg) was added and the volume was adjusted to 150 ml. The solution was kept at 37° C and 1-ml aliquots were taken at intervals (see Table I). Each sample was mixed with an equal volume of 2 *N* sulphuric acid and heated on a boiling water bath for 15 minutes to stop enzyme action. The heptulose content was then estimated by the method of Dische (7) with cysteine hydrochloride and sulphuric acid as follows. One milliliter of the sample was made up to 10 ml, and 1 ml of this solution was treated with 5 ml of sulphuric acid reagent at 0° C. The color at 5080 Å which developed after the solution had been left to stand for 18 hours was measured on a Unicam SP 600 spectrophotometer.

TABLE I

Yield of heptose as determined by the colorimetric procedure of Dische (7)

Time (hours)	Heptulose synthesis: aldolase, D-fructose 1,6-diphosphate, L-threose (log *E* 5080 Å)	Blank experiment: aldolase, dihydroxyacetone, L-threose (log *E* 5080 Å)
0	0.17	0.18
0.5	0.20	0.17
1.5	0.23	0.17
6.0	0.51	0.18
24	0.66	0.17
72	0.76	0.16

A calibration curve made by using D-galactoheptulose as the heptose sugar gave a linear relationship between concentration and intensity of color.

The pH of the reaction solution showed a drop towards lower values with time and this pH was adjusted to the original value by the addition of a few drops of sodium acetate solution. Sulphuric acid (2 *N*, 150 ml) was added to the solution which was heated at 100° C for 6 hours in order to hydrolyze phosphate esters. The sulphuric acid was partially neutralized with barium hydroxide and neutralization was completed with barium carbonate.

The barium salts were removed by centrifugation and the supernatant liquid was passed through a column of Amberlite IR4B (acetate) and IR 120 ion-exchange (H) resins. The eluate was reduced in volume by evaporation under diminished pressure to give a syrup which was separated into three fractions on a column of powdered cellulose using butane-1-ol and water (9:1) as eluent.

Fraction I.—Fraction I (0.030 g) co-chromatographed with dihydroxyacetone and gave the same color with the *p*-anisidine hydrochloride reagent as did dihydroxyacetone.

Fraction II.—Fraction II (0.082 g) co-chromatographed with D-fructose and gave the same color with the orcinol – trichloroacetic acid reagent.

Fraction III.—Fraction III (0.079 g) co-chromatographed with L-galactoheptulose and on trituration with ethanol gave L-galactoheptulose, m.p. and mixed m.p. 100–101°, $[\alpha]_D^{22°}$ −90° → −80° (*c*, 1.1 water).

Reaction of Dihydroxyacetone with L-*Threose and Aldolase at pH 6.5*

A solution of L-threose (0.30 g) and dihydroxyacetone (0.30 g) in water was adjusted to pH 6.5 with acetic acid, crystalline muscle aldolase (5 mg) was then added, the volume made up to 15.0 ml, and the solution kept at 37° C. One-milliliter aliquots were taken at 0, 0.5, 1.5, 6.0, 24, and 72 hours, and the heptulose estimated (7). The absorption at 5080 Å at the elapse of these times is recorded in the table.

The authors thank the National Research Council for grants and for a Postdoctoral Fellowship (to N. K. Matheson).

REFERENCES

1. Meyerhof, O. and Schulz, W. Biochem. Z. **289**, 87 (1936).
2. Topper, Y. J., Mehler, A. H., and Bloom, D. Science, **126**, 1287 (1957).
3. Hough, L. and Jones, J. K. N. J. Chem. Soc. 4047 (1952).
4. Jones, J. K. N. and Kelly, R. B. Can. J. Chem. **34**, 95 (1956).
5. Gorin, P. A. J. and Jones, J. K. N. J. Chem. Soc. 1537 (1953).
6. Klevstrand, R. and Nordal, A. Acta Chem. Scand. **4**, 1320 (1950).
7. Dische, Z. J. Biol. Chem. **204**, 983 (1953).
8. Stacey, M. Biological synthesis of carbohydrates. Roy. Inst. Chem. (London), Monograph No. 2, 6 (1956).
9. Gascoigne, J. A., Overend, W. G., and Stacey, M. Chem. & Ind. (London), 402 (1959).
10. Neish, A. C. Can. J. Chem. **32**, 334 (1954).

LYCOPODIUM ALKALOIDS

VIII. LYCOPODINE[1]

D. B. MacLean and W. A. Harrison[2]

ABSTRACT

Information pertaining to the position of the carbonyl group relative to the nitrogen atom and to the size of one of the nitrogen rings in lycopodine has been obtained through a study of the reactions of α- and β-cyanobromolycopodine.

Lycopodine, $C_{16}H_{25}ON$, is the major alkaloid of several species of *Lycopodium*. It is known that it contains a tertiary nitrogen atom, a carbonyl group, and no other functional groups, and it can be inferred that it has a combination of four carbocyclic and/or heterocyclic rings (1).

The first degradative work on lycopodine was carried out by Marion and Manske (2), who dehydrogenated the alkaloid and isolated from the reaction 7-methylquinoline and 5,7-dimethylquinoline along with several other uncharacterized bases. Thus, there may be present in the alkaloid a reduced quinoline ring system. The reaction of lycopodine with cyanogen bromide was studied by MacLean, Manske, and Marion (1) and later by Barclay and MacLean (3). From the cyanogen bromide reaction two isomeric cleavage products, α- and β-cyanobromolycopodine, I and II, respectively, were isolated. The bromo group in I was shown to be primary by its conversion to an acetate, hydrolysis of the acetate to an alcohol, and oxidation of the latter to a carboxylic acid without loss of carbon. An attempt to carry out an analogous series of reactions on II failed in the first step, for, instead of the expected acetate, a different compound III, $C_{17}H_{24}ON_2$, was formed, apparently in a cyclization reaction. The carbonyl group in lycopodine is ketonic and is present in a six-membered or larger ring on the basis of its absorption in the infrared near 1700 cm^{-1} (1). Barclay and MacLean (3) have shown that the carbonyl group is flanked on one side by a methylene group through the formation of a benzylidene derivative from α-cyanolycopodine. In the present study the reactions of α- and β-cyanobromolycopodine have been extended to give information on the size of one of the two nitrogen rings and on the position of the carbonyl group relative to the nitrogen atom.

α-Cyanobromolycopodine I was converted to the carboxylic acid IV reported by MacLean, Manske, and Marion (1). Reduction of the acid IV with sodium borohydride yielded the hydroxy acid V, $C_{17}H_{26}O_3N_2$. This hydroxy acid failed to form a lactone on treatment with catalytic amounts of *p*-toluene sulphonic acid in a boiling benzene solution and a close relationship between the carbonyl and the nitrogen in the direction of the α-cleavage is precluded. Hydrolysis of the acid IV with aqueous alcoholic hydrochloric acid yielded an impure amino acid hydrochloride VI. Treatment of a solution of VI in methanol with a solution of diazomethane in ether yielded a mixture from which the lactam VII, $C_{16}H_{23}O_2N$, was isolated. The lactam had ketonic absorption in its infrared spectrum at 1700 cm^{-1} and lactam absorption at 1635 cm^{-1}. The latter is in the region characteristic of six-membered or larger ring lactams. Reduction of VII with

[1]*Manuscript received June 25, 1959.*
Contribution from the Burke Chemical Laboratories, Hamilton College, McMaster University, Hamilton, Ontario. Part of this work was taken from the thesis of W. A. Harrison presented to the Faculty of Graduate Studies in May, 1957 in partial fulfillment of the requirements for the M.Sc. degree.
[2]*Holder of National Research Council Studentship 1956–57, 1957–58, and 1958–59.*

lithium aluminum hydride yielded dihydrolycopodine VIII, identified by comparison with an authentic sample prepared by the reduction of lycopodine with lithium aluminum hydride. It can be concluded that no rearrangements in the carbon skeleton occurred in the above reaction sequence.

MacLean, Manske, and Marion (1) reported that β-cyanobromolycopodine II reacted with potassium acetate in an unexpected manner and formed compound III in an elimination reaction rather than undergoing displacement to form an acetate. We have confirmed this result. We have found, however, that treatment of II with silver acetate in boiling benzene yielded a mixture of III and an acetate. The presence of the acetate in the reaction mixture was indicated by an examination of the infrared spectrum of the crude reaction product. To facilitate the separation of compound III from the other product of reaction, the mixture was hydrolyzed and then separated by chromatography into two components. The less strongly adsorbed fraction proved to be compound III formed in 82% yield, while the more strongly adsorbed proved to be the β-alcohol, $C_{17}H_{26}O_2N_2$, IX formed in 18% over-all yield from the β-bromide. The crude product IX had absorption bands in the infrared attributable to a carbonyl group and a hydroxyl group. In an alternate method of separation, the crude reaction mixture from the silver acetate reaction was treated directly with sodium borohydride in ethanol. Chromatographic separation of the product of this reduction yielded III in 72% yield and a new compound, $C_{17}H_{28}O_2N_2$, X in 23% yield. Compound X was also obtained by treatment of IX with sodium borohydride. Compound X showed no carbonyl absorption in its infrared spectrum, but had strong hydroxyl absorption as well as the usual cyanamide absorption. The compound X was oxidized by the Oppenauer method to the keto alcohol IX, and in this manner IX was obtained in crystalline form.

The low yield of alcohol in the silver acetate reaction coupled with the difficulty in isolation of the β-bromide II led us to seek an alternative source of the β-alcohol IX. In the reaction of lycopodine with cyanogen bromide, Barclay and MacLean (3) reported that an alcohol fraction was formed in small yield along with the two isomeric bromides. From this alcohol fraction they isolated, after treatment with acetic anhydride, α-cyanoacetoxylycopodine XI, previously reported by MacLean, Manske, and Marion (1). We have treated this alcohol fraction with sodium borohydride and have obtained a mixture from which we have isolated compounds III and X and a new compound XII. Compound XII proved to be identical with the product obtained when α-cyanohydroxylycopodine was reduced with sodium borohydride. In this manner a sufficient quantity of the β-alcohol was obtained for degradative study.

The chromic acid oxidation of IX yielded a non-crystalline acid XIII which was converted to a crystalline methyl ester XIV, $C_{18}H_{26}O_3N_2$, on treatment with diazomethane. The analysis indicated that no loss in carbon had occurred in the oxidation reaction and one can safely conclude that the alcohol IX is a primary alcohol. Reduction of the crude β-acid XIII with sodium borohydride yielded a neutral product XV, $C_{17}H_{24}O_2N_2$, with the properties of a lactone. It had no hydroxyl absorption in its infrared spectrum, but had a strong peak at 1743 cm^{-1} when the spectrum was determined in nujol mull, and at 1761 cm^{-1} when it was determined in a carbon tetrachloride solution. This is a borderline region between five-membered and six-membered lactones and it can be concluded that the carbonyl group is separated from the nitrogen atom by three or four carbon atoms about the periphery of the molecule in the direction of the β-cleavage.

In proposing a model to account for these reactions it is inviting to use the hexahydrojulolidine ring system which is present in annotinine, the only alkaloid of this group of

known structure (4, 5). In making use of this ring system it is convenient to place the carbonyl group in the position shown in the partial formula below.

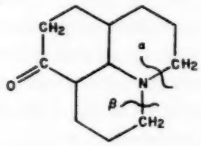

Those carbon atoms which are definitely known are so indicated, and the α- and β-cleavages are designated. This model is in agreement with the data presented here, namely, that the ring broken in the α-cleavage is six-membered and that the carbonyl group is located close to the nitrogen atom about the periphery of the molecule in the direction of the β-cleavage, but not in the direction of the α-cleavage. The model also accounts for the carbonyl frequency in the infrared spectrum of lycopodine. It does not attempt to account for the fourth ring of lycopodine nor for the C-methyl group which is present in the alkaloid.

EXPERIMENTAL

Lycopodine

The alkaloid was isolated from *L. flabelliforme* by the procedure described by Barclay and MacLean (3). It melted at 116° after recrystallization from petroleum ether. Calc. for $C_{16}H_{25}ON$: one C-methyl, 6.1%. Found: 5.0%.

Reaction of Lycopodine with Cyanogen Bromide

The reaction was carried out and the products isolated according to the procedure of Barclay and MacLean (3).

Oxidation of α-Cyanohydroxylycopodine

α-Cyanohydroxylycopodine (1.9 g), prepared by the method of MacLean, Manske, and Marion (1), was dissolved in 40 ml of 90% acetic acid and the solution added slowly to a solution of 4 g of chromium trioxide in 60 ml of 90% acetic acid. The temperature was maintained at −10 to −15° during the addition, and the mixture was stirred at this temperature for a further 4 hours. The excess chromic acid was destroyed with methanol and the mixture was then evaporated to dryness. Water was added to the residue and the mixture was exhaustively extracted with chloroform. The chloroform solution was extracted with sodium carbonate solution and the carbonate extract acidified and extracted with chloroform. Evaporation of the second chloroform solution yielded 1.2 g of non-crystalline acid. The crude acid crystallized on standing, but a suitable solvent system for its recrystallization was not found. It was characterized as its methyl ester reported previously (1).

Preparation of the Lactam VII

The acid IV (1.2 g) was dissolved in 12 ml of *n*-propanol and treated with 60 ml of 2 *M* hydrochloric acid. The mixture was heated on the steam bath for 15 hours and then evaporated to dryness. The residue was washed several times with warm ether to remove unreacted starting material. There remained a residue of 1.1 g of crude amino acid hydrochloride.

The hydrochloride was dissolved in methanol, an excess of diazomethane in ether was added, and the mixture allowed to stand for 1 hour before it was taken to dryness.

The crude product was dissolved in chloroform and washed with dilute hydrochloric acid. The chloroform solution yielded, on evaporation, 0.5 g of crude product which was purified by chromatography on an alumina column using chloroform as eluant. Practically all the material was eluted in a single band. The chloroform was evaporated and the residue dissolved in low boiling petroleum ether from which it crystallized in needles. Recrystallization from the same solvent gave an analytical sample which melted at 159–161°. Calc. for $C_{16}H_{23}O_2N$: C, 73.6; H, 8.88; N, 5.4%. Found: C, 73.9; H, 9.29; N, 5.2%. The infrared spectrum showed a strong band at 1635 cm^{-1} in the lactam region, as well as the usual carbonyl band at 1700 cm^{-1}. The over-all yield of lactam from α-cyanohydroxylycopodine was about 30%.

The acid washings from the purification of the lactam were worked up and yielded 0.3 g of an amino acid ester. The ester was slowly converted to the lactam by refluxing in xylene. This was shown by the infrared spectrum of the crude product, which exhibited a decrease in the intensity of the ester carbonyl absorption at 1730 cm^{-1} and the appearance of the lactam carbonyl band at 1635 cm^{-1}.

Reduction of the Lactam VII *with Lithium Aluminum Hydride*

A sample of the lactam VII (0.15 g), dissolved in anhydrous tetrahydrofuran, was added with stirring to a solution of lithium aluminum hydride (0.2 g) in tetrahydrofuran. The mixture was heated under reflux for 4 hours and then allowed to stand overnight. The excess hydride was decomposed with wet tetrahydrofuran, the solution filtered, and the precipitated hydroxides extracted thoroughly with chloroform. The combined tetrahydrofuran and chloroform extract was evaporated to dryness and the residue was purified by chromatography on an alumina column using chloroform as eluant. From the chloroform eluant a residue was obtained which crystallized from ether – petroleum ether. This material proved to be identical with a sample of dihydrolycopodine prepared by the reduction of lycopodine with lithium aluminum hydride. The melting point of a mixture of the two samples was not depressed and their infrared spectra were identical.

Reduction of the Acid IV *with Sodium Borohydride*

The acid IV (0.3 g) was dissolved in an aqueous sodium carbonate solution and treated with an excess of sodium borohydride. After the mixture had stood at room temperature for 12 hours, the excess sodium borohydride was destroyed with acetone and the mixture evaporated to dryness. The residue was taken up in water, acidified with hydrochloric acid, and the resulting mixture extracted with chloroform. The chloroform extract was dried and evaporated to yield a crystalline residue in virtually quantitative yield. Recrystallization from ether, in which the compound is only sparingly soluble, gave an analytical sample which melted at 193–194°. The compound analyzed for a monohydrate. Calc. for $C_{17}H_{26}O_3N_2 \cdot H_2O$: C, 62.9; H, 8.70; N, 8.6%. Found: C, 63.0; H, 8.35; N, 8.7%. Loss in weight on drying: Calc., 5.5%; found, 5.8%.

Reduction of α-Cyanohydroxylycopodine with Sodium Borohydride

α-Cyanohydroxylycopodine (0.2 g) was dissolved in ethanol and treated with an excess of sodium borohydride. After a period of 3 hours the excess borohydride was destroyed by the addition of acetone and the mixture evaporated to dryness. Water was added to the residue and the mixture was extracted with chloroform. The chloroform extract was dried and evaporated to dryness to yield a crystalline residue in virtually quantitative yield. Recrystallization from acetone yielded an analytical sample which

melted at 195–197°. Calc. for $C_{17}H_{28}O_2N_2$: C, 69.8; H, 9.65; N, 9.6%. Found: C, 70.1; H, 9.97; N, 9.2%.

Treatment of β-Cyanobromolycopodine II *with Silver Acetate*

Silver acetate (1.0 g) was added to a solution of 0.82 g of β-cyanobromolycopodine in benzene (80 ml) and the mixture heated under reflux for 5 hours. After the insoluble salts had been removed by filtration, the benzene solution was evaporated to give 0.67 g of non-crystalline material. The infrared spectrum (film) of the crude product showed bands at 1700 and 1735 cm^{-1}, attributed to ketone and acetate carbonyl groups respectively, as well as a strong band at 1675 cm^{-1} characteristic of the cyclized compound III.

To facilitate separation of the cyclized and non-cyclized products, the acetate which had been formed was hydrolyzed to the alcohol by treating the mixture for 2.5 hours with potassium hydroxide (0.8 g) in boiling methanol (20 ml). The methanol was evaporated, water added to the residue, and the mixture extracted with chloroform. The oil obtained on evaporation of the extract was chromatographed on alumina with chloroform as the eluant. The first fractions yielded 0.52 g (82%) of crystalline cyclized compound III, identified by comparison with a sample prepared according to the procedure of MacLean, Manske, and Marion (1). A yellow band which moved more slowly down the column yielded 0.12 g (18%) of an almost colorless oil, the infrared spectrum of which had absorption bands in the hydroxyl, cyanamide, and carbonyl regions. Reduction of this crude keto alcohol IX is described below.

A second silver acetate reaction was carried out using 0.47 g of β-cyanobromolycopodine. In this run the cyclized compound – acetate mixture was reduced with sodium borohydride and the resulting mixture separated by chromatography on alumina with chloroform as the eluant. This procedure yielded 0.26 g (72%) of the cyclized compound III and 0.09 g (23%) of compound X described below.

Reduction of β-Cyanohydroxylycopodine IX *with Sodium Borohydride*

The non-crystalline alcohol IX (0.12 g) obtained by the foregoing procedure was dissolved in 95% ethanol, sodium borohydride (0.1 g) added, and the mixture left overnight at room temperature. When the reaction mixture was worked up in the usual manner a nearly quantitative yield of a crystalline product was obtained which melted at 181–182° after recrystallization from acetone. Calc. for $C_{17}H_{28}O_2N_2$: C, 69.8; H, 9.65; N, 9.6%. Found: C, 69.9; H, 9.43; N, 8.9%.

The infrared spectrum of the compound showed a band at 3360 cm^{-1} in the hydroxyl region, cyanamide absorption at 2195 cm^{-1}, and no absorption in the carbonyl region.

Sodium Borohydride Reduction of the Alcohol Fraction from the Cyanogen Bromide Reaction

An ethanol solution containing the alcohol fractions (3.6 g) from a number of reactions of lycopodine with cyanogen bromide was added to a solution of 1.0 g of sodium borohydride in 95% ethanol. The reaction mixture was allowed to stand overnight at room temperature. The excess hydride was destroyed by the addition of formalin and the solution taken to dryness. Water was added to the residue, the mixture extracted with chloroform, and the chloroform extract washed with dilute hydrochloric acid. The non-crystalline basic material which was recovered from the acid washings weighed 0.22 g. The neutral fraction obtained on evaporation of the chloroform solution was dissolved in acetone. Concentration of the acetone solution yielded 0.31 g of a crystalline com-

pound, m.p. 193–196°, which was identical with compound XII obtained by borohydride reduction of α-cyanohydroxylycopodine.

The material recovered by evaporation of the mother liquors from the crystallization above was dissolved in chloroform and adsorbed on an alumina column. Elution with 99:1 chloroform–methanol first yielded a fraction containing 0.43 g of cyclized compound III, followed by a brown band (0.43 g) from which no crystalline compounds could be isolated. Evaporation of the next fractions yielded an additional 0.78 g of crystalline compound XII. This diol was closely followed down the column by another compound (0.22 g, m.p. 179–181°) which was found by a mixed melting point determination and comparison of infrared spectra to be identical with that obtained by sodium borohydride reduction of β-cyanohydroxylycopodine. Further elution of the column yielded only non-crystalline material of complex composition. The yields of cyclized compound III, α-cyanohydroxydihydrolycopodine XII, and β-cyanohydroxydihydrolycopodine X were 12%, 30%, and 6%, respectively.

Oppenauer Oxidation of β-Cyanohydroxydihydrolycopodine X

To 0.60 g of β-cyanohydroxydihydrolycopodine X partially dissolved in anhydrous benzene (70 ml) were added 5 ml of acetone and 1.5 g of aluminum isopropoxide. The mixture was heated under reflux for 11 hours and then poured into water. The benzene layer was separated and the aqueous phase extracted with more benzene. The crude product obtained by evaporation of the combined benzene extract was dissolved in chloroform and adsorbed on an alumina column. Evaporation of the fractions collected on elution with chloroform yielded 0.38 g of β-cyanohydroxylycopodine which melted at 123–124° after crystallization from ether – petroleum ether. Calc. for $C_{17}H_{26}O_2N_2$: C, 70.3; H, 9.03; N, 9.7%. Found: C, 69.8; H, 8.82; N, 10.0%.

The infrared spectrum showed absorption bands at 3475 cm^{-1} in the hydroxyl region, 2195 cm^{-1} in the cyanamide region, and 1685 cm^{-1} in the carbonyl region. The spectrum of a non-crystalline film of the compound was found to be identical with that of the non-crystalline alcohol obtained by hydrolysis of the product of the reaction of β-cyanobromolycopodine with silver acetate.

Elution of the column with 95:5 chloroform–methanol gave a fraction containing 0.09 g of unreacted diol.

Oxidation of β-Cyanohydroxylycopodine with Chromic Acid

A solution of 0.15 g of β-cyanohydroxylycopodine (m.p. 123–124°) in 90% acetic acid was added dropwise over 1.5 hours to a stirred solution of chromium trioxide (0.3 g) in 90% acetic acid maintained at −5 to −10°. The reaction mixture was stirred 3 hours longer, during which time the temperature rose to 0°. After the excess chromium trioxide had been destroyed by the addition of methanol, the mixture was evaporated under reduced pressure. Water was added to the residue and the mixture extracted repeatedly with chloroform. The chloroform solution was extracted with aqueous sodium bicarbonate and the bicarbonate solution acidified and extracted with chloroform. Evaporation of the chloroform yielded 0.11 g (70%) of a non-crystalline acid, whose infrared spectrum (film) showed absorption maxima at 1695 (ketone carbonyl), 1710 (acid carbonyl), and 2200 cm^{-1} (cyanamide), and absorption in the hydroxyl region.

A sample of the acid (35 mg) was converted to the methyl ester by dissolving it in methanol and treating it with an excess of an ether solution of diazomethane. After it had stood for 2 hours the solution was evaporated and the residue dissolved in chloro-

form. The chloroform solution was washed with aqueous sodium bicarbonate and then evaporated. The product crystallized readily and melted at 127–129° after recrystallization from ether – petroleum ether. Calc. for $C_{18}H_{26}O_3N_2$: C, 67.9; H, 8.23; N, 8.8%. Found: C, 67.8; H, 8.41; N, 8.9%.

The infrared spectrum of the ester showed absorption at 1700 (ketone carbonyl), 1725 (ester carbonyl), and 2210 cm^{-1} (cyanamide).

Reduction of the Acid XIII *with Sodium Borohydride*

A solution of the non-crystalline acid XIII (70 mg) in aqueous sodium bicarbonate was added to an ethanolic solution of sodium borohydride. After the reaction mixture had stood at room temperature for 2 hours, the excess hydride was destroyed by adding formalin, and the mixture evaporated. The residue was acidified with dilute hydrochloric acid and extracted with chloroform. The chloroform extract was washed with aqueous sodium bicarbonate and then evaporated to give 45 mg (68%) of a crystalline neutral compound. A small amount of starting material was recovered when the bicarbonate washings were acidified and extracted with chloroform, but no hydroxy acid was detected. Recrystallization of the neutral compound from ether yielded colorless needles, m.p. 201–203°. Calc. for $C_{17}H_{24}O_2N_2$: C, 70.8; H, 8.39; N, 9.7%. Found: C, 70.7; H, 8.52; N, 9.8%.

The infrared spectrum of the neutral compound exhibited cyanamide absorption and a single band in the carbonyl region which appeared at 1761 cm^{-1} when the spectrum was determined in carbon tetrachloride solution, and at 1743 cm^{-1} when determined in nujol mull. There was no absorption in the hydroxyl region.

ACKNOWLEDGMENTS

We wish to express our thanks to the National Research Council and the Ontario Research Foundation for financial assistance.

REFERENCES

1. MacLean, D. B., Manske, R. H. F., and Marion, L. Can. J. Research, B, **28**, 460 (1950).
2. Marion, L. and Manske, R. H. F. Can. J. Research, B, **20**, 153 (1942).
3. Barclay, L. R. C. and MacLean, D. B. Can. J. Chem. **34**, 1519 (1956).
4. Przybylska, M. and Marion, L. Can. J. Chem. **35**, 1075 (1957).
5. Wiesner, K., Valenta, Z., Ayer, W. A., Fowler, L. R., and Francis, J. E. Tetrahedron, **4**, 87 (1958).

THE CONSTITUTION OF THE SODIUM – ACID PHOSPHATE GLASSES[1, 2]

A. E. R. Westman, M. Joyce Smith, and P. A. Gartaganis

ABSTRACT

The preparation of phosphate glasses containing sodium and hydrogen is described. The over-all composition was calculated from the Na/P ratio of the starting mixture and the hydrogen content determined by a zinc oxide ignition. The chemical constitution was determined paper-chromatographically employing recent improvements in technique.

Close resemblance between the molecular weight distributions of the sodium–acid glasses and the strong phosphoric acids is shown by the results, but it is also shown that there is no sharp transition to the molecular weight distribution shown by the sodium, potassium, and lithium glasses.

The importance of stoichiometry on the constitution of glass is discussed, together with the statistical models from which several theories are derived to predict the distribution of the polymers in a glass. The theories of Van Wazer and Parks, which show the most satisfactory agreement with the experimental results, receive detailed consideration.

INTRODUCTION

Glasses with compositions in the Na_2O–H_2O–P_2O_5 system between the orthophosphate and the metaphosphate compositions were studied, in particular glasses containing both hydrogen and sodium cations. New methods of preparation involved the progressive dehydration of orthophosphate mixtures to give a series of compositions following the lines on Fig. 1. In the preliminary examination compositions on the line $T = 20$ were also studied.

The development of the separation of phosphate anions by paper chromatography has been described by Hettler (1). The latest techniques used in this laboratory, especially a

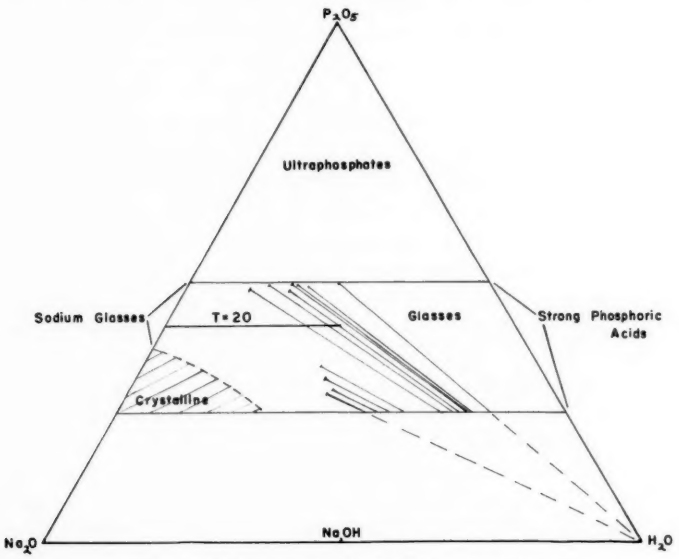

FIG. 1. Glasses in the Na_2O–H_2O–P_2O_5 system.

[1]*Manuscript received June 17, 1959.*

Contribution from the Ontario Research Foundation, 43 Queen's Park, Toronto 5, Ontario. This paper was presented at the American Chemical Society Symposium on Phosporus, Boston, April 5–10, 1959.

[2]*Published with the permission of the American Chemical Society.*

new method of quantitative estimation of phosphorus, have been described recently (2) and give greater precision and reliability.

The chromatographic separation of the condensed phosphate anions made it possible to determine the constitutions of the soluble glasses, i.e. the proportions of each chain length. The first study of the change in the size distribution with composition was carried out by Westman and Crowther (3) on the Na_2O–P_2O_5 system, the sodium glasses. However, only glasses with a number-average chain length, $\bar{n}$, higher than 3 were obtainable crystal-free. Many attempts to obtain clear sodium glasses of lower $\bar{n}$ have not yet yielded satisfactory results, although experiments are still in progress, notably with the through-flame apparatus originally devised by Haller (4). Secondly, the system H_2O–P_2O_5, the strong phosphoric acids, was studied by Huhti and Gartaganis (5) and also by Thilo and Sauer (6) and Ohashi and Sugatani (7). Some modification of techniques was necessary because these compositions give rise to hygroscopic, syrupy liquids at room temperatures. Certain significant differences were observed between the distributions obtained for the sodium glasses and the acids from these two studies, the principal being the absence of orthophosphate in sodium glasses and the existence of "free-water" in the acids. Two further investigations into the effect of the cation on distribution were begun. The distributions obtained from glasses containing lithium and potassium as cations have already been published (8). They were similar to those of the original sodium glasses, no orthophosphate being detected; however there were differences too large to be ascribed to experimental error alone. The object of the present study was to obtain the distribution patterns of glasses having a sodium–hydrogen ratio of unity, and to determine the effect of the substitution of sodium by hydrogen at one particular cation to phosphorus ratio.

EXPERIMENTAL

Preliminary Works

Attempts to prepare sodium–acid glasses with Na/H = 1 by heating phosphorus pentoxide with sodium hydrogen pyrophosphate in a sealed pyrex flask, as in the case of the strong phosphoric acids, were unsuccessful and dangerous because the pyrex, leached by the phosphate, became brittle and exploded. "Vycor" brand, 96% silica glass was found to be resistant to attack and so small tubes of Vycor were prepared as containers.

Starting materials consisted of $Na_2H_2P_2O_7$ and either P_2O_5 or an equimolecular mixture of Na_2HPO_4 and NaH_2PO_4. (The $Na_2H_2P_2O_7$, Na_2HPO_4, and NaH_2PO_4 were previously dried at 110° C.) The mixtures were homogenized by vigorous shaking, a portion was sealed in a Vycor tube and placed in a furnace at 650° or 800° C. A clear liquid was obtained in 10 minutes. The tube was carefully removed (the worker wearing protective shields) and plunged horizontally into a bath of water. When cool the tube was broken open and a sample of the glass was dissolved in alkaline solution and chromatographed. Tubes were processed singly due to the frequency of explosion, both in the furnace and on quenching.

Despite the difficulties, data were obtained for a range of number-average chain lengths, $\bar{n}$ = 1.1 to 9.0. These were communicated to Van Wazer and Parks to illustrate their distribution theory and were published by them as preliminary values (9). In this laboratory, publication of the detailed results was delayed because an error was detected in the preparation. When the number of molecules per 100 atoms of phosphorus indicated by the chromatographic analysis, "N", was compared with the number derived from the cation to phosphorus ratio of the starting material, the agreement was found to be unsatisfactory at high cation–phosphorus ratios. Appreciable quantities of water had

escaped from the liquid phase and, on quenching, condensed on the upper portion of the tube, leaving the bulk of glass poor in hydrogen and with a correspondingly increased average chain length. This was confirmed by experiment showing that packing the tubes as fully as possible lowered the average chain length again and that the surface layer of the glass with adsorbed water had a very different constitution from the bulk of the glass. The techniques adopted to avoid this error are described later.

The glass prepared by the earlier technique with an average chain length $\bar{n} = 5$ was sufficiently defined to be used in admixture with a sodium glass $\bar{n} = 5$ to examine the effect of a change in cation. The mixtures were melted quickly in a platinum crucible over a burner and quenched between copper blocks. No general increase in average chain length was detected.

Final Preparation of Glasses

Efforts were made to avoid the unknown composition change due to loss of water to the vapor phase. A lowering of the temperature required to give a clear melt was sought in an alternative starting mixture including sodium – acid tetrametaphosphate (10) but no significant improvement in results was observed. Finally, a method was adopted whereby the composition (%) with respect to hydrogen was determined after the glass was made by ignition with zinc oxide. The standard deviation of this determination was 0.12.

Glasses of number-average chain length greater than three were obtained by quenching between copper blocks, at 1-minute intervals, the liquids resulting from melting and partially dehydrating certain mixtures of pure monobasic sodium orthophosphate and standard orthophosphoric acid (85.454%) in a platinum crucible over a Meeker burner. Usually six glasses of decreasing water content resulted from one starting mixture. A second series covering a smaller range of compositions, due to shorter intervals of dehydration, permitted glasses to be obtained with Na/H near unity. Most were clear, brittle, crystal-free glasses, but if insufficient water was removed, very viscous liquids similar to the strong phosphoric acids resulted. The end of a dehydration series was controlled by the formation of fibrous "hypoly" material, as the metaphosphate composition was approached. This appeared crystalline under the petrographic microscope and would not remelt.

The chemical constitution of each glass was determined by dissolving a few fragments in sodium bicarbonate solution maintaining the pH at approximately 8, separating the various molecular species on a filter paper chromatogram, and analyzing by the new technique (2). By adding the other fragments to a weighed, fired crucible containing zinc oxide (approx. 2 g), the water content (in %) was determined from the loss in weight from firing at 550° C for 1 hour.

Glasses having a sodium to phosphorus ratio greater than .83 (i.e. $\bar{n} = 3$ when Na = H) required a starting mixture of mono- and di-basic orthophosphates without orthophosphoric acid. These mixtures lost almost all of their water content before melting. Glasses of these compositions were obtained, however, by returning to a sealed Vycor-tube technique. Mixtures of the correct sodium to phosphorus ratio, but rich in water content (i.e. using $NaH_2PO_4.H_2O$ crystals in part), were sealed into Vycor tubes and heated to 350° C for about one hour. The liquid was homogenized by rolling the tube over the floor of the furnace (with all due precautions) and then removed vertically and allowed to cool to room temperature. The coefficients of expansion of the Vycor and the phosphate glass were sufficiently different to allow the phosphate lump to be lifted cleanly away from the fractured Vycor tube. Carefully avoiding the upper surface layer and possible absorbed water, we chromatographed part of the lump and ignited part to determine the water

content and thus the composition of the bulk of the phosphate glass. Again, a series of varying composition was obtained by varying the proportion of hydrated and anhydrous NaH_2PO_4; slight variations were also effected by using tubes of various lengths and different temperatures of melting, both of the latter influencing the proportion of the water existing in the vapor phase.

DATA

The constitution of some 150 glasses with compositions located along the solid lines in Fig. 1 were obtained. For these glasses it was found that the Na/H ratio had little effect on the observed constitutions so all of the results, including those for Na = H, could be represented adequately by the curves in Fig. 2 (11). The abscissa "T" is defined by

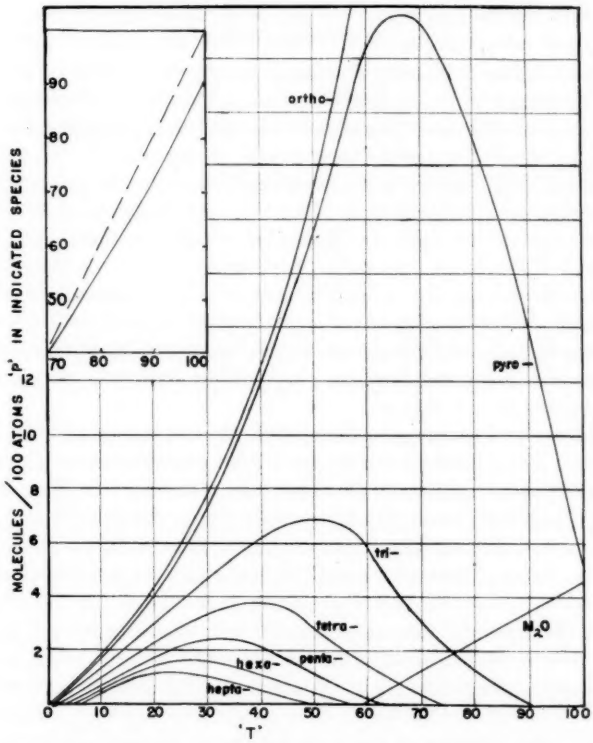

FIG. 2. The variation of distributions with T for the sodium–acid glasses. Inset: solid line, extension of orthophosphate curve; broken line, orthophosphate proportion in a system containing only ortho- and pyro-fractions.

$T = 50(M/P-1)$ where M/P is the cation to phosphorus atomic ratio (see also Stoichiometry later), "T" therefore represents the number of molecules per 100 phosphorus atoms for the particular composition. The ordinate indicates the number of molecules appearing in each fraction for a total of 100 atoms of phosphorus. The value of "T" for each glass was calculated from its water content using the following equation:

[1] $$T = 100/\bar{n} = 50\,(x+w(ax+b)/(1-w)-1)$$

where w = % water content/100, $a = Na_2O/H_2O = 3.440$, $b = P_2O_5/H_2O = 7.885$, and x = molecular ratio $Na_2O:P_2O_5$. The curve marked "M_2O", i.e. "free water or sodium hydroxide" in Fig. 2 is derived from the difference between "T" and "N", the latter being the total of the molecules observed in the chromatographic analysis per 100 atoms of phosphorus, i.e. those molecules not detected chromatographically, "hypoly" being negligible. At smaller values of "T" the number-average chain length of the hypoly material can be deduced from $T-N$. A check on the methods of preparation and chromatographic analyses is provided when both M_2O and "hypoly" are negligible.

DISCUSSION

Qualitative Comparisons

The distributions observed in Fig. 2 are similar to those of the strong phosphoric acids in that free M_2O and orthophosphate are present; the latter does not occur in the sodium glasses. When only ortho- and pyro-phosphate are present their proportion is fixed as indicated by the broken line in the insert on Fig. 2, but the experimental points for both the sodium–acid glasses and the strong phosphoric acids tend to follow the lower solid line. This was explained by Huhti and Gartaganis (5) in the case of the acids by assuming "free water" to exist in equilibrium with the phosphoric acids. Their auxiliary experiments and those of other workers (6, 7) confirmed this explanation. In the case of the sodium–acid glasses, free M_2O may again explain the points below the theoretical line. However, it was difficult to prepare bubble-free glasses in this region and it was possible for moisture trapped in the bubbles to result in a higher value of T. This was borne out when the deliberate analysis of specimens containing some bubbles showed values for % total phosphorus as orthophosphate, approximately 5% lower than the samples without bubbles indicated by the solid line in the inset on Fig. 2. More experiments, possibly with other techniques, are needed in this region.

A closer comparison of the curves in Fig. 2 with the corresponding curves for the strong acids and the alkali metal glasses revealed the following differences:

(*a*) The orthophosphate content of the acid glasses was greater than that of either the strong acids or the sodium glasses, the latter being zero. The preliminary experiments at $\bar{n} = 5$ described above showed that as hydrogen replaced sodium as cation, the orthophosphate content of the glasses increased *gradually* to a very flat maximum or plateau over the acid glass compositions before dropping very slightly at the strong phosphoric acid composition. Thus, there was no particular arrangement of hydrogen and sodium atoms necessary for the development of orthophosphate.

(*b*) The maximum in the curve for pyrophosphate in Fig. 2 is to the right of that for the strong acids.

(*c*) The sodium–acid glasses and the acids had much higher hypoly contents than the sodium glasses. At low values of T the sodium–acid glasses contained less hypoly than the acids; at high T values, more hypoly; the hypoly contents being the same at about $T = 20$.

(*d*) Free water occurred in much the same mole percentages and over the same range of T in both the acid glasses and acids.

(*e*) The ring phosphates found in the alkali metal glasses were not found in either the acids or the sodium–acid glasses studied. Studies of compositions closer to the left side of Fig. 1 are indicated.

Some of the above comparisons are seen later in Fig. 4 where the agreement between theoretical and experimental results is shown for three of the fractions.

Phase Relations

Morey (12) investigated phase relations in sealed tubes for systems with compositions along a line in Fig. 1 from H_2O to $NaPO_3$. A comparison with the data of this paper is of interest in connection with the much discussed question of the relation of glass constitution to the constitution of the primary phase. The molecules, or molecule-ions, that form the primary phase may exist as such in the glass or may be formed from smaller units as the crystal grows. There is evidence for the first of these possibilities in this case. The cyclic trimetaphosphate crystals (Morey's $NaPO_3I$) grow in glasses containing trimetaphosphate rings near the $NaPO_3$ composition.

STOICHIOMETRY

For a particular cation or combination of cations M, the chromatographic analysis of a properly fused and quenched glass depends solely on the M/P atomic ratio of that glass. This means that stoichiometry is an important factor in determining the constitution of a glass.

Stoichiometric ideas can be introduced in several ways. The method developed in papers from this laboratory starts from the number-average chain length. Other approaches include that of Stevels (13) and Van Wazer and Parks (9).

Number-average Chain Length

If only polymers of the general formula $M_{n+2}P_nO_{3n+1}$ are involved, then the number-average chain length, $\bar{n}$, is related to the M/P atomic ratio by the equation

$$\bar{n} = 2/(M/P-1) \qquad [2]$$

where M and P stand for corresponding numbers of cation and phosphorus atoms respectively. If for a particular $\bar{n}$, we consider 100 phosphorus atoms, then on stoichiometric grounds alone the constitution might be such that all the polymers had the same formula $MO_{\frac{1}{2}}.(MPO_3)_{\bar{n}}.O_{\frac{1}{2}}M$ and there would be $100/\bar{n}$ such polymers. The MPO_3 units, 100 in all, could then be distributed in other ways among the $100/\bar{n}$ polymers. The number of polymers per 100 phosphorus atoms remains the same, depending only on $\bar{n}$, and being given by [1] above.

When ring compounds are formed, the number of linear polymers per 100 phosphorus atoms is unchanged, but there are fewer MPO_3 groups to distribute among them. A single long linear polymer can also rearrange according to equation [5] (following) to form a branched or cross-linked polymer with the same M/P ratio and without altering the above empirical formula so long as the "length" of the new polymer is defined by the number of phosphorus atoms it contains. However, when branching or cross-linking is accompanied by an increase in molecular weight, as when two polymers go together to form the new polymer, splitting off M_2O, then the M/P ratio of the polymer decreases.

When the M/P atomic ratio = 1 the number-average chain length becomes infinite (equation [2]). For M/P atomic ratios < 1, branching or cross-linking accompanied by higher molecular weights, postulated by Van Wazer, creates "ultraphosphates" (14). As the M/P ratio is reduced through unity a sharp change from finite linear polymers to infinite (wall-to-wall) polymers, or cross-linked structures, is unlikely. In the experimental

data for glasses just below the metaphosphate line there is some indication of branched or cross-linked material.

Bridging and Non-bridging Oxygens

A number of glass technologists, notably Stevels (13), introduce stoichiometric ideas into the discussion of silicate glasses by distinguishing between bridging and non-bridging oxygens.

Stevels defines the number of non-bridging oxygens per silicon atom, X, and the number of bridging oxygens per silicon atom, Y, as follows:

$$X = 2(O/Si) - 4 \quad [3]$$

$$Y = 8 - 2(O/Si) \quad [4]$$

where the symbols O and Si stand for numbers of atoms of oxygen and silicon respectively and $X + Y = 4$.

Criteria for finite chains, infinite chains, and cross-linked structures are then given in terms of Y, as $O < Y < 2$, $Y = 2$, and $Y > 2$ respectively. The silicate glasses of commerce have values of Y from 3 to 3.4. Glasses can be made in the laboratory having Y values between 3 and 2 and, by special means, below 2.

When this approach is applied to phosphate glasses it is found to be algebraically equivalent to the methods just given, except that there is no provision for unreacted M_2O or rings. A phosphorus–oxygen tetrahedron is only capable of bonding to three other tetrahedra and cannot form a three-dimensional network, as do the SiO_4 tetrahedra. In its usual crystalline modification P_4O_{10} consists of isolated cage structures each built of four PO_4 tetrahedra. In other forms sheets of PO_4 tetrahedra occur but no three-dimensional networks. Thus, it is interesting to note: (*a*) that the silicate glasses of commerce on this basis have a more cross-linked structure than even P_2O_5 in the phosphate series; (*b*) that bonding a cation to a SiO_4 tetrahedron renders it equivalent to a PO_4 tetrahedron, i.e. NaSi may substitute for P; and (*c*) that, using Stevels' equations [3] and [4], the phosphate glasses with which this paper is concerned are in the range of $O < Y < 2$ or very much below the commercial silicate glasses. Each of these comments is illustrated in Table I.

TABLE I

Stoichiometric comparison of silicate and phosphate compositions

Composition of silicate	X	Y	O/Si or O/P ratio	Composition of phosphate
SiO_2	0	4	2	
$Na_2Si_2O_5$	1	3	2.5	P_2O_5
Na_2SiO_3	2	2	3	$NaPO_3$
	3	1	3.5	$Na_4P_2O_7$
	4	0	4	Na_3PO_4

Parks–Van Wazer Approach

Parks and Van Wazer (9) define chemical groups to which chemical symbols and names are assigned as follows:

Symbol	Name	Symbol	Name
o = M_3PO_4	Ortho group	**b** = $PO_{2.5}$	Branching group
e = $M_2PO_{3.5}$	End group	**u** = MOM	Unreacted M_2O
m = MPO_3	Middle group	(**2e**) = $M_4P_2O_7$	Pyro group

They also define R as the M/P ratio.

All polymers and molecules envisaged in a glass may be constructed from these building units and are subject to the chemical equations

[5] $$2\mathbf{m} = \mathbf{b}+\mathbf{e}$$

[6] $$2\mathbf{e} = \mathbf{m}+\mathbf{o}$$

[7] $$2\mathbf{o} = 2\mathbf{e}+\mathbf{u}$$

or

[8] $$2\mathbf{o} = (\mathbf{2e})+\mathbf{u}.$$

The compound $\mathbf{u} = M_2O$ is not considered to break down further.

Equilibrium constants designated K_1, K_2, K_3, and K'_3 are written for equations [5], [6], [7], and [8] respectively in terms of mole fractions represented by the corresponding italicized letters. This approach is proving very useful for classifying a wide variety of polymer systems. The choice of the constants K_1, K_2, K_3, K'_3 to fit the experimental results as closely as possible permits deductions concerning the degree of ionization of the cations. Conversely, if previous assumptions regarding ionization are made, the change in ortho and unreacted units with composition (M/P) is forecast. In general the shapes of the curves obtained by calculation agree well with the experimental results. This is clearly shown in Fig. 3 where the solid lines indicate the experimental data for the acid glasses and the broken lines the curves derived from the selection of the constants as $K_1 = 0$, $K_2 = 0.08$, and $K_3 = 0.02$. However, no choice of K values will bring the maximum for ends anywhere but at $R = 2$, which does not agree with the experimental data. One must assume in this case that the K values change slightly with composition.

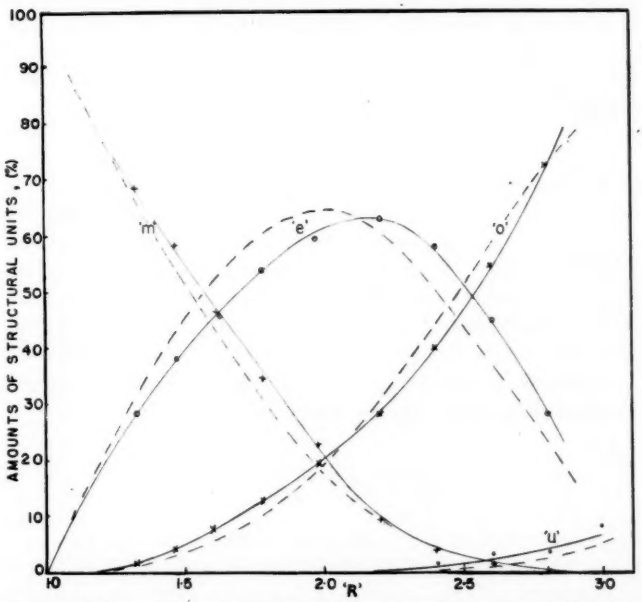

FIG. 3. Comparison of theoretical and experimental amounts of structural units ('*m*', middles; '*e*', ends; '*o*', ortho; '*u*', unreacted M_2O). (Theoretical curves (broken lines) obtained using $K_1 = 0$, $K_2 = 0.08$, and $K_3 = 0.02$.)

Distribution Theories

Since knowledge of the structural units present and their proportions does not define the distribution of polymers to be expected in a glass, various statistical models have been proposed. Van Wazer has discussed a Poisson model; a random reorganization model, based on a flexible chain theory; and, with Parks, a rigid-rod model (9).

The Poisson model has been shown to fit only a limited range of compositions and does not fit the data given in this paper so it will not be discussed further.

It is also possible to invoke mass law theory, which is essentially statistical in origin. This was applied to the chromatographic data for the strong phosphoric acids (5).

Mass Law Theory

This can be applied in as many ways since one can write chemical equations purporting to govern the dynamic equilibrium occurring in the molten glass, or liquid state, etc. In the paper cited, the equilibrium between water, pyrophosphoric acid, and orthophosphoric acid was considered. Thus, unreacted M_2O, i.e. water, was the common factor. This could have been extended to the higher acids present but two difficulties are encountered: (*a*) the number of equilibrium constants involved becomes very large and (*b*) the data required to confirm their validity would have to be very comprehensive and accurate. This is one reason why Van Wazer and Parks worked with structural units, since five or six such units suffice for all polymers.

An alternative method would be to regard orthophosphate as a common factor in all the equilibria since, whatever the mechanism, the polymers gain or lose PO_4 tetrahedra in maintaining an equilibrium. This method has possibilities in the low molecular weight acid glasses and acids, but suffers the two disadvantages already given for the mass law approach and, in addition, when dealing with the non-acid glasses, the difficulty arises that charge density considerations suppress the formation of orthophosphate, as explained by Van Wazer (9). On the other hand, hydrolysis studies indicate that linear phosphate polymers tend to degrade by splitting orthophosphate groups off the end so this approach would have the benefit of starting from chemical knowledge of the polymer properties. One could only hope for some empirical relation relating the equilibrium or other constants with chain length.

Van Wazer–Parks Distributions

Another approach, followed by Van Wazer–Parks, is to set up a statistical model, being guided more or less by the known properties of phosphates and the nature of the distributions to be fitted. They used the results for the strong acids (5) and the authors' preliminary results for the sodium-acid glasses and showed that with some smoothing of the data, a reasonable fit could be obtained using the flexible chain model but not the rigid-rod model. Since the preliminary data do not differ markedly from the more reliable data reported here, a theoretical distribution based on the flexible chain model in the limiting case where there is no branching was computed from

$$[9] \qquad w_n = \frac{n}{\bar{n}(\bar{n}-1)}\left(\frac{\bar{n}-2}{\bar{n}-1}\right)^{n-2}\left(1-\frac{o}{1-u}\right)$$

where n = the chain length of a polymer; w_n = the weight fraction of the total phosphorus in polymers of length n; and $\bar{n}$ = the number-average chain length of the glass, computed by including only the polymers having $n \geqslant 2$. Allowance is made in the equation [9] for "o" and "u", the mole fractions of orthophosphate and unreacted M_2O,

which are not considered to be polymers but diluents. Their proportion was predicted by the selection of K_1, K_2, and K_3 as shown in Fig. 3.

The comparisons afforded by Table II show that the Van Wazer–Parks distribution (9) fits the observed values remarkably well, considering that the probabilities are introduced from very general physical ideas. The individual chemical properties of the polymers are most likely to influence the system which contains only a few species, especially when these exhibit the striking differences associated with the first members of a homologous series. Thus the ability of statistical models to fit the high molecular weight contributions but not the low ones is understandable. The slight differences between sodium, potassium, and lithium glasses can similarly be attributed to chemical influences.

If the distribution for $T = 10$ is plotted in terms of molecules, it will be seen that, although the number-average chain length is 10, the maximum is still at $n = 2$. Most statistical models result in distributions in which the mode moves away from the origin quickly as the mean is increased.

It will be noted that the observed values for $T = 20$ and $T = 10$ in Table II are practically constant for $n = 2$ or greater. If this holds for the hypoly fraction, it indicates a very flat and long distribution above $n = 7$ which accentuates the difficulty just mentioned.

In Fig. 4 the agreement between distributions derived from the flexible chain model and the results of both the acid – sodium phosphate glasses and the strong phosphoric acids has been indicated in the case of pyro-, tri-, and hypoly-phosphate. Clearly the distributions in the sodium glass system require a modified theory such as that provided by the rigid-rod model.

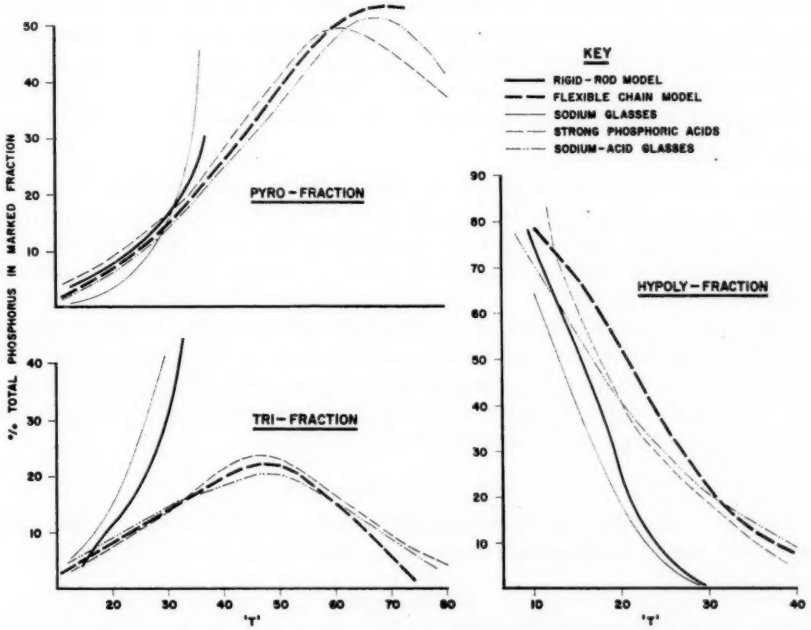

FIG. 4. Comparison of the theoretical and experimental distributions.

TABLE II

Sodium–acid glasses
(Comparisons of experimental and theoretical distributions)

		Ortho	Pyro		Tri		Tetra		Penta		Hexa		Hepta		Hypoly	
T	*u*	*E**	*E*	[9]	*E*	[9]	*E*	[9]	*E*	[9]	*E*	[9]	*E*	[9]	*E*	[9]
90	3.5	72.4	28.0		0.3											
80	2.9	54.5	42.3		4.1											
70	1.4	39.8	50.6	52.9	9.5	6.5	1.4	0.7								
60		28.3	48.4	50.3	17.2	15.6	5.4	4.3	1.1	1.1		0.3				
50		19.5	35.2	37.2	20.6	21.8	11.2	11.3	5.9	5.5	3.1	2.6	0.8	1.2	3.8	0.9
40		12.7	24.0	24.8	18.6	20.3	15.2	14.8	10.0	10.0	7.2	6.6	3.8	4.2	9.2	6.6
30		7.8	14.9	14.1	14.1	14.4	13.7	13.1	11.7	11.2	9.6	9.2	7.7	7.3	20.8	22.9
20		3.9	8.9	6.5	9.0	7.8	8.8	8.3	9.0	8.3	9.0	7.9	8.4	7.4	43.0	49.9
10		1.5	3.4	1.6	4.2	2.2	3.8	2.6	4.1	3.0	4.2	3.2	3.5	3.4	73.5	82.5

*E, experimental values; [9], values calculated from eq. [9].

CONCLUSIONS

Change of Cation

From the discussion of the experimental results in the first part of this paper, it will be evident that a distribution theory which fits the strong acids will give a reasonable fit for glass compositions in the Na_2O–P_2O_5–H_2O diagram, Fig. 2, as far as the center line where Na/H atomic ratio = 1. At higher ratios the effect of the smooth reduction of both orthophosphate and hypoly will have to be taken into account. Also, it has been shown that a shift of cation to K or Li makes a significant but small change in the nature of the distributions.

The postulation of statistical models, however, has served a useful purpose. While not always fitting the data within the experimental error, the fit has been good enough to support the general thesis that some sort of reorganization governed largely by chance encounters is taking place in a molten phosphate glass, that the equilibrium can be frozen in by quick quenching, and that it governs the distributions observed by means of filter paper chromatography as well as by the physical methods used by Van Wazer.

Statistical Models

More than one statistical model plus certain stoichiometrical conditions derived from experiment are necessary in general to give a good fit to the observed molecular weight distributions. However, the most general conclusion is that, despite the differences which have been pointed out, the distributions of molecular weight are much the same over a considerable range of cations.

The relations of the constitution of the phosphate glasses to that of the silicate glasses will be better understood when more work has been done on the silicate glasses having a higher M/Si atomic ratio and on the phosphate glasses with a lower M/P ratio.

More work on the physical properties of the phosphate glasses whose constitution has been established appears to be a logical development.

ACKNOWLEDGMENTS

The authors wish to express their gratitude to Anne Mueller for her careful technical assistance and also to the Research Corporation, New York, for their support.

REFERENCES

1. HETTLER, H. J. Chromatog. **1**, 389 (1958).
2. SMITH, M. J. Anal. Chem. **31**, 1023 (1959).

3. WESTMAN, A. E. R. and CROWTHER, J. J. Am. Ceram. Soc. **37**, 420 (1954).
4. LANDIS, B. M. M.Sc. Thesis presented to the University of Toledo, Toledo, Ohio. 1956. (Work supervised by W. Haller.)
5. HUHTI, A.-L. and GARTAGANIS, P. A. Can. J. Chem. **34**, 785 (1956).
6. THILO, E. and SAUER, R. J. prakt. Chem. **4**, 324 (1957).
7. OHASHI, S. and SUGATANI, H. Bull. Chem. Soc. Japan, **30**, 864 (1957).
8. WESTMAN, A. E. R. and GARTAGANIS, P. A. J. Am. Ceram. Soc. **40**, 293 (1957).
9. (*a*) VAN WAZER, J. R. and PARKS, J. R. J. Am Chem. Soc. **79**, 4890 (1957).
(*b*) VAN WAZER, J. R. Phosphorus and its compounds. Vol. I. Interscience Publishers, Inc., New York. 1958.
10. GRIFFITH, E. J. J. Am. Chem. Soc. **73**, 3867 (1956).
11. SMITH, M. J. M.Sc. Thesis presented to the University of Birmingham, Birmingham, England. 1959. (Now available from University Microfilm Center, Ann Arbor, Michigan.)
12. MOREY, G. W. J. Am. Chem. Soc. **75**, 5794 (1953).
13. STEVELS, J. M. Glass Ind. **35**, 657 (1954).
14. VAN WAZER, J. R. and GRIFFITH, E. J. J. Am. Chem. Soc. **77**, 6140 (1955).

THE PREPARATION OF D-RIBOSE-1-C^{14}, D-ARABINOSE-1-C^{14}, AND D-2-DEOXYRIBOSE-1-C^{14} [1]

D. H. MURRAY AND G. C. BUTLER

ABSTRACT

D-Ribose-1-C^{14} and D-arabinose-1-C^{14} have been synthesized by a modified Sowden–Fischer procedure in which the mixed sodium nitropentitols resulting from the condensation of erythrose and $C^{14}H_3NO_2$ have been submitted to a Nef reaction. The epimeric labelled pentoses were isolated by cellulose column chromatography in an over-all radiochemical yield of 19%.

Mixed nitropentitols-1-C^{14} have been acetylated, partially deacetylated with sodium bicarbonate in a non-polar solvent, and hydrogenated to yield triacetoxy-1-nitropentane-1-C^{14}. The mixture of this material and the accompanying undeacetylated nitropentitols gave rise, via a Nef reaction, to D-2-deoxyribose-1-C^{14} (6.3%), D-ribose-1-C^{14} (3.1%), and D-arabinose-1-C^{14} (2.9%).

INTRODUCTION

The Fischer cyanhydrin (1–4) and the Sowden–Fischer (5, 6, 7) methods of lengthening an aldose chain have both been employed in the preparation of labelled aldoses. The cyanhydrin procedure has generally afforded better radiochemical yields of the desired aldoses but is somewhat tedious. Most of the procedures reported to date employing either method have involved separation of epimeric compounds at an early stage, thus necessitating twice the manipulation of labelled compounds. It is more convenient to carry isomeric materials through one series of reactions and to separate them at a terminal stage. Chromatography on cellulose columns (8) constitutes a convenient method for achieving such separation on a preparative scale.

Rappoport and Hassid (6) have employed a Sowden–Fischer procedure and cellulose column chromatography in preparing L-arabinose-1-C^{14}. Although the yield of labelled pentose reported was only 3% based on the starting C^{14}-nitromethane, the simplicity of the method was attractive. The Sowden–Fischer method has also been adapted to the preparation of deoxyaldoses, and it thus appeared possible that it might be employed for the preparation of the two sugars of nucleic acids, D-ribose and D-2-deoxyribose in Cl-labelled form. Figure 1 shows the routes followed.

D-*Ribose-1*-C^{14} *and* D-*Arabinose-1*-C^{14}

D-Erythrose was condensed with an equimolecular amount of C^{14}-nitromethane in sodium methoxide solution. The mixed sodium nitropentitols formed were submitted to a Nef reaction according to the reaction conditions employed by Mahler (5), with two modifications. First, because of the ready decomposition of sodium nitroalditols in aqueous solutions, the alkaline solution of mixed sodium nitropentitols was added to concentrated acid from a jacketed funnel maintained at 0°. Second, it was to be expected that toward the end of the addition the dilution which had occurred would reduce the concentration of acid to a point where the Nef reaction would not take place. To avoid this possibility, the sodium nitropentitols were dissolved in a minimal volume of ice water and added to a larger amount of concentrated acid than that reported by Sowden (9). The pentoses formed were separated using a cellulose column and aqueous acetone as eluting solvent. The yield of pentose-1-C^{14} based on C^{14}-nitromethane was 19%.

[1] *Manuscript received June 26, 1959.*
Contribution from the Department of Biochemistry, University of Toronto, Toronto, Ontario.

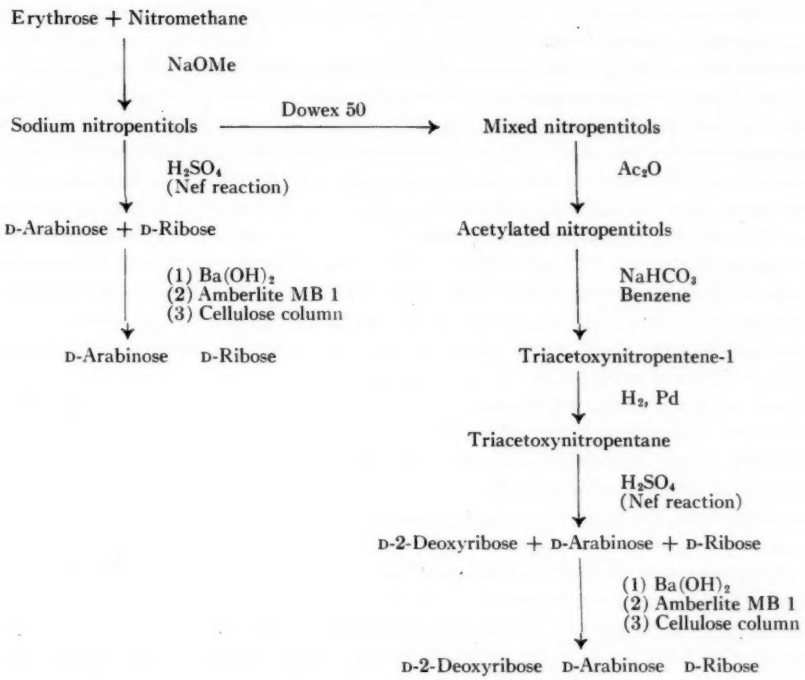

FIG. 1. Scheme of synthesis for labelled pentoses.

A fast-running radioactive fraction containing a small amount of tetrose-1-C^{14} (10) was eluted from the column ahead of the ribose-1-C^{14}. When excess nitromethane was employed in preliminary non-radioactive experiments, a similar small fraction was regularly observed but yields of pentose up to 65% were obtained. With the smaller amounts of C^{14}-nitromethane a reduction in the yield of pentose-1-C^{14} occurred. The reasons for this are discussed in a separate communication (10).

D-*2-Deoxyribose-1*-C^{14}

There seemed to be three potentially feasible routes to deoxyribose-1-C^{14}. Application of a Fischer glycal method (11) starting from D-arabinose-1-C^{14} (1), or a Ruff degradation of the metasaccharinic acids (12) resulting from the alkaline isomerization of D-glucose-2-C^{14} (13) would produce the desired labelled sugar. Both these routes, however, could be anticipated to give low radiochemical yields. On first consideration a Sowden–Fischer procedure starting from erythrose and nitromethane seemed equally unpromising. Although Sowden has prepared D-2-deoxyribose in over-all yield of 21% based on the starting erythrose (14), other workers have obtained less than 1% yields of the deoxy sugar by this route (15). On further examination it appeared that Sowden (9) adequately explained the reasons for this low yield and we therefore undertook the preparation of D-2-deoxyribose-1-C^{14} by his method.

In most cases the erythrose used for the preparation of ribose and arabinose was obtained from 4,6-ethylidene glucose. As discussed elsewhere (10), use of this material in the preparation of the deoxyribose may result in a small but significant contamination

of the desired deoxy sugar. By employing benzylidene sorbitol as the source of erythrose this contamination could be avoided.

Erythrose was condensed with an equimolecular amount of C^{14}-nitromethane to yield a mixture of epimeric C-nitropentitols which, after acetylation and subsequent treatment with bicarbonate in a non-polar solvent, gave rise to an acetylated nitroölefin. Partial hydrogenation of this material afforded the 1-nitro-1,2-deoxy-3,4,5-triacetoxypentane.

The intermediate compounds in the above procedure are crystallizable with difficulty (15). However, Sowden has shown (7) that acceptable yields of deoxyribose are attainable without separation of intermediates. Moreover, in the interest of best utilization of carbon-14, advantage was taken of the fact that nitropentitols which were not acetylated, as well as acetylated nitropentitols which were not deacetylated (and would not therefore be available for hydrogenation), would both give rise, via the Nef reaction, to ribose-1-C^{14} and arabinose-1-C^{14}, and the whole preparative procedure could be made to yield these two pentoses in addition to deoxyribose-1-C^{14}.

The total product of the hydrogenation step, in alkaline solution, was submitted to a Nef reaction. After deionization the mixture of pentoses was separated on a cellulose column using aqueous acetone. A radiochemical yield of 12% of pentoses based on nitromethane was obtained.

As in the synthesis of ribose-1-C^{14} and arabinose-1-C^{14} a fast-running fraction carrying significant radioactivity was observed. This was concluded to be 2-deoxytetrose-1-C^{14}, for reasons given in a separate communication (10). As for the ribose–arabinose case, the reactions leading to this by-product, when equimolecular amounts of erythrose and C^{14}-nitromethane were used in the initial condensation reaction, led to a considerable reduction in the yield of deoxyribose-1-C^{14}. In pilot experiments employing excess non-radioactive nitromethane, yields of about 30% of deoxyribose based on the starting erythrose were obtained.

EXPERIMENTAL

D-*Ribose and* D-*Arabinose-1*-C^{14}

D-Erythrose was prepared from 4,6-ethylidene-D-glucose (m.p. 181–183°) by the procedure described for L-erythrose (6). C^{14}-Nitromethane was obtained from Merck and Company, Montreal, and had a specific activity of about 4 mc per g.

Sodium Nitropentitols-1-C^{14}

A sodium methoxide solution (2.4 g of sodium in 50 ml of absolute methanol) was added dropwise, with stirring, to a solution of erythrose (8.3 g) and C^{14}-nitromethane (3.7 ml) in 50 ml of methanol. After 2 hours the reaction mixture was cooled to 0–10° in an ice bath. The cooled mixture was stirred for a further 12 hours, 100 ml of cold anhydrous ether added, and the precipitated sodium nitropentitols collected by filtration. They were washed on the filter with cold methanol – ether (1:1) and ether – petroleum ether (1:1). While still moist the sodium salts were transferred rapidly to a vacuum desiccator containing P_2O_5, which was then evacuated until all solvent had been removed. The yield of dry sodium nitropentitols was 8.28 g (60% based on nitromethane).

Nef Reaction

A solution of the sodium nitropentitols (2.5 g in 15 ml of ice water) was added dropwise, over a 2-hour period, from a cold (0–5°) jacketed dropping funnel to a cold (−20 to −18°) stirred solution of 6 ml of concentrated sulphuric acid and 7.5 ml of water. After the addition was complete, the stirred reaction mixture was allowed to approach 0° slowly over a period of 1 hour.

Deionization and Separation of Pentoses

The resulting solution was diluted by slow addition of 200 ml of ice water and adjusted to pH 4.0 with cold barium hydroxide solution. A few drops of glacial acetic acid were added; the barium sulphate was removed by centrifugation and washed eight times with water. The combined supernatant and washings were concentrated to a small volume at a temperature below 35°, charcoaled, and passed, under suction, through a column of 40 g of Amberlite-MB 1. The column was washed with 200 ml of water, and 0.1 *M* sodium sulphate was passed through the resin until the first faint positive test of sulphate was obtained in the eluate. A few milligrams of resin were added to the eluate, stirred, and removed by filtration. After concentration at reduced pressure (below 35° C), powdered cellulose was added and concentration continued to dryness. To remove the last traces of water, alcohol, and subsequently acetone, were added and removed under reduced pressure. The dry cellulose powder (on which the C^{14}-pentoses were absorbed) was washed with dry acetone on to a cellulose column (5 cm by 50 cm) through which absolute acetone had been passed for 4–6 hours. A pad of filter paper was placed above the cellulose and pressed down firmly. The column was developed with 98% acetone until the fast-running fractions were eluted. Ribose was eluted with 93% acetone and arabinose with 80% acetone. A 40-minute collection time and a flow rate of about 1 ml per minute were used throughout. Pentose was located in the eluate with orcinol reagent (16).

The ribose-containing fractions were combined and concentrated to a syrup at reduced pressure. Alcohol was added and distilled at reduced pressure, twice, to remove the last traces of acetone. The syrup was dissolved in water, charcoaled, and passed through a bacterial filter. The arabinose-containing fractions were combined and treated similarly. No attempt was made to crystallize the pentoses since it was convenient to use aqueous solutions directly in biological experiments. Aliquots of the solutions were taken for determination of pentose and of radioactivity. The pentoses were identified by orcinol reactions and paper strip chromatography with the appropriate authentic samples as markers.

The yields of labelled pentose were: D-ribose-1-C^{14}, 300 mg, 17,400 counts/min mg; D-arabinose-1-C^{14}, 297 mg, 18,100 counts/min mg. The total yield of C^{14}-pentose was 19.1% based on nitromethane.

D-*2-Deoxyribose-1*-C^{14}

D-*Erythrose*

Twenty grams of β-benzyl-4,6-benzylidene-D-glucoside (17, 18) in methanol solution was hydrogenated with 3 g of Raney nickel catalyst, at 3 atmospheres pressure, for 72 hours. After removal of the catalyst, excess of benzene was added to the methanol filtrate. Concentration under reduced pressure removed methanol. Further benzene was added and concentration continued until precipitation occurred. The crude benzylidene sorbitol was collected by filtration, stirred with 50 ml of ethylacetate–chloroform (1:1), refiltered, washed, and dried. One crystallization from ethanol yielded pure benzylidene sorbitol (m.p. 132–134°). From this material D-erythrose was obtained in 85% yield by periodate oxidation as described by Sowden (14).

Acetylated Nitropentitols-1-C^{14}

A solution of 0.85 g of sodium in 40 ml of absolute methanol was added dropwise over a half-hour period to a stirred, cool (10° C) solution of erythrose (3.04 g) and C^{14}-nitromethane (0.5 ml diluted to 1.3 ml with non-radioactive nitromethane) dissolved in 40 ml of methanol. The cool reaction mixture was stirred for a further 15 hours, stored

in the cold room overnight, and the sodium nitropentitols collected as described in the procedure for ribose-1-C^{14} and arabinose-1-C^{14}. The sodium nitropentitols were dissolved in 200 ml of ice water and the sodium removed by passage through a cooled column of 40 ml of Dowex 50 (hydrogen form). The eluate and further water washings of the column were charcoaled, filtered, and concentrated to dryness at a temperature below 35°. Alcohol was added to the resulting partly crystalline mass and distilled under reduced pressure. This procedure was repeated three times to remove the last traces of water. After storage over P_2O_5 *in vacuo* the product weighed 2.36 g (51% based on nitromethane). Acetic anhydride (30 ml) and one small drop of concentrated sulphuric acid were added and stirred for 6 hours until the syrupy nitropentitols had dissolved. The reaction mixture was heated at 95° with stirring for 30 minutes, cooled, and 100 ml of ice water added to hydrolyze the excess acetic anhydride. After being stirred for 20 minutes the cold mixture was extracted with three 75-ml portions of chloroform. The combined chloroform extracts were washed twice with ice water, dried over calcium chloride, charcoaled, filtered, and concentrated to a syrup. Benzene was added and removed under reduced pressure. This procedure was repeated eight times to remove the last traces of acetic acid. The product weighed 3.83 g corresponding to an 84% yield of the acetylated nitropentitols.

Deacetylation and Hydrogenation

The acetylated compound, 60 ml of dry benzene and 4.5 g of sodium bicarbonate were refluxed with rapid stirring for 2½ hours, cooled, charcoaled, filtered, and concentrated to a syrup. Alcohol was added and removed under reduced pressure. The syrup was finally completely freed of solvent under high vacuum to yield 2.83 g of presumed triacetoxynitropentene-1. The syrup was dissolved in 50 ml of ethanol, 300 mg of palladium black was added, and hydrogenation carried out at room temperature and atmospheric pressure. After 21 minutes the rate of uptake of hydrogen had become slow and the hydrogenation was terminated. The catalyst was removed by filtration and the ethanol filtrate concentrated to a syrup.

Nef Reaction

The syrup was dissolved in 8 ml of ethanol, cooled to 10°, and 24 ml of 2 *N* NaOH also at 10° was added dropwise with rapid stirring over a 20-minute period. The resulting alkaline solution was employed in a Nef reaction under the same conditions as those for the preparation of ribose-1-C^{14} and arabinose-1-C^{14}. (Eight milliliters of concentrated sulphuric acid and 10 ml of water were used.)

Deionization and Separation of Pentoses

The resulting solution was deionized and the mixture of pentoses transferred to a cellulose column by the same procedure given for the ribose–arabinose case. The column was developed with 99% acetone for 8 hours. (Forty-minute collection time and elution rate of 1 ml per minute.) After 8 hours the eluting solvent was changed to 97% acetone until the deoxyribose-1-C^{14} was eluted; ribose and arabinose were eluted as described previously. The three pentoses were obtained as syrups and, as previously described, dissolved in water for biological experiments. Aliquots were taken for determination of pentose and of radioactivity. The three pentoses were identified by diphenylamine (19) (for the deoxyribose-1-C^{14}) and orcinol (for the ribose-1-C^{14} and arabinose-1-C^{14}) reactions and by paper strip chromatography with the appropriate authentic samples as markers. The yields of labelled pentoses (based on nitromethane) were: D-2-deoxyribose-1-C^{14}, 202 mg (6.3%), 6800 counts/min mg; D-ribose-1-C^{14}, 112 mg (3.1%), 7200 counts/min mg; D-arabinose-1-C^{14}, 106 mg (2.9%), 7100 counts/min mg.

ACKNOWLEDGMENT

The authors are grateful to the National Research Council of Canada for funds which defrayed part of the cost of this study.

REFERENCES

1. FRUSH, H. L. and ISBELL, H. S. J. Research Natl. Bur. Standards, **51**, 307 (1953).
2. ISBELL, H. S., KARABINOS, J. V., FRUSH, H. L., HOLT, N. B., SCHWEBEL, A., and GALKOWSKI, T. T. J. Research Natl. Bur. Standards, **48**, 163 (1952).
3. ISBELL, H. S., FRUSH, H. L., and HOLT, N. B. J. Research Natl. Bur. Standards, **53**, 217 (1954).
4. ISBELL, H. S., FRUSH, H. L., and HOLT, N. B. J. Research Natl. Bur. Standards, **53**, 325 (1954).
5. MAHLER, H. R. U.S. Atomic Energy Comm. Document AECD-2400 (1948).
6. RAPPOPORT, D. A. and HASSID, W. Z. J. Am. Chem. Soc. **73**, 5524 (1951).
7. SOWDEN, J. C. J. Biol. Chem. **180**, 55 (1949).
8. BINKLEY, W. W. Advances in Carbohydrate Chem. **10**, 55 (1955).
9. SOWDEN, J. C. Advances in Carbohydrate Chem. **6**, 291 (1951).
10. MURRAY, D. H. and BUTLER, G. C. To be published.
11. OVEREND, W. G. and STACEY, M. Advances in Carbohydrate Chem. **8**, 68 (1953).
12. SOWDEN, J. C. J. Am. Chem. Soc. **76**, 3541 (1954).
13. ISBELL, H. S., FRUSH, H. L., and SCHAFFER, R. J. Research Natl. Bur. Standards, **54**, 201 (1955).
14. SOWDEN, J. C. J. Am. Chem. Soc. **72**, 808 (1950).
15. OVEREND, W. G., STACEY, M., and WIGGINS, L. F. J. Chem. Soc. 1358 (1949).
16. MCRARY, W. L. and SLATTERY, M. C. Arch. Biochem. **6**, 151 (1945).
17. RAYMOND, A. L., TYSON, R. S., and LEVENE, P. A. J. Biol. Chem. **130**, 47 (1939).
18. RICHTMYER, N. K. J. Am. Chem. Soc. **56**, 1633 (1934).
19. DAVIDSON, J. N. and WEYMOUTH, C. Biochem. J. **38**, 379 (1944).

NOTES

A RAPID DETERMINATION OF SOME SURFACE PROPERTIES OF SOLIDS

H. P. Schreiber and M. H. Waldman

INTRODUCTION

Among the important properties of a solid used as an adsorbent, catalytic agent, filler, etc., are its specific surface area ($\bar{A}$) and its maximum adsorption capacity ($\bar{V}_{max}$) for a given adsorbate. Standard techniques are available for accurate determinations of these quantities; for example, surface areas can be measured by the B.E.T. method (1) or by electron microscopy (2), adsorption capacities from suitable adsorption isotherms. When routine determinations of such surface properties are required and demands on accuracy are not too stringent, these techniques become overly time consuming. In such cases a rapid method of determination is wanted. To this end, a simplification of the B.E.T. procedure has recently been reported (3). This note is believed to describe a more widely applicable and rapid method of estimating the desired surface properties.

BASIS OF METHOD

The present method relies on a correlation between the surface area and adsorption capacity of a solid on the one hand, and the heat of adsorption in the given system, on the other. For the coverage of any fraction θ of surface per gram of adsorbent,

$$(\bar{A}) = k(\Delta\bar{H}_\theta) \qquad [1]$$

and

$$(\bar{V}_{max}) = k'(\Delta\bar{H}_\theta) \qquad [2]$$

where $(\Delta\bar{H}_\theta)$ denotes the integral heat of adsorption per gram of adsorbent, and k and k' are unspecified proportionality parameters. Thus, provided k and k' are known, an experimental evaluation of $(\Delta\bar{H}_\theta)$ would give an estimate of the required solid characteristic in any specified system.

In this method, a quantity proportional to the heat of adsorption is measured rapidly using apparatus characteristic of differential thermal analysis (d.t.a.). Since results are always comparative, the proportionality between the true and the measured reaction quantity need not be known explicitly.

EXPERIMENTAL

The quantity proportional to the heat of adsorption is measured in apparatus, the essentials of which are shown in Fig. 1. The d.t.a. cell is connected through a manifold system to the usual high vacuum components. Cup A of the cell holds the experimental sample; cup B is the reference arm, containing sintered glass of small specific surface. Chromel–alumel thermocouples (T_1 and T_2) are immersed into the cups, and connected to a Leeds–Northrup Type 9835B d-c. amplifier, the latter to a single pen recording potentiometer. The reservoir R contains the adsorbate, the vapor pressure of which can be read on the constant-volume mercury manometer. Provision was made to append additional d.t.a. cells as indicated. About one gram of adsorbent is weighed into the

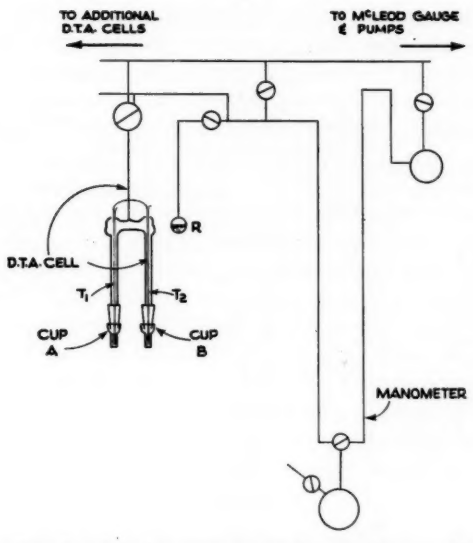

FIG. 1. Sample cell and vacuum system for reaction area determination.

reaction cup. The adsorbent is evacuated for about one hour at room temperature, or sufficiently long to establish a residual pressure of about 10^{-5} mm over the sample. The sample cell is then thermostated at the desired temperature, the dead space volume is exposed to the adsorbate, and the vapor finally admitted to the evacuated sample. The course of the interaction is recorded until no temperature gradient exists between sample and reference arms of the cell. In general, this involves about 10 minutes' operating time. The area under the time–temperature curve is found using a planimeter. This area, divided by the mass of adsorbent involved, is taken to be proportional to the heat of adsorption. Hereafter, the quantity is referred to as the "reaction area".

RESULTS AND DISCUSSION

The procedure for rapid surface area and adsorption capacity measurements was established using commercially available carbon blacks as adsorbents. Water, *n*-butane, and ethyl chloride were chosen as convenient adsorbates. Nine carbon blacks were involved in the water adsorption work, carried out at 25.5° C. Three types of carbon black were used in conjunction with the butane and ethyl chloride, these experiments being done at 0° C. In order to evaluate the parameters k and k', conventional values of $\bar{A}$ and $\bar{V}_{max}$ were needed (equations [1], [2]). Surface areas of the carbon blacks were obtained by the usual nitrogen adsorption technique in a B.E.T. apparatus (1). Maximum adsorption capacities were found only for butane and ethyl chloride adsorption, from the 0° C isotherms.

A description of the carbon black samples, their nitrogen adsorption and various "reaction areas", and the pertinent maximum adsorption capacities, are recorded in Table I. Each "reaction area" is the mean of two separate results. These did not deviate more than 8% about the mean. A correlation seems to exist between the "reaction areas" and the surface areas and maximum adsorption capacities. This is more readily seen by evaluating the proportionality parameters k and k'. In so doing, the pertinent

"reaction area" was substituted for the heat of adsorption. The values are given in Table II.

TABLE I

Surface areas, adsorption capacities, and reaction areas for adsorption of water, butane, and ethyl chloride on carbon blacks

Sample	Description	N_2 surface areas (m^2/g)	Reaction areas (cm^2/g)			$\bar{V}_{max}$ (cc/g)	
			H_2O (25.5° C)	n-C_4H_{10} (0° C)	EtCl (0° C)	n-C_4H_{10} (0° C)	EtCl (0° C)
1	Fine porous channel	327	88.0	54.2	50.6	470	300
2	Medium porous channel	139	42.0	—	—	—	—
3	Coarse porous channel	106	31.0	—	—	—	—
4	Coarse porous channel	112	35.5	—	—	—	—
5	Medium porous channel	125	36.5	—	—	—	—
6	Medium porous channel	140	38.0	—	—	—	—
7	Fine non-porous furnace	131	15.0	23.2	21.3	205	110
8	Medium non-porous furnace	76	8.8	—	—	—	—
9	Medium non-porous furnace	80	—	13.5	13.0	115	50
10	Coarse non-porous furnace	43	5.5	—	—	—	—

TABLE II

Proportionality parameters for adsorption of water, butane, and ethyl chloride on carbon blacks

Sample	$k \times 10^{-4}$			k' (cm)	
	H_2O	n-C_4H_{10}	EtCl	n-C_4H_{10}	EtCl
1	3.80	6.10	6.50	8.70	5.90
2	3.30	—	—	—	—
3	3.40	—	—	—	—
4	3.20	—	—	—	—
5	3.40	—	—	—	—
6	3.70	—	—	—	—
7	8.70	5.60	6.10	8.80	5.20
8	8.50	—	—	—	—
9	—	5.80	6.10	8.50	4.00
10	7.80	—	—	—	—

The parameter k appears to be constant for each interacting pair. The "reaction area" can therefore serve as a measure of the apparent surface area of the adsorbent in each system. Similarly, the value k' appears to be a constant characteristic of the interacting system, although there is a relatively large spread in the case of ethyl chloride adsorption. Thus, in each specified system an estimate of $\bar{V}_{max}$ is possible from the reaction datum. Provided, therefore, a given adsorbent–adsorbate system has been calibrated by means of a standard determination of surface area or maximum adsorption capacity, the described technique can be used to estimate these characteristics absolutely with an accuracy of some 15%. The total determination time of under two hours constitutes a very pronounced time saving over standard techniques.

A further use of this technique should be in routine control of the surface properties of a given solid. The precision of the "reaction area" determination is about 10–15%, so that changes in the quantity beyond this limit in a selected adsorption process indicate significant changes in the surface characteristics of the adsorbent under consideration. If absolute values are not required, there is no need for prior calibration of the system. If several d.t.a. cells are used, up to 30 or 40 such "surface characterizations" can be

performed per day by a single operator. Although the method had been utilized only in conjunction with carbon blacks, it should be broadly applicable to any adsorbent.

Some further aspects of the data merit brief discussion. Table II shows that k changes only slightly from the butane to the ethyl chloride system. This is reasonable; the apparent surface area is not likely to vary greatly when the probe molecules are approximately equal in size, as is the case here. In the case of water adsorption, the k value is sensitive to differences between channel and furnace blacks, but seems constant in each group. The absence of pore structure in the furnace blacks doubtless lowers the effective number of sites for water adsorption, thus raising the value of k. The water molecule is, presumably, sufficiently small to gain entry into some of the pores of the channel blacks, resulting in a relatively large heat of adsorption, hence a low k value. The apparent constancy of k for ethyl chloride and butane adsorption suggests that little penetration of the pore structure of the channel blacks occurs with these adsorbates.

The proportionality parameter k' is considerably greater for butane than for ethyl chloride. Since the "reaction areas" in these cases are approximately equal (see Table I), a given surface region of the black seems to accommodate greater amounts of butane than ethyl chloride prior to bulk liquefaction. In view of the polar nature of the ethyl chloride molecule, this result seems reasonable.

1. Brunauer, S., Emmett, P. H., and Teller, E. J. Am. Chem. Soc. **60**, 309 (1938).
2. Anderson, R. B. and Emmett, P. H. J. Appl. Phys. **19**, 367 (1948).
3. Starkweather, F. M. and Palumbo, D. T. J. Electrochem. Soc. **104**, 287 (1957).

Received April 24, 1959.
Canadian Industries Limited,
Central Research Laboratory,
McMasterville, Quebec.

STEROIDS. CXV. THE SYNTHESIS OF HALOGENATED STEROID HORMONES, 4-CHLORO-19-NOR HORMONE ANALOGS*

O. Mancera and H. J. Ringold

In an earlier paper (1) we noted that halogenation of progesterone at C-4 virtually eliminates progestational activity. It was thus of considerable interest to convert the extremely potent progestational agents (2), 19-nor: 17α-methyl- (3), 17α-ethynyl- (3), 17α-vinyl- (4), and 17α-ethyltestosterone (5) as well as 19-norprogesterone (6) into their 4-chloro analogs for evaluation of gestational activity. This transformation was readily accomplished by converting the parent steroids I into their 4,5-oxides (II) by reaction with alkaline hydrogen peroxide followed by hydrochloric acid treatment to yield directly the 4-chloro-Δ^4-3-ketones (III). This sequence is one first described in the cholesterol series by Shaw and Stevenson (7) and later described in the hormones series by ourselves (1) and by Camerino *et al.* (8). An alternate synthesis involving direct halogenation has been described by Petrow and co-workers (9) while a later paper by a Schering group (10) describes the synthesis of 4-halo hormone analogs by the addition of hypohalous acid to Δ^4-3-ketones.

In the case at hand 17α-methyl-19-nortestosterone (I*a*), 17α-ethynyl-19-nortestosterone (I*b*), and 19-norprogesterone (I*e*) were each reacted for periods of 35 minutes to 1 hour

*Paper CXIV, Kincl, F. A. and Garcia, M. Ber. **92**, 595 (1959).*

with alkaline hydrogen peroxide in cold methanol solution to give a mixture (1) of the corresponding 4β,5β- and 4α,5α-epoxides. Without purification the epoxide mixtures were treated for 1 hour with concentrated hydrochloric acid in acetone solution (1), thus giving a high yield of the 4-chloro-Δ^4-3-keto compounds II*a*, II*b*, and II*e*.

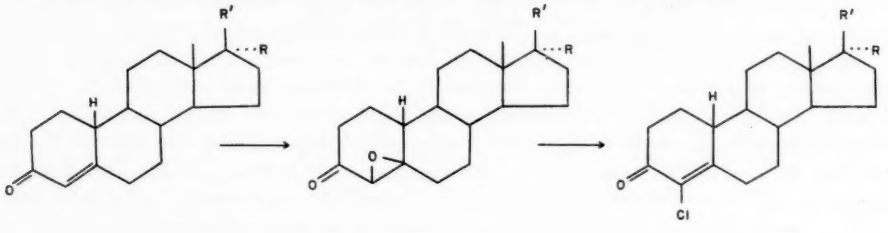

(I) (II)

(*a*) R = CH_3; R' = OH
(*b*) R = C≡CH; R' = OH
(*c*) R = CH=CH_2; R' = OH
(*d*) R = CH_2CH_3; R' = OH
(*e*) R = H; R' = $COCH_3$

Hydrogenation of 4-chloro-17α-ethynyltestosterone (II*b*) in pyridine (11) over a palladium – calcium carbonate catalyst and interrupted at 1.1 equivalents hydrogen uptake gave 4-chloro-17α-vinyltestosterone (II*c*) in 70% yield, while hydrogenation of II*b* in dioxane (12) with palladium – barium sulphate, interrupted at 2.1 moles uptake, gave the 17α-ethyl compound (II*d*) in 60% yield. When tested* in the Clauberg assay by either the oral or subcutaneous route, compounds II exhibited only a relatively low order of progestational activity.

EXPERIMENTAL

Melting points are uncorrected. Rotations were determined in chloroform and ultraviolet absorption spectra in 96% ethanol.

4-Chloro-17α-methyl-19-nortestosterone (II*a*).—A solution of 17α-methyl-19-nortestosterone (I*a*) (10 g) in methanol (250 ml) was cooled to 0° and then treated dropwise and successively with 35% hydrogen peroxide (40 ml) and 10% sodium hydroxide (16 ml). After it had been left to stand for 35 minutes at 0–5° the solution was poured into water and extracted with ethyl acetate. Evaporation of the washed extract gave 11 g of crude epoxide as a semicrystalline product exhibiting no selective absorption in the ultraviolet. The epoxide without further purification was dissolved in acetone (100 ml), and concentrated hydrochloric acid (10 ml) was added. The solution, after being kept for 1 hour at room temperature, was poured into salt water and the product extracted with methylene chloride. The extract was washed successively with water, sodium carbonate solution, water, and then evaporated. The residue in 200 ml of benzene–hexane (1:1) was adsorbed on 300 g of neutral alumina, whereupon acetone–hexane crystallization of the benzene eluate gave 6.32 g of 4-chloro-17α-methyl-19-nortestosterone (II*a*), m.p. 145–148°. The analytical specimen from acetone–ether exhibited m.p. 148–151°, λ_{max} 255 mμ, log ϵ 4.12, $[\alpha]_D$ +42°.† Anal. Calc. for $C_{19}H_{27}ClO_2$: C, 70.67; H, 8.43; Cl, 10.98. Found: C, 70.68; H, 8.39; Cl, 10.61.

**Bio-assays by The Endocrine Laboratories, Madison, Wisc.*

†After completion of our work this compound was reported by Camerino et al. (ref. 8b) with m.p. 151–152°, λ_{max} 255 mμ, log ϵ 4.14.

4-Chloro-17α-ethynyl-19-nortestosterone (II*b*).—17α-Ethynyl-19-nortestosterone (I*b*) (10 g) was epoxidized and then treated with acid as described above for the 17-methyl analog. The residue was chromatographed on neutral alumina and the benzene and benzene–ether 4:1 fractions crystallized from acetone–hexane to yield 5.54 g of II*b*, m.p. 186–188°, λ_{max} 225 mμ, log ε 4.11, $[\alpha]_D$ +7°. Anal. Calc. for $C_{20}H_{25}ClO_2$: C, 72.16; H, 7.57; Cl, 10.65. Found: C, 72.49; H, 7.46; Cl, 10.69.

4-Chloro-19-norprogesterone (II*e*).—19-Norprogesterone (0.8 g) in methanol (100 ml) at 0° was treated with 3.5 ml of 35% hydrogen peroxide and 1.4 ml of 10% sodium hydroxide and stirred for 1 hour at 0–5°. A small amount of insoluble material was removed and the filtrate poured into salt water. The crude epoxide mixture (0.83 g) was isolated by ethyl acetate extraction and then dissolved in 40 ml of acetone, and 1 ml of concentrated hydrochloric acid was added. After the solution had stood for 1 hour at room temperature, water, salt, and ice were added, the precipitate was collected, washed, dried, and recrystallized from acetone–hexane, yielding 0.61 g of II*e*, m.p. 169–172°. Recrystallization from the same solvents afforded the analytical sample, m.p. 174–177°, λ_{max} 256 mμ, log ε 4.11, $[\alpha]_D$ +127°. Anal. Calc. for $C_{20}H_{27}O_2Cl.\frac{1}{2}C_3H_6O$: C, 70.96; H, 8.31; Cl, 9.74%. Found: C, 71.01; H, 7.93; Cl, 9.68.

4-Chloro-17α-vinyl-19-nortestosterone (II*c*).—4-Chloro-17α-ethynyl-19-nortestosterone (5 g) in pyridine (100 ml) was hydrogenated at 25° and 580 mm over 2 g of pre-reduced 2% palladium – calcium carbonate catalyst. When hydrogen uptake reached 1.1 equivalents (2 to 3 hours in general) the reduction was interrupted, the catalyst removed, and the solvent concentrated *in vacuo*. The oily residue was taken up in ethyl acetate, the solution washed with dilute acid, carbonate solution, and then water. Evaporation and crystallization of the product from acetone–hexane gave 3.54 g of the vinyl compound (II*c*), m.p. 115–118°. Two recrystallizations from the same solvent pair produced the analytical specimen, m.p. 124–126°, λ_{max} 255 mμ, log ε 4.13, $[\alpha]_D$ +51°. Anal. Calc. for $C_{20}H_{27}ClO_2$: C, 71.69; H, 8.15; Cl, 10.59. Found: C, 71.42; H, 8.05; Cl, 10.71.

4-Chloro-17α-ethyl-19-nortestosterone (II*d*).—The reduction at 25° and 580 mm of 2 g of 4-chloro-17α-ethynyl-19-nortestosterone (II*b*) in 160 ml of dioxane over 0.8 g of pre-hydrogenated 10% palladium – barium sulphate catalyst was stopped after the uptake of 2.1 equivalents of hydrogen (ca. 3 hours). The catalyst was filtered and the solution concentrated to dryness, whereupon acetone–hexane crystallization of the reduced product gave 1.20 g of 17α-ethyl compound (II*d*), m.p. 122–125°. Repeated crystallization yielded the pure substance, m.p. 126–128° (mixture melting point depression with II*c*), λ_{max} 256 mμ, log ε 4.14, $[\alpha]_D$ +47°. Anal. Calc. for $C_{20}H_{29}O_2Cl$: C, 71.34; H, 8.68; O, 9.50. Found: C, 71.30; H, 8.69; O, 9.58.

1. Ringold, H. J., Batres, E., Mancera, O., and Rosenkranz, G. J. Org. Chem. **21**, 1432 (1956).
2. McGinty, D. and Djerassi, C. Ann. N. Y. Acad. Sci. **71**, 500 (1958).
3. Djerassi, C., Miramontes, L., Rosenkranz, G., and Sondheimer, F. J. Am. Chem. Soc. **76**, 4092 (1954).
4. Sandoval, A., Miramontes, L., Rosenkranz, G., and Sondheimer, F. J. Am. Chem. Soc. **75**, 4117 (1953).
5. Colton, F. B., Nysted, L. N., Riegel, B., and Raymond, A. L. J. Am. Chem. Soc. **79**, 1123 (1957).
6. Miramontes, L., Rosenkranz, G., and Djerassi, C. J. Am. Chem. Soc. **73**, 3540 (1951).
7. Shaw, J. I. and Stevenson, R. J. Chem. Soc. 3549 (1955).
8. (*a*) Camerino, B., Patelli, B., and Vercellone, A. J. Am. Chem. Soc. **78**, 3540 (1956). (*b*) Camerino, B., Modelli, R., and Patelli, B. Farmaco, (Pavia), **13**, 52 (1958); Chem. Abstr. **52**, 13768 (1958).
9. Kirk, D. N., Patel, D. K., and Petrow, V. J. Chem. Soc. 1184 (1956).
10. Oliveto, E. P., Gerold, C., and Hershberg, E. B. J. Am. Chem. Soc. **79**, 3596 (1957).

11. RUZICKA, L. and MÜLLER, P. Helv. Chim. Acta, **22**, 755 (1939).
12. HERSHBERG, E. B., OLIVETO, E. P., GEROLD, C., and JOHNSON, L. J. Am. Chem. Soc. **73**, 5073 (1951).

RECEIVED JUNE 12, 1959.
RESEARCH LABORATORIES,
SYNTEX, S. A.,
APDO. POSTAL 2679,
MEXICO, D. F.

THE STREAMING BIREFRINGENCE OF CELLULOSE MICELLES: A CONFIRMATION OF THE THEORY FOR RIGID RODS

D. F. MACLENNAN* AND S. G. MASON

INTRODUCTION

Theories of streaming birefringence have been reviewed by Edsall (1) and by Cerf and Scheraga (2). Peterlin and Stuart (3, 4) have developed a theory for the orientation of rigid ellipsoids of revolution which permits the calculation of particle lengths from streaming birefringence data. Donnet (5) has made a comparison of the lengths of tobacco mosaic virus particles measured directly from electron micrographs and those calculated from flow birefringence measurements using the theory of Peterlin and Stuart. Good agreement between the two methods was obtained.

This note deals with similar measurements on a cellulose sol.

EXPERIMENTAL

Apparatus

The streaming birefringence apparatus, used in this work, is the concentric cylinder type with rotating outer cylinder. A longitudinal section of the cylinders and optical system is shown in Fig. 1.

The outer cylinder, made of stainless steel, has an internal diameter of 3.40 cm and an inside length of 6.35 cm. Four interchangeable stainless steel inner cylinders, 6.30 cm long and having different diameters, make it possible to vary the annular gap from 1.5 mm to 0.2 mm and the velocity gradient up to 10^4 sec^{-1}.

The light source is a General Electric A-H4 100-watt mercury arc with a filter combination to isolate the 546-mμ mercury line.

Cellulose Sol

The sol was prepared (6) by boiling 10 g bleached sulphite wood pulp in 5 *N* sulphuric acid for 3.5 hours, and the residue, after it was washed, was dispersed in 2 l. of distilled water.

To narrow the distribution of particle sizes the sol was then centrifuged at 3500 *g* for 1 hour in a Spinco preparatory ultracentrifuge and the supernatant sol was used for the measurements.

Electron micrographs of the rod-like cellulose particles were made using palladium-shadowed specimens.

RESULTS AND DISCUSSION

The distribution of particle lengths from the electron micrographs is given in Table I. The experimental values of the extinction angle χ over a range of gradients G and using three different stators are plotted in Fig. 2.

The electron micrographs indicate that the cellulose particles range in length from 1500 Å to 6500 Å. From this information a theoretical extinction angle curve, character-

Holder of a Studentship (1951–52) and a Fellowship (1952–53) from the National Research Council of Canada.

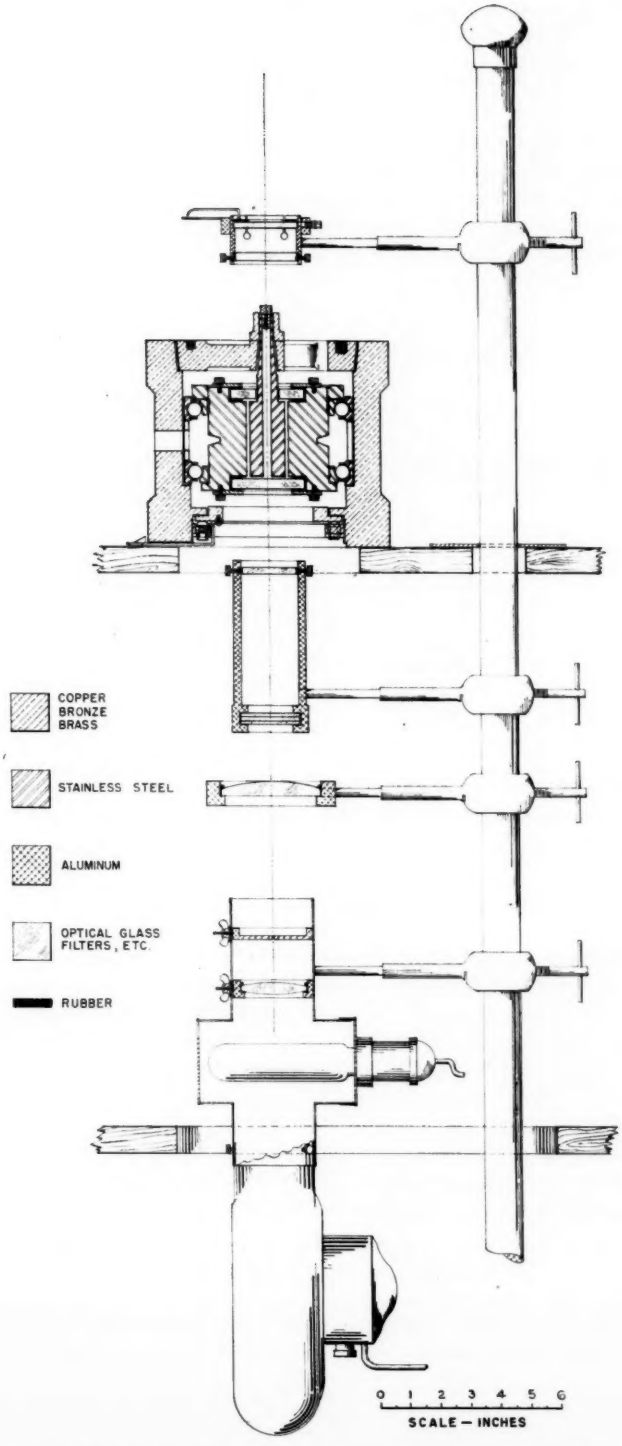

FIG. 1. Sectional view of the streaming birefringence apparatus.

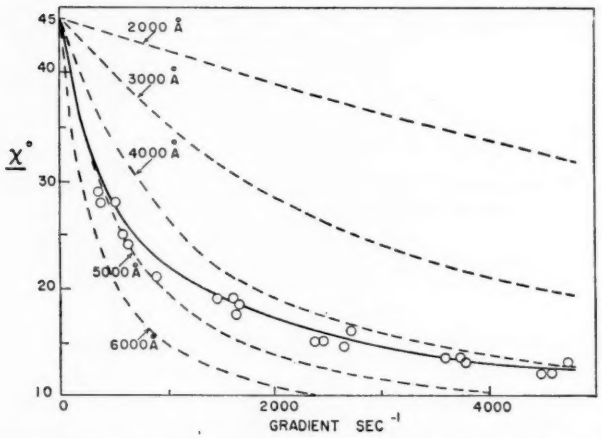

FIG. 2. Extinction angle at various gradients. The points represent experimental values with three different annular gaps in the apparatus. The solid line is calculated from the measured length distribution, and the broken lines are calculated for monodisperse particles of the lengths indicated.

TABLE I
Length distribution from electron micrographs

Range (Å)	Percentage of particles
1500–2500	12
2500–3500	21
3500–4500	27
4500–5500	22
5500–6500	18

istic of a solution of particles having this length distribution, has been calculated.

A rotary diffusion constant, θ, has been calculated for each length range using the Perrin formula (7)

$$[1] \qquad \theta = \frac{3kT}{16\pi\eta a^3}(-1+2\log_e 2p)$$

where k is the Boltzmann constant, T is the absolute temperature, η is the solvent viscosity, a is the length of the semimajor axis, and p is the axis ratio.

Since, as may be seen from eq. [1], θ is much more sensitive to a than to p, the use of an approximate value of p in these calculations is permissible. The latter was taken to be 16, the approximate value estimated from the electron micrographs.

From values of θ and p, theoretical values of χ can be obtained for any velocity gradient from the tables of Scheraga, Edsall, and Gadd (8).

Values for a polydisperse sol, made up of particles of the measured lengths in the proper proportions, have been calculated using the theory of Sadron (9). According to this theory the extinction angle of a polydisperse system is given by

$$[2] \qquad \tan 2\chi = \left(\sum_i \delta_i \sin 2\psi_i\right) \Big/ \left(\sum_i \delta_i \cos 2\psi_i\right)$$

where ψ_i is the extinction angle, and δ_i the birefringence which would be produced by the ith component alone in a given solvent at a given velocity gradient.

According to Peterlin and Stuart (4) the birefringence Δn of a polydisperse system is given by

$$[3] \qquad \Delta n = \frac{2\pi c}{n_0}(g_1 - g_2) f(\alpha, p)$$

where c is the concentration of the particles expressed as volume fraction, n_0 is the index of refraction of the isotropic solution at rest, $(g_1 - g_2)$ is an optical factor, and $f(\alpha, p)$ is an orientation factor. If $(g_1 - g_2)$ is assumed to be constant, δ_i may be replaced in eq. [2] by $c_i f_i$ where c_i is the concentration and f_i the orientation factor of the ith component of the sol. The relative values of c_i were taken from the distribution (Table I) and f_i and ψ_i were obtained from the tables (8).

The modified equation is

$$[4] \qquad \tan 2\chi = \sum_i c_i f_i \sin 2\psi_i \Big/ \sum_i c_i f_i \cos 2\psi_i.$$

The curve calculated from eq. [4] is shown as the solid line in Fig. 2. Included for comparison as broken lines are the calculated values for monodisperse sols of various lengths. It is seen that the experimental values are in good agreement with the theoretical curve based on the measured length distribution.

1. Edsall, J. T. Advances in Colloid Sci. **1**, 269 (1942).
2. Cerf, R. and Scheraga, H. A. Chem. Revs. **51**, 185 (1952).
3. Peterlin, A. Z. Physik, **111**, 232 (1938).
4. Peterlin, A. and Stuart, H. A. Z. Physik, **112**, 1, 129 (1939).
5. Donnet, J. B. J. Polymer Sci. **12**, 53 (1954).
6. Ranby, B. G. Discussions Faraday Soc. **11**, 158 (1951).
7. Perrin, F. J. phys. radium, **5** (7), 497 (1934).
8. Scheraga, H. A., Edsall, J. T., and Gadd, J. O., Jr. J. Chem. Phys. **19**, 1101 (1951).
9. Sadron, C. J. phys. radium, **9** (7), 381 (1938).

Received June 9, 1959.
Physical Chemistry Division,
Pulp and Paper Research Institute of Canada and
Department of Chemistry, McGill University,
Montreal, Quebec.

NOTE ON THE REACTION OF HYDROGEN ATOMS WITH CYANOGEN*

Catherine Haggart† and C. A. Winkler

During a study of the reactions of CN radicals formed in mixtures of cyanogen and active nitrogen, it became of interest to know the extent to which cyanogen was capable of reacting with hydrogen atoms and CN radicals with molecular hydrogen. Using a fast flow system, Geib and Harteck (1) observed that hydrogen atoms react with cyanogen to produce hydrogen cyanide and traces of methylamine and ammonia. Pease and Robertson (2) reported that, in a static system at 550° C, the reaction of cyanogen and molecular hydrogen followed a chain mechanism, initiated by the formation of CN radicals, and they suggested that hydrogen cyanide was formed by the reactions of CN radicals with molecular hydrogen and of hydrogen atoms with cyanogen. The reaction of molecular hydrogen with CN radicals, formed in the sodium flame reaction with cyanogen, was observed by Hartel and Polanyi (3) to produce hydrogen cyanide and to require an activation energy of some 7 kcal.

**Financial assistance received from the Canadian Industries Limited, and the National Research Council.*
†*Holder of a C.I.L. Fellowship, 1958–59.*

The reaction between hydrogen atoms and cyanogen was studied over a range of temperatures up to 430° C, at various flow rates of cyanogen. Hydrogen atoms were formed in a conventional Wood–Bonhoeffer (4) system. Hydrogen cyanide and unreacted cyanogen were the only substances trapped at liquid air temperature after reaction had occurred and no polymer was formed during the reaction. Analysis for hydrogen cyanide in the presence of cyanogen was made as described by Rhodes (5), by absorbing both products in a known volume of acidified silver nitrate solution, from which cyanogen was quantitatively recovered by slowly drawing nitrogen through the absorber and then into a train of Wallis bubblers (6) containing sodium hydroxide solution. The excess silver nitrate was titrated with potassium thiocyanate using ferrous ammonium sulphate as indicator, and the cyanide content of the bubblers was estimated by titration with silver nitrate with potassium iodide as indicator (7).

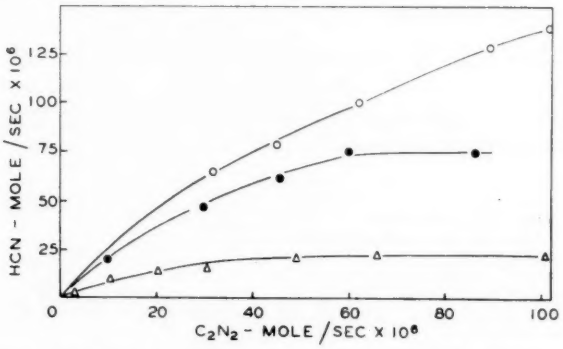

FIG. 1. Production of hydrogen cyanide in the reaction of hydrogen atoms with cyanogen. Temperature in ° C: △, 68; ●, 268; ○, 430.

The relations between the hydrogen cyanide production and cyanogen flow rate at three temperatures are shown in Fig. 1. Even at the lowest temperature used (68° C), the maximum rate of hydrogen cyanide production exceeded by a factor of three the flow rate of hydrogen atoms as determined from the maximum amount of hydrogen bromide that could be decomposed under comparable conditions (8). As the temperature was increased, the maximum production of hydrogen cyanide increased rapidly, until at 430° C it was some twenty times the flow rate of hydrogen atoms from the discharge tube. It seems quite apparent, therefore, that the reaction occurs by a chain mechanism, presumably as follows:

$$(CN)_2 + H \rightarrow HCN + CN \quad [1]$$

$$CN + H_2 \rightarrow HCN + H. \quad [2]$$

Termination of the chain might, of course, occur by recombination of hydrogen atoms or CN radicals, or by the interaction of hydrogen atoms and CN radicals.

1. GEIB, K. H. and HARTECK, P. Ber. B, **66**, 1815 (1933).
2. PEASE, R. N. and ROBERTSON, N. C. J. Am. Chem. Soc. **64**, 1880 (1942).
3. HARTEL, P. and POLANYI, M. Z. physik. Chem. B, **11**, 97 (1930).
4. BONHOEFFER, K. F. Z. physik. Chem. **113**, 199 (1924).
5. RHODES, F. N. Ind. Eng. Chem. **4**, 652 (1912).
6. WALLIS, T. Ann. **345**, 352 (1906).
7. KOLTHOFF, I. M. and SANDELL, E. B. Textbook of quantitative inorganic analysis. Rev. ed. The MacMillan Co., New York. 1948.

8. WILES, D. M. and WINKLER, C. A. J. Phys. Chem. **61**, 620 (1957).

RECEIVED JUNE 22, 1959.
PHYSICAL CHEMISTRY LABORATORY,
MCGILL UNIVERSITY,
MONTREAL, QUEBEC.

THE MERCURY-DISCHARGE REDUCTION OF PHOSPHORUS TRICHLORIDE

ARTHUR FINCH

Little information is available concerning the preparation or properties of simple halogen compounds containing the P—P bond; P_2Br_4 and P_2F_4 are unknown, and only P_2I_4 is well characterized (1). Early work by Besson (2) on the effect of an electrodeless discharge on mixtures of phosphorus trichloride and hydrogen resulted in the production of (presumably) P_2Cl_4, and similar recent work by Gutmann (3) led to unidentified liquid products. Attempts to make the tetrachloride by chemical reactions using P_2I_4 have been unsuccessful (4). The work reported below involves the reduction of phosphorus trichloride vapor by a high-voltage mercury arc, using conditions successfully adopted by Schlesinger and collaborators (5) for the continuous production of unstable boron subhalides.

EXPERIMENTAL

Apparatus and Materials

A "square-four" design discharge tube, similar to that previously used (5) was employed, with a discharge path of about 6 cm. A 2000-volt, 15-ma output transformer was operated under conditions appropriate to give a satisfactory discharge; the potential actually used varied between 1000 volts and 1300 volts, depending on the pressure in the system.

Phosphorus trichloride was redistilled at 74° C, passed into a high-vacuum line of conventional design, and fractionated through a −45.2° bath into a −78° trap. The vapor pressure of the purified compound was 65 mm at about −10°, in agreement with published results (6). Phosphorus trichloride vapor was circulated through the discharge cell either by a circulating pump or by distillation from a −63° bath to a −196° trap.

Results

Extensive decomposition occurred, with the production of dark red and yellow involatile solids on the walls of the discharge tubes, a dark grey scale on the surface of the mercury electrodes, and small quantities of a volatile liquid.

The volatile fraction was transferred to a fractionating system, and condensed as white crystals at −45° after passing a −23° bath. Using the Stock melting-point technique, and a pentane thermometer calibrated at the National Physical Laboratory to ±1°, the crystals were found to melt sharply between −34° and −35° C. The colorless liquid produced on melting the crystals decomposed at room temperature in vacuum, giving yellow involatile solids, and phosphorus trichloride, identified by measurements in a micro vapor-pressure apparatus. The liquid fumed in air, and reacted vigorously with water. Samples were distilled into weighed tubes under vacuum, hydrolyzed, and analyzed for chlorine and phosphorus, using standard procedures. Typical results calculated for P_2Cl_4 (Cl, 69.5%; P, 30.5%) were as follows. Sample 1: weight, 0.3041 g; Cl, 69.3%; P, 29.8%. Sample 2: weight, 0.2520 g; Cl, 69.6%; P, 30.4%. During the hydrolysis some non-condensable gas, presumably hydrogen, was evolved, suggesting the breaking of a P—P bond, though measurement was not possible in the apparatus available. The nature

of the hydrolysis products in the analogous compound P_2I_4 has been studied in detail by Kolitowska (9), who has shown that the final products include HI, H_3PO_2, H_3PO_3, PH_3, ($P_{12}H_6$), and it is expected that similar results obtain for the present compound. Molecular weight determinations by depression of vapor tension of carbon tetrachloride gave the values 191 and 194 for different samples (calculated for P_2Cl_4, 204). Thus the liquid was P_2Cl_4, and exhibited the general appearance and properties described by Besson, though the melting point was 6° lower. Using a single cell, some 200 mg per day were formed by a semiautomatic process.

Lack of volatility at low temperatures, and the rate of decomposition at room temperature, precluded vapor-pressure measurements. By analogy with the fluorination of B_2Cl_4 to form a more volatile and stable compound (7), attempts were made to replace the chlorine by fluorine, using similar Swarts-type reactions. No evidence for volatile compounds other than phosphorus trichloride, and very small amounts of a very volatile gas, presumably phosphorus trifluoride, was obtained. Further experiments to synthesize the tetrafluoro compound are in progress.

The electrode scale was completely soluble in warm nitric acid without apparent evolution of phosphine. Complete analysis, using standard gravimetric techniques, gave the following results. Sample 1: Hg, 86.4%; Cl, 10.7%; P, 2.6%. Sample 2: Hg, 86.2%; Cl, 10.9%; P, 2.6%. Thus in distinction to Gutmann's experiments with copper electrodes, a simple metal phosphide was not formed. It is of interest to note, that mercury tetratritaphosphide Hg_3P_4 is produced by the action of P_2I_4 on mercury at elevated temperatures (8), and the electrode scale is presumably a mixture of this with other mercury phosphides and chlorides.

The colored involatile deposits on the walls of the tubes were pyrophoric, and were similar to the mixture of red and yellow phosphorus described by Gutmann.

ACKNOWLEDGMENTS

It is a pleasure to acknowledge helpful discussions from Dr. A. G. Foster, and financial assistance from Imperial Chemical Industries Limited.

1. Leung, Y. C. and Waser, J. J. Phys. Chem. **60**, 539 (1956).
2. Besson, A. and Fournier, L. Compt. rend. **150**, 102 (1910).
3. Gutmann, V. Monatsh. Chem. **86**, 98 (1954).
4. Gautier, A. Compt. rend. **78**, 286 (1874).
5. Urry, G., Wartik, T., Moore, R. E., and Schlesinger, H. I. J. Am. Chem. Soc. **76**, 5293 (1954).
6. International Critical Tables, III, 213 (1933).
7. Finch, A. and Schlesinger, H. I. J. Am. Chem. Soc. **80**, 3573 (1958).
8. Van Haaren, A. and Partheil, A. Arch. Pharm. **238**, 35 (1900).
9. Kolitowska, J. H. Roczniki Chem. **15**, 29 (1935).

Received June 12, 1959.
Department of Chemistry,
Royal Holloway College,
University of London,
Englefield Green, England.

INFRARED SPECTRUM OF AMMONIUM HYDROPEROXIDE

Osvald Knop* and Paul A. Giguère

Ammonia and hydrogen peroxide form a 1:1 compound which is remarkable in that its melting point, 25° C (1), lies some 100° above that of the ammonia–water analogue (2).

**Present address: Department of Chemical Engineering, Nova Scotia Technical College, Halifax, N.S.*

Solid ammonia hydrates are known from various investigations (3–5) to be of the molecular, or addition type: $NH_3 \cdot H_2O$, etc. On the other hand, the Raman spectra of the ammonia – hydrogen peroxide compound in the molten state as well as in aqueous solutions (6, 7) show no indication whatsoever of the characteristic bands of the NH_4^+ ion, thereby confirming that under such conditions both component molecules essentially preserve their identity. In view of its relatively high melting point it is conceivable that in the solid state the ammonia – hydrogen peroxide compound is ionic, $NH_4^+O_2H^-$, like the alkali metal hydroperoxides. To answer the question we decided to measure its infrared spectrum. In the meantime we came across a short note by Simon and Kriegsman (8) establishing definitely the ionic nature of crystalline ammonium hydroperoxide from the NH_4^+ ion bands at 3041 and 3152 cm^{-1}. The present results lead to the same conclusion and provide further data on the O_2H^- ion.

Preparation of samples suitable for the infrared spectra presented considerable difficulty due to the marked tendency of the solid to decompose and react with atmospheric moisture. The usual methods of (*a*) grinding of the bulk solid to a fine powder, (*b*) mull in Nujol, (*c*) evaporation of a solution in alcohol, and (*d*) pressing in a KBr disk were tried without success. Satisfactory results could be obtained only by the deposition technique (9) using an evacuated glass absorption cell. First, hydrogen peroxide vapor from a liquid sample 99.9% pure was condensed in a thin film on a rock salt plate cooled with liquid nitrogen. Then a suitable amount of ammonia gas was deposited on top of the solid peroxide film. Mixing of the two vapors before condensation turned out to be unsuitable because of the large difference in the volatility of the two components. As long as the temperature remained in the neighborhood of −180° C no reaction took place between the two solids; when the liquid nitrogen was replaced by acetone – dry ice the compound was formed readily, and the excess ammonia was then pumped off. Traces of water, either from leakage of moisture or from decomposition of the peroxide vapor, yielded complex spectra arising presumably from some ternary compounds, identified since by means of thermal analysis (10).

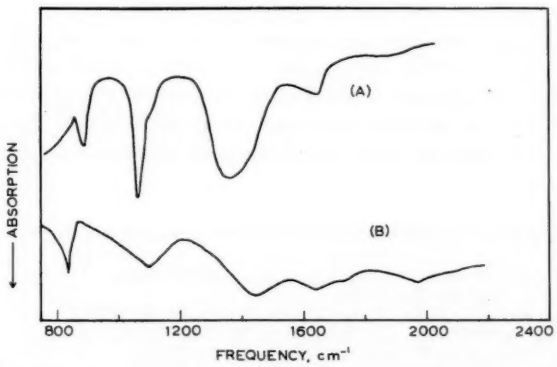

FIG. 1. Infrared spectra of (*a*) unreacted films of anhydrous ammonia and hydrogen peroxide deposited at −180° C, and (*b*) ammonium hydroperoxide.

The infrared spectrum in the rock salt region (Fig. 1) shows the well-known bands of the NH_4^+ ion at 1630 and 1450 cm^{-1} (11), plus a medium-intense band at 1100 cm^{-1} and the sharp O—O stretching band at 836 cm^{-1}. The latter, which coincides exactly with the

Raman band, represents an appreciable decrease from the corresponding frequency in hydrogen peroxide, 880 cm^{-1} (12). This implies a lowering of some 10% in the force constant and a lengthening of about 0.02 Å of the O—O bond. Undoubtedly the formal negative charge on the O_2H^- ion is responsible for this effect through (*a*) increase in covalent radius of the terminal O atom and (*b*) repulsion between the latter and the bonding electron cloud. Another example of this is the isocyanate ion (13) the fundamental frequencies of which are noticeably lower that those of isocyanic acid (14). Conversely, the formal positive charge on the hydroxylammonium ion increases the NO stretching frequency and shortens the N—O distance, as shown recently by infrared spectroscopy (15).

The 1100 cm^{-1} band reported here for the first time is not found in the spectra of ammonium salts; therefore it must belong to the O_2H^- ion, most likely to the bending mode. The only other possibility is an overtone or combination involving some lattice frequency, but this seems precluded by its relatively high intensity. Although somewhat low for an OH bending mode (ν_6 = 1380 cm^{-1} in crystalline H_2O_2), the present assignment is reasonable since lengthening of the O—O bond must reduce appreciably the OH bending frequency. Lastly the OH stretching band could not be identified positively in infrared because of strong interference from the NH stretching bands of the ammonium ion. In the Raman spectrum (8) a band at 3112 cm^{-1} has been assigned tentatively to the hydrogen-bonded OH in agreement with the above reasoning. As no X-ray data are available on crystalline hydroperoxides one can only surmise that hydrogen bonds of the type O—H . . . O exist between the neighboring perhydroxyl ions.

It seemed desirable to supplement this work by a study of an alkali metal hydroperoxide. To that effect some NaO_2H was prepared by reacting (in a dry box) pure, reagent grade sodium peroxide with absolute ethanol. The dry solid was ground under an inert atmosphere and the finer particles were allowed to settle on a salt window. The spectra showed bands at 718 (w), 814 (s), 873 (s), 1009 (s), 1325 (s), 1361 (w), 1427 (s), 1555 (w), and 1622 (s) cm^{-1}, indicating that, in spite of all precautions, the sample had reacted with atmospheric carbon dioxide and possibly contained traces of a hydroperoxidate, $2NaO_2H \cdot H_2O_2 \cdot 4H_2O$ (12).

In conclusion it appears that the acid strength of hydrogen peroxide, though greater than that of water (pK = 11.65 at 25°), is not sufficient to ionize ammonia in the liquid state. Only when thermal agitation is reduced on cooling do the strong hydrogen bonds O—H . . . N ionize and the resulting field leads to spatial organization of the ions. On the other hand, with a stronger base like tetramethylammonium, hydrogen peroxide ionizes even in solution (6).

The authors are grateful to the National Research Council for financial help.

1. Maass, O. and Hatcher, W. H. J. Am. Chem. Soc. **44**, 2472 (1922).
2. Postma, S. Rec. trav. chim. **39**, 516 (1920).
3. Waldrom, R. L. and Hornig, D. F. J. Am. Chem. Soc. **75**, 6079 (1953).
4. Gutowsky, H. S. and Fujiwara, S. J. Chem. Phys. **22**, 1782 (1954).
5. Siemons, W. J. and Templeton, D. H. Acta Cryst. **7**, 194 (1954).
6. Simon, A. and Marchand, M. Zeit. anorg. Chem. **262**, 191 (1950).
7. Simon, A. and Uhlig, U. Ber. **85**, 977 (1952).
8. Simon, A. and Kriegsman, H. Naturwissenschaften, **42**, 14 (1955).
9. Wagner, E. L. and Hornig, D. F. J. Chem. Phys. **18**, 296 (1950).
10. Chin, D. Unpublished results.
11. Miller, F. A. and Wilkins, C. H. Anal. Chem. **24**, 1253 (1952).
12. Schumb, W. C., Satterfield, C. N., and Wentworth, R. L. Hydrogen peroxide. Reinhold Publishing Corp., New York. 1955.
13. Pal, N. N. and Sen Gupta, P. N. Indian J. Phys. **5**, 13 (1930).

14. HERZBERG, G. and REID, C. Discussions Faraday Soc. **9**, 92 (1950).
15. FRASCO, D. L. and WAGNER, E. L. J. Chem. Phys. **30**, 1124 (1959).

RECEIVED JUNE 29, 1959.
DEPARTMENT OF CHEMISTRY,
LAVAL UNIVERSITY,
QUÉBEC, QUÉBEC.

NOTES TO CONTRIBUTORS

Canadian Journal of Chemistry

MANUSCRIPTS

General.—Manuscripts, in English or French, should be typewritten, double spaced, on paper 8½×11 in. **The original and one copy are to be submitted.** Tables and captions for the figures should be placed at the end of the manuscript. Every sheet of the manuscript should be numbered. Style, arrangement, spelling, and abbreviations should conform to the usage of recent numbers of this journal. Greek letters or unusual signs should be written plainly or explained by marginal notes. Characters to be set in bold face type should be indicated by a wavy line below the characters. Superscripts and subscripts must be legible and carefully placed. Manuscripts and illustrations should be carefully checked before they are submitted. Authors will be charged for unnecessary deviations from the usual format and for changes made in the proof that are considered excessive or unnecessary.

Abstract.—An abstract of not more than about 200 words, indicating the scope of the work and the principal findings, is required, except in Notes.

References.—These should be designated in the text by a key number and listed at the end of the paper, with the number, in the order in which they are cited. The form of the citations should be that used in this journal; in references to papers in periodicals, titles should not be given and only initial page numbers are required. The names of periodicals should be abbreviated in the form given in the most recent *List of Periodicals Abstracted by Chemical Abstracts.* All citations should be checked with the original articles and each one referred to in the text by the key number.

Tables.—Tables should be numbered in roman numerals and each table referred to in the text. Titles should always be given but should be brief; column headings should be brief and descriptive matter in the tables confined to a minimum. Vertical rules should not be used. Numerous small tables should be avoided.

ILLUSTRATIONS

General.—All figures (including each figure of the plates) should be numbered consecutively from 1 up, in arabic figures, and each figure referred to in the text. The author's name, title of the paper, and figure number should be written in the lower left corner of the sheets on which the illustrations appear. Captions should not be written on the illustrations.

Line drawings.—Drawings should be carefully made with India ink on white drawing paper, blue tracing paper, or co-ordinate paper ruled in blue only; any co-ordinate lines that are to appear in the reproduction should be ruled in black ink. Paper ruled in green, yellow, or red should not be used. All lines must be of sufficient thickness to reproduce well. Decimal points, periods, and stippled dots must be solid black circles large enough to be reduced if necessary. Letters and numerals should be neatly made, preferably with a stencil (**do NOT use typewriting**), and be of such size that the smallest lettering will not be less than 1 mm high when the figure is reduced to a suitable size. Many drawings are made too large; originals should not be more than 2 or 3 times the size of the desired reproduction. Wherever possible two or more drawings should be grouped to reduce the number of cuts required. In such groups of drawings, or in large drawings, full use of the space available should be made; the ratio of height to width should conform to that of a journal page (5½×7¼ in.) but allowance must be made for the captions. **The original drawings and one set of clear copies (e.g. small photographs) are to be submitted.**

Photographs.—Prints should be made on glossy paper, with strong contrasts. They should be trimmed so that essential features only are shown and mounted carefully, with rubber cement, on white cardboard, with no space between those arranged in groups. In mounting, full use of the space available should be made. **Photographs are to be submitted in duplicate;** if they are to be reproduced in groups one set should be mounted, the duplicate set unmounted.

REPRINTS

A total of 50 reprints of each paper, without covers, are supplied free. Additional reprints, with or without covers, may be purchased at the time of publication.

Charges for reprints are based on the number of printed pages, which may be calculated approximately by multiplying by 0.5 the number of manuscript pages (double-space typewritten sheets, 8½×11 in.) and including the space occupied by illustrations. Prices and instructions for ordering reprints are sent out with the galley proof.

Contents

Printed in Canada *by* University of Toronto Press